

---

# The standard model and beyond in the light of $\varepsilon'$

---

Doctoral dissertation presented by

Philippe Mertens

in fulfilment of the requirements for the degree of Doctor in Sciences

Prof. Jean-Marc Gérard (Advisor)	UCLouvain
Prof. Vincent Lemaitre (Chairman)	UCLouvain
Prof. Eduardo Cortina Gil	UCLouvain
Prof. Emi Kou	LAL-IN2P3/CNRS
Prof. Fabio Maltoni	UCLouvain
Prof. Christopher Smith	LPSC-IN2P3/CNRS

---

May 2014



### *Remerciements*

*Tout d'abord, je tiens à remercier le Professeur Jean-Marc Gérard d'avoir accepté de me guider tout au long de cette aventure. Je le remercie autant pour ses enseignements de qualité et ses conseils avisés que pour la patience et la confiance dont il a fait preuve à mon égard.*

*Je remercie le Professeur Christopher Smith de m'avoir momentanément pris sous son aile et ensuite soutenu tout au long du trajet restant. Je lui dois, entre autres choses, mon gout pour les calculs en  $\chi$ PT au NLO sans crayon ni papier.*

*Je suis honoré de pouvoir remercier les Professeurs Eduardo Cortina, Emi Kou, Vincent Lemaitre et Fabio Maltoni d'avoir accepté de faire partie de mon jury de thèse.*

*Un tout grand merci à Megan Manin pour sa précieuse et attentive relecture du manuscrit.*

*Merci à tous les membres du CP3, anciens et actuels, de faire de ce centre ce qu'il est, un endroit où il fait autant bon vivre et travailler qu'il est triste de quitter.*

*Merci aux amis, vous m'avez été d'un soutien sans faille comme toujours.*

*Enfin et surtout, merci à mes parents, inébranlables guides et professeurs de la première heure, et à mes sœurs, supportrices inconditionnelles et attentives.*



# Contents

<b>Introduction</b>	<b>i</b>
<b>1 The standard model</b>	<b>1</b>
1.1 Flavor structure . . . . .	4
1.2 CP violation . . . . .	6
1.3 Flavor Changing Neutral Currents . . . . .	10
1.3.1 At short distances . . . . .	11
1.3.2 At long distances . . . . .	18
<b>2 <math>s \rightarrow d\gamma</math> in the SM</b>	<b>29</b>
2.1 Phenomenological windows . . . . .	29
2.2 Standard Model predictions . . . . .	32
2.2.1 $K \rightarrow \pi\pi\gamma$ . . . . .	33
2.2.2 $K_{L,S} \rightarrow \gamma\gamma$ . . . . .	42
2.2.3 Rare semileptonic decays . . . . .	46
2.2.4 Virtual effects in $\varepsilon'/\varepsilon$ . . . . .	50
2.3 Conclusions . . . . .	54

<b>3</b>	<b><math>s \rightarrow d\gamma</math> beyond the SM</b>	<b>57</b>
3.1	Model-independent analysis . . . . .	60
3.2	Tree-level FCNC . . . . .	64
3.3	Loop-level FCNC . . . . .	68
3.4	Conclusions . . . . .	82
<b>4</b>	<b>Weakly-induced strong CP-violation</b>	<b>85</b>
4.1	$\eta^{(\prime)} \rightarrow \pi\pi$ from strong interactions . . . . .	86
4.2	$\eta^{(\prime)} \rightarrow \pi\pi$ from weak interactions . . . . .	89
4.3	From $\delta_{\text{CKM}}$ to $\theta_{\text{QCD}}$ . . . . .	91
4.4	Conclusion . . . . .	96
	<b>Conclusions</b>	<b>97</b>
<b>A</b>	<b>Useful formulae</b>	<b>101</b>
A.1	The $\Gamma(z)$ function . . . . .	101
A.2	Dilogarithmic functions . . . . .	103
A.3	Scalar one-loop functions . . . . .	104
A.4	Particular one-loop functions . . . . .	106
<b>B</b>	<b>Effective Lagrangians</b>	<b>111</b>
B.1	Effective QCD at $\mathcal{O}(p^4)$ . . . . .	112
B.2	The Wess-Zumino-Witten Lagrangian . . . . .	112
B.3	Effective $ \Delta S  = 1$ sector . . . . .	113
B.3.1	The effective Lagrangian at $\mathcal{O}(p^2)$ . . . . .	117
B.3.2	The effective Lagrangian at $\mathcal{O}(p^4)$ . . . . .	118

<b>C</b>	<b>Amplitudes in ChPT</b>	<b>121</b>
C.1	Renormalization . . . . .	122
C.2	$K \rightarrow \gamma\gamma$ . . . . .	126
C.3	$K \rightarrow \pi\pi(\gamma)$ . . . . .	130
C.4	$\eta^{(\prime)} \rightarrow \pi\pi$ . . . . .	150





# Introduction

Our current understanding of the fundamental laws ruling the dynamics of the elementary matter building blocks is encoded in the Standard Model of elementary particles (SM). Even though its physical reality has been experimentally confirmed many times, this should not be the end of the story. Among the several indications supporting this statement, the strongest one might be that the *SM does not include gravity yet*, as Einstein's theory of General Relativity seems to be incompatible with the quantum field descriptions we have regarding the three other fundamental interactions identified so far. Even so, as the SM will certainly reveal itself as an inevitable piece of a unified theory of all fundamental interactions, yet to be discovered if existing at all, it is important to address its internal issues such as:

- the *unexplained hierarchies* observed in the fermion mass spectrum and the mixing matrix,
- the *SM hypothesis of massless neutrinos*, which is not only at variance with neutrino mixing observations but could also cover up CP violating phenomenon relevant for *successful baryo- and lepto-genesis explanations*,
- the *SM inability to accommodate possible Dark Matter* which, if present, would constitute 25% of the Universe's content,
- the *strong CP problem* [1], which is still a problem as we do not yet understand why experimental measurements constrain the apparently free  $\theta_{\text{QCD}}$  parameter to lie below the  $10^{-10}$  level.

These unanswered questions drove physicists to consider alternative theories referred to as New Physics (NP) models within which some (but not all) SM weakness(es) could be overcome. For instance, supersymmetric (SUSY) models provide Dark Matter candidates while the strong CP problem might be solved by the Peccei-Quinn mechanism [2]. These are two possible alternatives among

many others, which are all characterized by their own phenomenology and enlarged particle spectrum. In SUSY we find super-partner particles, the axion is predicted by the Peccei-Quinn mechanism, Kaluza-Klein excitations appear in Extra-Dimension models and technicolor models predict the existence of strongly interacting techniquarks. To unravel and/or discriminate between such NP scenarios, strategies must be set up. They basically fall into two categories: *direct* and *indirect* searches.

Direct searches, pursued at the LHC for instance, consist in trying to directly produce and observe new degrees of freedom. Unfortunately, no direct observation of particle beyond the SM has been confirmed so far. However, these negative results have already set strong constraints on various NP models.

Indirect searches tend to detect NP by measuring its possible quantum effects. For instance, NP could manifest itself in flavor changing neutral K- or B-meson decay branching fractions through virtual loop contributions involving new degrees of freedom. By comparing their SM predictions with experimental measurements, we hope to identify tensions that could signal something beyond the SM is at play. Yet, in order to be efficient, these observables must satisfy several criteria. As we are testing the SM at the one-loop level, they must be precisely predicted in the SM. If not, NP contributions could be buried in uncertainties. Ideally, these observables should be highly suppressed or even forbidden in the SM. Indeed, the SM mechanism, responsible for the suppression or the prohibition of a particular process, may not be a feature of the NP model under consideration. Finally, and for obvious reasons, these observables should be either measured or measurable in a near future.

In this indirect hunt, the radiative  $b \rightarrow s\gamma$  and  $\mu \rightarrow e\gamma$  transitions have received considerable attention. Since both are neutral flavor changing transitions, they are loop suppressed in the SM. While the suppression of the former is not so effective,  $\text{Br}(\bar{B} \rightarrow X_s\gamma)_{\text{th}} = 3.15(23) \cdot 10^{-4}$ , the latter is extremely suppressed as it proceeds through neutrino mixing effects, in fact,  $\text{Br}(\mu \rightarrow e\gamma)_{\text{th}} < 10^{-40}$ . The former is known to NNLO precision in the SM [3], and has been measured accurately at the  $B$  factories [4],  $\text{Br}(\bar{B} \rightarrow X_s\gamma)_{\text{exp}} = 3.55(26) \cdot 10^{-4}$  with  $E_\gamma > 1.6$  GeV. It is now one of the most constraining observables for NP models. The latter is so small in the SM that its experimental observation would immediately point toward the presence of NP [5]. Further, most models do not suppress this transition as effectively as the SM, with rates within reach of the current MEG experiment at PSI [6].

In view of the expected high luminosities of several  $K$  decay experiments starting in the next few years, such as NA62 at CERN, KOTO at J-Parc, and KLOE-II at the LNF, new effective strategies to constrain or signal NP may

open up. In the Kaon sector, one of the golden targets is the  $K^+ \rightarrow \pi^+ \nu \bar{\nu}$  decay mode, which, in the SM, is exclusively driven by  $s \rightarrow dZ$  penguin and, therefore, very precisely predicted:  $\text{Br}(K^+ \rightarrow \pi^+ \nu \bar{\nu})_{\text{th}} = 8.25(64) \cdot 10^{-11}$ . Incidentally, one of the main purposes of the second phase of the NA68 experiment is to record  $\mathcal{O}(100)$  events in order to reach a ten percent precision on  $\text{Br}(K^+ \rightarrow \pi^+ \nu \bar{\nu})_{\text{exp}}$ . This would represent a great improvement compared to the current  $\text{Br}(K^+ \rightarrow \pi^+ \nu \bar{\nu})_{\text{exp}} = 1.73_{-1.05}^{+1.15} \cdot 10^{-10}$  measurement extracted from the seven events recorded by the E787-949 experiments at BNL [7]. If such a precision is achieved, the  $K^+ \rightarrow \pi^+ \nu \bar{\nu}$  would constitute a perfect probe for NP in the  $s \rightarrow dZ$  penguin.

In principle, another powerful probe for NP is the  $\varepsilon'$  parameter. Indeed, this observable, which quantifies the small amount of direct CP violation in  $K \rightarrow \pi\pi$  decays, is loop induced and well measured:  $\text{Re}(\varepsilon') = (2.5 \pm 0.4) \cdot 10^{-6}$  with  $\phi_{\varepsilon'} \simeq \pi/4$ . Furthermore, it has the advantage to probe the SM directly at the amplitude level rather than at the branching one. Sadly, its ability to constrain NP is quite limited by our current theoretical control over the electroweak and QCD penguins hadronic dynamics, which is not good enough to resolve precisely the destructive interference occurring between the  $s \rightarrow dg$  and the  $s \rightarrow d\{Z, \gamma\}$  penguins in  $\varepsilon'$ . Yet, with the  $s \rightarrow dZ$  transition controlled by  $K^+ \rightarrow \pi^+ \nu \bar{\nu}$  in a near future, the situation could be further improved if we manage to control the  $s \rightarrow d\gamma$  transition independently of  $\varepsilon'_{\text{th}}$ . Supplemented with such orthogonal correlations,  $\varepsilon'_{\text{th}}$  could eventually become a good probe for the  $s \rightarrow dg$  penguin only.

The main purpose of the present work is, therefore, a complete and most updated analysis of the best observables (other than  $\varepsilon'_{\text{th}}$ ) giving a direct access to the  $s \rightarrow d\gamma$  transition, both in and beyond the SM. This analysis is not only profitable to the  $s \rightarrow d\{Z, \gamma, g\}$  penguins disentanglement in  $\varepsilon'$ , it is also complementary to the  $b \rightarrow s\gamma$  and  $\mu \rightarrow e\gamma$  studies. Indeed, as shown in the following table, these three radiative decays are complementary from the point of view of their respective SM suppression and sensitivity to hadronic effects:

	SM suppression	Hadronic effects	Experiment
$\text{Br}(b \rightarrow s\gamma)_{\text{inc}}$	$3.15(23) \cdot 10^{-4}$	small: $E_\gamma > 1.6 \text{ GeV}$	$3.55(26) \cdot 10^{-4}$
$\text{Br}(s \rightarrow d\gamma)_{\text{exc}}$	$\sim 10^{-6}$	large: $E_\gamma < 0.2 \text{ GeV}$	which mode?
$\mu \rightarrow e\gamma$	$< 10^{-40}$	absent	$< 1.2 \cdot 10^{-11}$

Since in the SM, the  $s \rightarrow d\gamma$  transition is more suppressed than the  $b \rightarrow s\gamma$  one, we naively expect the former to be more efficient to constrain NP effects (in its own flavor sector). However, this suppression argument overlooks hadronic uncertainties, which are very important in  $s \rightarrow d\gamma$  and under good control

in  $b \rightarrow s\gamma$ . Consequently, two issues have severely hampered the  $s \rightarrow d\gamma$  ability to probe NP up to now. First, the  $s \rightarrow d\gamma$  decay takes place deep within the QCD non-perturbative regime, and thus requires control over the low-energy hadronic physics. Second, these hadronic effects strongly enhance the SM contribution, to the point that identifying a possible deviation from NP is very challenging both theoretically and experimentally. To circumvent these difficulties is one of the goal of the present thesis.

In chapter 2, we demonstrate that a good theoretical control over the hadronic dynamics of  $s \rightarrow d\gamma$  is now reached. In particular, these effects, handled within Chiral Perturbation Theory (ChPT), involve local interactions which were unknown up to now. Thanks to our improved NLO computations combined with recent experimental results concerning the  $K^+ \rightarrow \pi^+\pi^0\gamma$  decay obtained by NA48 [8], we are now able to extract these problematic contributions directly from experiment. As a matter of fact, we provide the first experimental extraction of a previously unknown local term which intervenes in several  $K \rightarrow \pi\pi\gamma$  decays and we find it to be small, as expected.

The most promising observables to probe the  $s \rightarrow d\gamma$  high energy dynamics and thereby possible NP effects, are then identified. Those are the radiative  $K$  decay CP asymmetries in the case of real emissions and the CP violating contributions to the  $K_L \rightarrow \pi^0\ell^+\ell^-$  decay modes in the case of virtual emissions. While the current experimental situation regarding these observables will surely benefit from forthcoming high luminosity K experiments, we have, for the time being, systematically improve their SM predictions. The theoretical control over these CP violating observables is now achieved, in and beyond the SM, by using a systematic and original parametrization of the hadronic penguins in terms of the well measured  $\varepsilon'_{\text{exp}}$  parameter.

This parametrization procedure does not suffer from the hadronic uncertainties encountered in  $\varepsilon'_{\text{th}}$ , except in one place where it actually serves our purpose. Indeed, our updated analysis of the CP asymmetries in  $K \rightarrow \gamma\gamma$  decays reveals a new phenomenological relation between one of these measurable CP parameter and the pure QCD penguin contribution to  $\varepsilon'$ . This simple link is particularly interesting as it suggests a way to eventually resolve the destructive interference at play in  $\varepsilon'$ .

In chapter 3, the correlations between rare and radiative K decays as well as  $\varepsilon'$ , established in chapter 2, are exploited to quantify the possible impact of NP on the  $s \rightarrow d\gamma$  process. Subsequent strategies, which differ from usual parameter scan procedures, are then suggested to resolve possible interference among various NP sources. Doing so, a special care is taken to minimize model dependencies and fine-tuning. The NP scenarios considered there are organized

into three broad classes within which each NP source is bounded once turned on one at a time. The discriminatory informations on possible NP which could be gained from our results concerning the  $s \rightarrow d\gamma$  are also highlighted on a model dependent basis.

In chapter 4, the relevance of the experimental information we have about  $\varepsilon'$  is illustrated in another (almost) independent context. Namely, a novel method to estimate the electroweak corrections affecting  $\theta_{\text{QCD}}$  is suggested. Contrary to previous complementary but controverted attempts, this new method uses  $\varepsilon'$  to express the physical quantum corrections to  $\theta_{\text{QCD}}$  in a simple and direct way.

The main results of the present thesis have already been presented in the following publications:

- [9] P. Mertens and C. Smith, The  $s \rightarrow d\gamma$  gamma decay in and beyond the Standard Model, *JHEP* **1108** (2011) 069 ,
- [10] J.-M. Gérard and P. Mertens, Weakly-induced strong CP-violation, *Phys. Lett. B* **716** (2012) 316 ,

as well as in a conference proceeding [11].



# Chapter 1

## The standard model

As far as we know, two types of elementary matter particles exist: the leptons and the quarks. It is also believed and experimentally confirmed that their dynamics emerge from a symmetry principle, the gauge principle [12–16], applied on the group

$$G_{\text{SM}} \doteq SU(3)_C \otimes SU(2)_L \otimes U(1)_Y ,$$

which constitutes the cornerstone of the SM. The strong interactions are encoded in the  $SU(3)_C$  factor while the electroweak interactions emerge from the  $SU(2)_L \otimes U(1)_Y$  one. According to this picture, the dynamics of a particle  $\psi$  is determined by its transformation law under  $G_{\text{SM}}$  or, equivalently, by its membership to a given multiplet of  $G_{\text{SM}}$ . In the SM, fermions are organized into chiral multiplets. In the lepton sector, they are defined as

$$L^I \doteq \begin{pmatrix} \nu_{\ell^I} \\ \ell^I \end{pmatrix}_L , \quad E^I \doteq \ell^I_R , \quad (1.1)$$

where  $I$  runs over the three known lepton flavors ( $I = e, \mu, \tau$ ) and where, by construction, there is no right-handed neutrino. In the quark sector, we find six different flavors organized as

$$Q^I \doteq \begin{pmatrix} u^I \\ d^I \end{pmatrix}_L , \quad U^I \doteq u^I_R , \quad D^I \doteq d^I_R , \quad (1.2)$$

with  $(u^1, u^2, u^3) = (u, c, t)$  and  $(d^1, d^2, d^3) = (d, s, b)$ . The gauge transformation properties of these multiplets are specified by their covariant derivatives

$$D_\mu \psi = (\partial_\mu - ig_s s_\psi T^a G_\mu^a - ig l_\psi \tau^k W_\mu^k - ig' y_\psi B_\mu) \psi ,$$

$\psi$	$Q$	$U$	$D$	$L$	$E$
$s_\psi$	$1_{2 \times 2}$	1	1	$0_{2 \times 2}$	0
$l_\psi$	1	0	0	1	0
$y_\psi$	$\frac{1}{6} 2 \times 2$	$\frac{2}{3}$	$-\frac{1}{3}$	$-\frac{1}{2} 2 \times 2$	-1

**Tab. 1.1:**  $SU(3)_C \otimes SU(2)_L \otimes U(1)_Y$  charges of the SM chiral multiplets in  $g_s$ ,  $g$  and  $g'$  unit.

where  $\psi$  stands for any of the five chiral multiplets introduced in Eqs.(1.1) and (1.2) and where the various charges  $(s, l, y)_\psi$  are given in Tab.(1.1). The  $SU(3)_C$  and  $SU(2)_L$  generators are respectively given by  $T^a \doteq \lambda_a/2$  and  $\tau^k = \sigma^k/2$  where  $\lambda_a$  denote the Gell-Mann matrices and  $\sigma^k$  the Pauli matrices. The gluons, the weak-isospin and the hypercharge gauge boson fields are, for their part, represented by  $G_\mu^a$ ,  $W_\mu^i$  and  $B_\mu$ , respectively. Following the gauge principle, the fermion-gauge boson interactions are encoded in  $G_{\text{SM}}$ -invariant Lagrangian:

$$\mathcal{L} = \bar{\psi} i \gamma^\mu D_\mu \psi + \text{pure gauge terms} , \quad (1.3)$$

where weak and electromagnetic forces are still unified. To disentangle them,  $\mathcal{L}$  may be decomposed into charged and neutral current interactions as

$$\mathcal{L} = \mathcal{L}_{\text{CC}} + \mathcal{L}_{\text{NC}} + \mathcal{L}_{\text{QED}} + \text{kinetic terms} .$$

The charged current interactions described by

$$\mathcal{L}_{\text{CC}} = \frac{g}{\sqrt{2}} W_\mu^\dagger \left[ \bar{u}^I \gamma^\mu \gamma_L d^I + \bar{\nu}_{\ell I} \gamma^\mu \gamma_L \ell^I \right] + \text{h.c.} \quad (1.4)$$

are driven by the complex gauge boson  $W_\mu = (W_\mu^1 + iW_\mu^2)/\sqrt{2}$ , while QED and weak Neutral Current (NC) interactions are obtained once the weak rotation

$$\begin{pmatrix} Z_\mu \\ A_\mu \end{pmatrix} = \begin{pmatrix} \cos \theta_W & -\sin \theta_W \\ \sin \theta_W & \cos \theta_W \end{pmatrix} \begin{pmatrix} W_\mu^3 \\ B_\mu \end{pmatrix}$$

where  $\sin \theta_W \doteq s_W = g'/(g^2 + g'^2)^{1/2}$  and the conditions defining the electrical charge in  $|e|$  unit,

$$|e| = g \sin \theta_W = g' \cos \theta_W \quad \text{and} \quad Q_\psi = l_\psi \tau^3 + y_\psi , \quad (1.5)$$

are imposed. As a result,  $\mathcal{L}_{\text{QED}}$  is completely disentangled from the  $Z$  driven NC interactions encoded in

$$\mathcal{L}_{\text{NC}} = \frac{|e|}{\sin \theta_W \cos \theta_W} Z_\mu \bar{\psi} \gamma_\mu \left[ \tau^3 - \sin^2 \theta_W Q_\psi \right] \psi . \quad (1.6)$$



As such, the SM electroweak sector suffers from a very bad drawback: its gauge symmetry forbids the  $W_\mu$  and  $Z_\mu$  to acquire masses while it is experimentally observed that [17]

$$M_W = 80.385(15) \text{ GeV} \quad \text{and} \quad M_Z = 91.1876(21) \text{ GeV} .$$

A similar problem appears in the fermionic sector as chirality flipping mass terms, needed to account for the experimental measurements [17]

$$m_\tau = 1776.82(16) \text{ MeV} \quad \text{and} \quad m_t = 173.5(1) \text{ GeV} ,$$

for instance, explicitly break the electroweak gauge symmetry. These clear discrepancies demonstrate that the  $SU(2)_L \otimes U(1)_Y$  gauge symmetry must be broken.

In the SM, the required electroweak symmetry breaking is insured by the Brout-Englert-Higgs (BEH) mechanism [18–21], which describes how the ground state of the theory is responsible for the spontaneous symmetry breaking

$$G_{\text{SM}} \rightarrow SU(3)_C \otimes U(1)_{em} , \quad (1.7)$$

where  $U(1)_{em}$  is the unbroken electromagnetic gauge symmetry defined in accordance with the electric charge assignments of Eq.(1.5). This kind of symmetry breaking mechanism not only preserves the gauge symmetry of the interaction laws and, thereby, their description in terms of gauge invariant Lagrangians, it also guaranties that the SM is renormalizable [1,22]. The minimal ingredient required to achieve this symmetry breaking is the gauge invariant introduction of a complex weak-isospin scalar doublet  $\Phi$ . While its dynamic is governed by  $\mathcal{L}_\Phi = |D_\mu \Phi|^2 - V(\Phi)$ , its coupling to the fermions are governed by the Yukawa Lagrangian

$$\mathcal{L}_Y = -\bar{Q}\Phi\mathbf{Y}_d D - \bar{Q}\tilde{\Phi}\mathbf{Y}_u U - \bar{L}\Phi\mathbf{Y}_\ell E + \text{h.c.} , \quad (1.8)$$

with  $\tilde{\Phi} \doteq i\sigma_2 \Phi^*$  and where the Yukawa couplings  $\mathbf{Y}_{d,u,\ell}$  are arbitrary matrices defined in the flavor space. In order for the spontaneous symmetry breaking to occur, the scalar potential  $V(\Phi)$  must be chosen to provide  $\Phi$  its vacuum expectation value (vev). The most general gauge symmetric and renormalizable potential being given by  $V(\Phi) = \mu^2 \Phi^\dagger \Phi + \lambda (\Phi^\dagger \Phi)^2$ , we can conclude that if  $\mu^2 < 0$  and  $\lambda > 0$ ,  $\Phi$  acquires a non vanishing vev

$$\langle \Phi \rangle = (0 \ v/\sqrt{2})^T \quad \text{with} \quad v \doteq \sqrt{-\mu^2/\lambda} ,$$

which is invariant under the action of  $U(1)_{em}$ . Accordingly, the Goldstone theorem [23] implies the existence of three massless scalar fields  $\omega_i$  parametrized as

$$\Phi(x) = \frac{1}{\sqrt{2}} (0 \ v + h(x))^T e^{i\tau^i \omega_i(x)} , \quad (1.9)$$

which, thanks to the gauge invariance of the Lagrangian, may be rotated away to provide the missing longitudinal degree of freedom of the weak gauge bosons. The corresponding masses, originating from the  $\Phi$  kinetic term, read

$$M_W = \frac{g}{2}v \quad \text{and} \quad M_Z = \frac{M_W}{\cos \theta_W} , \quad (1.10)$$

while the unbroken  $U(1)_{em}$  still protects the photon from a mass as, in fact,  $M_\gamma < 10^{-18}$  eV, see Ref. [17]. Using the experimental gauge boson masses together with the conditions of Eq.(1.5) and  $\alpha_{em} \simeq 1/137$ , Eq.(1.10) indicates that the spontaneous electroweak symmetry breaking should occur around  $v \simeq 250$  GeV.

Contrary to the  $\omega_i$  fields, the extra scalar degree of freedom  $h(x)$  appearing in Eq.(1.9) can not be gauged away. This degree of freedom, called the Higgs boson, is a striking prediction of the BEH mechanism and its tree-level mass is predicted to be

$$m_h = \sqrt{2\lambda}v .$$

Until fairly recently we had no direct theoretical information about it as we did not know  $\lambda$ . The situation has changed since the fourth of July 2012. On that day, the two CERN experiments dedicated to the Higgs boson hunt, namely ATLAS and CMS, announced the discovery of a resonance around 125 GeV consistent with the SM Higgs boson [24, 25]. Since then, evidences in favor of the SM Higgs have gotten stronger even though a lot of its properties must still be carefully measured before we can be sure it is the Higgs boson. In particular, most of its couplings to fermions are not accurately measured yet.

## 1.1 Flavor structure

The SM fermion-gauge sector enjoys an accidental flavor symmetry: any flavor rotation of a given chiral multiplet will remain unnoticed. The only place where a non trivial flavor structure enters the SM is the Yukawa sector which reads

$$\mathcal{L}_Y = -\frac{1}{\sqrt{2}}(v+h) [\bar{d}_L \mathbf{Y}_d d_R + \bar{u}_L \mathbf{Y}_u u_R + \bar{\ell}_L \mathbf{Y}_\ell \ell_R + \text{h.c.}] ,$$

once the  $\omega_i$  are gauged away. As the Yukawa couplings are arbitrary (complex) matrices, flavor symmetry breaking effects emerge from  $\mathcal{L}_Y$ . In particular, because they are proportional to  $v\mathbf{Y}$ , fermion mass terms call for fermion fields rotations

$$u_{R,L} \rightarrow V_{R,L}^u u_{R,L}, \quad d_{R,L} \rightarrow V_{R,L}^d d_{R,L}, \quad \ell_{R,L} \rightarrow V_{R,L}^\ell \ell_{R,L} \quad (1.11)$$

that render the full Yukawa interactions diagonal:

$$\mathcal{L}_Y = - \left( 1 + \frac{h}{v} \right) \left[ \bar{d}_L \mathbf{m}_d d_R + \bar{u}_L \mathbf{m}_u u_R + \bar{\ell}_L \mathbf{m}_\ell \ell_R + \text{h.c.} \right] ,$$

provided that

$$\mathbf{m}_\ell \doteq \frac{v}{\sqrt{2}} V_L^{\ell\dagger} \mathbf{Y}_\ell V_R^\ell = \text{diag}(m_e, m_\mu, m_\tau) ,$$

$$\mathbf{m}_{u(d)} \doteq \frac{v}{\sqrt{2}} V_L^{u(d)\dagger} \mathbf{Y}_{u(d)} V_R^{u(d)} = \text{diag}(m_{u(d)}, m_{c(s)}, m_{t(b)}) .$$

The structure of Higgs couplings to the fermion is now explicit: they are proportional to the physical fermion masses. Consequently, the scalar-fermion sector develops a highly hierarchical flavor structure as the fermion mass spectrum covers several orders of magnitude. For instance, we observe that

$$\frac{m_u}{m_t} \simeq 1.3 \cdot 10^{-5}, \quad \frac{m_\mu}{m_t} \simeq 6.1 \cdot 10^{-2}, \quad \frac{m_t}{v} \simeq \frac{1}{\sqrt{2}} .$$

This is not the only place where a non trivial flavor structure emerges. The rotations in Eq.(1.11) affect the fermion-gauge sector as well. Yet, these rotations have only a limited impact on the flavor structure of this sector. Indeed, as they are unitary, the  $V_{R,L}^{u,d,\ell}$  matrices leave the ( $\gamma$  and  $Z$  driven) neutral currents diagonal in the flavor space. As a result, there is no tree-level Flavor Changing Neutral Current (FCNC) in the SM. This restriction, proper to the SM and referred to as the Glashow-Iliopoulos-Maiani or GIM mechanism, was suggested in Ref. [26] as a generalization of the work of Cabibbo [27]. The flavor structure of charged current interactions of Eq.(1.4) is, for its part, affected: under the rotations defined in Eq.(1.11) these currents become

$$\mathcal{L}_{CC} \rightarrow \frac{g}{\sqrt{2}} W_\mu^\dagger \left[ \bar{u} V \gamma^\mu \gamma_L d + \bar{\nu}_\ell \gamma^\mu \gamma_L \ell \right] + \text{h.c.} , \quad (1.13)$$

where the unitary matrix

$$V \doteq V_L^{u\dagger} V_L^d = \begin{pmatrix} V_{ud} & V_{us} & V_{ub} \\ V_{cd} & V_{cs} & V_{cb} \\ V_{td} & V_{ts} & V_{tb} \end{pmatrix}$$

is called the Cabibbo-Kobayashi-Maskawa (CKM) matrix. Historically, this matrix was introduced to account for CP violating effects. Its ability to provide a single source for such effects is, however, conditional to the existence of a third family of quark (the bottom and top quarks) predicted in Ref. [29]. Indeed, the unitarity of the CKM matrix allows for CP violation only if the number of quark family is at least equal to 3. In that case, this matrix may be parametrized

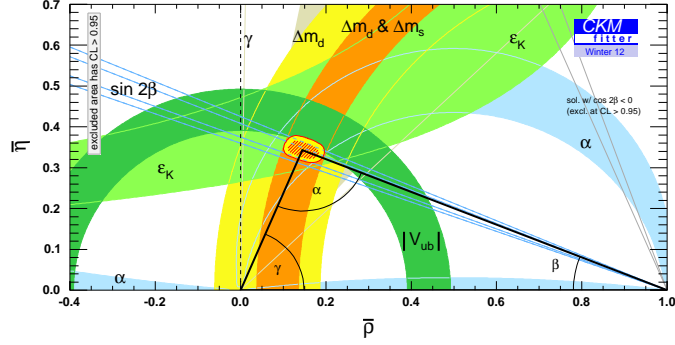


**Fig. 1.1:** Current CKMFitter  $(\bar{\rho}, \bar{\eta})$  confidence region at  $1\sigma$ . Figure taken from Ref. [28].

by three Euler angles and one complex phase  $e^{i\delta_{\text{CKM}}}$ . For example, in the Wolfenstein parametrization we may write

$$V = \begin{pmatrix} 1 - \lambda^2/2 & \lambda & A\lambda^3(\bar{\rho} - i\bar{\eta}) \\ -\lambda & 1 - \lambda^2/2 & A\lambda^2 \\ A\lambda^3(1 - \bar{\rho} - i\bar{\eta}) & -A\lambda^2 & 1 \end{pmatrix} + \mathcal{O}(\lambda^4), \quad (1.14)$$

where the various parameters are extracted from experimental data. Several groups are dedicated to that purpose and, according to the CKMFitter group [28],  $A \simeq 0.80$  and  $\lambda \simeq 0.22$ , while

$$\bar{\rho} \simeq 0.14 \quad \text{and} \quad \bar{\eta} \simeq 0.34.$$

These values are obtained from several measurements which, as shown in Fig.(1.1), are quite consistent. In particular, in the usual phase convention where  $V_{ub} \propto e^{-i\delta_{\text{CKM}}}$  the angle

$$\delta_{\text{CKM}} \simeq \tan^{-1} \left( \frac{\bar{\eta}}{\bar{\rho}} \right) \simeq 67^\circ \quad (1.15)$$

clearly demonstrates the existence of CP violation in the weak interactions.

## 1.2 CP violation

To prepare the ground for forthcoming developments, we review the main aspects of the CP violation phenomenon in the context of the neutral kaon (or K) system. This system consists in a subset of the  $SU(3)$  octet  $(\pi, K, \eta)$  made

out of the two pseudo-scalar particles  $K^0 \sim d\bar{s}$  and  $\bar{K}^0 \sim s\bar{d}$ . These strong eigenstates are CP conjugate of each other,

$$CP K^0 = -\bar{K}^0 \quad \text{and} \quad CP \bar{K}^0 = -K^0, \quad (1.16)$$

but differ from the mass eigenstates, which are expanded over the CP eigenstates defined by  $K_{1(2)} \doteq (K^0 \mp \bar{K}^0)/\sqrt{2}$  as

$$K_{S(L)} = \frac{1}{(1 + |\bar{\varepsilon}|^2)^{-1/2}} (K_{1(2)} + \bar{\varepsilon} K_{2(1)}),$$

where the mixing parameter  $\bar{\varepsilon}$  is related to the weak phase of the matrix element  $M \doteq A(K^0 \rightarrow \bar{K}^0)$ . The first experimental confirmation for a non-zero  $\bar{\varepsilon}$  goes back to Ref. [30] whilst current semi-leptonic  $K$  decays measurements indicate that

$$2\text{Re}\bar{\varepsilon} = (3.32 \pm 0.06) \cdot 10^{-3}.$$

This result has important consequences. Let us consider  $K_L$  meson decays for instance. Since  $\bar{\varepsilon} \neq 0$ , this particle is described as a mixture a  $\text{CP}_{\text{even}}$  state,  $K_1$ , and a  $\text{CP}_{\text{odd}}$  state,  $K_2$ .  $K_L$  may therefore decay into a  $\text{CP}_{\text{even}}$  state either via its  $\text{CP}_{\text{even}}$  component or via its  $\text{CP}_{\text{odd}}$  component. Both transitions are CP violating: the former process is allowed because the mixing matrix element  $M$  carries a CP violating phase and the latter proceeds through the direct CP violating decay amplitude  $A(K_2 \rightarrow \text{CP}_{\text{even}})$ . These two different CP violating mechanisms are referred to as *indirect* CP violation (ICPV) and *direct* CP violation (DCPV), respectively. Let us now develop these concepts in the context of the  $K \rightarrow \pi\pi$  decays in more detail.

In order to be consistent with unitarity, the description of  $K \rightarrow \pi\pi$  decay amplitudes has to take into account the strong  $\pi\pi$  re-scattering. If  $S_s$  represents the S-matrix of strong interaction, these phases are the asymptotic phase shifts defined by

$$\langle \pi\pi_I | S_s | \pi\pi_I \rangle \doteq e^{i2\delta_I} \quad \text{with} \quad I = 0 \text{ or } 2. \quad (1.17)$$

In Eq.(1.17), we assume isospin invariance and the  $\pi\pi$  state is decomposed into its isospin components  $\pi\pi_I$ . In principle, to fully re-construct the phases  $\delta_I$  we have to expand  $S_s$  to all orders in perturbation. Such a task is, a priori, impossible to achieve using perturbative techniques. A commonly used solution to overcome this issue consists in unitarizing the isospin decay amplitudes as

$$A(K^0 \rightarrow \pi\pi_I) \doteq \sqrt{3/2} A_I e^{i\delta_I}.$$

In other words, the strong phases  $\delta_I$  are factorized out from the amplitude (the weak phases being kept in  $A_I$ ) and are fitted from experiment. If so, the following decompositions arise

$$A(K^0 \rightarrow \pi^+\pi^-) = A_0 e^{i\delta_0} + A_2 e^{i\delta_2} / \sqrt{2}, \quad (1.18a)$$

$$A(K^0 \rightarrow \pi^0\pi^0) = A_0 e^{i\delta_0} - \sqrt{2} A_2 e^{i\delta_2}, \quad (1.18b)$$

$$A(K^+ \rightarrow \pi^+\pi^0) = (3/2) A_2 e^{i\delta_2}, \quad (1.18c)$$

which, thanks to the CPT theorem, fix automatically the  $\overline{K^0}$  decay amplitudes to be

$$A(\overline{K^0} \rightarrow \pi\pi_I) = \sqrt{3/2} A_I^* e^{i\delta_I}.$$

Focusing now on the  $K_L$  decays into  $\pi\pi$  states, i.e.,  $\text{CP}_{\text{even}}$  states, we introduce the following physical ratios

$$\eta_{+-} \doteq \frac{A(K_L \rightarrow \pi^+\pi^-)}{A(K_S \rightarrow \pi^+\pi^-)} \simeq \varepsilon + \frac{\varepsilon'}{1 + \frac{\omega}{\sqrt{2}} e^{-i\delta_{02}}}, \quad (1.19a)$$

$$\eta_{00} \doteq \frac{A(K_L \rightarrow \pi^0\pi^0)}{A(K_S \rightarrow \pi^0\pi^0)} \simeq \varepsilon - \frac{2\varepsilon'}{1 - \sqrt{2}\omega e^{-i\delta_{02}}}, \quad (1.19b)$$

which are, here, linearly parametrized in terms of the  $\varepsilon$  and  $\varepsilon'$  parameters, properly defined below, and

$$\delta_{02} \doteq \delta_0 - \delta_2 \quad \text{and} \quad \omega \doteq \frac{\text{Re}A_2}{\text{Re}A_0}.$$

In Eqs.(1.19),  $\varepsilon$  appears as a common contribution to both  $\eta_{+-}$  and  $\eta_{00}$  since it originates from the  $\text{CP}_{\text{even}}$  component of  $K_L$ . As such, it measures the amount of indirect CP violation in  $K_L \rightarrow \pi\pi$  decays. In fact, since by definition

$$\varepsilon \doteq \frac{A(K_L \rightarrow \pi\pi_0)}{A(K_S \rightarrow \pi\pi_0)},$$

it turns out that  $\varepsilon$  and  $\bar{\varepsilon}$  are indeed intimately related through

$$\varepsilon \doteq \frac{\bar{\varepsilon} + i\xi_0}{1 + i\bar{\varepsilon}\xi_0} \simeq \bar{\varepsilon} + i\xi_0 \quad \text{where} \quad \xi_0 \doteq \frac{\text{Im}A_0}{\text{Re}A_0}. \quad (1.20)$$

Consequently and contrary to  $\bar{\varepsilon}$ ,  $\varepsilon$  is a physical parameter: it does not depend on the overall phase of the  $K^0$  wave function. This can be observed either from the definition of  $\varepsilon$ , given in terms of physical amplitudes, or from Eq.(1.20) where the  $K^0$  phase dependence of  $\varepsilon$  cancels in the combination  $\bar{\varepsilon} + i\xi_0$ . The remaining  $\varepsilon'$  pieces in Eqs.(1.19) measure for their parts non-mixing induced

CP violation, i.e., direct CP violation. Experimentally, both parameters are rather precisely determined [17]:

$$|\varepsilon|_{\text{exp}} = (2.228 \pm 0.011) \cdot 10^{-3}, \quad \text{Re}(\varepsilon'/\varepsilon)_{\text{exp}} = (1.65 \pm 0.26) \cdot 10^{-3}, \quad (1.21)$$

while the current strong phases fits provide [31]

$$\phi_{\varepsilon'} \doteq -\delta_{02} + \pi/2 = (42.3 \pm 1.5)^\circ,$$

which is accidentally very close to the  $\varepsilon$  phase measured to be  $\phi_\varepsilon = (43.51 \pm 0.05)^\circ$ . From the  $K \rightarrow \pi\pi$  decay widths and given the smallness of CP violation effects it is also possible to extract the following information:

$$\omega \simeq 1/22.$$

The dominance of  $\Delta I = 1/2$  transitions over  $\Delta I = 3/2$  transitions, known as the  $\Delta I = 1/2$  rule, is due to the strong interaction dynamics. However, our limited ability to handle these effects at low energy have hampered a precise theoretical computation of  $\omega$ . In fact, the theoretical descriptions of the CP violation parameters

$$\varepsilon = e^{i\phi_\varepsilon} \sin \phi_\varepsilon \left( \frac{\text{Im}M_{12}}{\Delta M_K} + \xi_0 \right) \quad (1.22)$$

and

$$\text{Re}(\varepsilon'/\varepsilon) = -\frac{\omega}{\sqrt{2}|\varepsilon|} \xi_0 (1 - \Omega), \quad (1.23)$$

where

$$\Omega \doteq \frac{1}{\omega} \frac{\text{Im}A_2}{\text{Im}A_0}, \quad (1.24)$$

are not in perfect agreement with experiment either. These discrepancies may be appreciated by comparing the experimental measurements in Eqs.(1.21) with their corresponding current theoretical determinations:

$$|\varepsilon|_{\text{th}} = (1.81 \pm 0.28) \cdot 10^{-3}, \quad (1.25)$$

taken from Ref. [32] and

$$\text{Re} \left( \frac{\varepsilon'}{\varepsilon} \right)_{\text{th}} = 1.9_{-0.9}^{+1.1} \cdot 10^{-3}, \quad (1.26)$$

taken from [33,34]. Regarding  $\varepsilon$ , the main theoretical issues are the calculation of the  $A_0$  and  $M_{12} \doteq \langle K^0 | H_W^{\Delta S=2} | \overline{K^0} \rangle$  matrix elements (the weak effective

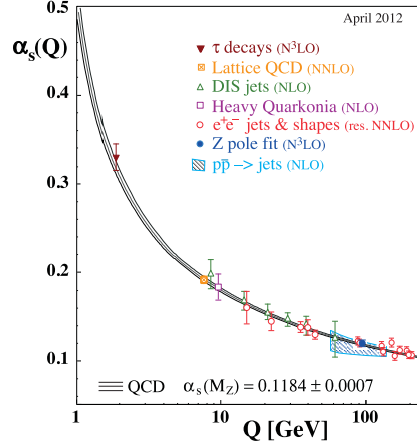


**Fig. 1.2:** Summary of the  $\alpha_s(Q)$  measurements versus the energy scale  $Q$ . Figure taken from Ref. [17].

Hamiltonian  $H_W^{\Delta S=2}$  is introduced in Eq.(1.30)). In the case of  $\varepsilon'$ , both  $A_0$  and  $A_2$  (see the definition of  $\Omega$  in Eq.(1.24)) amplitudes are equally important. The theoretical investigation of these parameters is a perfect starting point to our journey across the dynamics of FCNC in and beyond the SM. In particular, this will allow us to present the main difficulties we will have to face during our forthcoming study of  $s \rightarrow d\gamma$ .

### 1.3 Flavor Changing Neutral Currents

In the SM, flavor violating processes are governed by the weak interaction. More precisely, only charged  $W$  exchange processes are able to produce flavor violating transitions through the CKM matrix, see Eq.(1.13). Yet, in order to get a complete description of these processes it is crucial to take into account QCD effects as well. Unfortunately, these effects are as important as they complicate the analysis of FCNC. The fundamental reason being that QCD is not perturbative at low energy.

Due to quantum corrections, the strong coupling constant  $g_s$  is subject to renormalization: in a  $SU(N_C)$  version of QCD with  $N_F$  quark flavors a one-loop perturbative computation shows that the strong coupling constant is given by

$$\alpha_s(Q) \doteq \frac{g^2}{4\pi} = \frac{4\pi}{\beta_0 \ln(Q^2/\Lambda_{\text{QCD}}^2)} \quad \text{with} \quad \beta_0 = 11\frac{N_C}{3} - 2\frac{N_F}{3}, \quad (1.27)$$



where  $\Lambda_{\text{QCD}}$  is determined once  $\alpha_s(Q)$  is measured at a given energy scale  $Q$ . The current world average measurement,  $\alpha_s(M_Z) = 0.1184(7)$ , combined with many other measurements shown in Fig.(1.2), confirms the running behavior of  $\alpha_s$  predicted by the  $SU(3)_C$  version of QCD. As a consequence, quarks are asymptotically free [35, 36]: the more the energy increases or, equivalently, the more distances decrease, the less quarks feel strong interaction to the point where they become asymptotically free as  $\lim_{Q \rightarrow +\infty} \alpha_s(Q) = 0$ . On the other hand, the limit  $\lim_{Q \rightarrow 0} \alpha_s(Q)$  makes no sense since  $\alpha_s(Q)$  is computed through perturbative methods, which are meaningful as long as  $\alpha_s(Q)$  is small enough. We simply don't know, from perturbative methods, how  $\alpha_s(Q)$  behaves at energies below 1 GeV. This particular scale set the border between two different regimes of QCD.

Above, the QCD coupling constant is small enough for perturbative techniques based on quark and gluon description to apply. Below, we invoke the confinement conjecture to explain why quarks bound together to form hadrons and we rely on non-perturbative techniques to make computations. This is, of course, of high relevance regarding FCNC processes where physical observables generally involve hadronic states such as pions, kaons or B-mesons. When considering such flavor violating processes, two different regimes must therefore be taken into account: the short distances or high energy dynamics described in terms of quarks and gluons and the low energy or long distances dynamics described in terms of hadrons. While the former is handled by usual perturbative methods, the latter requires the use of alternative methods.

### 1.3.1 At short distances

To illustrate the problem let us consider the Z-penguin diagrams displayed on Fig.(1.3.a) that produce the  $\Delta S = -1$  local operators

$$Q_{q,i}^Z = 4 \frac{G_F}{\sqrt{2}} \frac{\alpha_{em}}{\pi} \lambda_i C_0(x_i) (\bar{s} \gamma^\mu \gamma_L d) (\bar{q} \gamma_\mu \gamma_q q) \quad \text{with} \quad x_i \doteq \frac{m_i^2}{M_W^2}, \quad (1.28)$$

once the up-type quark  $u_i$  and the  $W$  boson are integrated out<sup>1</sup>. The CKM factors depend on the flavor of the quark which runs into the loop and appear in the form of the product  $\lambda_i \doteq V_{is}^* V_{id}$ , while the Inami-Lim function  $C_0$  results from the loop integration [37]. Even though it is one specific example, it turns

<sup>1</sup>We defined  $\gamma_q \doteq e_q [\gamma_R + (1 - \sin^{-2} \theta_W) \gamma_L]$ ,  $e_q$  being the electric charge of the  $q$  quark in  $|e|$  unit and the Fermi constant has been introduced as

$$G_F / \sqrt{2} \doteq g^2 / 8M_W^2.$$

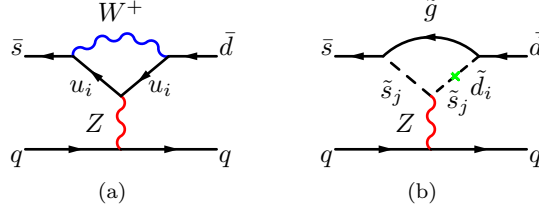


**Fig. 1.3:** FCNC represented by the Z penguins in the SM (a) and beyond (b).

out that all the FCNC are loop induced in the SM. This particular feature, proper to the SM, has important consequences on FCNC:

- They are non trivially suppressed. Their suppression is not only due to the product of the loop factor with the relevant coupling constant,  $\alpha_{em}$  in the case of the Z-penguin, it is also conditional to the Inami-Lim functions abilities to break the GIM mechanism. In a world where  $m_u = m_c = m_t$ , the GIM mechanism would be fully effective since the unitarity of the CKM matrix, that guaranties  $\lambda_u + \lambda_c + \lambda_t = 0$ , would force the sum of the Z-penguins, as defined above, to vanish. FCNC inherit, therefore, the strong hierarchy observed in the quark mass spectrum, through the Inami-Lim functions, as well as in the CKM matrix, through the CKM factors  $\lambda_i$ . Note that, in the particular case of the Z-penguin,  $C_0(x)$  scales like  $x$  as  $x \rightarrow \infty$  and like  $x \log x$  as  $x \rightarrow 0$ .
- While being CP conserving at long distances, they produce CP violation at short distances. This statement depends, of course, on the CKM matrix parametrization. Following the standard parametrization, where the CP violating phase enters the CKM entries as in Eq.(1.14), we have  $\text{Im}\lambda_u = 0$ . In this particular convention, the CP violating components of the FCNC are generated by heavy quark flavors loops (such as the charm- and top-quark because  $\text{Im}\lambda_c = -\text{Im}\lambda_t \neq 0$ ) whilst the up-quark loop is CP conserving.
- They provide well designed probes for NP as large enhancements compared to their very suppressed SM predictions can be expected. Even if NP tree-level induced FCNC are forbidden, they might still reveal non SM contribution appearing as

$$C_0(x) \rightarrow C_0(x) + \delta C_0 ,$$

where the perturbation represents, for instance, a SUSY contribution to the Z-penguin depicted by a green cross in Fig.(1.3.b). In that case, the flavor violation originates from the squarks non-diagonal mass matrix.

The FCNC efficiency to unravel NP is, however, conditional to their accurate predictability in the SM at both short and long distances. Their proper and systematic treatment at short distances proceeds through the Operator Product Expansion (OPE) leading to the construction of effective weak Hamiltonians of the form [38]

$$H_{\text{eff}} = \frac{G_F}{\sqrt{2}} \sum_i C_i(\mu) Q_i(\mu) ,$$

where the effective operators  $Q_i$  are weighted the by Wilson coefficients  $C_i$ . The latter encode all the QCD and EW corrected evolution of the Wilson coefficient taken at  $\mu \simeq M_W$ , where they are related to simple Inami-Lim functions, down to lower  $\mu$  scales. This perturbative approach does not only include the sequential integration of degrees of freedom heavier than  $\mu$ , but also takes into account renormalization group effects inherent to the running of  $\alpha_s$ . It is important to notice that at a given energy scale  $\mu$  the Wilson coefficients appear as mere effective coupling constants while the process dependencies appear at the matrix element level. Namely, if we are interested in a  $A(i \rightarrow f)$  decay amplitude, the effective Hamiltonian formulation tells us that

$$A(i \rightarrow f) = \langle f | H_{\text{eff}} | i \rangle = \frac{G_F}{\sqrt{2}} \sum_i C_i(\mu) \langle f | Q_i(\mu) | i \rangle , \quad (1.29)$$

where the process dependent matrix elements  $\langle f | Q_i(\mu) | i \rangle$  are still to be evaluated and where the Wilson coefficients are determined regardless of what  $i$  and  $f$  stand for.

$|\Delta S| = 2$  **processes** As a first example, we consider the  $|\Delta S| = 2$  effective Hamiltonian responsible for  $\bar{s}d \rightarrow s\bar{d}$  transitions, which is of particular relevance for  $\varepsilon$ . Around the 1 GeV scale, only one effective operator  $Q^{\Delta S=2} \doteq (\bar{s}\gamma^\mu\gamma_L d)(\bar{s}\gamma^\mu\gamma_L d)$  matters and enters the corresponding effective Hamiltonian as [38]

$$H_W^{\Delta S=2} = \frac{G_F}{(4\pi)^2} M_W^2 [\lambda_c^2 \eta_c S_{cc} + \lambda_t^2 \eta_t S_{tt} + 2\lambda_c \lambda_t \eta_{ct} S_{ct}] \times \\ \times b(\mu) Q^{\Delta S=2}(\mu) , \quad (1.30)$$

where  $S_{ij}$  are Inami-Lim functions and where the functions  $\eta_i b(\mu)$  equal one if QCD is turned off. These corrections are given at NLO in Ref. [38] while NNLO improvements of  $\eta_{ct}$  and  $\eta_{cc}$  may be found in Refs. [39] and [32], respectively. In the context of  $\varepsilon$ , a direct use of Eq.(1.30) leads to the theoretical prediction

$$|\varepsilon| = \kappa_\varepsilon C_\varepsilon \hat{B}_K |V_{cb}|^2 \lambda^2 \bar{\eta} (|V_{cb}|^2 (1 - \bar{\rho}) \eta_{tt} S_{tt} + \eta_{ct} S_{ct} - \eta_{cc} S_{cc}) \quad (1.31)$$

$$= (1.81 \pm 0.28) \cdot 10^{-3} \quad \text{according to [32]} , \quad (1.32)$$

where  $\kappa_\varepsilon$  accounts for both  $\phi_\varepsilon$  and  $\xi_0$  and where  $C_\varepsilon$  is a numerical constant. For more details, see Ref. [40]. The non-perturbative parameter  $\hat{B}_K$  parametrizes, for its part, the hadronic matrix element

$$\hat{B}_K \doteq \frac{3}{2} b(\mu) \frac{\langle \bar{K}^0 | Q^{\Delta S=2}(\mu) | K^0 \rangle}{F_K^2 M_K^2} ,$$

where  $F_K$  and  $M_K$  denote the decay constant and the mass of the neutral kaon, respectively. The low value of Eq.(1.32) has generated some concerns about possible NP contributions needed to accommodate its experimental determination [40, 41] quoted in Eq.(1.21). It should, however, be noticed that this theoretical prediction relies on improving results from both K and B sector and on partial long distances computations. In particular, the CKM entry  $V_{cb}$  is not well known as it may currently sit somewhere in between  $38.7 \cdot 10^{-3}$  and  $42.6 \cdot 10^{-3}$ , see Ref. [17]. Since  $V_{cb}$  enters  $\varepsilon$  at the fourth power, it has a huge impact on  $|\varepsilon|_{\text{th}}$ . In our opinion and for the time being,  $|\varepsilon|_{\text{th}}$  does not point towards an NP manifestation. In fact, using the 2013 updated inputs used by the CKMFitter collaboration given in Ref. [28] where, in particular, the inclusive value  $|V_{cb}| = (41.15 \pm 0.33 \pm 0.59) \cdot 10^{-3}$  is stable under the fit, we actually find

$$|\varepsilon|_{\text{th}} = (1.96 \pm 0.25) \cdot 10^{-3} ,$$

which is in better agreement with the experimental measurement. While Lattice determinations of the non-perturbative  $\hat{B}_K$  parameter seem to converge right below its upper bound predicted at Large- $N_C$  [42, 43], i.e.  $\hat{B}_K = 3/4$ , we must also wonder about the long distances contributions to  $\varepsilon$  estimated by  $\kappa_\varepsilon$  (for a review see e.g. Ref. [44]). These corrections originate, in particular, from the  $|\Delta S| = 1$  parameter  $\xi_0$  defined in Eq.(1.24) whose estimation remains very challenging.

**$|\Delta S| = 1$  processes** Following the OPE approach, the study of  $\xi_0$  as well as  $\varepsilon'$  starts with the construction of the  $H_W^{\Delta S=1}$  effective Hamiltonian, which encodes the  $|\Delta S| = 1$  short-distance dynamics. Around  $\mu \simeq 1$  GeV, it is expanded over ten effective four-quark operators:

$$H_W^{\Delta S=1} = 4 \frac{G_F}{\sqrt{2}} \sum_{i=1}^{10} C_i(\mu) Q_i(\mu) . \quad (1.33)$$

The first two represent QCD corrected current-current operators [45, 46]

$$Q_1 = (\bar{s}_\alpha \gamma_\mu \gamma_L u_\beta)(\bar{u}_\beta \gamma^\mu \gamma_L d_\alpha) \quad \text{and} \quad Q_2 = (\bar{s} \gamma_\mu \gamma_L u)(\bar{u} \gamma^\mu \gamma_L d) ,$$

where Greek indexes stand for color. The next four operators

$$Q_3 = (\bar{s}\gamma_\mu\gamma_L d)(\bar{q}\gamma^\mu\gamma_L q), \quad Q_4 = (\bar{s}_\alpha\gamma_\mu\gamma_L d_\beta)(\bar{q}_\beta\gamma^\mu\gamma_L q_\alpha),$$

$$Q_5 = (\bar{s}\gamma_\mu\gamma_L d)(\bar{q}\gamma^\mu\gamma_R q), \quad Q_6 = (\bar{s}_\alpha\gamma_\mu\gamma_L d_\beta)(\bar{q}_\beta\gamma^\mu\gamma_R q_\alpha),$$

where a sum over the light flavors  $q = u, d, s$  is understood, emerge from the Fierz decomposition of the QCD penguin operator [47], while the last four, given by

$$Q_7 = \frac{3}{2}(\bar{s}\gamma_\mu\gamma_L d)(\bar{q}e_q\gamma^\mu\gamma_R q), \quad Q_8 = \frac{3}{2}(\bar{s}_\alpha\gamma_\mu\gamma_L d_\beta)(\bar{q}_\beta e_q\gamma^\mu\gamma_R q_\alpha),$$

$$Q_9 = \frac{3}{2}(\bar{s}\gamma_\mu\gamma_L d)(\bar{q}e_q\gamma^\mu\gamma_L q), \quad Q_{10} = \frac{3}{2}(\bar{s}_\alpha\gamma_\mu\gamma_L d_\beta)(\bar{q}_\beta e_q\gamma^\mu\gamma_L q_\alpha),$$

correspond to the Fierz decomposition of the EW penguins. To these ten operators correspond ten Wilson coefficients conventionally decomposed as  $C_i(\mu) \doteq \lambda_u z_i(\mu) - \lambda_t y_i(\mu)$ , which are calculable perturbative quantities as long as  $\mu$  is above the 1 GeV scale. They can be found at various scales in Ref. [38], for instance.

A straightforward application of this  $|\Delta S| = 1$  operator product expansion in the context of the  $K \rightarrow \pi\pi$  decay amplitudes leads to the usual expressions for

$$\xi_0 \simeq -\frac{G_F}{\sqrt{2}\text{Re}A_0} \text{Im}\lambda_t y_6(\mu) \langle Q_6(\mu) \rangle_0$$

and

$$\frac{\varepsilon'}{\varepsilon} \simeq \frac{G_F \omega}{2|\varepsilon|\text{Re}A_0} \text{Im}\lambda_t \left[ y_6 \langle Q_6 \rangle_0 - \frac{1}{\omega} y_8 \langle Q_8 \rangle_2 \right], \quad (1.36)$$

where only the dominant contributions have been kept. These are the QCD  $\langle Q_6(\mu) \rangle_0 \doteq 4\langle \pi\pi_0 | Q_6(\mu) | K^0 \rangle$  and EW  $\langle Q_8 \rangle_2 \doteq 4\langle \pi\pi_2 | Q_8 | K^0 \rangle$  penguins contributions. In order to get precise predictions for both  $\varepsilon$  and  $\varepsilon'$ , these hadronic matrix elements (together with other sub-leading contributions) are still to be evaluated. This is in fact a huge problem as nobody knows how to deal with such non-perturbative quantities. Two main kinds of attempts have been offered so far: effective approaches (such as  $1/N_C$ -expansion or Chiral Perturbation Theory) or Lattice calculations. While the QCD penguin remains a big challenge for all these non-perturbative approaches (for a review see e.g. Ref. [48]), some recent progress in Lattice calculation regarding the determination of  $\langle Q_8 \rangle_2$ , published in Ref. [49], should be noticed. Yet, a further complication occurs in  $\varepsilon'$ : a destructive interference appears between two poorly known quantities, which, unfortunately, turn out to be of similar size. On the one hand, the EW contribution to  $\varepsilon'$ , naively expected to be suppressed with

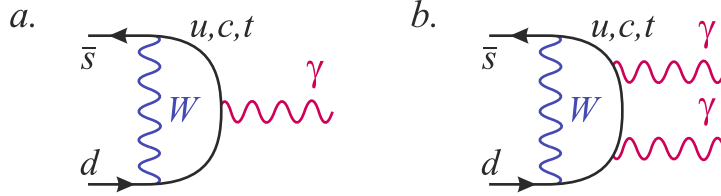


**Fig. 1.4:** The flavor-changing electromagnetic currents in the Standard Model.

respect to the QCD one, is enhanced by the  $\Delta I = 1/2$  rule, see the  $\omega^{-1}$  factor in Eq.(1.36), and, on the other hand, isospin breaking effects tend to confuse the QCD contribution as it should in fact be re-scaled as  $\langle Q_6 \rangle_0 \rightarrow \langle Q_6 \rangle_0 (1 - \Omega_{\text{iso}})$  in  $\varepsilon'$  where, according to Ref. [50],  $\Omega_{\text{iso}} = 0.06 \pm 0.08$ .

In conclusion, even though the evaluation of hadronic matrix elements is improving, the current situation is such that precise theoretical determination of  $\varepsilon$  and  $\varepsilon'$  are still out of reach. However, we will show in the present thesis that phenomenological links with radiative kaon decays might be used to improve the current situation.

**Radiative  $|\Delta S| = 1$  processes** In order to generalize  $H_W^{\Delta S=1}$  to include radiative processes, we have to supplement it with the single photon penguin of Fig.(1.4.a). When QCD is turned off, and  $m_{s,d} \ll m_{u,c,t}$ , this is achieved by adding the local effective interactions of dimension greater than four

$$H_{\text{eff}}^\gamma = C_\gamma^\pm Q_\gamma^\pm + C_{\gamma^*}^\pm Q_{\gamma^*}^\pm + \text{h.c.} \quad (1.37)$$

to  $H_W^{\Delta S=1}$ . The magnetic and electric operators are defined by

$$Q_\gamma^\pm = \frac{Q_d e}{16\pi^2} (\bar{s}_L \sigma^{\mu\nu} d_R \pm \bar{s}_R \sigma^{\mu\nu} d_L) F_{\mu\nu}, \quad (1.38a)$$

$$Q_{\gamma^*}^\pm = \frac{Q_d e}{16\pi^2} (\bar{s}_L \gamma^\nu d_L \pm \bar{s}_R \gamma^\nu d_R) \partial^\mu F_{\mu\nu}, \quad (1.38b)$$

where  $2\sigma^{\mu\nu} = i[\gamma^\mu, \gamma^\nu]$  and  $Q_d = -1/3$  is the down-quark electric charge. For a real photon emission only the magnetic operators contribute. Indeed, in this particular case, the electric operators are proportional to  $\partial^\mu F_{\mu\nu} = 0$ . The corresponding Wilson coefficients are [38]

$$Q_d(C_\gamma^+ \pm C_\gamma^-) = \sqrt{2} G_F \lambda_i D'_0(x_i) m_{d(s)}, \quad (1.39)$$

and

$$Q_d(C_{\gamma^*}^+ + C_{\gamma^*}^-) = -2\sqrt{2} G_F \lambda_i D_0(x_i), \quad Q_d(C_{\gamma^*}^+ - C_{\gamma^*}^-) \simeq 0, \quad (1.40)$$

where  $D_0^{(l)}$  are two new Inami-Lim functions detailed in Ref. [38], for instance. While  $D_0(x)$  breaks GIM logarithmically both for  $x \rightarrow \infty$  and  $x \rightarrow 0$ ,  $D_0'(x)$  is suppressed for light quarks. However, QCD corrections significantly soften the quadratic GIM breaking of  $D_0'(x)$  in the  $x \rightarrow 0$  limit [51–53], and exacerbate the logarithmic one of  $D_0(x)$  [54], making light-quark contributions significant for both operators. The evolution of these Wilson coefficients in the context of the  $s \rightarrow d\gamma$  effective Hamiltonian is not known. The reason being that the community has focused on  $s \rightarrow d$  transitions, relevant for non-radiative kaon decays, for which,  $Q_{\gamma(c^*)}^\pm$  operators are irrelevant [55]. Yet, numerically, to account for the large QCD corrections, the well known Wilson coefficient of the magnetic operator in  $b \rightarrow s\gamma$  can be used for  $\text{Im } C_\gamma^\pm$ , since the CKM elements for the  $u$ ,  $c$  and  $t$  contributions scale indeed similarly. With  $m_s(2 \text{ GeV}) = 101_{-21}^{+29} \text{ MeV}$  [17] and  $C_{7\gamma}(2 \text{ GeV}) \simeq -0.36$  from Ref. [38], we shall, therefore, use<sup>2</sup>

$$\begin{aligned} \frac{\text{Im } C_\gamma^\pm(2 \text{ GeV})_{\text{SM}}}{G_F m_K} &= \mp \sqrt{2} \frac{C_{7\gamma}(2 \text{ GeV})}{Q_d} \frac{m_s(2 \text{ GeV})}{m_K} \text{Im } \lambda_t \\ &= \mp 0.31(8) \times \text{Im } \lambda_t, \end{aligned} \quad (1.41)$$

to be compared to  $\mp 0.17 \text{Im } \lambda_t$  with only the top quark. In view of the large error on  $m_s$ , the LO approximation is adequate. For  $\text{Re } C_\gamma^\pm$ , contrary to the situation in  $b \rightarrow s\gamma$ , the top quark is strongly suppressed as  $\text{Re } \lambda_c \approx -\text{Re } \lambda_u \gg \text{Re } \lambda_t$ . With the light quarks further enhanced by QCD corrections, an estimate is delicate. Naively rescaling the above result gives

$$\frac{\text{Re } C_\gamma^\pm(2 \text{ GeV})_{\text{SM}}}{G_F m_K} \simeq \frac{\text{Re } \lambda_c}{\text{Im } \lambda_c} \times \frac{\text{Im } C_\gamma^\pm(2 \text{ GeV})_{\text{SM}}}{G_F m_K} \simeq \mp 0.06. \quad (1.42)$$

Evidently, one should not take this as more than a rough estimate of the order of magnitude of the  $c$  quark and high-virtuality  $u$  quark contributions. In any case, we will be mostly concerned by CP-violating observables in the following, so we will not be using Eq.(1.42).

With the help of the standard QED interactions, the  $H_{\text{eff}}^\gamma$  operators also contribute to processes with more than one photon, where they compete with the effective operators directly involving several photon fields. For example, for two real photons, the dominant operators are

$$Q_{\gamma\gamma,||}^\pm = (\bar{s}_L d_R \pm \bar{s}_R d_L) F_{\mu\nu} F^{\mu\nu}, \quad Q_{\gamma\gamma,\perp}^\pm = (\bar{s}_L d_R \pm \bar{s}_R d_L) F_{\mu\nu} \tilde{F}^{\mu\nu}, \quad (1.43)$$

with  $\tilde{F}^{\mu\nu} = \varepsilon^{\mu\nu\rho\sigma} F_{\rho\sigma}/2$ . In the SM, the additional quark propagator in the two-photon penguin induces an  $x^{-1}$  GIM breaking by the loop function (see

<sup>2</sup>For convenience, the same normalization by  $G_F m_K$  will be adopted throughout this work. Also, if not explicitly written, the  $C_\gamma^\pm$  are always understood at the  $\mu = 2 \text{ GeV}$  scale.

Fig.1.4.b). Hence, the  $c$  and  $t$ -quark contributions are completely negligible compared to the  $u$ -quark loop. Therefore, whenever it contributes, the double photon penguin represents an irreducible CP-conserving long-distance SM background for the SD processes. Indeed, NP effects in these operators should be very suppressed since they are at least of dimension seven. The same is true for transitions with more than two photons, with the NP (up-quark loop) even more suppressed (enhanced). Therefore, those will not be considered here.

### 1.3.2 At long distances

Having presented the short-distance dynamics of the FCNC considered in this work, it is time to wonder about their challenging long-distance dynamics. Since the QCD confinement is such that colored quark always bound into hadrons,  $q\bar{q}$  bound states called mesons or  $qqq$  bound states called baryons, the question is: how to go from a description of QCD based on quarks and gluons to a description based on hadronic states ?

**Strong sector** For the lightest meson spectrum made of  $u, d$  and  $s$  quark one of the possibilities, which will be the one used in the present work, is to rely on Chiral Perturbation Theory (ChPT). This effective description is based on the approximate global chiral symmetry of QCD. In the massless or chiral limit, the QCD Lagrangian truncated to the  $u, d$  and  $s$  quarks enjoys a global  $U(3)_L \otimes U(3)_R$  chiral symmetry acting in the  $(u, d, s)$  flavor space defined by

$$\psi_{L,R} \rightarrow g_{L,R} \psi_{L,R} \quad \text{with} \quad g_{L,R} \in U(3)_{L,R} .$$

Beyond the classical level, this chiral symmetry is too large since, even in the chiral limit, anomalous quantum effects break it into  $SU(3)_L \otimes SU(3)_R \otimes U(1)_V$  [56–58]. In the following we will leave aside the vectorial  $U(1)$  associated with the baryon number as it will not concern us. On the other hand, some aspects of the  $U(1)_A$  anomaly will be investigated in chapter 4. The remaining  $SU(3)_L \otimes SU(3)_R$  chiral symmetry is still too large as it would imply a parity degenerated hadronic spectrum. The non observation of such a spectrum suggests that  $SU(3)_L \otimes SU(3)_R$  is, in fact, spontaneously broken into its vectorial subgroup,  $SU(3)_V$ . In the context of the BEH mechanism, the spontaneous breaking of the electroweak symmetry is insured by the Higgs field vev. In the present case, no particular field seems to play the same role. Yet, the required spontaneous symmetry breaking might as well be produced by the vev of a composite fields, represented by composite operators  $\mathcal{O}^a$  (one for each broken axial generator  $Q_A^a$ ). Of course, in order to preserve all the unbroken symmetries, the operators



$\mathcal{O}^a$  are not arbitrary: they must be Lorentz and color singlets. The simplest choices are obviously the axial densities  $\mathcal{O}^a \doteq \bar{\psi}\gamma_5\lambda^a\psi$  and a condition for the spontaneous chiral symmetry breaking to actually happen might be

$$\langle 0 | [Q_A^a, \mathcal{O}^b] | 0 \rangle = -\frac{2}{3}\delta^{ab}\langle 0 | \bar{\psi}\psi | 0 \rangle \neq 0 .$$

This condition is, indeed, fulfilled if  $Q_A^a|0\rangle \neq 0$ , which is the explicit manifestation of a spontaneous symmetry breaking. In conclusion, the quark condensates

$$\langle 0 | \bar{u}u | 0 \rangle = \langle 0 | \bar{d}d | 0 \rangle = \langle 0 | \bar{s}s | 0 \rangle \neq 0$$

might play the role of the order parameter (or vev) of the chiral symmetry breaking. If so, the Goldstone theorem predicts the existence of eight massless scalar particles sharing the quantum numbers of the broken axial generators  $Q_A^a$ . These Goldstone Bosons (GB)  $\phi^a$  fields are collected in a unitary matrix [59, 60], which transforms under  $SU(3)_L \otimes SU(3)_R$  as

$$U(\phi) \rightarrow g_R U(\phi) g_L^\dagger ,$$

where  $\phi \doteq \sum_a \phi^a \lambda^a$  is a generic  $SU(3)$  matrix. Without loss of generality,  $U$  may be expanded as

$$U = 1 + \sum_{n=1}^{\infty} a_n \left( i\sqrt{2} \frac{\phi}{F} \right)^n$$

where  $F$  is normalized such that  $a_1 = 1$ . The remaining expansion parameters are restricted by the unitarity of  $U$  to assume the following values

$$a_2 = 1/2, \quad a_3 = b, \quad a_4 = b - 1/8, \quad \dots ,$$

where the real parameter  $b$  is arbitrary and, therefore, not physical. It indicates the freedom we have for the  $U$  matrix parametrization [61, 62]. For instance, the usual exponential parametrization is recovered for  $b = \frac{1}{6}$ . The key point here is that we have at our disposal an octet of light pseudo-scalars, namely, the three pions ( $\pi^\pm, \pi^0$ ), the four kaons ( $K^\pm, K^0, \bar{K}^0$ ) and the  $\eta$ , which might be considered as the GB of the spontaneous chiral symmetry breaking of QCD and, which enter the  $U$  matrix as

$$\phi = \begin{pmatrix} \pi^0 + \frac{\eta_8}{\sqrt{3}} & \sqrt{2}\pi^+ & \sqrt{2}K^+ \\ \sqrt{2}\pi^- & -\pi^0 + \frac{\eta_8}{\sqrt{3}} & \sqrt{2}K^0 \\ \sqrt{2}K^- & \sqrt{2}K^0 & -\frac{2}{\sqrt{3}}\eta_8 \end{pmatrix} . \quad (1.44)$$

The dynamics of these GB is described by an effective Lagrangian whose constructing rules are simple [63, 64]: it must contain all the terms allowed by the

assumed symmetry, here  $SU(3)_L \otimes SU(3)_R$ , built from the relevant asymptotic states, here  $U$ . This Lagrangian produces then the most general  $S$  matrix compatible with analyticity, perturbative unitarity, cluster decomposition and underlying symmetries. Given the unitarity of  $U$ , the simplest term we can construct is  $f^2 \langle \partial_\mu U \partial^\mu U^\dagger \rangle$  where  $f$  is an undetermined mass scale and  $\langle \dots \rangle$  denotes the trace over flavors. Expanding it up to  $\mathcal{O}(\phi^2)$ , canonical kinetic terms emerge for all the  $\phi^a$  if  $f = F/\sqrt{2}$  and the corresponding effective Lagrangian reads

$$\mathcal{L}_s = \frac{F^2}{4} \langle \partial_\mu U \partial^\mu U^\dagger \rangle . \quad (1.45)$$

This Lagrangian is too minimal: it does not include  $SU(3)_V$  breaking mass terms present in the fundamental QCD Lagrangian and it does not contain all possible chiral invariant operators. As the number of such operators is infinite, we will come back to this issue once a classification scheme will be introduced. For now, let us handle the former issue.

$\mathcal{L}_s$  can be generalized in a generic way by gauging its  $SU(3)_L \otimes SU(3)_R$  symmetry in order to introduce the external fields  $\ell_\mu$ ,  $a_\mu$  and  $s$  transforming as

$$\ell_\mu \rightarrow g_L \ell_\mu g_L^\dagger + i g_L \partial_\mu g_L^\dagger, \quad r_\mu \rightarrow g_R r_\mu g_R^\dagger + i g_R \partial_\mu g_R^\dagger, \quad s \rightarrow g_R s g_L^\dagger .$$

These external sources enter  $\mathcal{L}_s$  either through the covariant derivative

$$\partial_\mu U \rightarrow D_\mu U \doteq \partial_\mu U - i r_\mu U + i U \ell_\mu$$

or as extra terms collected in the generalized effective Lagrangian

$$\mathcal{L}_s^{(2)} = \frac{F^2}{4} \langle D_\mu U D^\mu U^\dagger + \chi^\dagger U + U^\dagger \chi \rangle \quad \text{with} \quad \chi \doteq 2B_0 s . \quad (1.46)$$

It is now a child-play to introduce the required  $SU(3)_V$  breaking mass term by freezing the external field  $s$  to  $\text{diag}(m_u, m_d, m_s)$ . This explicit symmetry breaking will be effective provided that the mass parameter  $B_0 \neq 0$ . This condition is, in fact, insured by the spontaneous chiral symmetry breaking pattern introduced above. Indeed, because the density  $\bar{\psi}^j \psi^i$  is obtained from the variation of the mass term of the fundamental QCD Lagrangian as  $\bar{\psi}^j \psi^i = -\delta \mathcal{L} / \delta s^{ij}$ , its effective realization is given by

$$\bar{\psi}^j \psi^i \rightarrow -\frac{\delta \mathcal{L}_s^{(2)}}{\delta s^{ij}} = -\frac{F^2}{2} B_0 [U + U^\dagger]^{ij} , \quad (1.47)$$

from which the simple relation

$$B_0 = -\frac{\langle 0 | \bar{\psi} \psi | 0 \rangle}{F^2} \neq 0 \quad (1.48)$$

follows. The corresponding pseudo-scalar mass spectrum can be carried out from the non derivative quadratic terms in  $\phi$  of  $\mathcal{L}_s^{(2)}$  with the result

$$m_{\pi^\pm}^2 = 2\hat{m}B_0, \quad m_{\pi^0}^2 = 2\hat{m}B_0 + \mathcal{O}((m_u - m_d)^2), \quad (1.49a)$$

$$m_{K^\pm}^2 = (m_u + m_s)B_0, \quad m_{K^0}^2 = (m_d + m_s)B_0, \quad (1.49b)$$

whilst the  $\eta_8$  mass fulfilled the Gell-Mann-Okubo relation

$$m_{\eta_8}^2 = \frac{1}{3}(4m_K^2 - m_\pi^2) + \mathcal{O}(m_u - m_d). \quad (1.50)$$

The external fields introduced above allow the calculation of other hadronic currents as well. For instance, the left- and right-handed hadronized quark currents are obtained from the following variations

$$J_L^\mu \doteq \frac{\delta \mathcal{L}_s^{(2)}}{\delta \ell_\mu} = i \frac{F^2}{2} D^\mu U^\dagger U, \quad (1.51a)$$

$$J_R^\mu \doteq \frac{\delta \mathcal{L}_s^{(2)}}{\delta r_\mu} = i \frac{F^2}{2} D^\mu U U^\dagger. \quad (1.51b)$$

In particular, we may now evaluate the following transition matrix

$$\langle 0 | J_A^\mu(0) | \phi^a(p) \rangle \doteq \langle 0 | J_L^\mu(0) - J_R^\mu(0) | \phi^a(p) \rangle \doteq i\sqrt{2}Fp_\mu, \quad (1.52)$$

where the meaning of  $F$  is now explicit: it represents the decay constant of the pseudo-scalar  $\phi^a$ , which is unique and may be identified with the pion one, i.e.,

$$F = F_\pi = 92.3 \text{ MeV}. \quad (1.53)$$

Let us now address the second issue of  $\mathcal{L}_s$  by noting that the mass spectrum and decay constants found so far are valid at the leading order (LO) in the *chiral expansion*. This expansion constitutes a power counting scheme in which all possible terms entering the strong effective Lagrangian are classified according to their dimension  $p^{2n}$ , where  $p$  indicates one power of derivative or (equivalently) one power of mass. Since they are derived from the  $\mathcal{L}_s^{(2)}$ , which involves at most  $\mathcal{O}(p^2)$  operators, the mass spectrum in Eqs.(1.49) and (1.50), as well as the decay constant given in Eq.(1.53), are  $\mathcal{O}(p^2)$  or LO results. However, in principle, we cannot discard chiral symmetric terms like  $\langle D_\mu U D^\mu U^\dagger \rangle^2$ , which involve four derivatives nor terms built from the field strength tensors

$$F_X^{\mu\nu} \doteq \partial^\mu x^\nu - \partial^\nu x^\mu - i[x^\mu, x^\nu] \quad \text{with } x = \ell, r,$$

which due to the Lorentz invariance, will be of at least  $\mathcal{O}(p^4)$ . In fact, any hadronic amplitude may be expanded in power of  $p$  up to a given order  $p^{d_x}$

where  $d_\chi \doteq 2n$  is called the chiral dimension of the amplitude. It has been shown by Weinberg that the chiral dimension of an amplitude built up from a connected  $L$ -loop diagram with  $V_d$  vertices of order  $p^d$  is [63]

$$d_\chi = 2 + 2L + \sum_d (d-2)V_d ,$$

where  $d$  assumes only non zero natural even values because of Lorentz invariance<sup>3</sup>. Consequently,  $d_\chi = 2$  amplitudes are built up from tree-level diagrams involving  $\mathcal{O}(p^2)$  vertices only, while  $d_\chi = 4$  amplitudes originate from either one-loop diagrams with only  $\mathcal{O}(p^2)$  vertices or tree-level diagrams involving one  $\mathcal{O}(p^4)$  vertex.

As  $p^2$  scales typically like  $m_{K,\pi}^2$  in ChPT, an expansion in this parameter seems to be appropriate. Yet, to get an naive idea of the relative size of  $\mathcal{O}(p^4)$  and  $\mathcal{O}(p^2)$  contributions, we may easily realize that a one-loop amplitude will drag a typical  $(4\pi F_\pi)^{-2}$  loop factor. Taking the typical energy scale of this loop amplitude at or below  $m_K$ , the natural energy scale for a ChPT calculation, the chiral expansion parameter is

$$\frac{m_K^2}{(4\pi F_\pi)^2} \simeq 20\% .$$

Even though this estimate is quite naive, as it does not even take into account possible large chiral logarithms, it shows that  $\mathcal{O}(p^4)$  corrections might indeed be important. It is even more true as some amplitudes start at that order. It is, therefore, desirable to extend  $\mathcal{L}_s^{(2)}$  up to  $\mathcal{O}(p^4)$  by supplementing it with all possible  $\mathcal{O}(p^4)$  operators.

The  $\mathcal{O}(p^4)$  effective QCD Lagrangian is divided into two distinct sectors. The first contains a minimal set of  $\mathcal{O}(p^4)$  chirally invariant operators derived in Ref. [65] and presented in App.B.1. The structure of these effective operators is dictated by the chiral counting rules and the chiral symmetry properties of the underlying theory. The renormalized counter-terms  $L_i$ , which multiply these operators, cannot be computed from first principles. Instead, they have to be fixed experimentally, exactly like the  $\mathcal{O}(p^2)$  constants  $F$ . The corresponding NLO mass spectrum and decay constants are analyzed in App.C.1. The second sector is particular since it originates from a parity symmetry mismatch between the fundamental QCD Lagrangian and its effective realization. As this Lagrangian will only play a minor role in the present work, we refer the reader to App.B.2 and Refs. [66, 67] for further details.

---

<sup>3</sup>Note that the chiral dimension of  $\chi$  is 2, see Eq.(1.46) and (1.48).

**Electroweak sector** The effective description of the EW interaction follows the exact same lines already used to construct the strong effective Lagrangian. The only difference here is that, by nature, the EW interaction violates the chiral symmetry. Consequently, at low energy, they are represented by hadronic operators which share the chiral symmetries of the corresponding weak effective Hamiltonian. In the context of this thesis, we are interested in the  $|\Delta S| = 1$  interactions given in Eq.(1.33) and the radiative  $|\Delta S| = 1$  interactions given in Eq.(1.37). Let us first investigate the four-quark weak operators.

By inspecting the chiral structure of the operators in Eq.(1.33), we conclude that the  $|\Delta S| = 1$  effective Hamiltonian belongs to the  $U(3)_L \otimes U(3)_R$  direct sum

$$(8_L, 1_R) \oplus (27_L, 1_R) \oplus (8_L, 8_R) . \quad (1.54)$$

The first two pure left-handed multiplets embody the current-current, the QCD penguin and the EW operators  $Q_9$  and  $Q_{10}$ , while the third multiplet encodes the EW penguin operators  $Q_7$  and  $Q_8$ . Note also that the effective Hamiltonian in Eq.(1.33) satisfies an additional symmetry [68] called the CPS symmetry which combines the CP symmetry and the exchange of the  $d$  and  $s$  quarks. This symmetry will be implicitly taken into account in the following. In App.B.3 it is shown that by matching their chiral structures, the four-quark weak current-current and penguin operators are represented at LO by [61, 62]

$$\mathcal{L}_8 = F^4 G_8 \langle \lambda_6 L_\mu L^\mu \rangle , \quad (1.55a)$$

$$\begin{aligned} \mathcal{L}_{27} = & \frac{F^4}{18} G_{27}^{1/2} (\langle \lambda_1 L_\mu \rangle \langle \lambda_4 L^\mu \rangle + \langle \lambda_2 L_\mu \rangle \langle \lambda_5 L^\mu \rangle - \\ & - 10 \langle \lambda_6 L_\mu \rangle \langle \lambda_3 L^\mu \rangle + 18 \langle \lambda_6 L_\mu \rangle \langle Q L^\mu \rangle + \\ & + \frac{5F^4}{18} G_{27}^{3/2} (\langle \lambda_1 L_\mu \rangle \langle \lambda_4 L^\mu \rangle + \langle \lambda_2 L_\mu \rangle \langle \lambda_5 L^\mu \rangle + \\ & + 2 \langle \lambda_6 L_\mu \rangle \langle \lambda_3 L^\mu \rangle) , \end{aligned} \quad (1.55b)$$

$$\mathcal{L}_{ew} = F^6 e^2 G_{ew} \langle \lambda_6 U^\dagger Q U \rangle , \quad (1.55c)$$

where  $L^\mu \doteq U^\dagger D^\mu U$  and  $G_{27} \equiv G_{27}^{3/2} = G_{27}^{1/2}$  in the isospin limit. If QCD was perturbative down to the hadronic scale, the low-energy constants  $G_8$ ,  $G_{27}$  and  $G_{ew}$  could be computed from the Wilson coefficients at that scale. However, the ChPT scale is too low for this to be possible. Instead, the low-energy constants are fixed from experiment, especially from  $K \rightarrow \pi\pi$  branching ratios, see e.g. Ref. [69]. The corresponding  $\mathcal{O}(p^4)$  Lagrangians are presented in Eqs.(B.16), (B.17) and (B.18) of App.B.3.2. These Lagrangians are not the most general ones but they are complete enough in the context of the present work.

Regarding radiative decays, if  $\mathcal{L}_8$ ,  $\mathcal{L}_{27}$ , or  $\mathcal{L}_{ew}$  contribute at three-level, it is only through bremsstrahlung amplitudes [70–72]. The dynamics is therefore trivial at  $\mathcal{O}(p^2)$  because Low’s theorem [73] shows that such emissions are entirely fixed in terms of the non-radiative amplitudes. Thus, the non-trivial dynamics corresponding to the low-energy tails of the photon penguins arise at  $\mathcal{O}(p^4)$ , where they are represented in terms of non-local meson loops, as well as additional  $\mathcal{O}(p^4)$  local effective interactions, which are detailed in App.B.3.2.

The set of interactions included within ChPT is complete, in the sense that all the possible effective interactions with the required symmetries are present at a given order. So, it may appear that at  $\mathcal{O}(p^4)$ , once the weak interactions in Eq.(1.55) are added to the strong dynamics of Eq.(1.46), and including the weak counter-terms presented in Eq.(B.16), (B.17) and (B.18), there is no more need to separately include the SD electromagnetic operators of Eq.(1.37). All their effects would be accounted for in the values of the low-energy constants. Indeed, these constants should sum up the physics taking place above the mesonic scale, i.e. the hadronic degrees of freedom just above the octet of pseudoscalar mesons [74, 75] as well as the quark and gluon degrees of freedom above the GeV scale [76, 77]. This actually holds for  $Q_{\gamma^*}^\pm$ , but not for  $Q_\gamma^\pm$ . Indeed, only the former have the same chiral structures as the weak counter-terms. Whenever  $Q_{\gamma^*}^\pm$  contribute, so do the weak counter-terms, but  $Q_\gamma^\pm$  can contribute to many modes where the weak counter-terms are absent (see Tab.2.1 in the next chapter). The  $Q_\gamma^\pm$  operators must therefore appear explicitly in the effective theory.

Before going through their hadronization, let us first notice that the mismatch between the effective weak Lagrangians of Eqs.(1.55) and  $Q_\gamma^\pm$  operators has an important dynamical implication since the weak counter-terms reflect the chiral structures of the meson loops built on the  $Q_{1,\dots,10}$  operators at  $\mathcal{O}(p^4)$ . While the meson loops can genuinely represent the low-energy tail of the virtual photon penguin, i.e. the  $\log(x_u)$  singularity of the  $D_0(x)$  function, they never match the chiral representation of  $Q_\gamma^\pm$ . The meson dynamics lacks the required  $m_{s,d}$  chirality flip at  $\mathcal{O}(p^4)$ , relying instead on the long-distance dynamics, i.e. momenta. One can understand this phenomenon as the low-energy equivalent of the known importance of the  $Q_2^s = (\bar{s}c)_{V-A} \otimes (\bar{c}b)_{V-A}$  contribution to  $b \rightarrow s\gamma$  [51–53]. Clearly,  $s \rightarrow d\gamma$  has to be even more affected than  $b \rightarrow s\gamma$  by QCD corrections since the photon is never hard ( $q_\gamma^2 < m_K^2$ ). So for  $s \rightarrow d\gamma$ , the  $Q_2^u = (\bar{s}u)_{V-A} \otimes (\bar{u}d)_{V-A}$  contribution, represented through  $Q_{1,\dots,10}$ , corresponds to a whole class of purely long-distance processes, often including IR divergent bremsstrahlung radiations. They are not suppressed at all, contrary to the naive expectation from  $D'_0(x) \rightarrow x$  as  $x \rightarrow 0$ , but instead dominate most of the

radiative processes<sup>4</sup>. Furthermore, the meson loops are always finite at  $\mathcal{O}(p^4)$ , except for  $K_1 \rightarrow \pi^+ \pi^- \pi^0 \gamma(\gamma)$  [70]. This means that not only the SD part of the magnetic operators decouples, but also to some extent the intermediate QCD degrees of freedom. By contrast, the weak counter-terms combinations occurring for the modes induced by  $Q_{\gamma^*}^\pm$  are always scale dependent, somewhat reminiscent of the factorization of the low-energy part of the virtual photon penguin. From these observations, we can reasonably expect that whenever a finite combination of weak counter-terms occurs for a process with only real photons, it should be significantly suppressed. Indeed, not only the divergences cancel among the weak counter-terms, but also the large  $Q_{\gamma^*}^\pm$  contribution embedded into them (this was already noted using large  $N_C$  arguments in Ref. [79]), as well as the resonance effects describing the purely strong structure of the photon. As our analysis of  $K^+ \rightarrow \pi^+ \pi^0 \gamma$  in Chapter 2 will show, this suppression is supported by the recent experimental data, see Eq. (2.9).

Let us now tackle the chiral realization of the tensor currents in  $Q_\gamma^\pm$  which starts at  $\mathcal{O}(p^4)$  since two derivatives are needed to get the correct Lorentz structure. Further, it cannot be entirely fixed but involves specific low-energy constants. By imposing charge conjugation and parity invariance (valid for QCD), the antisymmetry under  $\mu \leftrightarrow \nu$ , and the identity  $i\varepsilon^{\alpha\beta\mu\nu}\sigma_{\mu\nu} = 2\sigma^{\alpha\beta}\gamma_5$ , only two free real parameters  $a_T$  and  $a'_T$  remain (parts of these currents were given in Refs. [80, 81])

$$\begin{aligned} \bar{q}^J \sigma_{\mu\nu} \gamma_L q^J &= -i \frac{F^2}{2} a_T (D_\mu U^\dagger D_\nu U U^\dagger - D_\nu U^\dagger D_\mu U U^\dagger - \\ &\quad - i\varepsilon_{\mu\nu\rho\sigma} D^\rho U^\dagger D^\sigma U U^\dagger)^{JI} + \\ &\quad + \frac{F^2}{2} a'_T ((F_{\mu\nu}^L - i\tilde{F}_{\mu\nu}^L) U^\dagger + U^\dagger (F_{\mu\nu}^R - i\tilde{F}_{\mu\nu}^R))^{JI} , \end{aligned} \quad (1.56a)$$

$$\begin{aligned} \bar{q}^J \sigma_{\mu\nu} \gamma_R q^J &= -i \frac{F^2}{2} a_T (D_\mu U D_\nu U^\dagger U - D_\nu U D_\mu U^\dagger U + \\ &\quad + i\varepsilon_{\mu\nu\rho\sigma} D^\rho U D^\sigma U^\dagger U)^{JI} + \\ &\quad + \frac{F^2}{2} a'_T (U (F_{\mu\nu}^L + i\tilde{F}_{\mu\nu}^L) + (F_{\mu\nu}^R + i\tilde{F}_{\mu\nu}^R) U)^{JI} . \end{aligned} \quad (1.56b)$$

Numerically, we will use the lattice estimate [82]

$$B_T(2 \text{ GeV}) = 2m_K a_T = 1.21(12) . \quad (1.57)$$

Being derived from a study of the  $\langle \pi | \bar{s} \sigma_{\mu\nu} d | K \rangle$  matrix element,  $SU(3)$  corrections are under control. A similar estimate of  $B'_T = 2m_K a'_T$  is not available

<sup>4</sup>By comparison, though the Inami-Lim function  $C_0(x)$  for the  $Z$  penguin scale like  $D'_0(x)$  in the  $x \rightarrow 0$  limit, this behavior survives to QCD corrections, and the light-quark contributions are very suppressed, see Ref. [78].

yet. Instead, we can start from  $\langle \gamma | \bar{u} \sigma_{\mu\nu} \gamma_5 d | \pi^- \rangle$  and invoke the  $SU(3)$  symmetry. Ref. [83], through a study of the  $VT$  correlator, gets  $a'_T = B_0/M_V^2$  and thus  $B'_T = 2.7(5)$ , assuming the standard ChPT sign conventions for the matrix elements. Another route is to use the magnetic susceptibility of the vacuum,  $\langle 0 | \bar{q} \sigma_{\mu\nu} q | 0 \rangle_\gamma$ . From the lattice estimate in Ref. [84], we extract using  $a'_T = -\chi_T B_0/2$  the value  $B'_T(2 \text{ GeV}) = 2.67(17)$ . Both techniques give similar results though their respective scales do not match. In addition, sizeable  $SU(3)$  breaking effects cannot be ruled out since there is no Ademollo-Gatto protection for the tensor currents. So, to be conservative, we shall use

$$B'_T(2 \text{ GeV}) = 2m_K a'_T = 3(1). \quad (1.58)$$

At  $\mathcal{O}(p^4)$ , the magnetic operators contribute to decay modes with at most two photons. With the chiral suppression expected for higher order terms, decays with three or more (real or virtual) photons should have a negligible sensitivity to  $Q_\gamma^\pm$ , hence are not included in our study. Note finally that since in the SM the local operators sum up the short-distance part of the real photon penguins, the factor  $m_{s,d} \sim \mathcal{O}(p^2)$  in Eq.(1.39) are not included in the bosonization. Instead, they are kept as perturbative parameters in the Wilson coefficients  $C_\gamma^\pm$ , to be evaluated at the same scale as the form factors  $B_T$  and  $B'_T$ .

Let us conclude this chapter by summarizing the anatomy of the  $s \rightarrow d\gamma$  process in the SM and beyond by the Fig.(1.5).



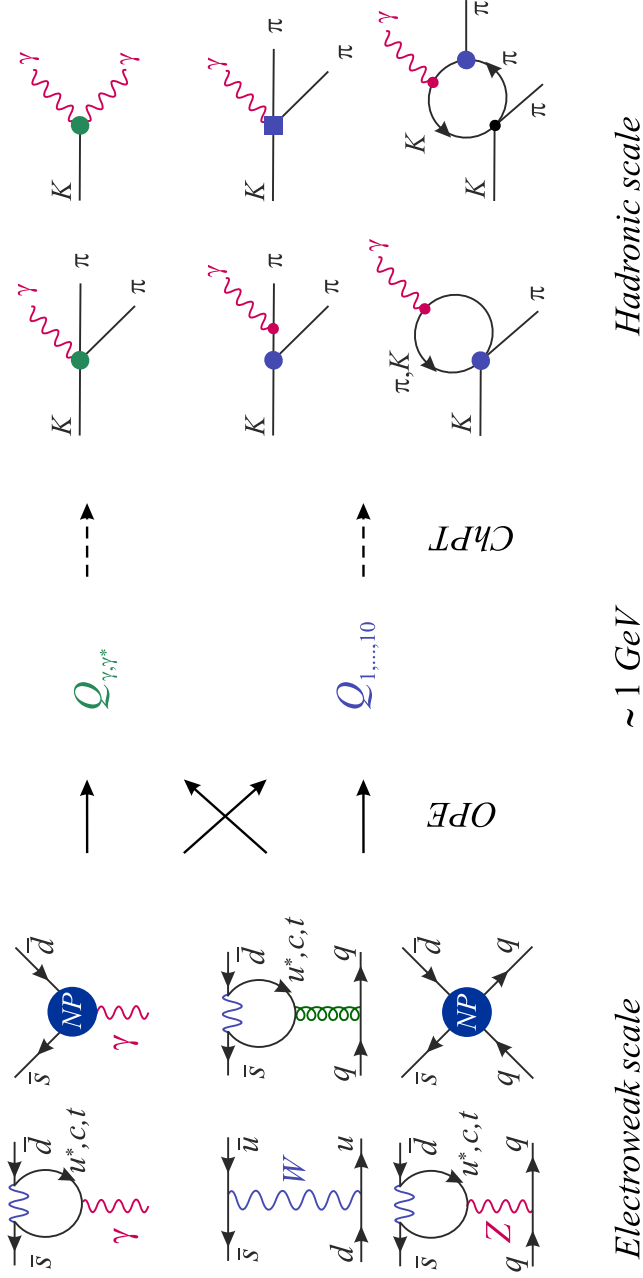


**Fig. 1.5:** Description of the radiative  $K$  decays, starting with the electroweak scale interactions down to chiral perturbation theory, with illustrative examples of mesonic processes (the photons can be real or virtual). The green vertices arise from the currents in Eqs.(1.51) and (1.56), the blue disks and square from the  $\mathcal{O}(p^2)$  weak Lagrangians Eq.(1.55) and  $\mathcal{O}(p^4)$  weak counter-terms Eqs.(B.16), (B.17) and (B.18), respectively, and finally, the strong (black) and QED (red) vertices from Eq.(1.46).



# Chapter 2

## $s \rightarrow d\gamma$ in the SM

From general considerations developed in chapter 1, the best windows to probe the  $s \rightarrow d\gamma$  decays are, in the present chapter, identified. These observables are then analyzed in details in the SM and beyond. Particular attention is paid to their sensitivity to short-distance effects and, thereby, to possible NP contributions. In the presence of NP, new mechanisms could produce the  $s \rightarrow d\gamma$  transition. Since the NP energy scale is presumably above the electroweak scale, these effects would simply enter into the Wilson coefficients of the same effective local operators (1.37). This is the shift we want to extract phenomenologically. In this respect, the magnetic operators are, a priori, most sensitive to NP for two reasons. Firstly, the electric transition is essentially left-handed and the magnetic operators are very suppressed in the SM because right-handed external quarks  $(s, d)_R$  are accompanied by the chiral suppression factor  $m_{s,d}$ . These strong suppressions may be lifted in the presence of NP, where larger chirality flip mechanisms can be available. Secondly, the magnetic operators are formally of dimension five and are thus, a priori, less suppressed by the NP energy scale than the dimension six electric operators. Sizeable NP effects could, therefore, show up, as will be quantitatively analyzed in chapter 3.

### 2.1 Phenomenological windows

The  $K$  decay channels where the electromagnetic operators contribute are listed in Tab.(2.1), together with their CP signatures. For the electric operators, at least one of the photons needs to be virtual, i.e. coupled to a Dalitz pair  $\ell^+\ell^-$ .

		$\perp$	$\parallel$	$-$
$K_2 \rightarrow \gamma\gamma$	$a'_T$	$\text{Re } C_\gamma^+$	$\text{Im } C_\gamma^-$	$-$
$K_2 \rightarrow \pi^0\gamma\gamma$	$a'_T$	$\text{Im } C_\gamma^-$	$\text{Re } C_\gamma^+$	$-$
$K^+ \rightarrow \pi^+\gamma\gamma$	$3a_T + a'_T$	$C_\gamma^-$	$C_\gamma^+$	$-$
$K_2 \rightarrow \pi^0\pi^0\gamma\gamma$	$a'_T$	$\text{Re } C_\gamma^+$	$\text{Im } C_\gamma^-$	$-$
$K_2 \rightarrow \pi^+\pi^-\gamma\gamma$	$a_T, a'_T$	$\text{Re } C_\gamma^+$	$\text{Im } C_\gamma^-$	$-$
$K^+ \rightarrow \pi^+\pi^0\gamma\gamma$	$a_T, a'_T$	$C_\gamma^+$	$C_\gamma^-$	$-$
$K_2 \rightarrow 3\pi^0\gamma\gamma$	$a'_T$	$\text{Im } C_\gamma^-$	$\text{Re } C_\gamma^+$	$-$
		$M$	$E$	$L$
$K_2 \rightarrow \pi^0\gamma$	$a_T$	$-$	$-$	$\text{Im } C_{\gamma^{(*)}}^+$
$K^+ \rightarrow \pi^+\gamma$	$a_T$	$-$	$-$	$C_{\gamma^{(*)}}^+$
$K_2 \rightarrow \pi^0\pi^0\gamma$	$a_T$	$-$	$-$	$\text{Re } C_{\gamma^{(*)}}^-$
$K_2 \rightarrow \pi^+\pi^-\gamma$	$a_T$	$\text{Re } C_\gamma^+$	$\text{Im } C_\gamma^-$	$\text{Re } C_{\gamma^{(*)}}^-$
$K^+ \rightarrow \pi^+\pi^0\gamma$	$a_T$	$C_\gamma^+$	$C_\gamma^-$	$C_{\gamma^{(*)}}^-$
$K_2 \rightarrow 3\pi^0\gamma$	$a_T$	$-$	$-$	$\text{Im } C_{\gamma^{(*)}}^+$

**Tab. 2.1:** Dominant processes where the electromagnetic operators contribute, omitting the  $K \rightarrow (n\pi)\gamma^*\gamma^{(*)}$ ,  $n \geq 0$  decays. The  $K_1 \simeq K_S$  processes are obtained from  $K_2 \simeq K_L$  by inverting real and imaginary parts. The symbol  $\perp$  ( $\parallel$ ) means the photon pair in an odd (even) parity state, i.e. a  $F_{\mu\nu}\tilde{F}^{\mu\nu}$  ( $F_{\mu\nu}F^{\mu\nu}$ ) coupling, and similarly,  $M$  ( $E$ ) means odd (even) parity magnetic (electric) emissions. For  $\pi\pi$  modes, the lowest multipole is understood (i.e.,  $\pi\pi$  in a  $S$  wave for  $\gamma\gamma$  modes, and a  $P$  wave for  $\gamma$  modes). The last column denotes longitudinal off-shell photon emissions, proportional to  $q^2 g^{\alpha\beta} - q^\alpha q^\beta$  with  $q$  the photon momentum, for which the  $Q_{\gamma^*}^\pm$  operators also enters. The  $K \rightarrow 3\pi\gamma(\gamma)$  decays with charged pions are not included since they are dominated by bremsstrahlung radiations off  $K \rightarrow 3\pi$  [70]. Finally,  $a_T$  and  $a'_T$  are the low-energy constants entering the tensor current (1.56).

In this respect, we note that all the electromagnetic operators produce the  $\ell^+\ell^-$  pair in the same  $1^{--}$  state, so the electric and magnetic operators can only be disentangled using real photon decays. For most of the decays in Tab.(2.1), the LD contributions are dominant, obscuring the SD parts where NP could be evidenced. The situation is, thus, very different from  $b \rightarrow s\gamma$ , where the  $u$  quark contribution is suppressed by  $V_{ub} \ll 1$ . However, in  $K$  physics, the long-distance contributions are essentially CP-conserving. Indeed, CP-violation from the four-quark operators is known to be small from  $\text{Re}(\varepsilon'/\varepsilon)_{\text{exp}}$ . In the SM, this follows from the CKM scalings  $\text{Re } \lambda_u \gg \text{Re } \lambda_t \sim \text{Im } \lambda_t$  and  $\text{Im } \lambda_u = 0$ . So, for CP-violating observables, one recovers a situation reminiscent of  $b \rightarrow s\gamma$ , with the dominant SM contributions arising from the charm

and top quarks, both of similar size a priori. Only for such observables can we hope that the interesting short-distance physics in  $Q_\gamma^\pm$  and  $Q_{\gamma^*}^\pm$  emerges from the long-distance SM background.

All the decays in Tab.(2.1) have a CP-conserving contribution and, thus, in most cases the best available CP-violating observables are CP-asymmetries. Since they arise from CP-odd interferences between the various decay mechanisms, the dominant CP-conserving processes must be under sufficiently good theoretical control. In addition, these CP-asymmetries being usually small, the decay rates should be sufficiently large and not completely dominated by bremsstrahlung radiations. Indeed, even though these radiations are under excellent theoretical control, thanks to Low's theorem [73], they would render the short-distance physics too difficult to access experimentally.

Imposing these conditions on the modes in Tab.(2.1), the best windows for the electromagnetic operators are:

- *Real photons:* Since the branching ratios decrease as the number of pions increases, the best candidates to constrain  $Q_\gamma^\pm$  are the  $K_{L,S} \rightarrow \gamma\gamma$  decays for two real photons and the  $K \rightarrow \pi\pi\gamma$  decays for a single real photon. All the other modes with real photons are either significantly more suppressed (see e.g. Refs. [71, 80] for a study of  $K \rightarrow \pi\gamma\gamma$ ), or dominated by bremsstrahlung contributions. By contrast, these radiations are suppressed for  $K_L \rightarrow \pi^+\pi^-\gamma$  since  $K_L \rightarrow \pi^+\pi^-$  is CP-violating, and for  $K^+ \rightarrow \pi^+\pi^0\gamma$  thanks to the  $\Delta I = 1/2$  rule. The relevant CP-violating asymmetries are either those between  $K_L - K_S$  decay amplitudes, or between  $K^+ - K^-$  differential decay rates or finally in some phase-space variables. This latter possibility usually requires some additional information on the photon polarization, accessible for example through Dalitz pairs. But, besides the significant suppression of the total rates, this brings in the electric operators, making the analysis much more involved, so these observables will not be considered here (see e.g. Refs. [85–88]).
- *Virtual photons:* The best candidates to probe the electric operators are the  $K_L \rightarrow \pi^0\ell^+\ell^-$  ( $\ell = e, \mu$ ) decays, for which  $K_L \rightarrow \pi^0\gamma^*[\rightarrow \ell^+\ell^-]$  is CP-violating and, hence, free of the up-quark contribution (see e.g. Ref. [89]). As detailed in Sec. 2.2.3 (see Fig.(2.4)), there are, nevertheless, an indirect CP-violating piece from the small  $\varepsilon K_2$  component of the  $K_L$  and a CP-conserving contribution from the four-quark operators with two intermediate photons. These contributions are, however, suppressed and under control [90,91]. The direct CP-asymmetry in  $K^\pm \rightarrow \pi^\pm\ell^+\ell^-$  is not competitive because of its small  $\sim 10^{-9}$  branching ratio and because of

the hadronic uncertainties affecting the long-distance contributions [54, 92]. With  $K_L \rightarrow \pi^0 \ell^+ \ell^-$  sensitive to  $Q_{\gamma^*}^+$ , information on  $Q_{\gamma^*}^-$  would also be needed to disentangle the left and right-handed currents. But since  $\langle \gamma | Q_{\gamma^*}^- | K^0(q) \rangle \sim q^\nu q^\mu F_{\mu\nu} = 0$ , and with  $K \rightarrow \pi \gamma^* \gamma$  sensitive again to  $Q_{\gamma^*}^+$ , the simplest observables are the  $K \rightarrow \pi \pi \gamma^*$  and  $K \rightarrow \pi \pi \gamma^* \gamma^{(*)}$  modes, which are suppressed and dominated by LD contributions. For the time being, we will, thus, only concentrate on  $Q_{\gamma^*}^+$ .

In summary, the best windows to probe for the electromagnetic operators are the CP-asymmetries in the  $K_{L,S} \rightarrow \gamma\gamma$ ,  $K_{L,S} \rightarrow \pi^+ \pi^- \gamma$ , and  $K^+ \rightarrow \pi^+ \pi^0 \gamma$  decays, and the  $K_L \rightarrow \pi^0 \ell^+ \ell^-$  decay rates. For completeness, it should be mentioned that the magnetic operators also contribute to radiative hyperon decays [93–95] or to the  $B_s \rightarrow B_d^* \gamma$  transition [96], which will not be analyzed here.

## 2.2 Standard Model predictions

In order to get clear signals of NP, the SM contributions have to be under good theoretical control. We rely on the available OPE analyses for the Wilson coefficients in the SM [38] and concentrate on the remaining long-distance parts of these contributions. For CP-violating observables, they originate either indirectly from the hadronic penguins  $Q_3 \rightarrow Q_{10}$  or directly from the magnetic operators  $Q_\gamma^\pm$ . Since the former indirect contributions are suppressed, while the  $C_\gamma^\pm$  are very small in the SM, both often end up being comparable. These LD contributions have to be estimated in ChPT. This is rather immediate for  $Q_\gamma^\pm$  given the hadronic representations (1.56), but significantly more involved for the hadronic penguins, requiring a detailed analysis of the meson dynamics relevant for each process. In addition, some free low-energy constants necessarily enter, which have to be fixed from other observables.

Thus, the goal of this section is threefold:

1. the observables relevant for the study of  $Q_\gamma^\pm$  are presented. This includes the  $K \rightarrow \pi \pi \gamma$  rate and CP-asymmetries, the  $K_{L,S} \rightarrow \gamma\gamma$  direct CP-violation parameters, the rare semileptonic decays  $K \rightarrow \pi \ell^+ \ell^-$ , and finally, the hadronic parameter  $\varepsilon'$ ,
2. the hadronic penguin contributions to the radiative decay observables are brought under control by relating them to well-measured parameters like  $\varepsilon'$ . In doing this, special care is paid to the possible impacts of NP in  $Q_3 \rightarrow Q_{10}$ , which have to be separately parametrized.

3. we extract the contributions from  $Q_\gamma^\pm$ , where NP could also be present, to establish the master formulas for all the observables relevant in the study of  $Q_\gamma^\pm$ , which will form the basis of the NP analysis of the next chapter.

### 2.2.1 $K \rightarrow \pi\pi\gamma$

Having a detailed calculation of the  $K \rightarrow \pi\pi\gamma$  decays, up to  $\mathcal{O}(p^4)$ , in App.C.3 we focus here on their physical consequences. These radiative decays are described by two terms,  $E(z_i)$  and  $M(z_i)$ , which are respectively the dimensionless electric and magnetic amplitudes [97]. Note that they do not interfere in the rate once summed over the photon polarizations. The reduced kinematical variables  $z_{1,2}$  are related to the energies of the two pions and  $z_3 = z_1 + z_2 = E_\gamma/m_K$  is the photon energy in the  $K$  rest-frame. The electric part can be further split into a bremsstrahlung and a direct emission term:

$$E(z_1, z_2) \doteq E_{IB}(z_1, z_2) + E_{DE}(z_1, z_2), \quad (2.1)$$

while the magnetic part is a pure direct emission,  $M \doteq M_{DE}$ . When the photon energy goes to zero, only  $E_{IB}$  is divergent and, according to Low's theorem [73], entirely fixed from the non-radiative process  $K \rightarrow \pi_1\pi_2$ , while the direct emission terms  $E_{DE}$  and  $M_{DE}$  are constant in that limit. In addition, they can be expanded in multipoles, according to the angular momentum of the two pions [98], see Appendix C.3 for more details.

#### $K^+ \rightarrow \pi^+\pi^0\gamma$

For the  $K^+ \rightarrow \pi^+\pi^0\gamma$  decay, the standard phase-space variables are chosen as the  $\pi^+$  kinetic energy  $T_c^*$  and  $W^2 \doteq (P_\gamma \cdot P_K)(P_\gamma \cdot P_{\pi^+})/m_{\pi^+}^2 m_K^2$  [98]. Pulling out the bremsstrahlung contribution, we can write the differential rate as

$$\begin{aligned} \frac{\partial^2 \Gamma}{\partial T_c^* \partial W^2} &= \frac{\partial^2 \Gamma_{IB}}{\partial T_c^* \partial W^2} \left( 1 - 2 \frac{m_{\pi^+}^2}{m_K} \operatorname{Re} \left( \frac{E_{DE}}{e A_{IB}} \right) W^2 + \right. \\ &\quad \left. + \frac{m_{\pi^+}^4}{m_K^2} \left( \left| \frac{E_{DE}}{e A_{IB}} \right|^2 + \left| \frac{M_{DE}}{e A_{IB}} \right|^2 \right) W^4 \right), \end{aligned} \quad (2.2)$$

where  $A_{IB} \doteq A(K^+ \rightarrow \pi^+\pi^0)$  is constant while  $E_{DE}$  and  $M_{DE}$  are functions of  $W^2$  and  $T_c^*$ . The main interest of  $K^+ \rightarrow \pi^+\pi^0\gamma$  is clearly apparent:  $A_{IB}$  is pure  $\Delta I = 3/2$  hence suppressed, making the direct emission amplitudes easier to access. Note that the strong phase of  $A_{IB}$  is that of the  $\pi\pi$  rescattering in

the  $I = 2, L = 0$  state, as confirmed by a full  $\mathcal{O}(p^4)$  computation. This is not trivial, a priori, since both Watson's and Low's theorem deal with asymptotic states. Actually, Low's theorem takes place after Watson's theorem, in agreement with the naive expectation from the relative strength of QED and strong interactions.

**Total and differential rates** Given its smallness, we can assume the absence of CP-violation when discussing these observables. Experimentally, the electric and magnetic amplitudes (taken as constant) have been fitted by NA48/2 [8] in the experimental phase-space (PS) range

$$\text{PS} \doteq T_c^* \leq 80 \text{ MeV} \cup 0.2 < W < 0.9 . \quad (2.3)$$

Using their parametrization, we have

$$X_E = \frac{-\text{Re}(E_{DE}/eA_{IB})}{m_K^3 \cos(\delta_1^1 - \delta_0^2)} = (-24 \pm 4 \pm 4) \text{ GeV}^{-4} , \quad (2.4a)$$

$$X_M = \frac{|M_{DE}/eA_{IB}|}{m_K^3} = (254 \pm 6 \pm 6) \text{ GeV}^{-4} , \quad (2.4b)$$

with  $\delta_J^I$  the strong  $\pi\pi$  rescattering phase in the isospin  $I$  and angular momentum  $J$  state. The magnetic amplitude is dominated by the QED anomaly and will not concern us here (see e.g. Refs. [99–102]). For the electric amplitude, we obtain at  $\mathcal{O}(p^4)$ :

$$X_E = \frac{3G_8/G_{27}}{40\pi^2 F_\pi^2 m_K^2} \frac{\cos(\delta_{DE} - \delta_0^2)}{\cos(\delta_1^1 - \delta_0^2)} \left[ E^{loop}(W^2, T_c^*) - \frac{m_K^2 \text{Re} \bar{N}}{m_K^2 - m_\pi^2} \right] , \quad (2.5)$$

with the expression of  $E^{loop}$  given in Eq.(C.70). The  $\bar{N}$  term, given for its part in Eq.(C.66), contains both weak counter-terms [103] and  $Q_\gamma^-$  contributions and reads

$$\text{Re} \bar{N} \doteq (4\pi)^2 \text{Re}(N_{14} - N_{15} - N_{16} - N_{17}) - \frac{2G_F}{3G_8} B_T \frac{\text{Re} C_\gamma^-}{G_F m_K} , \quad (2.6)$$

if 27-plet counter-terms are neglected or rather parametrically included into the  $N_i$ , together with higher order momentum-independent chiral corrections. To a good approximation, the loop contribution  $E^{loop}(W^2, T_c^*)$  is dominated by the leading multipole  $E_1^{loop}(z_3)$ , in which case  $\delta_{DE} = \delta_1^1$ . Note that  $E_1^{loop}(z_3)$  is still a function of the photon energy, hence, indirectly of  $W^2$  and  $T_c^*$ . In our computation of  $E_1^{loop}$ , we include both the  $\mathcal{L}_8$  and  $\mathcal{L}_{27}$  contributions. Indeed, as shown in Fig.(2.1), the large  $\pi\pi$  loop occurs only for the  $\Delta I = 3/2$  channel, making it competitive with the  $\Delta I = 1/2$  contributions arising entirely from the



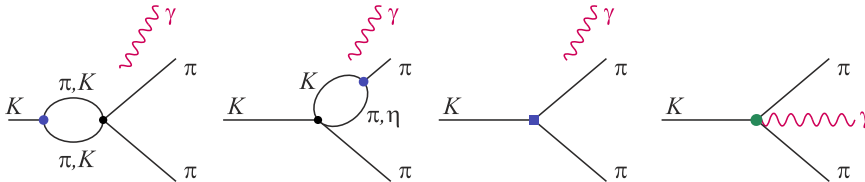


**Fig. 2.1:** Basic topologies for the  $K \rightarrow \pi\pi\gamma$  loops, with the vertices colored according to the conventions of Fig.(1.5). The photon is to be attached in all possible ways. However, in accordance with Low's theorem, most of these diagrams renormalize the  $\mathcal{O}(p^2)$  bremsstrahlung process, leaving only genuine subtracted three-point loops (thus involving at least one charged meson) for the direct emission amplitudes. The transition is  $\Delta I = 1/2$  ( $3/2$ ) when the weak vertex is  $K^+\pi^-\eta$  or  $K^0\pi^+\pi^-$  ( $K^+\pi^-\pi^0$ ). The counter-terms and  $Q_{\bar{\gamma}}$  contribute only to  $K^+ \rightarrow \pi^+\pi^0\gamma$  and  $K^0 \rightarrow \pi^+\pi^-\gamma$ .

small  $\pi K$  and  $\eta K$  loops. As a result, we find  $E_1^{loop}(0) = -0.25$ , to be compared to  $-0.16$  in Ref. [104]. In addition, the  $\pi\pi$  loop generates a significant slope. Though this momentum dependence is mild over the experimental PS, these cuts are far from the  $z_3 = 0$  point, resulting in a further enhancement. Indeed, over the experimental range (but not outside of it),  $E_1^{loop}$  is well described by

$$E_1^{loop}(W, T_c^*)_{\text{PS}} \simeq -0.260 - 0.051W + 0.089 \frac{T_c^*}{m_K}. \quad (2.7)$$

Since experimentally, no slope was included, we average  $E_1^{loop}$  over the experimental range (using the  $dT_c^*dW$  measure to match the binning procedure of Ref. [8]), and find

$$\left\langle E_1^{loop}(W, T_c^*) \right\rangle_{\text{PS}} = -0.280 \rightarrow X_E^{loop} = -17.6 \text{ GeV}^{-4}. \quad (2.8)$$

We checked that, in the presence of the slopes as predicted at  $\mathcal{O}(p^4)$ , the fitted values of  $X_E$  and  $X_M$  are not altered significantly.

Once  $E_1^{loop}$  is known, we can constrain the local term  $\bar{N}$  using the experimental measurement of  $X_E$ :

$$\text{Re } \bar{N} = 0.095 \pm 0.083. \quad (2.9)$$

This is much smaller than the  $\mathcal{O}(1)$  expected for the  $N_i$  on dimensional grounds or from factorization [103], but confirms the picture described in Sec. 2.1.3. Evidently, so long as the  $N_i$  are not better known, we cannot get an unambiguous

bound on  $\text{Re } C_\gamma^-$ . Still, barring a large fortuitous cancellation,

$$\frac{|\text{Re } C_\gamma^-|}{G_F m_K} \lesssim 0.1. \quad (2.10)$$

Note that this bound is rather close to our naive estimate (1.42) of the charm-quark contribution to the real photon penguin in the SM.

**Direct CP-violating asymmetries** CP-violation in  $K^+ \rightarrow \pi^+ \pi^0 \gamma$  is quantified by the parameter  $\varepsilon'_{+0\gamma}$ , defined from the interfering terms

$$\text{Re} \left( \frac{E_{DE}}{e A_{IB}} \right)_{K^\pm} \simeq \frac{\text{Re } E_{DE}}{e \text{Re } A_{IB}} [\cos(\delta_{DE} - \delta_0^2) \mp \sin(\delta_{DE} - \delta_0^2) \varepsilon'_{+0\gamma}], \quad (2.11)$$

as [69]

$$\varepsilon'_{+0\gamma} \doteq \frac{\text{Im } E_{DE}}{\text{Re } E_{DE}} - \frac{\text{Im } A_{IB}}{\text{Re } A_{IB}}. \quad (2.12)$$

To reach this form, we worked at the first order in  $\text{Im } A_{IB}/\text{Re } A_{IB}$  and used the fact that, contrary to the strong phase  $\delta_{DE}$  and  $\delta_0^2$ , both  $\text{Im } E_{DE}$  and  $\text{Im } A_{IB}$  change sign under CP. Since  $E_2$  has the same strong phase as  $A_{IB}$ , and higher multipoles are completely negligible, we can replace  $E_{DE}$  by the dipole emission  $E_1$  to an excellent approximation, so that  $\delta_{DE} = \delta_1^1$ .

Plugging Eq.(2.11) in Eq.(2.2), we get the differential asymmetry, which can be integrated over the phase-space according to various definitions. Still, no matter the choice, these phase-space integrations tend to strongly suppress the overall sensitivity to  $\varepsilon'_{+0\gamma}$  since the rate is dominantly CP-conserving [69]. For example, NA48/2 [8] use the partially integrated asymmetry

$$\begin{aligned} a_{CP}(W^2) &= \frac{\partial\Gamma^+/\partial W^2 - \partial\Gamma^-/\partial W^2}{\partial\Gamma^+/\partial W^2 + \partial\Gamma^-/\partial W^2} \\ &= \frac{-2m_{\pi^+}^2 m_K^2 X_E W^2 \sin(\delta_{DE} - \delta_0^2) \varepsilon'_{+0\gamma}}{1 + 2m_{\pi^+}^2 m_K^2 X_E W^2 + m_{\pi^+}^4 m_K^4 (|X_E|^2 + |X_M|^2) W^4}, \end{aligned} \quad (2.13)$$

where the dependences of  $X_E$  and  $X_M$  on  $T_c^*$  are dropped, which is a reasonable approximation within the considered phase-space. Combining the experimental values of  $X_E$  and  $X_M$  with  $\sin(\delta_1^1 - \delta_0^2) \simeq \sin(7^\circ) \simeq 0.12$ , taken from Refs. [8, 105], it turns out that  $a_{CP}(W^2) \lesssim 0.01 \varepsilon'_{+0\gamma}$  over the whole  $W^2$  range. Clearly, integrating over  $W^2$  to get the total rate charge asymmetry (or the induced direct CP-asymmetry in  $K^\pm \rightarrow \pi^\pm \pi^0$  [106]) would suppress the sensitivity even more. Because of this, the current bound is rather weak [8]

$$\sin(\delta_{DE} - \delta_2) \varepsilon'_{+0\gamma} = (-2.5 \pm 4.2) \times 10^{-2}. \quad (2.14)$$

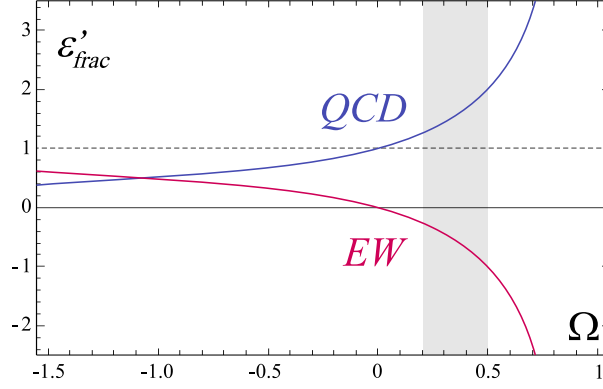


**Fig. 2.2:** Fractions of QCD and electroweak penguins in  $\varepsilon'$ . The absence of electroweak penguins corresponds to  $\Omega = 0$ . Destructive interference occurs for values between 0 and 1 (with a singularity at 1 since it corresponds to a complete cancellation between both types of penguins). Current analyses in the SM favor a limited destructive interference, i.e.  $\Omega \in [+0.2, +0.5]$  (see e.g. Refs. [33, 40, 107]).

Actually, thanks to the fact that  $X_E < 0$ , there is an alternative observable, which is not phase-space suppressed. Defining  $\partial^2\Gamma_{DE}^\pm = \partial^2\Gamma^\pm - \partial^2\Gamma_{IB}^\pm$ , and integrating over  $T_c^*$ , the direct emission differential rates  $\partial\Gamma_{DE}^+/\partial W^2$  and  $\partial\Gamma_{DE}^-/\partial W^2$  vanish at slightly different values of  $W^2$ , so we can construct the asymmetry,

$$a_{CP}^0 = \frac{W^2_{\partial\Gamma_{DE}^+/\partial W^2=0} - W^2_{\partial\Gamma_{DE}^-/\partial W^2=0}}{W^2_{\partial\Gamma_{DE}^+/\partial W^2=0} + W^2_{\partial\Gamma_{DE}^-/\partial W^2=0}} = -\tan(\delta_{DE} - \delta_2)\varepsilon'_{+0\gamma}. \quad (2.15)$$

The zeros are around  $W^2 \simeq 0.16$ , i.e. within the experimental range  $0.2 < W < 0.9$ . Of course, it remains to be seen whether the experimental precision needed to perform significant fits to the zeros of  $\partial\Gamma_{DE}^\pm/\partial W^2$  is not prohibitive.

Let us analyze the prediction for  $\varepsilon'_{+0\gamma}$  in the SM. At  $\mathcal{O}(p^4)$ , discarding (for now) the counter-terms and the electromagnetic operators, we obtain (see App.C.3)

$$\varepsilon'_{+0\gamma}(z_3) = \frac{\sqrt{2}|\varepsilon'|}{\omega} f(z_3, \Omega) \quad (2.16)$$

with

$$f(z_3, \Omega) = \frac{-1}{1 + \omega h_{20}(z_3)} - \frac{\Omega}{1 - \Omega} \frac{\omega \delta h_{20}(z_3)}{1 + \omega h_{20}(z_3)}, \quad (2.17)$$

where  $h_{20}(z_3) \doteq h_2(z_3)/h_0(z_3)$  is the ratio of the  $G_{27}$  and  $G_8$  loop functions, enhanced by the  $\pi\pi$  contributions to the former, while  $\delta h_{20}(z_3) \doteq \delta h_2(z_3)/h_0(z_3)$  is the ratio of the  $G_{ew}$  and  $G_8$  loop functions and is  $\mathcal{O}(1)$ . The parameter  $\Omega$ , defined in Eq.(1.24) represents the fraction of electroweak versus QCD penguins in  $\varepsilon'$ ,

$$\varepsilon' = \frac{e^{i\phi_{\varepsilon'}}}{\sqrt{2}} \xi_0 \omega (\Omega - 1). \quad (2.18)$$

As shown in Fig.(2.2), a conservative range is  $\Omega \in [-1, +0.8]$ . Values between  $[+0.2, +0.5]$  are favored by current analyses in the SM, but large NP cannot be ruled out. A crucial observation is that, contrary to  $\varepsilon'$ ,  $\varepsilon'_{+0\gamma}$  is rather insensitive to  $\Omega$ , because  $\omega \delta h_{20}(z_3)$  is suppressed by  $\omega$ , so that  $f(z_3, \Omega) \simeq -2/3$ . Varying  $\Omega$  in the large range  $[-1, +0.8]$ , as well as including the potential impact of the weak counter-terms, subject to the constraint Eq.(2.9), does not affect  $\varepsilon'_{+0\gamma}$  much. To get an estimate of the possible impact of higher order corrections affecting  $\varepsilon'_{+0\gamma}$ , let us include the counter-terms  $\bar{N}$  in Eq.(2.16), so that

$$\varepsilon'_{+0\gamma}(z) = \frac{\sqrt{2}|\varepsilon'|}{\omega} f(z, \Omega, \delta_N), \quad (2.19)$$

where

$$f(z, \Omega, \delta_N) = \frac{1 + \omega\Omega(h_{20}(z) + \delta h_{20}(z)) - \text{Im } \delta_N}{(\Omega - 1)(1 + \omega h_{20}(z) - \text{Re } \delta_N)} - \frac{1}{\Omega - 1} - 1, \quad (2.20)$$

with

$$\begin{aligned} \text{Re } \delta_N &= \frac{1}{h_0(z)} \frac{\sqrt{2}m_K^2}{m_K^2 - m_\pi^2} \text{Re } \bar{N}, \\ \text{Im } \delta_N &= \frac{\sqrt{2}}{h_0(z)} \frac{m_K^2}{m_K^2 - m_\pi^2} \xi_0^{-1} \text{Im } \bar{N}. \end{aligned} \quad (2.21)$$

Parametrically,  $\bar{N}$  accounts for all the  $\mathcal{O}(p^4)$  counter-terms, as well as for the momentum-independent parts of higher order effects. To proceed, some assumptions have to be made on its weak phase. From the experimental data, we know that  $\text{Re } \bar{N}$  is of the typical size expected for  $\mathcal{O}(p^6)$  corrections instead of  $\mathcal{O}(p^4)$ . Since both  $Q_6$  and  $Q_8$  contribute at  $\mathcal{O}(p^6)$  through two-loop graphs,  $\bar{N}$  receives, a priori, contributions from all the penguin operators, besides the current-current operators. On the other hand, the electromagnetic operators are too small to affect  $\text{Re } \bar{N}$ , allowing their impact to be pulled out and treated separately. So, inspired by the  $\mathcal{O}(p^4)$  loop result, we parametrically write:

$$\bar{N} = b((1 - a)A_0 + aA_2 + i\delta a \text{Im } A_2), \quad (2.22)$$

with  $b \sim \mathcal{O}(p^6)/\mathcal{O}(p^4)$ . Assuming the corrections parametrized in terms of  $A_0$  and  $A_2$  are of the same sign as at  $\mathcal{O}(p^4)$ , we take  $a \in [0, 1]$  to span from the pure QCD penguin to the pure electroweak penguin scenario, and  $a \approx (1 + \omega)^{-1} \approx 0.95$  if the  $\mathcal{O}(p^4)$  scaling between the  $G_8$  and  $G_{27}$  contributions survives at  $\mathcal{O}(p^6)$ . In a way similar to what happens at  $\mathcal{O}(p^4)$ , the parameter  $\delta a$  allows for additional  $Q_8$  contributions in the imaginary parts. Since at  $\mathcal{O}(p^4)$ , it emerges entirely from  $K \rightarrow \pi\eta$  and  $K \rightarrow KK$  vertices, and misses the  $K \rightarrow \pi\pi$  vertex and its associated loop, we expect  $\delta a \ll 1$ . With this,

$$\frac{\text{Im } \delta_N}{\text{Re } \delta_N} = \frac{(1 - a) + (a + \delta a)\omega\Omega}{(1 - a) + a\omega}. \quad (2.23)$$

By varying  $\Omega \in [-1, +0.8]$ ,  $a \in [0, 1]$ ,  $|\delta a| \leq 0.1$  and  $\text{Re } \bar{N}$  within  $1\sigma$  of the range (2.9), we get the final and conservative prediction

$$\varepsilon'_{+0\gamma}(Q_{3,\dots,10}) = -0.55(25) \times \frac{\sqrt{2}|\varepsilon'|}{\omega} = -0.64(31) \times 10^{-4}, \quad (2.24)$$

using  $\text{Re}(\varepsilon'/\varepsilon)_{\text{exp}} = (1.65 \pm 0.26) \times 10^{-3}$  [17]. The slight growth of  $\varepsilon'_{+0\gamma}$  with  $z_3$  is negligible compared to its error. Since it is based on the experimental value of  $|\varepsilon'|$ , and given the large range allowed for  $\Omega$ , this estimate is valid even in the presence of NP in the four-quark operators. This is the first example where the experimental information about  $\varepsilon'$  is extremely important!

The stability of this prediction actually means that even a precise measurement of  $\varepsilon'_{+0\gamma}$  would not help to understand the physical content of  $\varepsilon'$ , which would require measuring  $\Omega$ . However, it may help to unambiguously distinguish a contribution from  $Q_\gamma^-$ ,

$$\begin{aligned} \varepsilon'_{+0\gamma}(Q_\gamma^-) &= \frac{\text{Im } E_{DE}(Q_\gamma^-)}{\text{Re } E_{DE}} = \frac{B_T}{20\pi^2} \frac{G_F/G_{27}}{F_\pi^2(m_K^2 - m_\pi^2)X_E} \frac{\text{Im } C_\gamma^-}{G_F m_K} \\ &= +2.8(7) \frac{\text{Im } C_\gamma^-}{G_F m_K}, \end{aligned} \quad (2.25)$$

where we used the experimental determination of  $\text{Re } E_{DE}$  given in Eq.(2.4). So, the magnetic operator is competitive with the four-quark operators already in the SM as Eq.(1.41) implies that

$$\varepsilon'_{+0\gamma}(Q_\gamma^-)|_{\text{SM}} = +1.2(4) \times 10^{-4}. \quad (2.26)$$

Consequently, a significant cancellation occurs in the SM, which, by summing Eq.(2.24) and Eq.(2.26), translates into the following prediction

$$\varepsilon'_{+0\gamma}|_{\text{SM}} = 0.5(5) \times 10^{-4}. \quad (2.27)$$

This result is still far below the current bound on  $\varepsilon'_{+0\gamma}$  derived from Eq.(2.14), in such a way that it leaves ample room for NP effects, i.e.,

$$\frac{\text{Im } C_\gamma^-}{G_F m_K} = -0.08 \pm 0.13 . \quad (2.28)$$

$$K_L \rightarrow \pi^+ \pi^- \gamma$$

For this mode, the large  $\pi\pi$  loop is present in both the  $\Delta I = 1/2$  and  $\Delta I = 3/2$  channel, see Fig.(2.1). Therefore, including the latter does not change the picture for the total rate as, in the present case, the  $\Delta I = 1/2$  suppression is not dynamically compensated. On the other hand, the situation for the CP-violating parameter  $\bar{\varepsilon}'_{+-\gamma}$ , defined from [69]

$$\bar{\varepsilon}'_{+-\gamma} \doteq \eta_{+-\gamma} - \eta_{+-} , \quad (2.29)$$

where

$$\eta_{+-\gamma} \doteq \frac{A(K_L \rightarrow \pi^+ \pi^- \gamma)_{E_{IB}+E_1}}{A(K_S \rightarrow \pi^+ \pi^- \gamma)_{E_{IB}+E_1}} , \quad \eta_{+-} \doteq \frac{A(K_L \rightarrow \pi^+ \pi^-)}{A(K_S \rightarrow \pi^+ \pi^-)} , \quad (2.30)$$

is altered significantly. The restriction to the dipole terms originates in their dominance in the  $K_S$  decay. The parameter  $\eta_{+-\gamma}$  is then purely CP-violating since the  $K_L \rightarrow \pi^+ \pi^- \gamma$  dipole emissions violate CP. The direct dipole emission amplitudes  $E_1^{L,S}$  for  $K_{L,S} \rightarrow \pi^+ \pi^- \gamma$  are functions of the photon energy  $z_3$  only, and can be written as

$$E_1^S = \text{Re } E_{+-} , \quad E_1^L = i \text{Im } E_{+-} + \bar{\varepsilon} \text{Re } E_{+-} . \quad (2.31)$$

Parametrizing the CP-violating IB amplitude as  $E_{IB}^L = \eta_{+-} E_{IB}^S$ , including the strong phases but working to leading order in  $\omega$  and in the CP-violating quantities [69],

$$\bar{\varepsilon}'_{+-\gamma} = e^{i(\delta_1^+ - \delta_0^0)} \frac{m_K z_1 z_2}{e\sqrt{2}} \frac{\text{Re } E_{+-}}{\text{Re } A_0} \left( \varepsilon' + i \left( \frac{\text{Im } A_0}{\text{Re } A_0} - \frac{\text{Im } E_{+-}}{\text{Re } E_{+-}} \right) \right) . \quad (2.32)$$

As stated in Ref. [69],  $\bar{\varepsilon}'_{+-\gamma}$  is a measure of direct CP-violation. The  $z_1 z_2$  momentum dependence comes from the bremsstrahlung amplitude  $E_{IB}^S$ , which we write in terms of the  $K \rightarrow \pi\pi$  isospin amplitudes, using  $A(K_S \rightarrow \pi^+ \pi^-) = \sqrt{2}A_0 + A_2$ . Over the  $K^0 \rightarrow \pi^+ \pi^- \gamma$  phase-space,  $z_1 z_2$  is the largest when  $E_\gamma^*$  is at its maximum (and the bremsstrahlung at its minimum), but always strongly suppresses the asymmetry since  $z_1 z_2 \lesssim 0.030$ . Following Ref. [108], to avoid dragging this phase-space factor, we define the direct CP-violating parameter  $\varepsilon'_{+-\gamma}$

$$\varepsilon'_{+-\gamma} \doteq \frac{\bar{\varepsilon}'_{+-\gamma}}{z_1 z_2} = \frac{\eta_{+-\gamma} - \eta_{+-}}{z_1 z_2} . \quad (2.33)$$

Experimentally, this parameter has been studied indirectly through the time-dependence observed in the  $\pi^+\pi^-\gamma$  decay channel [109] (using material in the beam to regenerate  $K_S$  states), which is sensitive to the interference between the  $K_L \rightarrow \pi^+\pi^-\gamma$  and  $K_S \rightarrow \pi^+\pi^-\gamma$  decay amplitudes. Importantly, the experimental parameter  $\eta_{+-\gamma}$  used in Ref. [109] (also quoted by the PDG [17]) is not the same as the one in Eq.(2.29) but requires additional phase-space integrations. Following Ref. [108] in order to perform this integration, the experimental measurement  $\tilde{\eta}_{+-\gamma} = (2.35 \pm 0.07) \times 10^{-3}$  translates into

$$|\varepsilon'_{+-\gamma}| < 0.06 . \quad (2.34)$$

Theoretically, the  $E_{+-}$  amplitude can be predicted at  $\mathcal{O}(p^4)$  in ChPT, with the result (neglecting the counter-terms and electromagnetic operators for now)

$$\frac{\text{Im } E_{+-}}{\text{Re } E_{+-}} = \frac{\text{Im } A_0}{\text{Re } A_0} \frac{1 + \omega \Omega(h'_{20}(z_3) + \delta h'_{20}(z_3))}{1 + \omega h'_{20}(z_3)} , \quad (2.35)$$

where  $h'_{20}(z_3)$  and  $\delta h'_{20}(z_3)$  are ratios of loop functions (see Appendix C.3). Due to the fact that the  $\pi\pi$  loop is allowed in the  $\Delta I = 1/2$  channel,  $h'_{20}(z_3) \simeq 1/\sqrt{2} \ll \omega^{-1}$  while  $\delta h'_{20}(z_3)$  is tiny and can be safely neglected. Plugging this in  $\varepsilon'_{+-\gamma}$ , the sensitivity to  $\Omega$  disappears completely

$$\varepsilon'_{+-\gamma}(Q_{3,\dots,10}) = ie^{i(\delta_1^1 - \delta_0^0)} \frac{m_K}{e\sqrt{2}} \frac{\text{Re } E_{+-}}{\text{Re } A_0} |\varepsilon'| \left( e^{i(\delta_0^2 - \delta_0^0)} - 1 \right) . \quad (2.36)$$

As for  $\varepsilon'_{+0\gamma}$ , there is no possible way to learn something about  $\varepsilon'$  by measuring  $\varepsilon'_{+-\gamma}$ . Besides, note that  $\varepsilon'_{+-\gamma}$  is suppressed by the  $\Delta I = 1/2$  rule through its proportionality to  $|\varepsilon'|$ , contrary to  $\varepsilon'_{+0\gamma}$  in Eq.(2.24).

The same combination of counter-terms occur for  $K^0 \rightarrow \pi^+\pi^-\gamma$  and  $K^+ \rightarrow \pi^+\pi^0\gamma$ . The bound in Eq.(2.9) shows that this combination is of the same order of the  $\pi K$  and  $\eta K$  loops, which are much smaller than the  $\pi\pi$  loop, and it can, therefore, be safely neglected. As a result, we finally predict

$$\begin{aligned} \varepsilon'_{+-\gamma}(Q_{3,\dots,10}) &\simeq \frac{m_K^2}{(4\pi F_\pi)^2} h_0(z_3/2) \times |\varepsilon'| \times e^{-i\pi/3} \\ &= -1.5(5) \times 10^{-6} \times e^{-i\pi/3} , \end{aligned} \quad (2.37)$$

with  $h_0(z_3/2) \simeq -4\sqrt{2} \text{Re } h_{\pi\pi}(-z_3) \simeq -2.2$ ,  $\delta_0^2 - \delta_0^0 \simeq -45^\circ$ , and  $\delta_1^1 - \delta_0^2 \simeq 7^\circ$ . We conservatively added by hand a 30% error to account for the chiral corrections to the loop functions. This result is an order of magnitude below the bound derived in Ref. [69] because, having kept track of the  $G_8$ ,  $G_{27}$ , and  $G_{ew}$  contributions, we could prove that  $\varepsilon'_{+-\gamma}(Q_{3,\dots,10})$  is suppressed by the  $\Delta I = 1/2$  rule. As for  $\varepsilon'_{+0\gamma}$ , this estimate is valid even in the presence of NP

in the four-quark operators, since it is independent of  $\Omega$  and takes  $\text{Re}(\varepsilon'/\varepsilon)_{\text{exp}}$  as input.

With  $\varepsilon'_{+-\gamma}(Q_{3,\dots,10})$  extremely suppressed,  $\varepsilon'_{+-\gamma}$  becomes sensitive to the presence of the  $Q_{\gamma}^{-}$  operator, even in the SM. Its impact on  $E_{DE}^S$  is negligible given the bound (2.10) but  $E_{DE}^L$  receives an extra contribution, so that

$$\begin{aligned} \varepsilon'_{+-\gamma}(Q_{\gamma}^{-}) &= \frac{-G_F/G_8}{6(2\pi)^2} B_T \frac{m_K^4}{F_{\pi}^2(m_K^2 - m_{\pi}^2)} \frac{\text{Im} C_{\gamma}^{-}}{G_F m_K} e^{i\phi_{\gamma}} \\ &\simeq 0.2 \frac{\text{Im} C_{\gamma}^{-}}{G_F m_K} e^{i\phi_{\gamma}}, \end{aligned} \quad (2.38)$$

with  $\phi_{\gamma} \doteq \delta_1^1 - \delta_0^0 + \pi/2 \simeq 52^\circ$  and  $G_8 < 0$  in our conventions. With the SM value (1.41) for  $\text{Im} C_{\gamma}^{-}$ , this gives

$$\varepsilon'_{+-\gamma}(Q_{\gamma}^{-})_{\text{SM}} = +8(3) \times 10^{-6} \times e^{i\phi_{\gamma}}, \quad (2.39)$$

which is about five times larger than  $\varepsilon'_{+-\gamma}(Q_{3,\dots,10})$ , but still very small compared to  $\varepsilon'_{+0\gamma}$ . The current measurement (2.34) requires

$$\frac{|\text{Im} C_{\gamma}^{-}|}{G_F m_K} < 0.3, \quad (2.40)$$

which is slightly looser than the bound (2.28) obtained from the direct CP-asymmetry in  $K^+ \rightarrow \pi^+ \pi^0 \gamma$ .

## 2.2.2 $K_{L,S} \rightarrow \gamma\gamma$

CP-violating asymmetries for  $K \rightarrow \gamma\gamma$  can be defined through the parameters

$$\eta_{\gamma\gamma}^{\perp} = \frac{A(K_S \rightarrow (\gamma\gamma)_{\perp})}{A(K_L \rightarrow (\gamma\gamma)_{\perp})} = \varepsilon + \varepsilon'_{\perp}, \quad \eta_{\gamma\gamma}^{\parallel} = \frac{A(K_L \rightarrow (\gamma\gamma)_{\parallel})}{A(K_S \rightarrow (\gamma\gamma)_{\parallel})} = \varepsilon + \varepsilon'_{\parallel}, \quad (2.41)$$

if the conventions of Ref. [69] are adopted. Experimentally, these CP-violating parameters could be accessed through time-dependent interference experiments, i.e. with  $K^0$  or  $\bar{K}^0$  beams [110–112], so the photon polarization need not be measured using the suppressed decays with Dalitz pairs.

Let us parametrize the  $K^0 \rightarrow \gamma(k_1, \mu)\gamma(k_2, \nu)$  amplitudes as

$$A(K^0 \rightarrow (\gamma\gamma)_{\parallel}) = \frac{A_{\gamma\gamma}^{\parallel}}{\sqrt{2}} \times (\alpha_{em} G_F m_K) \times (k_1^{\nu} k_2^{\mu} - k_1 \cdot k_2 g^{\mu\nu}), \quad (2.42a)$$

$$A(K^0 \rightarrow (\gamma\gamma)_{\perp}) = \frac{A_{\gamma\gamma}^{\perp}}{\sqrt{2}} \times (\alpha_{em} G_F m_K) \times i\varepsilon^{\mu\nu\rho\sigma} k_{1,\rho} k_{2,\sigma}, \quad (2.42b)$$



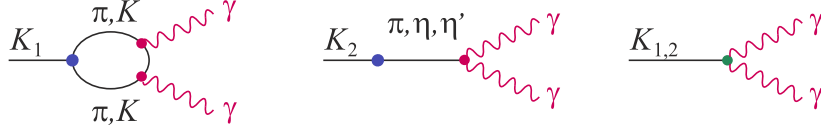


**Fig. 2.3:** The transition  $K \rightarrow \gamma\gamma$  in the SM, with the vertices colored according to the conventions of Fig.(1.5). The meson loop produces the  $\gamma\gamma_{\parallel}$  state, while the meson poles produce the  $\gamma\gamma_{\perp}$  state thanks to the QED anomaly. The direct  $Q_{\gamma}^{\pm}$  contributions produce both  $\gamma\gamma_{\parallel}$  and  $\gamma\gamma_{\perp}$  final states.

so that the direct CP-violating parameters are expressed as

$$\varepsilon'_{\parallel,\perp} = i \left( \frac{\text{Im } A_{\gamma\gamma}^{\parallel,\perp}}{\text{Re } A_{\gamma\gamma}^{\parallel,\perp}} - \frac{\text{Im } A_0}{\text{Re } A_0} \right). \quad (2.43)$$

We can fix  $|A_{\gamma\gamma}^{\parallel}| = 0.133(4)$  and  $|A_{\gamma\gamma}^{\perp}| = 0.0800(3)$  from the  $K_{L,S} \rightarrow \gamma\gamma$  decay rates [17], which are dominantly CP-conserving. In ChPT,  $A_{\gamma\gamma}^{\parallel}$  originates from a  $\pi^+\pi^-$  loop and  $A_{\gamma\gamma}^{\perp}$  is induced by the  $\pi^0$ ,  $\eta$ ,  $\eta'$  meson poles together with the QED anomaly, see Fig.(2.3) and Appendix C.3 for more details.

## Two-photon penguin contributions

In the absence of the electromagnetic operators,  $K^0 \rightarrow \gamma\gamma$  is induced by the two-photon penguin. The parameters  $\varepsilon'_{\parallel,\perp}$  are then generated indirectly by the  $Q_{3,\dots,10}$  contributions to the weak vertices in Fig.(2.3), and directly by the two photon penguins with  $c$  and  $t$  quarks (see Eq.(1.43)). However, as said in chapter 1, these short-distance contributions are suppressed by the quadratic decoupling of the heavy modes in the two-photon penguin loop [69]:

$$\frac{|\text{Re } A_{\gamma\gamma}^{\parallel,\perp}|_{c,t}}{|\text{Re } A_{\gamma\gamma}^{\parallel,\perp}|_u} < 10^{-4}, \quad (2.44)$$

which in turn implies

$$|\varepsilon'_{\parallel,\perp}|_{c,t} \simeq \frac{|\text{Im } A_{\gamma\gamma}^{\parallel,\perp}|_c}{|\text{Re } A_{\gamma\gamma}^{\parallel,\perp}|_u} < \frac{\text{Im } \lambda_c}{\text{Re } \lambda_c} \times 10^{-4} \simeq 10^{-7}. \quad (2.45)$$

This contribution will turn out to be negligible both for  $\varepsilon'_{\perp}$  and  $\varepsilon'_{\parallel}$ .

With regards to the long-distance contribution, let us start with  $\varepsilon'_{\parallel}$ . Since  $A_{\gamma\gamma}^{\parallel}$

is mainly<sup>1</sup> induced by a  $\pi\pi$  loop, CP-violation comes entirely from the  $K^0 \rightarrow \pi^+\pi^-$  vertex, as is obvious adopting a dispersive approach or using Eq.(C.26) in the safe limit where  $G_{ew} = 0$ . By using  $A(K_S \rightarrow \pi^+\pi^-) = \sqrt{2}A_0 + A_2$  (without strong phases), we recover the result of Ref. [113]

$$\varepsilon'_{||}(Q_{3,\dots,10}) = i \frac{\text{Im } A_0}{\text{Re } A_0} \left( \frac{\sqrt{2} + \omega\Omega}{\sqrt{2} + \omega} - 1 \right) = \frac{\varepsilon' e^{-i(\delta_0^2 - \delta_0^0)}}{1 + \omega/\sqrt{2}}. \quad (2.46)$$

As it is the case for  $\varepsilon'_{+0\gamma}$  and  $\varepsilon'_{+-\gamma}$ ,  $\varepsilon'_{||}$  is insensitive to  $\Omega$ , so this expression remains valid in the presence of NP. Also, being suppressed by the  $\Delta I = 1/2$  rule, the tiny value  $|\varepsilon'_{||}(Q_{3,\dots,10})| \simeq 4 \times 10^{-6}$  is obtained.

The situation is different for  $\varepsilon'_{\perp}$ . It was demonstrated in Ref. [114] that only the  $Q_1$  operator has the right structure to generate  $A_{\gamma\gamma}^{\perp}$  through the QED anomaly. Then,  $\text{Im } A_{\gamma\gamma}^{\perp} = 0$  since current-current operators are CP-conserving (proportional to  $\lambda_u$ ), leaving  $\varepsilon'_{\perp}$  as a pure and  $\Delta I = 1/2$  enhanced measure of the QCD penguins

$$\varepsilon'_{\perp}(Q_{3,\dots,10}) = -i\xi_0 = i \frac{\sqrt{2}|\varepsilon'|}{\omega(1 - \Omega)}. \quad (2.47)$$

One may be a bit puzzled by the appearance of  $\text{Im } A_0$  in this  $K \rightarrow \gamma\gamma$  observable. Actually, this originates from the very definition of  $\varepsilon$  in the  $K \rightarrow \pi\pi$  system. It is the choice made there to define a convention-independent physical parameter, which renders it implicitly dependent on  $K \rightarrow \pi\pi$  amplitudes. Besides, Eq.(2.47) is clearly only valid in the usual CKM phase-convention, contrary to Eq.(2.43), which is convention-independent. For example, if the Wu-Yang phase convention  $\text{Im } A_0 = 0$  is adopted [115], then  $\langle \gamma\gamma | Q_1 | K_L \rangle$  gets a non-zero weak phase, since  $\text{Im } \lambda_u \neq 0$ , while  $\varepsilon'_{\perp}$  stays the same.

Evidently, given the current information on the  $Q_6$  contribution to  $\varepsilon'$ , it is not possible to give a precise prediction for  $\varepsilon'_{\perp}$ . With  $\Omega \in [-1, +0.8]$ ,  $\varepsilon'_{\perp}$  spans an order of magnitude:

$$5 \times 10^{-5} < -i\varepsilon'_{\perp}(Q_{3,\dots,10}) < 7 \times 10^{-4}. \quad (2.48)$$

A value of a few  $10^{-4}$  is likely as  $\Omega \in [+0.2, +0.5]$  is favored in the SM, see Fig.(2.2).

This result is different from earlier estimates [113], obtained before the structure of the  $K_L \rightarrow \gamma\gamma$  amplitude was elucidated in Ref. [114]. Further, from that analysis, we do not expect that the residual  $Q_6$  contributions in  $K_2 \rightarrow \gamma\gamma$

<sup>1</sup>In fact, both  $\pi\pi$  and  $KK$  loops are present though the latter are suppressed by  $G_{ew}$ , see Eq.(C.26).

could alter Eq.(2.47), especially given its large  $\Delta I = 1/2$  enhanced value (2.48). Indeed, the origin of the vanishing of the  $K_2 \rightarrow \gamma\gamma$  amplitude at  $\mathcal{O}(p^4)$  is now understood as the inability of  $SU(3)$  ChPT to catch the  $Q_1$  contribution at leading order. But once accounted for, either through higher order counter-terms or by first working within  $U(3)$  ChPT, this  $Q_1$  contribution is seen to dominate the  $K_2 \rightarrow \gamma\gamma$  amplitude.

Though only ten times smaller than  $\varepsilon$ , measuring  $\varepsilon'_\perp$  would prove to be very challenging. Still, any information would be extremely rewarding: with its unique sensitivity to the QCD penguins, it could be used to finally resolve the physics content of  $\varepsilon'$ . Further, it would also help in estimating  $\varepsilon$  precisely, since the term  $i\xi_0$  enters directly  $\varepsilon'_\perp$  [40,116].

## Electromagnetic operator contributions

The magnetic operators  $Q_\gamma^\pm$  contribute to  $K \rightarrow \gamma\gamma$  as

$$A_{\gamma\gamma}^{\parallel,\perp} \rightarrow A_{\gamma\gamma}^{\parallel,\perp} + \frac{2F_\pi}{9\pi m_K} B'_T \frac{C_\gamma^{-,+}}{G_F m_K} . \quad (2.49)$$

Given the good agreement between theory and experiment for the  $K_{S,L} \rightarrow \gamma\gamma$  rate, we require that their contributions are less than 10% of the full amplitude, giving

$$\frac{|\operatorname{Re} C_\gamma^\pm|}{G_F m_K} \lesssim 0.3 . \quad (2.50)$$

The stronger bound (2.10) from  $K^+ \rightarrow \pi^+\pi^0\gamma$ , thus, shows that the impact of  $Q_\gamma^\pm$  on the total rates is negligible (assuming  $|\operatorname{Re} C_\gamma^+| \simeq |\operatorname{Re} C_\gamma^-|$ ).

Plugging Eq.(2.49) in Eq.(2.43), the  $Q_\gamma^\pm$  contribution to the direct CP-violation parameters are

$$|\varepsilon'_{\parallel}(Q_\gamma^-)| \simeq \frac{1}{3} \frac{|\operatorname{Im} C_\gamma^-|}{G_F m_K} , \quad |\varepsilon'_{\perp}(Q_\gamma^+)| \simeq \frac{1}{2} \frac{|\operatorname{Im} C_\gamma^+|}{G_F m_K} . \quad (2.51)$$

In the SM,  $|\varepsilon'_{\parallel}(Q_\gamma^-)| \simeq 1.4 \times 10^{-5}$  is nearly an order of magnitude larger than  $\varepsilon'_{\parallel}(Q_{3,\dots,10})$ , Eq.(2.46). On the contrary, the SM contribution  $|\varepsilon'_{\perp}(Q_\gamma^+)| \simeq 2 \times 10^{-5}$  is too small to compete with  $\varepsilon'_{\perp}(Q_{3,\dots,10})$ , Eq.(2.47). In the absence of a significant NP enhancement,  $\varepsilon'_\perp$ , thus, remains a pure measure of the QCD penguins.

### 2.2.3 Rare semileptonic decays

The  $K_L \rightarrow \pi^0 \ell^+ \ell^-$  decays are sensitive to several FCNC currents. In the SM, both the virtual and real photon penguins, as well as the  $Z$  penguins can contribute (together with their associated  $W$  boxes), see Fig.(2.4). Since NP could, a priori, affect all these FCNC in a coherent way, they have to be accounted for. Further, to separately constrain the  $Z$  penguins, we include the rare  $K \rightarrow \pi \nu \bar{\nu}$  decays in the analysis. So, in the present section, we collect the master formula for the  $K_L \rightarrow \pi^0 e^+ e^-$ ,  $K_L \rightarrow \pi^0 \mu^+ \mu^-$ ,  $K^+ \rightarrow \pi^+ \nu \bar{\nu}$  and  $K_L \rightarrow \pi^0 \nu \bar{\nu}$  decay rates, starting from the effective Hamiltonian

$$H_{\text{eff}} = -\frac{G_F \alpha_{em}}{\sqrt{2}} (C_{\nu,\ell} Q_{\nu,\ell} + C_{V,\ell} Q_{V,\ell} + C_{A,\ell} Q_{A,\ell}) + \text{h.c.}, \quad (2.52)$$

where

$$Q_{V,\ell} = \bar{s} \gamma^\mu d \otimes \bar{\ell} \gamma_\mu \ell, \quad (2.53a)$$

$$Q_{A,\ell} = \bar{s} \gamma^\mu d \otimes \bar{\ell} \gamma_\mu \gamma_5 \ell, \quad (2.53b)$$

$$Q_{\nu,\ell} = \bar{s} \gamma^\mu d \otimes \bar{\nu}_\ell \gamma_\mu (1 - \gamma_5) \nu_\ell, \quad (2.53c)$$

and where a sum over the leptonic flavors  $\ell = e, \mu, \tau$  is understood. As  $Q_{\gamma^*}^\pm$  are implicitly included in  $Q_{V,\ell}$ ,  $H_{\text{eff}}$  should be complemented by  $Q_\gamma^\pm$  operators only to account for radiative processes

#### Electric operators and SM predictions

Thanks to the excellent control on the vector currents (1.51), the branching ratios for  $K \rightarrow \pi \nu \bar{\nu}$  are very precisely predicted:

$$\text{Br}(K^+ \rightarrow \pi^+ \nu_\ell \bar{\nu}_\ell) = 0.1092(5) \cdot 10^{-11} \times r_{us}^2 \times |\omega_{\nu,\ell}|^2, \quad (2.54a)$$

$$\text{Br}(K_L \rightarrow \pi^0 \nu_\ell \bar{\nu}_\ell) = 0.471(3) \cdot 10^{-11} \times r_{us}^2 \times (\text{Im} \omega_{\nu,\ell})^2, \quad (2.54b)$$

with  $r_{us} = 0.225/|V_{us}|$  and  $\omega_{\nu,\ell} = C_{\nu,\ell}/10^{-4}$ . Since experimentally, the neutrino flavors are not detected, the  $K \rightarrow \pi \nu \bar{\nu}$  rate is the sum of the rates into  $\nu_{e,\mu,\tau}$ .

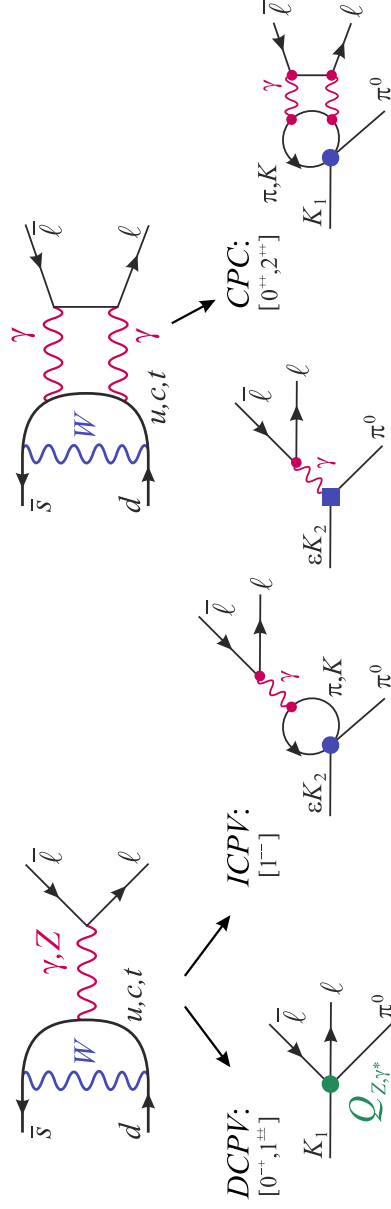


**Fig. 2.4:** The anatomy of the rare semileptonic decays, following the color coding defined in Fig.(1.5). For  $K \rightarrow \pi \nu \bar{\nu}$ , only the  $Z$  penguin contributes. For  $K_L \rightarrow \pi^0 \ell^+ \ell^-$ , in addition to the direct CP-violating contributions (DCPV) from the  $Z$  and  $\gamma^*$  penguins, the long-distance dominated indirect CP-violating contribution (ICPV) and the CP-conserving two-photon penguin contribution (CPC) also enter. The  $J^{PC}$  state of the lepton pair is indicated, showing that only the DCPV and ICPV processes can interfere in the  $1^{--}$  channel.

As shown in Fig.(2.4), the situation for  $K_L \rightarrow \pi^0 \ell^+ \ell^-$  is more complex because the indirect CP-violation  $K_L = \varepsilon K_1 \rightarrow \pi^0 \gamma^* [\rightarrow \ell^+ \ell^-]$  [54] and the CP-conserving contribution  $K_L \rightarrow \pi^0 \gamma \gamma [\rightarrow \ell^+ \ell^-]$  [90,91] have to be included:

$$\text{Br}(K_L \rightarrow \pi^0 \ell^+ \ell^-) = (C_{dir}^\ell r_{us}^2 + C_{int}^\ell \bar{a}_S r_{us} + C_{mix}^\ell \bar{a}_S^2 + C_{\gamma\gamma}^\ell) \cdot 10^{-12} \quad (2.55)$$

where

$$\begin{aligned} C_{dir}^e &= 2.355(13) (\omega_{V,e}^2 + \omega_{A,e}^2), & C_{dir}^\mu &= 0.553(3) \omega_{V,\mu}^2 + 1.266(12) \omega_{A,\mu}^2, \\ C_{int}^e &= 7.3(2) [-7.0(2)] \omega_{V,e}, & C_{int}^\mu &= 1.73(4) [-1.74(4)] \omega_{V,\mu}, \\ C_{mix}^e &= 12.2(4) [11.5(5)], & C_{mix}^\mu &= 2.81(6), \\ C_{\gamma\gamma}^e &\simeq 0, & C_{\gamma\gamma}^\mu &= 4.7(1.3), \end{aligned}$$

with  $\omega_{X,\ell} = \text{Im } C_{X,\ell} / 10^{-4}$ . These coefficients are sensitive to the  $K_S \rightarrow \pi \ell^+ \ell^-$  amplitude, which is entirely dominated by the virtual photon penguin:

$$A(K_1(P) \rightarrow \pi^0 \gamma^*(q)) = \frac{e G_F}{8\pi^2} W_S(z) (q^2 P^\mu - q^\mu P \cdot q), \quad (2.56)$$

with

$$W_S(z) = a_S + b_S z + W_S^{\pi\pi}(z), \quad (2.57)$$

where  $z = q^2/M_{K^0}^2$ . As detailed in Ref. [54], the only assumption behind the parametrization of the  $W_S(z)$  form-factor is that all the intermediate states other than  $\pi\pi$  are well described by a linear polynomial in  $z$  and, thus, can be absorbed in the unknown constants  $a_S$  and  $b_S$ . The  $\pi\pi$  loop function  $W_S^{\pi\pi}(z)$ , the only one to develop an imaginary part, was estimated including both the phenomenological  $K_S \rightarrow \pi^+ \pi^- \pi^0$  vertex (i.e., including slopes), and the physical  $\pi^+ \pi^- \rightarrow \gamma^*$  vertex (i.e., with its VMD behavior). Because  $K_S \rightarrow \pi^+ \pi^- \pi^0$  is dominantly CP-violating, and  $b_S$  is of higher order in the chiral expansion, the leading term  $a_S$  dominates.

Given the current error on the  $K_S \rightarrow \pi^0 \ell^+ \ell^-$  rates, setting  $b_S/a_S = 0.4$  and keeping only quadratic terms in  $a_S^2$ , give reasonable predictions for the  $K_L$  rates. However, in preparation for better measurements, we prefer to systematically account for the momentum dependence of the form-factor in extracting the coefficients of the master formula in Eq.(2.55). To this end, and contrary to previous parametrizations, it is not convenient to use  $a_S$  as the parameter entering Eq. (2.55), because this necessarily overlooks the other terms of  $W_S(z)$ . The alternative parameter  $\bar{a}_S$  entering Eq.(2.55) and defined in Ref. [9] is found to be given by  $\bar{a}_S = 1.25(22)$ .

Importantly, if there is some NP, it would enter through  $\omega_i$  only, all the rest is fixed from experimental data [89]. The theoretically disfavored case of destructive interference between the direct and indirect CP-violating contributions is indicated in square brackets [79,90].

In the SM, the QCD corrected Wilson coefficients  $\omega_{\nu,\ell}^{\text{SM}}$  are very precisely known. Though  $\omega_{\nu,\tau}^{\text{SM}}$  is slightly different than  $\omega_{\nu,e(\mu)}^{\text{SM}}$  owing to the large  $\tau$  mass, the standard phenomenological parametrization employs a unique coefficient,

$$\omega_{\nu}^{\text{SM}} = -\frac{\lambda_t X_t + \bar{\lambda}^4 \text{Re} \lambda_c (P_c + \delta P_{u,c})}{2\pi \sin^2 \theta_W \times 10^{-4}} = 4.84(22) - i1.359(96), \quad (2.58)$$

valid for  $\ell = e, \mu, \tau$ , with  $X_t = 1.465(16)$  [117],  $P_c = 0.372(15)$  [118–120],  $\delta P_{u,c} = 0.04(2)$  [78] (with  $\bar{\lambda} = 0.2255$ ). The difference  $\omega_{\nu,e(\mu)}^{\text{SM}} - \omega_{\nu,\tau}^{\text{SM}}$  is implicitly embedded into the definition of  $P_c$ , up to a negligible 0.2% effect [38]. With the CKM coefficients from Ref. [28], the rates in the SM are, thus,

$$\begin{aligned} \text{Br}(K^+ \rightarrow \pi^+ \nu \bar{\nu})^{\text{SM}} &= 8.25(64) \cdot 10^{-11}, \\ \text{Br}(K_L \rightarrow \pi^0 \nu \bar{\nu})^{\text{SM}} &= 2.60(37) \cdot 10^{-11}. \end{aligned} \quad (2.59)$$

For  $K_L \rightarrow \pi^0 \ell^+ \ell^-$ , the Wilson coefficients are  $\text{Im} C_i = \text{Im} \lambda_t y_i$  with  $y_{A,\ell}^{\text{SM}}(M_W) = -0.68(3)$  and  $y_{V,\ell}^{\text{SM}}(\mu \simeq 1 \text{ GeV}) = 0.73(4)$  [38]. Using again the CKM elements from Ref. [28] gives the rate

$$\text{Br}(K_L \rightarrow \pi^0 e^+ e^-)^{\text{SM}} = 3.23_{-0.79}^{+0.91} \cdot 10^{-11} [1.37_{-0.43}^{+0.55} \cdot 10^{-11}], \quad (2.60a)$$

$$\text{Br}(K_L \rightarrow \pi^0 \mu^+ \mu^-)^{\text{SM}} = 1.29_{-0.23}^{+0.24} \cdot 10^{-11} [0.86_{-0.17}^{+0.18} \cdot 10^{-11}]. \quad (2.60b)$$

The errors are currently dominated by that of  $\bar{a}_S$ . These predictions can be compared to the current experimental results

$$\begin{aligned} \text{Br}(K^+ \rightarrow \pi^+ \nu \bar{\nu})^{\text{exp}} &= 1.73_{-1.05}^{+1.15} \times 10^{-10} & [7], \\ \text{Br}(K_L \rightarrow \pi^0 \nu \bar{\nu})^{\text{exp}} &< 2.6 \times 10^{-8} & [121], \\ \text{Br}(K_L \rightarrow \pi^0 e^+ e^-)^{\text{exp}} &< 2.8 \times 10^{-10} & [122], \\ \text{Br}(K_L \rightarrow \pi^0 \mu^+ \mu^-)^{\text{exp}} &< 3.8 \times 10^{-10} & [123]. \end{aligned} \quad (2.61)$$

At 90% CL, this measurement of  $\text{Br}(K^+ \rightarrow \pi^+ \nu \bar{\nu})$  becomes an upper limit at  $3.35 \times 10^{-10}$  [7, 124]. Improvements are to be expected in the future, with J-Parc aiming at a hundred SM events for  $K_L \rightarrow \pi^0 \nu \bar{\nu}$ , and NA62 at a similar amount of  $K^+ \rightarrow \pi^+ \nu \bar{\nu}$  events. The  $K_L \rightarrow \pi^0 \ell^+ \ell^-$  modes are not yet included in the program of these experiments, but should be tackled in a second phase.

### Magnetic operators in $K^0 \rightarrow \pi^0 \ell^+ \ell^-$

Only the  $Q_{\gamma}^+$  operator occurs in the  $K^0 \rightarrow \pi^0 \ell^+ \ell^-$  decays:

$$A(K^0(P) \rightarrow \pi^0 \gamma^*(q))_{Q_{\gamma}^+} = -\frac{eG_F}{24\sqrt{2}\pi^2} B_T \frac{C_{\gamma}^+}{G_F m_K} (q^2 P^{\mu} - q^{\mu} P \cdot q). \quad (2.62)$$

For  $K_S \rightarrow \pi^0 \ell^+ \ell^-$ , this contribution is CP-conserving and parametrically included in  $a_S$  since it is fixed from experiment. If we require that there is no large cancellations, i.e. that the  $Q_\gamma^+$  operator accounts for, at most, half of  $|a_S| \simeq 1.2$ , we get [9]

$$\frac{|\operatorname{Re} C_\gamma^+|}{G_F m_K} \lesssim \frac{3|\bar{a}_S|}{2B_T} \simeq 1.5. \quad (2.63)$$

This bound is nearly an order of magnitude looser than the one derived from  $K_L \rightarrow \gamma\gamma$  in Eq.(2.50).

For  $K_L \rightarrow \pi^0 \ell^+ \ell^-$ , the whole effect of  $Q_\gamma^+$  is to shift the value of the vector current [89, 125]:

$$\omega_{V,\ell} \times 10^{-4} = \operatorname{Im} C_{V,\ell} + \frac{Q_d}{2\sqrt{2}\pi} \frac{B_T(0)}{f_+(0)} \frac{\operatorname{Im} C_\gamma^+}{G_F m_K} \simeq \operatorname{Im} C_{V,\ell} - \frac{1}{21.3} \frac{\operatorname{Im} C_\gamma^+}{G_F m_K}, \quad (2.64)$$

where we assume the slopes of  $B_T(z)$  and  $f_+(z)$  are both saturated by the same resonance (which is a valid first order approximation). The relative sign between the  $Q_\gamma^+$  and  $Q_{V,\ell}$  contributions agrees with Ref. [125].

In the SM,  $\operatorname{Im} C_{V,\ell} \simeq 0.99 \times 10^{-4}$  and  $|\operatorname{Im} C_\gamma^+|/G_F m_K \simeq 4 \times 10^{-5}$ , so the shift is negligible. However, in case there is some NP, it quickly becomes visible. In the absence of any other NP effects (which is a strong assumption, as we will see in the next chapter), the current experimental bounds (2.61) imply

$$K_L \rightarrow \pi^0 e^+ e^- \Rightarrow -0.018 < \frac{\operatorname{Im} C_\gamma^+}{G_F m_K} < +0.030, \quad (2.65a)$$

$$K_L \rightarrow \pi^0 \mu^+ \mu^- \Rightarrow -0.050 < \frac{\operatorname{Im} C_\gamma^+}{G_F m_K} < +0.063, \quad (2.65b)$$

at 90% confidence and treating all theory errors as Gaussian. This is about an order of magnitude tighter than the bound (2.28) on  $\operatorname{Im} C_\gamma^-$  derived from  $K^+ \rightarrow \pi^+ \pi^0 \gamma$ .

## 2.2.4 Virtual effects in $\varepsilon'/\varepsilon$

Up to now, the photon produced by the electromagnetic operators was either real or coupled to a Dalitz pair, but it could also couple to quarks. At the level of the OPE, such effects are dealt with as  $\mathcal{O}(\alpha_{em})$  mixing among the four-quark operators, and sum up at  $\mu \simeq 1$  GeV in the Wilson coefficients of Eq.(1.33). The non-perturbative tail of these mixings are computed as QED corrections to the matrix elements of the effective operators between hadron



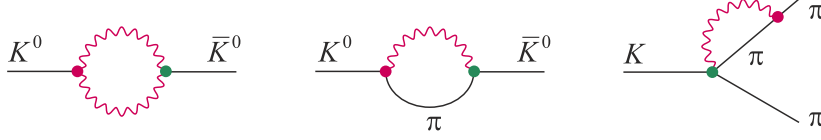


**Fig. 2.5:** The virtual effects from  $Q_\gamma^\pm$  on  $\Delta S = 2$  observables (reversed diagrams are understood) and on  $\varepsilon'$  from  $K^0 \rightarrow \pi^+\pi^-$ . Red vertices stand for the SM transitions (which are not necessarily local, see for example Fig.(2.3) ), while green vertices are induced by  $Q_\gamma^\pm$ .

states. Currently, only the left-handed electric operator (i.e., the virtual photon penguin) is included in the OPE [38] and in the  $K \rightarrow \pi\pi$  matrix elements and observables [50]. The magnetic operators are left aside given their strong suppression in the SM.

### Magnetic operators in hadronic observables

In the presence of NP, the magnetic operators could be much more enhanced than the electric operators, so their impact on hadronic observables must be quantified. Though, in principle, we should amend the whole OPE (i.e., initial conditions and running), we will instead compute only the low-energy part of these corrections. Indeed, the photon produced by  $Q_\gamma^\pm$  can be on-shell, so the dominant part of the mixing  $Q_\gamma^\pm \rightarrow Q_{1,\dots,10}$  is likely to arise at the matrix-element level. In any case, the missing SD contributions do not represent the main source of uncertainty. Indeed, the meson-photon loops induced by  $Q_\gamma^\pm$  are UV-divergent, requiring specific but unknown counter-terms. So, at best, the order of magnitude of the LD mixing effects can be estimated. To this end, the loops are computed in dimensional regularization and only the leading  $\log(\mu/m_\pi)$  or  $\log(\mu/m_K)$  is kept, with  $\mu \simeq m_\rho$ . Let us start with the impact of  $Q_\gamma^\pm$  on  $\varepsilon'$ . The third diagram of Fig.(2.5) induces a correction to  $\eta_{+-}$  (see Eq.(1.19a)) and, thereby, discarding strong phases for simplicity

$$\frac{|\text{Re}(\varepsilon'/\varepsilon)|_\gamma}{\text{Re}(\varepsilon'/\varepsilon)_{\text{exp}}} \simeq \frac{3\alpha_{em}}{256\pi^3} B_T \frac{G_F}{|G_8|} \frac{\log(m_\rho/m_\pi)}{|\varepsilon| \text{Re}(\varepsilon'/\varepsilon)_{\text{exp}}} \frac{|\text{Im} C_\gamma^-|}{G_F m_K} \simeq 2 \frac{|\text{Im} C_\gamma^-|}{G_F m_K}. \quad (2.66)$$

The photon loop is IR safe since  $Q_\gamma^-$  does not contribute to the bremsstrahlung amplitude in  $K^0 \rightarrow \pi^+\pi^-\gamma$ . Let us stress again that this is only an order of magnitude estimate. Besides the neglected SD mixings, unknown effects, of similar size than the contribution in Eq.(2.66), are necessarily present to absorb the divergence. Plugging in the bound on  $\text{Im} C_\gamma^-$  obtained from the measured

$K^+ \rightarrow \pi^+\pi^0\gamma$  direct CP-asymmetry, Eq.(2.28),

$$(\varepsilon'_{+0\gamma})^{\text{exp}} \Rightarrow \frac{|\text{Re}(\varepsilon'/\varepsilon)|_\gamma}{\text{Re}(\varepsilon'/\varepsilon)_{\text{exp}}} = (16 \pm 26)\% . \quad (2.67)$$

So, even in the presence of a large NP contribution to  $Q_\gamma^-$ , the impact on  $\varepsilon'$  remains smaller than its current theoretical error in the SM.

For completeness, let us also compute the contribution of the magnetic operators to the  $\Delta S = 2$  observables, for which perturbative QED corrections are significantly suppressed. At long distance, the magnetic operators contribute to  $\langle \bar{K}^0 | H_W | K^0 \rangle$  through the transitions  $K^0 \rightarrow \pi\gamma^* \rightarrow \bar{K}^0$  and  $K^0 \rightarrow \gamma\gamma \rightarrow \bar{K}^0$ , see Fig.(2.5). Neglecting the momentum dependences of the  $K \rightarrow \gamma\gamma$  and  $K \rightarrow \pi\gamma^*$  vertices and keeping only the leading  $\log(m_\rho/m_\pi)$ , we obtain

$$\mu_{12} \doteq \frac{\langle \bar{K}^0 | H_{\text{eff}}^\gamma | K^0 \rangle}{\Delta M_K^{\text{exp}}} = (a_{\gamma\gamma}^\perp + a_{\pi\gamma}) \frac{C_\gamma^+}{G_F m_K} + a_{\gamma\gamma}^\parallel \frac{C_\gamma^-}{G_F m_K} , \quad (2.68)$$

with (see Eq.(2.42) for the definition of  $A_{\gamma\gamma}^i$  and Eq.(2.57) for that of  $a_S$ )

$$|a_{\gamma\gamma}^i| \simeq \frac{\alpha_{em}^2}{72\pi^3} B_T' \frac{G_F^2 m_K^4 F_\pi}{\Delta M_K^{\text{exp}}} |A_{\gamma\gamma}^i| \log(m_\rho/m_K) \simeq 7 \times 10^{-6} |A_{\gamma\gamma}^i| , \quad (2.69a)$$

$$|a_{\pi\gamma}| \simeq \frac{\alpha_{em}}{512\pi^5} B_T |a_S| \frac{G_F^2 m_\pi^4 m_K}{\Delta M_K^{\text{exp}}} \log(m_\rho/m_\pi) \simeq 8 \times 10^{-7} . \quad (2.69b)$$

Even though they are not of the same order, it turns out that, numerically,  $a_{\pi\gamma} \simeq a_{\gamma\gamma}$ . This is due to the fact that a  $K^0 \rightarrow \pi^0\gamma^*$  vertex is absent at leading order, and because the momentum scale in the  $a_{\pi\gamma}$  loop is entirely set by the pion mass instead of the transferred momentum of  $\mathcal{O}(m_K)$ , as it is the case in  $a_{\gamma\gamma}$ . With such small values for  $a_{\gamma\gamma}$  and  $a_{\pi\gamma}$ , neither  $\Delta M_K(Q_\gamma^\pm) \sim \text{Re} \mu_{12}$  nor  $\varepsilon(Q_\gamma) \sim \text{Im} \mu_{12}$  can compete with the non-radiative  $\Delta S = 2$  processes, even in the presence of NP in  $Q_\gamma^\pm$ .

## Gluonic penguin operators

In complete analogy with the electromagnetic operators, gluonic FCNC are described by effective operators of dimensions greater than four. For instance, the chromomagnetic operators producing either a real or a virtual gluon are

$$\mathcal{H}_{eff}^\gamma = C_g^\pm Q_g^\pm + \text{h.c.} , \quad Q_g^\pm = \frac{g}{16\pi^2} (\bar{s}_L \sigma^{\alpha\beta} t^a d_R \pm \bar{s}_R \sigma^{\alpha\beta} t^a d_L) G_{\alpha\beta}^a . \quad (2.70)$$

The chromoelectric operators  $Q_{g^*}^\pm$ , whose form can easily be deduced from Eq.(1.38b), contribute only for a virtual gluon.

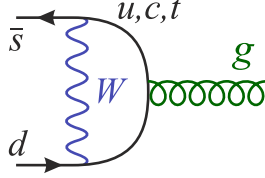


**Fig. 2.6:** The gluonic penguin in the SM.

In the SM, both  $Q_g^\pm$  and  $Q_\gamma^\pm$  arise from the diagram shown in Fig.(2.6). As for  $Q_\gamma^\pm$ , the former are suppressed by the light-quark chirality flips, hence, completely negligible, but the chromoelectric operators are sizeable and enter into the initial conditions for the four-quark operators [38]. They are, thus, hidden inside the weak low-energy constants, together with the hadronic virtual photon and  $Z$  penguins (see Fig.(1.5)).

The chromomagnetic operators are not included in the standard OPE, since they are negligible in the SM [55]. But, being of dimension-five, they could get significantly enhanced by NP. This would have two main effects. First, through the OPE mixing<sup>2</sup>,  $Q_g^\pm$  generate  $Q_\gamma^\pm$ . When both arise at a high-scale  $\mu_{NP} \gtrsim M_W$ , assuming only the SM colored particle content, neglecting the mixings with the four-quark operators, and working to LO [125]:

$$\begin{aligned} C_\gamma^\pm(\mu_c) &= \eta^2 [C_\gamma^\pm(\mu_{NP}) + 8(1 - \eta^{-1})C_g^\pm(\mu_{NP})] , \\ C_g^\pm(\mu_c) &= \eta C_g^\pm(\mu_{NP}) , \end{aligned} \quad (2.71)$$

where

$$\eta \doteq \eta(\mu_{NP}) = \left( \frac{\alpha_s(\mu_{NP})}{\alpha_s(m_t)} \right)^{2/21} \left( \frac{\alpha_s(m_t)}{\alpha_s(m_b)} \right)^{2/23} \left( \frac{\alpha_s(m_b)}{\alpha_s(\mu_c)} \right)^{2/25} . \quad (2.72)$$

Numerically,  $\eta(\mu) = 0.90, 0.89, 0.88$  for  $\mu = 0.1, 0.5, 1$  TeV, respectively. Indirectly, all the bounds on  $C_\gamma^\pm$  can, thus, be translated as bounds on  $C_g^\pm$ . However, there is another more direct impact of  $Q_g^\pm$  on phenomenology since it contributes to  $K \rightarrow \pi\pi$ , hence to  $\varepsilon'$  [125]

$$\text{Re}(\varepsilon'/\varepsilon)_g = \frac{11}{64\pi^2} \frac{\omega}{|\varepsilon| |\text{Re} A_0|} \frac{m_\pi^2 m_K^2}{F_\pi(m_s + m_d)} \eta B_G \text{Im} C_g^- \simeq 3B_G \frac{\text{Im} C_g^-}{G_F m_K} , \quad (2.73)$$

with, neglecting  $\Delta I = 3/2$  contributions,  $|\text{Re} A_0| = \sqrt{2} F_\pi (m_K^2 - m_\pi^2) |\text{Re} G_8|$  and  $F_\pi = 92.4$  MeV. The hadronic parameter  $B_G$  parametrizes the departure

<sup>2</sup>The  $Q_\gamma^\pm \rightarrow Q_g^\pm$  mixings are not included in Eq.(2.71), even though they become relevant if  $C_\gamma^\pm \gg C_g^\pm$ . However, such effects are presumably LD-dominated, and thus were already included in Eq.(2.66) together with  $Q_\gamma^\pm \rightarrow Q_{1,\dots,10}$ .

of  $\langle(\pi\pi)_0|Q_g^-|K^0\rangle$  from the chiral quark model, and presumably lies in the range  $1 \rightarrow 4$  [125]. Given that the SM prediction for  $\text{Re}(\varepsilon'/\varepsilon)$  is rather close to  $\text{Re}(\varepsilon'/\varepsilon)_{\text{exp}}$  [33], but its uncertainty is itself of the order of  $\text{Re}(\varepsilon'/\varepsilon)_{\text{exp}}$ , we simply impose that  $|\text{Re}(\varepsilon'/\varepsilon)_g| \leq \text{Re}(\varepsilon'/\varepsilon)_{\text{exp}}$ , which gives,

$$\frac{|\text{Im} C_g^-|}{G_F m_K} \lesssim 5 \times 10^{-4}. \quad (2.74)$$

For comparison, imposing that  $|\text{Re} A_0|_g$  is at most of the order of  $|\text{Re} A_0|^{\text{exp}}$  gives the much looser constraint  $|\text{Re} C_g^-|/G_F m_K \lesssim 10$ . Note, however, that the bound (2.74) is not to be taken too strictly. First, the  $B_G$  parameter is set to 1, but could be slightly smaller or bigger. Second,  $Q_g^\pm$  is not the only FCNC affecting  $\text{Re}(\varepsilon'/\varepsilon)$  (see Fig.(1.5)). This bound could get relaxed in the presence of NP in the other penguins. This will be analyzed in more detail in the next chapter.

## 2.3 Conclusions

In this chapter, the  $s \rightarrow d\gamma$  process has been thoroughly studied. The best phenomenological windows are the direct CP-violating parameters in radiative  $K$  decays for real photon emissions, and the rare  $K_L \rightarrow \pi^0 e^+ e^-$  and  $K_L \rightarrow \pi^0 \mu^+ \mu^-$  decays for the  $s \rightarrow d\gamma^*$  transition. For all these observables, a sufficiently good control over the purely long-distance SM contributions has to be achieved to access the short-distance physics, where NP effects could be competitive. So, in this chapter, the SM predictions were systematically reviewed, with the results:

1.  $K^+ \rightarrow \pi^+ \pi^0 \gamma$  We included the  $\Delta I = 3/2$  contributions, which were missing in the literature, and found that they enhance the loop amplitude by about 50%. As a result, the recent NA48 measurement [8] of the direct-emission electric amplitude can be well-reproduced without the inclusion of significant counterterm contributions. With regards to direct CP-violation, we identified an observable, Eq.(2.15), which is not phase-space suppressed and could, thus, help increase the experimental sensitivity to  $\varepsilon'_{+0\gamma}$ . Thanks to the improved experimental and theoretical analyses (using  $\varepsilon'$ ), the prediction for  $\varepsilon'_{+0\gamma}$  in the SM is under good control, though a large cancellation between the  $Q_{3,\dots,10}$  (four-quark operators, see Eq.(1.33)) and  $Q_{\bar{\gamma}}^-$  (magnetic operator, see Eq.(1.37)) contributions limits its overall precision,  $\varepsilon'_{+0\gamma} = 5(5) \times 10^{-5}$ .

2.  $\mathbf{K}^0 \rightarrow \pi^+\pi^-\gamma$  The inclusion of the  $\Delta I = 3/2$  contributions, together with the experimental extraction of the counter-terms from  $K^+ \rightarrow \pi^+\pi^0\gamma$ , permits to reach a good accuracy. Contrary to previous analyses, we found that the  $Q_{3,\dots,10}$  contribution to the direct CP-violating parameter  $\varepsilon'_{+-\gamma}$  is suppressed by the  $\Delta I = 1/2$  rule and negligible against that of  $Q_\gamma^-$ . Altogether, the very small value  $\varepsilon'_{+-\gamma} = 0.8(3) \times 10^{-5}$  is obtained in the SM.
3.  $\mathbf{K}^0 \rightarrow \gamma\gamma$  For the direct CP-violating parameter  $\varepsilon'_{||}$ , we confirmed the computation of Ref. [113] for the  $Q_{3,\dots,10}$  contribution. However, that of  $Q_\gamma^-$  was missing, and lead to a factor five enhancement to  $\varepsilon'_{||} \simeq 1.4 \times 10^{-5}$  in the SM. For the parameter  $\varepsilon'_\perp$ , the situation changes completely compared to Ref. [113]. Indeed, the anatomy of  $K_L \rightarrow \gamma\gamma$  has been clarified in Ref. [114], where the absence of QCD penguin contributions at leading order was proven. As a result, we got the striking prediction that  $\varepsilon'_\perp$  is a direct measure of these QCD penguins,  $\varepsilon'_\perp(Q_{3,\dots,10}) = -i\xi_0$ , while the  $Q_\gamma^+$  contribution is much smaller in the SM. So, this  $\Delta I = 1/2$ -enhanced observable could resolve the QCD versus electroweak penguin fraction in  $\varepsilon'$  (to which  $\varepsilon'_{+0\gamma}$ ,  $\varepsilon'_{+-\gamma}$ , and  $\varepsilon'_{||}$  have essentially no sensitivity), and could improve the theoretical prediction of  $\varepsilon$ .
4.  $\mathbf{Re}(\varepsilon'/\varepsilon)$  We have computed the long-distance part of the magnetic operator contribution to  $\varepsilon'$ , as well as to  $\Delta M_K$  and  $\varepsilon$ . While it is (as expected) negligible for the last two, it could, a priori, be sizeable for  $\varepsilon'$  if  $Q_\gamma^-$  is enhanced by NP. Even though this contribution cannot be predicted accurately, and the short-distance part is lacking, we proved that the recent NA48 bound [8] on  $\varepsilon'_{+0\gamma}$  ensures that it does not exceed about 30% of  $\text{Re}(\varepsilon'/\varepsilon)_{\text{exp}}$ , and, thus, for the time being, can be neglected.



# Chapter 3

## $s \rightarrow d\gamma$ beyond the SM

In most models of New Physics, new degrees of freedom and additional sources of flavor breaking offer alternative mechanisms to induce the FCNC transitions. The goal of the present chapter is to quantify the possible phenomenological impacts of NP in the dimension-five magnetic operators  $Q_\gamma^\pm$  of Eq.(1.37). As discussed in detail in the previous chapter, CP-conserving processes are fully dominated by the SM long-distance contributions. So, throughout this chapter, we concentrate exclusively on CP-violating observables, from which the short-distance physics can be more readily accessed along with possible signals of NP.

The cleanest observables to identify a large enhancement of  $Q_\gamma^\pm$  are the direct CP-asymmetries in  $K \rightarrow \pi\pi\gamma$  and  $K \rightarrow (\gamma\gamma)_{||}$ , which would then satisfy

$$\frac{1}{3}|\varepsilon'_{+0\gamma}(Q_\gamma^-)| \simeq 5|\varepsilon'_{+-\gamma}(Q_\gamma^-)| \simeq 3|\varepsilon'_{||}(Q_\gamma^-)| \simeq \frac{|\text{Im } C_\gamma^-|}{G_F m_K}. \quad (3.1)$$

Indeed, the contributions from the four-quark operators (QCD and electroweak penguins) are small and under control,

$$\frac{3\omega}{2\sqrt{2}}|\varepsilon'_{+0\gamma}(Q_{3,\dots,10})| \simeq \frac{5}{2}|\varepsilon'_{+-\gamma}(Q_{3,\dots,10})| \simeq |\varepsilon'_{||}(Q_{3,\dots,10})| \simeq |\varepsilon'|, \quad (3.2)$$

with  $\omega = 1/22.4$ . By using the experimental  $\varepsilon'$  value, these estimates are independent of the presence of NP in  $Q_{3,\dots,10}$ . On the other hand, the  $K_{S,L} \rightarrow (\gamma\gamma)_\perp$  asymmetry is very sensitive to  $\Omega$ , representing the ratio of the electroweak to the QCD penguin contributions in  $\varepsilon'$ :

$$\varepsilon'_\perp(Q_{3,\dots,10}) = -i\xi_0 = i\frac{\sqrt{2}|\varepsilon'|}{\omega(1-\Omega)}, \quad |\varepsilon'_\perp(Q_\gamma^+)| \simeq \frac{1}{2}\frac{|\text{Im } C_\gamma^+|}{G_F m_K}. \quad (3.3)$$

So, knowing the impact of  $Q_\gamma^+$ , the asymmetry  $\varepsilon'_\perp$  can be used to extract the otherwise inaccessible QCD penguin contributions to  $\varepsilon'$ .

The experimental information on these four asymmetries is, however, limited with only the loose bound (2.14) on  $\varepsilon'_{+0\gamma}$  and (2.34) on  $\varepsilon'_{+-\gamma}$  currently available. Therefore, to get some information on  $Q_\gamma^\pm$ , two routes will be explored.

First, we can use the  $K_L \rightarrow \pi^0 \ell^+ \ell^-$  decay rates, for which the experimental bounds are currently in the  $10^{-10}$  range. As shown in Fig.(3.1), these modes are rather sensitive to  $Q_\gamma^+$  once  $|\text{Im } C_\gamma^+|/G_F m_K$  is above a few  $10^{-3}$ . In the absence of any other source of NP, the experimental bounds (2.61) give

$$K_L \rightarrow \pi^0 e^+ e^- \Rightarrow -0.018 < \frac{\text{Im } C_\gamma^+}{G_F m_K} < +0.030, \quad (3.4a)$$

$$K_L \rightarrow \pi^0 \mu^+ \mu^- \Rightarrow -0.050 < \frac{\text{Im } C_\gamma^+}{G_F m_K} < +0.063. \quad (3.4b)$$

To compare with the direct CP-asymmetries (3.1), sensitive to  $Q_\gamma^-$ , we first need to study how NP could affect the relationship between  $Q_\gamma^+$  and  $Q_\gamma^-$ . If the SM relation  $C_\gamma^+ \simeq -C_\gamma^-$  survives, the direct CP-asymmetries could be relatively large, with for example  $-8\% < \varepsilon'_{+0\gamma} < 5\%$  from  $K_L \rightarrow \pi^0 e^+ e^-$ . Then, since NP can enter in  $K_L \rightarrow \pi^0 \ell^+ \ell^-$  through other FCNC, by affecting the electroweak penguins for example, we must also study their possible interferences with  $Q_\gamma^+$ , and quantify how broadly the bounds (3.4) could get relaxed.

A second route is to use  $\varepsilon'$ . Indeed, in many NP models, the magnetic operators  $Q_\gamma^\pm$  are accompanied by chromomagnetic operators  $Q_g^\pm$ , which contribute directly to  $\varepsilon'$ ,

$$\text{Re}(\varepsilon'/\varepsilon)_g \simeq 3B_G \frac{\text{Im } C_g^-}{G_F m_K}, \quad (3.5)$$

with  $B_G$  a hadronic bag parameter of  $\mathcal{O}(1)$ , a priori. If the Wilson coefficients of  $Q_\gamma^\pm$  and  $Q_g^\pm$  are similar, the current measurement  $\text{Re}(\varepsilon'/\varepsilon)_{\text{exp}}$  imposes strong constraints, and would naively imply that the direct CP-asymmetries in Eq.(3.1) are at most of  $\mathcal{O}(10^{-3})$ . However, not only the relationship between  $Q_g^\pm$  and  $Q_\gamma^\pm$  is model-dependent but, as for  $K_L \rightarrow \pi^0 \ell^+ \ell^-$ , many other FCNC enter in  $\varepsilon'$  and their possible correlations with  $Q_g^\pm$  must be analyzed.

The only way to relate the NP occurring in the various FCNC is to adopt a specific picture for the NP dynamics. Evidently, this cannot be done model-independently. Instead, the strategy will be to classify the models into broad classes and, within each class, to stay as model-independent as possible. In practice, these classes are in one-to-one correspondence with the choice of basis



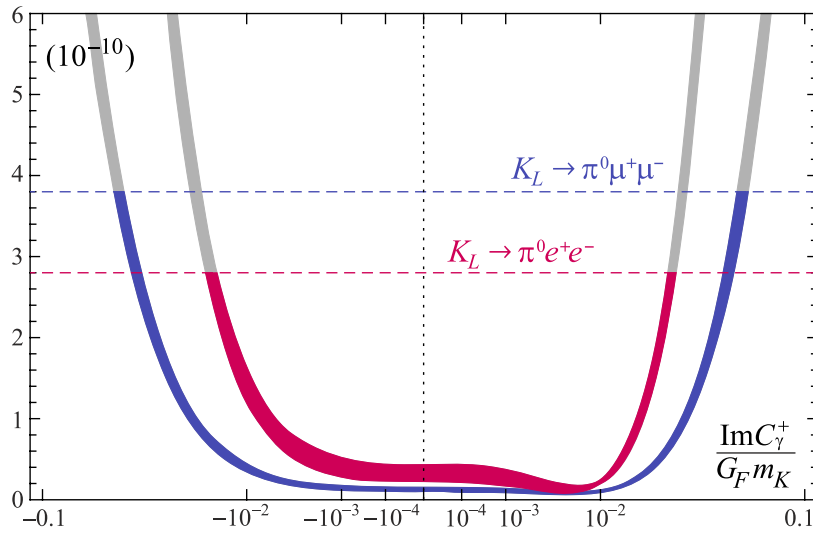


**Fig. 3.1:** The sensitivity of the  $K_L \rightarrow \pi^0 \ell^+ \ell^-$  decays to the magnetic penguin operator  $Q_\gamma^+$ , in the absence of any other source of NP. These curves are actually parabolas, but blown out to emphasize the small  $\text{Im} C_\gamma^+ / G_F m_K$  region (whose SM value is in the  $10^{-5}$  range). The horizontal lines signal the experimental bounds on  $K_L \rightarrow \pi^0 \ell^+ \ell^-$ . The contours stand for 90% confidence regions given the current theoretical errors in Eq.(2.55). Their apparent thinning as  $|\text{Im} C_\gamma^+|$  increases is purely optical, except just below  $10^{-2}$  where the  $Q_\gamma^+$  contribution precisely cancel out with the SM one in the vector current (positive DCPV–ICPV interference is assumed).

made for the effective semileptonic FCNC operators. Once a basis is chosen, bounds on the Wilson coefficients of these operators are derived by turning them on one at a time. In this way, fine-tunings between the chosen operators are explicitly ruled out. This is where the model-dependence enters [126]. On the other hand, the magnetic operators are kept on at all times, since it is precisely their interference with the semileptonic FCNC which we want to resolve. Note that the alternative procedure of performing a full scan over parameter space is (usually) basis independent, but we prefer to avoid that method as the many possible fine-tuning among the semileptonic operators would obscure those with the magnetic ones. Further, we will see that with our method, it is possible to get additional insight because the bounds do depend on the basis and, thus allow discrimination among the NP scenarios.

### 3.1 Model-independent analysis

The most model-independent operator basis is the one minimizing the interferences between the NP contributions in physical observables [126]. It is the one in Eq.(2.52), which we reproduce here for convenience:

$$\mathcal{H}_{\text{Pheno}} = -\frac{G_F \alpha_{em}}{\sqrt{2}} (C_{\nu,\ell} Q_{\nu,\ell} + C_{V,\ell} Q_{V,\ell} + C_{A,\ell} Q_{A,\ell}) + C_\gamma^\pm Q_\gamma^\pm + \text{h.c.} , \quad (3.6)$$

The four-fermion operators, defined in Eqs.(2.53), do not interfere in the rates since they produce different final states, while  $Q_\gamma^+$  and  $Q_\gamma^-$  have opposite CP-properties (see Tab.(2.1)). On the other hand,  $Q_\gamma^\pm$  and  $Q_{V,\ell} \ni Q_{\gamma^*}^\pm$  involve an intermediate photon, hence, necessarily interfere. Note that the coefficients in Eq.(3.6) are understood to be purely induced by the NP: the SM contributions have to be added separately.

Given the current data, the bounds on the CP-violating parts of the Wilson coefficients are

$K^+ \rightarrow \pi^+ \pi^0 \gamma$	$-160 < \rho \text{Im} C_\gamma^- < 80$	), (3.7)
$K_L \rightarrow \pi^0 e^+ e^-$	$-14 < \text{Im} C_{V,e} - \rho \text{Im} C_\gamma^+ < 8$ $\oplus$ $[-10 < \text{Im} C_{A,e} < 11 \wedge -8 < \rho \text{Im} C_\gamma^+ < 14]$	
$K_L \rightarrow \pi^0 \mu^+ \mu^-$	$-29 < \text{Im} C_{V,\mu} - \rho \text{Im} C_\gamma^+ < 24$ $\oplus$ $[-16 < \text{Im} C_{A,\mu} < 18 \wedge -24 < \rho \text{Im} C_\gamma^+ < 29]$	
$K^+ \rightarrow \pi^+ \nu \bar{\nu}$	$-14 < \text{Im} C_{\nu,\ell} < 17 \quad (\ell = e \oplus \mu \oplus \tau)$	

where all the numbers are in unit of  $10^{-4}$  and where  $\rho^{-1} \doteq 21.3G_F m_K$  from Eq.(2.64). The symbol  $\oplus$  stands for the exclusive alternative, since  $C_{A,\ell}$  and  $C_{V,\ell}$  are not turned on simultaneously for example, while  $\wedge$  means that the bounds are correlated, i.e. the coefficients fall within an elliptical contour in the corresponding plane. For comparison,  $\text{Im } C_{V,\ell}^{\text{SM}}$ ,  $\text{Im } C_{A,\ell}^{\text{SM}}$  and  $\text{Im } C_{\nu,\ell}^{\text{SM}}$  are all around  $10^{-4}$ . For the magnetic operators, the SM value in Eq.(1.41) implies  $\rho \text{Im } C_{\gamma}^{\pm,\text{SM}} \simeq \mp 0.015 \text{Im } \lambda_t \sim \mathcal{O}(10^{-6})$ .

For the neutrino modes, NP is separately turned on in each  $\text{Im } C_{\nu,\ell}$ ,  $\ell = e, \mu, \tau$ . Assuming leptonic universality would decrease the bound by about  $\sqrt{3}$  since all three  $C_{\nu,e} = C_{\nu,\mu} = C_{\nu,\tau}$  would simultaneously contribute. The direct bounds on  $\text{Im } C_{\nu,\ell}$  from  $K_L \rightarrow \pi^0 \nu \bar{\nu}$  are currently not competitive. The experimental bound on the  $K^+ \rightarrow \pi^+ \nu \bar{\nu}$  mode is, therefore, used setting  $\text{Re } C_{\nu,\ell} = 0$ . The maximal value for  $K_L \rightarrow \pi^0 \nu \bar{\nu}$  can then be predicted:

$$\text{Br}(K_L \rightarrow \pi^0 \nu \bar{\nu}) < 1.2 \times 10^{-9}, \quad (3.8)$$

which corresponds to a saturation of the Grossman-Nir Bound [127] (including the isospin breaking effects in the vector form-factor, but forbidding a destructive interference between the CP-conserving SM and NP contributions since  $\text{Re } C_{\nu,\ell} = 0$ ). This is more than an order of magnitude below the current experimental limit, but about 50 times larger than the SM prediction.

For  $K_L \rightarrow \pi^0 \ell^+ \ell^-$ , the bound on the vector current is less strict than on the axial-vector current because of the interference with the indirect CP-violating contribution. The theoretically favored case of positive DCPV-ICPV interference is assumed here as relaxing this assumption would not change the numbers much. Finally, the impact of  $Q_{\gamma}^-$  on  $\varepsilon'$  is neglected as it is estimated to be below 30% of its experimental value given the bound from  $K^+ \rightarrow \pi^+ \pi^0 \gamma$ , see Eq.(2.67).

To resolve the bound in the vector current and, thereby, disentangle  $C_{\gamma}^+$  and  $C_{V,\ell}$ , one is forced to specify at which level a destructive interference becomes a fine-tuning, see Fig.(3.2). This introduces some model-dependence since a specific NP model could generate  $Q_{\gamma}^{\pm}$  and  $Q_{V,\ell}$  (or  $Q_{\gamma^*}^{\pm}$ ) coherently. In this respect, it should be noted that the basis of four-fermion operators in Eq.(3.6) is not complete. It lacks the scalar, pseudoscalar, tensor and pseudotensor four-fermion operators. Naively, all these operators produce the lepton pair in different states and do not interfere in the rate [89]. Introducing large NP in any of them would, thus, render the bounds (3.7) weaker. There is, however, one exception. In  $K_L \rightarrow \pi^0 \ell^+ \ell^-$ , the tensor operators,

$$Q_{T,\ell} = \bar{s} \sigma^{\mu\nu} d \otimes \bar{\ell} \sigma_{\mu\nu} \ell, \quad (3.9)$$

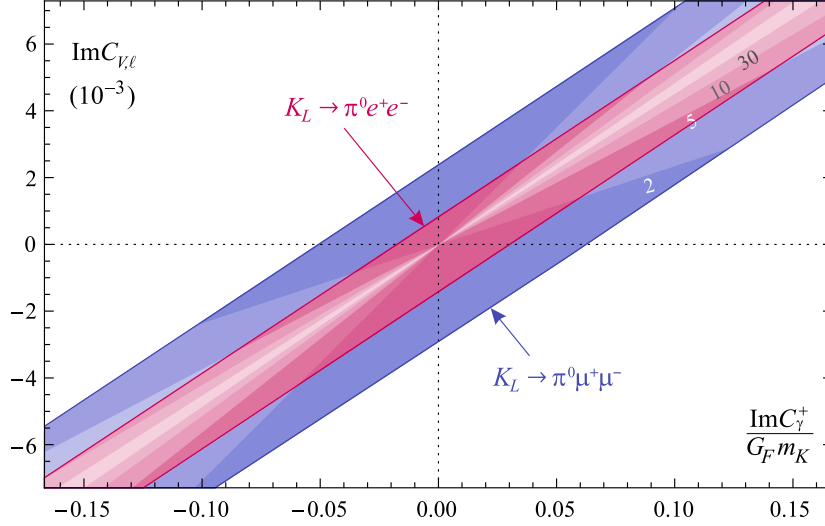


**Fig. 3.2:** The band in the  $\text{Im } C_{V,\ell} - \text{Im } C_\gamma^+$  plane allowed by the  $K_L \rightarrow \pi^0 \ell^+ \ell^-$  experimental bounds. The degree of fine-tuning is represented by the lighter areas, where  $|\text{Im } C_{V,\ell} - \rho \text{Im } C_\gamma^+| / |\rho \text{Im } C_\gamma^+| < 1/r$ ,  $r = 2, 5, 10, 30$ . Assuming  $\text{Im } C_\gamma^+ = -\text{Im } C_\gamma^-$ ,  $\varepsilon'_{+0\gamma}$  could, thus, reach its  $K^+ \rightarrow \pi^+ \pi^0 \gamma$  experimental bound for  $r \gtrsim 5$ .

do produce the leptons in the same  $1^{--}$  state as  $Q_{V,\ell}$  and  $Q_\gamma^+$  [89]. So, effectively,  $Q_{T,\ell}$  can be absorbed into  $Q_{V,\ell}$ . But then, owing to their similar structures, it is not impossible that  $Q_\gamma^\pm$  and  $Q_{T,\ell}$  are generated simultaneously and, thus, that  $Q_\gamma^\pm$  is tightly correlated to this effective  $Q_{V,\ell}$ .

In the next two sections, several NP scenarios are considered, in order to investigate under which circumstances the bounds on  $C_\gamma^+$  and  $C_{V,\ell}$  can be resolved. Of course, ultimately, better measurements of the direct CP-asymmetries are the cleanest option to get to  $C_\gamma^\pm$ . But before pushing for an experimental effort in that direction, it is essential to have a more precise idea of their maximal sizes under a large spectrum of NP scenarios.

### Hadronic current and Minimal Flavor Violation

The NP scenarios are organized into two broad classes according to the way the leptonic currents of the effective operators are parametrized. Before entering that discussion, let us first consider their hadronic parts, whose generic features transcend the various scenarios.

Only the vector current  $\bar{s}\gamma_\mu d$  enters in Eq.(3.6) because the axial-vector current  $\bar{s}\gamma_\mu\gamma_5 d$  drops out of the  $K \rightarrow \pi\nu\bar{\nu}$  and  $K_L \rightarrow \pi^0\ell^+\ell^-$  hadronic matrix elements. It would, therefore, be equivalent to replace  $\bar{s}\gamma_\mu d$  by the  $SU(2)_L \otimes U(1)_Y$  invariant forms  $\bar{Q}\gamma_\mu Q$  and  $\bar{D}\gamma_\mu D$ . By contrast, the magnetic operators require an extra Higgs doublet field to reach an  $SU(2)_L$  invariant form:

$$Q_\gamma^\pm \sim (\bar{Q}\sigma^{\mu\nu}D\Phi \pm \bar{D}\sigma^{\mu\nu}Q\Phi^*)F_{\mu\nu}. \quad (3.10)$$

After spontaneous electroweak symmetry breaking, this operator collapses to that in Eq.(1.38a). Consequently, if the NP respects the  $SU(2)_L \otimes U(1)_Y$  gauge symmetry,  $Q_\gamma^\pm$  and semileptonic operators are equally suppressed by the NP scale as they are all of dimension six. However, the magnetic operators are, a priori, much more sensitive to the electroweak symmetry breaking mechanism, so that the scaling between the two types of operators cannot be assessed model-independently. Its phenomenological extraction is, thus, important and could help discriminate among different models.

The effective operators in Eq.(3.6) induce the  $s \rightarrow d$  flavor transition, whilst the leptonic currents (or the photon) are flavor diagonal. Model-independently, the underlying gauge symmetry properties of an operator does not preclude anything about its flavor-breaking capabilities. However, the situation changes if we ask for the NP to have no more sources of flavor breaking than the SM. This is the Minimal Flavor Violation hypothesis [128–132]. For the operators at hand, it implies that the hadronic currents scale as

$$\begin{aligned} \bar{Q}^I\gamma_\mu(\mathbf{Y}_u\mathbf{Y}_u^\dagger)^{IJ}Q^J, \\ \bar{D}^I\gamma_\mu(\mathbf{Y}_d^\dagger\mathbf{Y}_u\mathbf{Y}_u^\dagger\mathbf{Y}_d)^{IJ}D^J, \\ \bar{Q}^I\sigma^{\mu\nu}(\mathbf{Y}_u\mathbf{Y}_u^\dagger\mathbf{Y}_d)^{IJ}D^J, \end{aligned} \quad (3.11)$$

with  $\mathbf{Y}_d = \sqrt{2}\mathbf{m}_d/v$ ,  $\mathbf{Y}_u = \sqrt{2}V^\dagger\mathbf{m}_u/v$ . The CKM matrix  $V$  is put in  $\mathbf{Y}_u$  so that the down-quark fields in the operators of Eq.(3.6) are mass eigenstates. Also, we limit the MFV expansions to the leading sources of flavor-breaking (i.e., minimal number of  $\mathbf{Y}_{u,d}$ ) for simplicity.

Under MFV, the NP operators acquire many SM-like properties. First,  $\bar{D}\gamma_\mu D$  is doubly suppressed by the light quark Yukawa couplings and is, thus, not competitive with  $\bar{Q}\gamma_\mu Q$ . Second, the chirality flip in  $\bar{Q}^I\sigma^{\mu\nu}D^J$  comes from the external light quark masses and are, thus, significantly suppressed. Finally, the  $s \rightarrow d$  transitions become correlated to the  $b \rightarrow d$  and  $b \rightarrow s$  transitions since

$$v^2(\mathbf{Y}_u^\dagger\mathbf{Y}_u)^{IJ} \simeq m_t^2 V_{3I}^* V_{3J}. \quad (3.12)$$

Of course, this correlation is not always strict as additional terms in the MFV expansion can be relevant. Still, it drives the overall scale of the observables in each sector.

We do not intend to perform a full MFV analysis here. Instead, our goal is to quantify, under the MFV ansatz, the maximal NP effects  $Q_\gamma^\pm$  could induce given the current situation in  $b \rightarrow s\gamma$ . From Eqs.(3.10), (3.11) and (3.12), discarding  $m_{s(d)}$  against  $m_{b(s)}$ , we get

$$Q_\gamma^\pm|_{d_R^I \rightarrow d_L^J} \sim C_{7\gamma}(\mu_{EW}) (\bar{Q}^J \sigma^{\mu\nu} (\mathbf{Y}_u \mathbf{Y}_u^\dagger \mathbf{Y}_d)^{JI} D^I) H F_{\mu\nu} \quad (3.13)$$

such that

$$\frac{Q_\gamma^\pm|_{s \rightarrow d}}{Q_\gamma^\pm|_{b \rightarrow s}} \sim \frac{V_{ts}^* V_{td} m_s}{V_{ts}^* V_{tb} m_b}. \quad (3.14)$$

The flavor-universality of the Wilson coefficient  $C_{7\gamma}(\mu_{EW})$  embodies the MFV hypothesis. The NP shift still allowed by  $b \rightarrow s\gamma$  is [133]

$$\delta C_{7\gamma}(\mu_{EW}) = [-0.14, 0.06] \cup [1.42, 1.62], \quad (3.15)$$

for constructive and destructive interference with the SM contributions. The latter has a lower probability and would require significant cancellations among the NP effects in  $B \rightarrow X_s \ell^+ \ell^-$ . From Eq.(1.41), and including the LO QCD reduction [38], such a shift can be written in our conventions as

$$\frac{\text{Im } C_\gamma^\pm|_{\text{MFV}}}{G_F m_K} - \frac{\text{Im } C_\gamma^\pm|_{\text{SM}}}{G_F m_K} \simeq \pm \frac{2}{3} \text{Im } \lambda_t \delta C_{7\gamma}(\mu_{EW}). \quad (3.16)$$

For comparison, the SM prediction is  $\mp 0.31(8) \times \text{Im } \lambda_t$ . So, there would be no visible effects for  $\delta C_{7\gamma}(\mu_{EW}) \in [-0.14, 0.06]$  and at most a factor four enhancement for  $\delta C_{7\gamma}(\mu_{EW}) \in [1.42, 1.62]$ .

This is hardly sufficient to push any of the asymmetries within the experimentally accessible range, while the impact on  $K_L \rightarrow \pi^0 \ell^+ \ell^-$  would be buried in the theoretical errors, see Fig.(3.1). However, it is well-known that MFV is particularly effective for  $K$  physics since it suppresses the NP contributions by the small  $V_{ts}^* V_{td} \sim 10^{-4}$ . This is proved to be the best place to test MFV as a deviation with respect to the strict ansatz (3.14) could lead to visible effects.

## 3.2 Tree-level FCNC

The basis of operators in Eq.(3.6) maximally breaks the  $SU(2)_L \otimes U(1)_Y$  symmetry. Neutrinos are completely decoupled from the charged leptons, and the vector and axial-vector operators (as well as  $Q_\gamma^+$  and  $Q_\gamma^-$ ) maximally mix currents of opposite chiralities. To be specific, the  $SU(2)_L \otimes U(1)_Y$  invariant

basis [134] is, after projecting the hadronic currents of semileptonic operators on their vector components,

$$\mathcal{H}_{\text{Gauge}} = -\frac{G_F \alpha_{em}}{\sqrt{2}} (C_{L,\ell} Q_{L,\ell} + C'_{L,\ell} Q'_{L,\ell} + C_{R,\ell} Q_{R,\ell}) + C_{\gamma}^{L,R} Q_{\gamma}^{L,R} + \text{h.c.}, \quad (3.17)$$

where

$$\begin{aligned} Q_L &\doteq \bar{s}\gamma^\mu d \otimes \bar{L}\gamma_\mu L, \quad Q'_L \doteq \bar{s}\gamma^\mu d \otimes \bar{L}\gamma_\mu \sigma^3 L, \quad Q_R \doteq \bar{s}\gamma^\mu d \otimes \bar{E}\gamma_\mu E, \\ Q_{\gamma}^L &= \frac{Q_{de}}{16\pi^2 v} \bar{s}_R \sigma^{\mu\nu} d_L \Phi^* F_{\mu\nu}, \\ Q_{\gamma}^R &= \frac{Q_{de}}{16\pi^2 v} \bar{s}_L \sigma^{\mu\nu} d_R \Phi F_{\mu\nu}, \end{aligned}$$

and where a sum over the leptonic chiral multiplet flavors  $\ell = e, \mu, \tau$  is understood. It is related to the phenomenological basis (3.6) through the transformations

$$\begin{aligned} \begin{pmatrix} C_{\nu,\ell} \\ C_{V,\ell} \\ C_{A,\ell} \end{pmatrix} &= \frac{1}{2} \begin{pmatrix} 1 & 1 & 0 \\ 1 & -1 & 1 \\ -1 & 1 & 1 \end{pmatrix} \begin{pmatrix} C_{L,\ell} \\ C'_{L,\ell} \\ C_{R,\ell} \end{pmatrix}, \\ \begin{pmatrix} C_{\gamma}^- \\ C_{\gamma}^+ \end{pmatrix} &= \frac{1}{2} \begin{pmatrix} 1 & -1 \\ 1 & 1 \end{pmatrix} \begin{pmatrix} C_{\gamma}^R \\ C_{\gamma}^L \end{pmatrix}, \end{aligned} \quad (3.18)$$

for each  $\ell = e, \mu, \tau$ . As in Eq.(3.6), the SM contributions are not encoded into  $\mathcal{H}_{\text{Gauge}}$  and have to be added separately.

The  $\mathcal{H}_{\text{Gauge}}$  basis represents a class of models where the four-fermion effective operators arise entirely from some high-scale  $SU(2)_L \otimes U(1)_Y$  invariant tree-level interactions. It is characterized by the correlations it imposes among the phenomenologically non interfering operators in  $\mathcal{H}_{\text{Pheno}}$ . A well-known example of model within this class is the MSSM with R-parity violating couplings [135–138], but more generic leptoquark models are also of this form [139]. Note that in these two cases, the  $Q_{\gamma}^{R,L}$  operators, nevertheless, arise only at the loop level since both the photon and the Higgs (see Eq.(3.10)) have flavor-diagonal couplings at tree-level.

The  $\mathcal{H}_{\text{Gauge}}$  basis completely decouples the three leptonic flavors. This is adequate because generic leptoquark couplings do not respect leptonic universality. Actually, one would expect that lepton-flavor violating (LFV) operators should arise, inducing in particular  $K \rightarrow (\pi)e\mu$ , which corresponds to an  $s + \mu \rightarrow d + e$  transition. Those modes are very constrained experimentally, with bounds often lower than for lepton-flavor conserving (LFC) modes. So, if LFV and

LFC couplings have similar sizes, there can be no large effects in the LFC modes. However, to relate the LFC and LFV couplings is far from immediate and requires some additional inputs on the dynamics (see e.g. Refs. [140–142] for studies within MFV). In the present work, we, therefore, concentrate exclusively on LFC decay channels. Still, let us emphasize again that leptonic universality is not expected to hold in the present scenario.

Adopting the  $SU(2)_L \otimes U(1)_Y$  invariant basis, the Wilson coefficients of the semileptonic operators in Eq.(3.17) are turned on one at a time while either  $C_\gamma^L$  or  $C_\gamma^R$  is kept on. The bounds are then completely resolved and rather strict:

$K_L \rightarrow \pi^0 e^+ e^-$	$ \begin{aligned} & -\text{Im } C_{L,e} \\ & \oplus \\ -20 < \text{Im } C'_{L,e} < 24 \quad \wedge \quad -14 < \rho \text{Im } C_\gamma^+ < 19 \\ & \oplus \\ & \text{Im } C_{R,e} \end{aligned} $	), (3.19)
$K_L \rightarrow \pi^0 \mu^+ \mu^-$	$ \begin{aligned} & -\text{Im } C_{L,\mu} \\ & \oplus \\ -33 < \text{Im } C'_{L,\mu} < 37 \quad \wedge \quad -30 < \rho \text{Im } C_\gamma^+ < 36 \\ & \oplus \\ & \text{Im } C_{R,\mu} \end{aligned} $	
$K^+ \rightarrow \pi^+ \nu \bar{\nu}$	$ \begin{aligned} & \text{Im } C_{L,\ell} \\ -28 < \oplus < 34 \quad \text{with} \quad \ell = e \oplus \mu \oplus \tau \\ & \text{Im } C'_{L,\ell} \end{aligned} $	

with all numbers in units of  $10^{-4}$ . Indeed,  $C_\gamma^L$  and  $C_\gamma^R$  cannot grow unchecked since the bounds from  $K_L \rightarrow \pi^0(\ell^+\ell^-)_{1--}$  would then require a large interference with  $C_L$ ,  $C'_L$ , or  $C_R$ . But these Wilson coefficients also contribute either to the neutrino modes (via  $Q_{\nu,\ell}$ ) or to the axial-vector current (via  $Q_{A,\ell}$ ), which are separately bounded since non-interfering. So,  $C_L$ ,  $C'_L$ , or  $C_R$  have maximal allowed values and so do  $C_\gamma^L$  and  $C_\gamma^R$ . The slight asymmetries between minimal and maximal values are due to the SM contributions. As in Eq.(3.7),  $\oplus$  denotes exclusive alternatives and  $\wedge$  means that the bounds are correlated. For example, both  $\text{Im } C_{L,\ell}$  and  $\text{Im } C_\gamma^+$  cannot reach their maximal values simultaneously, but rather should fall within the elliptical contour in the  $\text{Im } C_{L,\ell}$ - $\text{Im } C_\gamma^+$  plane, see Fig.(3.3). Looking at these contours, the bound from  $K_L \rightarrow \pi^0 e^+ e^-$  is clearly tighter than that from  $K^+ \rightarrow \pi^+ \nu \bar{\nu}$ , but  $K_L \rightarrow \pi^0 \mu^+ \mu^-$  is less constraining (except of course for  $C_{R,\mu}$ ). Thus, as long as leptonic universality is not imposed,  $C_{L,\mu}$  and  $C'_{L,\mu}$  are only bounded by  $K^+ \rightarrow \pi^+ \nu \bar{\nu}$ , and  $K_L \rightarrow \pi^0 \nu \bar{\nu}$  can reach its maximal model-independent bound (3.8). Still, even if  $K^+ \rightarrow \pi^+ \nu \bar{\nu}$  limits  $C_{L,\mu}^{(\prime)}$ , the  $K_L \rightarrow \pi^0 \mu^+ \mu^-$  rate can always reach its current experimental limit either through  $C_{R,\mu}$  or with the help of  $Q_\gamma^+$ .



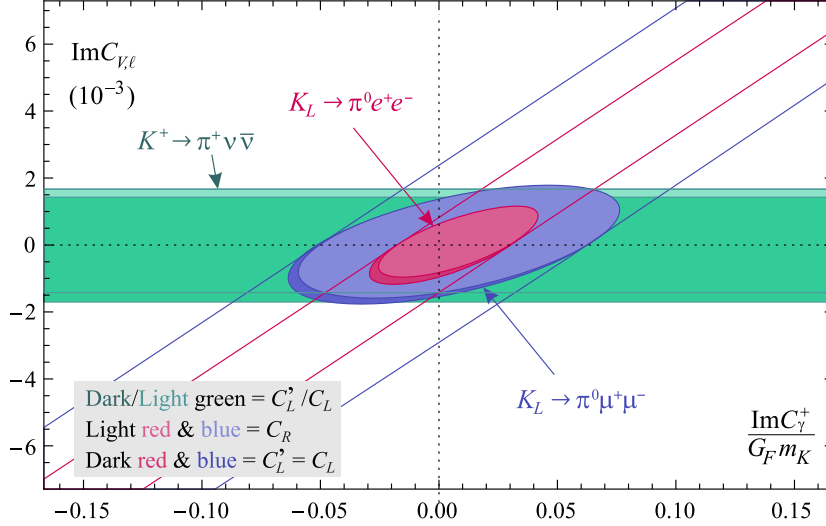


**Fig. 3.3:** Tree-level FCNC scenario, with  $C_{\gamma}^{L,R}$  together with either  $C_L^{\prime}$ ,  $C_L$ , or  $C_R$  turned on. The diagonal bands show the model-independent limits of Fig.(3.2).

The comparison of these bounds with Eq.(3.7) illustrates the consequence of introducing some model-dependence. A scenario with tree-level FCNC is completely bounded by the data. Further, both  $Q_{\gamma}^{L,R}$  contribute to all the decays in Tab.(2.1), since  $C_{\gamma}^{-} = +(-)C_{\gamma}^{+}$  when  $C_{\gamma}^{R(L)}$  is turned on. Thus, we give in Eq.(3.19) the bounds on  $\text{Im } C_{\gamma}^{+}$ , which directly translates as maximal values for all the direct CP-asymmetries in Eqs.(3.1) and (3.3). Since leptonic universality holds for  $Q_{\gamma}^{\pm}$ , the tightest bound from  $K_L \rightarrow \pi^0 e^+ e^-$  must be satisfied, i.e.

$$-0.03 < \frac{\text{Im } C_{\gamma}^{+}}{G_F m_K} < 0.04. \quad (3.20)$$

This represents only a slight extension of the range (3.4), obtained in the absence of NP but in  $Q_{\gamma}^{\pm}$ .

Scalar or tensor four-fermion operators are not included in Eq.(3.17), even though they could arise from leptoquark exchanges. The reason is that they cannot alter the bounds (3.19) if we write them in  $SU(2)_L \otimes U(1)_Y$  invariant forms. The only four-fermion operators able to interfere with the vector ones are  $Q_{T,\ell}$  of Eq.(3.9), but they must be replaced here by

$$Q_{T,\ell}^L = \bar{s} \sigma^{\mu\nu} d \otimes \bar{L} \sigma_{\mu\nu} E, \quad Q_{T,\ell}^R = \bar{s} \sigma^{\mu\nu} d \otimes \bar{E} \sigma_{\mu\nu} L. \quad (3.21)$$

Each of these operators has a pseudotensor piece  $\bar{s}\sigma^{\mu\nu}d \otimes \bar{\ell}\sigma_{\mu\nu}\gamma_5\ell$ , which is the only current able to produce the lepton pair in a  $1^{+-}$  state [89]. There is, thus, no entanglement, and  $Q_{T,\ell}^L$  and  $Q_{T,\ell}^R$  are both directly bound by the total  $K_L \rightarrow \pi^0\ell^+\ell^-$  rate. Hence numerically, the bounds are similar to those in Eq.(3.19), and Eq.(3.20) is not affected.

### 3.3 Loop-level FCNC

For a given lepton flavor, the  $\mathcal{H}_{\text{Gauge}}$  basis maximally couples the semileptonic operators, while the  $\mathcal{H}_{\text{Pheno}}$  basis maximally decouples them. An intermediate picture emerges if the NP generates FCNC only at the loop level. This can be due to some discrete symmetries (like  $R$ -parity) or to some generalized GIM mechanism. By construction, most NP models are of this type, for example the MSSM (see Sec. 3.3), little Higgs [143–145], left-right symmetry [108,146], fourth generation [147,148], some extra dimension models [149],..., because the loop suppression of the FCNC naturally allows for the NP particles to be lighter, hopefully within range of the LHC.

An appropriate basis to study this scenario is derived from the situation in the SM. Indeed, the NP should induce the quark flavor transition  $s \rightarrow d$ , but the lepton pair is flavor-diagonal and could still be produced by SM currents, i.e.,  $\gamma$  and/or  $Z$  bosons. So, in the absence of new vector interactions, the SM basis is adequate:

$$\mathcal{H}_{\text{PB}} = -\frac{G_F\alpha_{em}}{\sqrt{2}}(C_Z Q_Z + C_A Q_A + C_B Q_B) + C_\gamma^{L,R}Q_\gamma^{L,R} + \text{h.c.}, \quad (3.22)$$

with ( $s_W^2 \doteq \sin^2\theta_W = 0.231$ )

$$Z \text{ penguin} : Q_Z \doteq s_W^2 Q_L + (1 - s_W^2)Q'_L + 2s_W^2 Q_R, \quad (3.23a)$$

$$\gamma^* \text{ penguin} : Q_A \doteq \frac{s_W^2}{4}(Q_L - Q'_L + 2Q_R), \quad (3.23b)$$

$$W \text{ boxes} : Q_B \doteq -\frac{3}{2}Q_L - \frac{5}{2}Q'_L. \quad (3.23c)$$

In the presence of NP at the loop-level, it is natural to use the SM-like  $Q_\gamma^{L,R}$  operators of Eq.(3.17) since the chirality flip is, a priori, different for the  $L \rightarrow R$  and  $R \rightarrow L$  transitions. Indeed, even though the drastic SM scaling  $C_\gamma^L \sim m_s \gg C_\gamma^R \sim m_d$  needs not survive in the presence of NP, it is nevertheless expected that  $(C_\gamma^L + C_\gamma^R)/(C_\gamma^L - C_\gamma^R)$  is of  $\mathcal{O}(1)$ .

The  $Q_L$ ,  $Q'_L$  and  $Q_R$  operators are never independent in this scenario, even before the electroweak symmetry breaking takes place. Indeed, though there

is a one-to-one correspondence between the  $W_3^\mu$  penguin and  $Q'_L$ , the  $B^\mu$  penguin generates both  $Q_L$  and  $Q_R$  with a fixed (“fine-tuned”) relative coefficient. Combined with Eq.(3.18), the transformation back to the phenomenological basis is

$$\begin{pmatrix} C_{\nu,\ell} \\ C_{V,\ell} \\ C_{A,\ell} \end{pmatrix} = \frac{1}{2} \begin{pmatrix} 1 & 0 & -4 \\ 4s_W^2 - 1 & s_W^2 & 1 \\ 1 & 0 & -1 \end{pmatrix} \begin{pmatrix} C_Z \\ C_A \\ C_B \end{pmatrix}, \quad (3.24)$$

while the  $Q_\gamma^{L,R}$  operators are related to the  $Q_\gamma^\pm$  as in Eq.(3.17). In the SM without QCD, the semileptonic coefficients are directly given in terms of the Inami-Lim functions as (beware that the SM contributions are not included in  $\mathcal{H}_{\text{PB}}$ , which parametrizes only the NP contributions) [38]

$$C_{\{A,Z,B\}}^{\text{SM}} = -\frac{\lambda_t}{\pi s_W^2} \{D_0(x_t), C_0(x_t), B_0(x_t)\}, \quad (3.25)$$

so the  $\mathcal{H}_{\text{PB}}$  basis coincides with Penguin-Box expansion of Ref. [150]. Note that lepton universality is strictly enforced to match the physical picture of NP entering only for the  $s \rightarrow d$  penguins, but this can easily be lifted. Also, (pseudo)scalar or (pseudo)tensor operators are not introduced, as none of the SM penguins can produce them.

In the SM, only specific combinations of the electroweak penguins and boxes are gauge invariant [150]. Those combinations are precisely those entering into  $C_{\nu,\ell}$ ,  $C_{V,\ell}$ , and  $C_{A,\ell}$ , since their operators are directly producing different physical states. Of course, by construction, the  $\mathcal{H}_{\text{Gauge}}$  basis (3.17) is also gauge invariant. To check this starting with the SM expressions (3.25) requires extending the basis of Eq.(3.22) first to differentiate the boxes according to the weak isospin state of the lepton pairs [150]

$$Q_{B,\pm 1/2} \doteq \frac{1}{2}(Q_L \pm Q'_L) \Leftrightarrow \begin{pmatrix} Q_B \\ Q'_B \end{pmatrix} = \begin{pmatrix} -4 & 1 \\ -1 & 1 \end{pmatrix} \begin{pmatrix} Q_{B,+1/2} \\ Q_{B,-1/2} \end{pmatrix}. \quad (3.26)$$

The combination  $Q_B$  occurs in Eq.(3.23) because its Wilson coefficient is separately gauge invariant, see Ref. [150], while  $Q'_B$  is redundant once the gauge is fixed (we work in the t'Hooft-Feynman gauge).

So, if one insists on gauge invariance, the  $\mathcal{H}_{\text{PB}}$  basis collapses either onto the  $\mathcal{H}_{\text{Pheno}}$  or on the  $\mathcal{H}_{\text{Gauge}}$  basis. Still, using directly the  $\mathcal{H}_{\text{PB}}$  basis for parametrizing NP makes sense as its operators encode different physics [150, 151]. Indeed, the dominant NP contribution in the  $Z$  penguin effectively comes from a dimension-four operator after electroweak symmetry breaking [152], while the  $\gamma^*$  penguin is of dimension six. The box operator  $Q_B$  is there to

complete the basis, but is rather suppressed in general. Finally, the magnetic operators  $Q_\gamma^{L,R}$  are separately gauge-invariant, of dimension five after the electroweak symmetry breaking, and require a chirality flip mechanism. Consequently, it is only if there is a new gauge boson, and a corresponding new penguin not necessarily aligned with the SM structures, that significant fine-tunings between the  $\mathcal{H}_{\text{PB}}$  operators could arise. This will be dealt with in the next section.

Coincidentally, the  $\mathcal{H}_{\text{PB}}$  basis is rather close to the model-independent basis  $\mathcal{H}_{\text{Pheno}}$  because  $4s_W^2 \simeq 1$ . Indeed,  $Q_Z$  essentially drops out from the vector current, leaving  $Q_A$  and  $Q_\gamma^+$  completely entangled in  $K_L \rightarrow \pi^0(\ell^+\ell^-)_{1--}$ , while the  $Q_B$  and  $Q_Z$  pair is fully resolved through the non-interfering  $C_{\nu,\ell}$  and  $C_{A,\ell}$  contributions to  $K \rightarrow \pi\nu\bar{\nu}$  and  $K_L \rightarrow \pi^0(\ell^+\ell^-)_{1++},_{0+-}$ . The main difference between the  $\mathcal{H}_{\text{PB}}$  and  $\mathcal{H}_{\text{Pheno}}$  bases is in the magnetic penguins, since the former relates  $Q_\gamma^+$  and  $Q_\gamma^-$  through  $(C_\gamma^L + C_\gamma^R)/(C_\gamma^L - C_\gamma^R) \sim \mathcal{O}(1)$ .

Turning on  $C_Z$ ,  $C_A$ , and  $C_B$  one at a time while keeping  $C_\gamma^{R,L}$  on, the bounds, in units of  $10^{-4}$ , are

$K_L \rightarrow \pi^0 e^+ e^-$	$-14 < (s_W^2/2) \text{Im } C_A - \rho \text{Im } C_\gamma^+ < 8$ $\oplus$ $\text{Im } C_Z$ $-20 < \oplus < 24 \wedge -8 < \rho \text{Im } C_\gamma^+ < 14$ $- \text{Im } C_B$	(3.27)
$K_L \rightarrow \pi^0 \mu^+ \mu^-$	$-29 < (s_W^2/2) \text{Im } C_A - \rho \text{Im } C_\gamma^+ < 24$ $\oplus$ $\text{Im } C_Z$ $-33 < \oplus < 37 \wedge -24 < \rho \text{Im } C_\gamma^+ < 29$ $- \text{Im } C_B$	
$K^+ \rightarrow \pi^+ \nu \bar{\nu}$	$\text{Im } C_Z$ $-15 < \oplus < 21$ $-4 \text{Im } C_B$	

As before,  $\wedge$  denotes a contour in the corresponding plane within the quoted extremes, while  $\oplus$  is the exclusive alternative. Comparing with Eq.(3.7), the presence of  $Q_Z$  or  $Q_B$  in the vector current has no impact on the range for  $\text{Im } C_\gamma^+$ . The bounds from  $K^+ \rightarrow \pi^+ \nu \bar{\nu}$  are more strict because leptonic universality is now imposed. This actually enables to combine all the modes, so that  $\text{Im } C_Z$  is best constrained by  $K_L \rightarrow \pi^0 e^+ e^-$  together with  $K^+ \rightarrow \pi^+ \nu \bar{\nu}$ , and  $\text{Im } C_B$  entirely by  $K^+ \rightarrow \pi^+ \nu \bar{\nu}$  thanks to the factor  $-4$  in Eq.(3.24). The photon operators  $Q_A$  and  $Q_\gamma^\pm$  are unconstrained at this level, so let us investigate how to resolve this ambiguity within the present scenario.

### Hadronic Electroweak penguins

The photon and the  $Z$  boson are also coupled to quarks and, thus, affect  $\varepsilon'$ . If NP generates the  $Q_Z$  and  $Q_A$  operators entirely through these SM gauge interactions, we must impose

$$\text{Re}(\varepsilon'/\varepsilon)^{\text{NP}} \simeq \pi s_W^2 \text{Im} [11.3 \times C_Z + 3.1 \times C_A + 2.9 \times C_B] . \quad (3.28)$$

This simplified formula is obtained from Ref. [33] by parametrizing the NP contributions to the OPE initial conditions at  $M_W$  in terms of  $C_{Z,A,B}$ , setting the bag factors to their large  $N_C$  values and taking  $m_s(m_c) = 121$  MeV. We do not include the  $Q_\gamma^-$  contribution to  $\varepsilon'$  since the experimental bound (2.28) implies that it is below 30% of  $\text{Re}(\varepsilon'/\varepsilon)^{\text{exp}}$ , see Eq.(2.67). It should be clear that this formula is only a rough estimate. Deviations with respect to the strict large  $N_C$  limits are likely, even though the coefficients of  $C_Z$  and  $C_A$  are most dependent on  $B_8^{3/2}$ , which is better known than  $B_6^{1/2}$  (see Ref. [33]). To account simultaneously for this uncertainty and that of the SM contribution, we conservatively require  $|\text{Re}(\varepsilon'/\varepsilon)^{\text{NP}}| < 2 \text{Re}(\varepsilon'/\varepsilon)^{\text{exp}}$ .

Even if rather imprecise, the constraints from  $\text{Re}(\varepsilon'/\varepsilon)$  are currently tighter than those coming from rare decays for  $C_Z$  and  $C_A$ . Numerically, turning on one semileptonic operator at a time, Eq.(3.28) imposes (all numbers are in units of  $10^{-4}$ )

$$\text{Re}(\varepsilon'/\varepsilon) \Rightarrow |\text{Im} C_Z| < 4 \oplus |\text{Im} C_A| < 15 \oplus |\text{Im} C_B| < 16 . \quad (3.29)$$

As shown in Fig.(3.4), for such values, the contributions to  $C_{V,\ell}$  are tiny. Thus, the maximal values for  $\text{Im} C_\gamma^+$  are the same as without any other NP sources, see Eqs.(3.4), which requires that  $K_L \rightarrow \pi^0 e^+ e^-$  saturates its current experimental limit. Since lepton universality holds, the  $K_L \rightarrow \pi^0 \mu^+ \mu^-$  rate is smaller but tightly correlated to  $K_L \rightarrow \pi^0 e^+ e^-$ , see Fig.(3.4). Concerning  $K \rightarrow \pi \nu \bar{\nu}$ , if one assumes that  $C_B \ll C_Z$ , as in the SM, then  $K \rightarrow \pi \nu \bar{\nu}$  is strongly limited by  $\varepsilon'$ :

$$C_A = C_B = 0 \Rightarrow \begin{cases} 0 < \text{Br}(K_L \rightarrow \pi^0 \nu \bar{\nu}) < 16 \times 10^{-11} , \\ 7 \times 10^{-11} < \text{Br}(K^+ \rightarrow \pi^+ \nu \bar{\nu}) < 12 \times 10^{-11} . \end{cases} \quad (3.30)$$

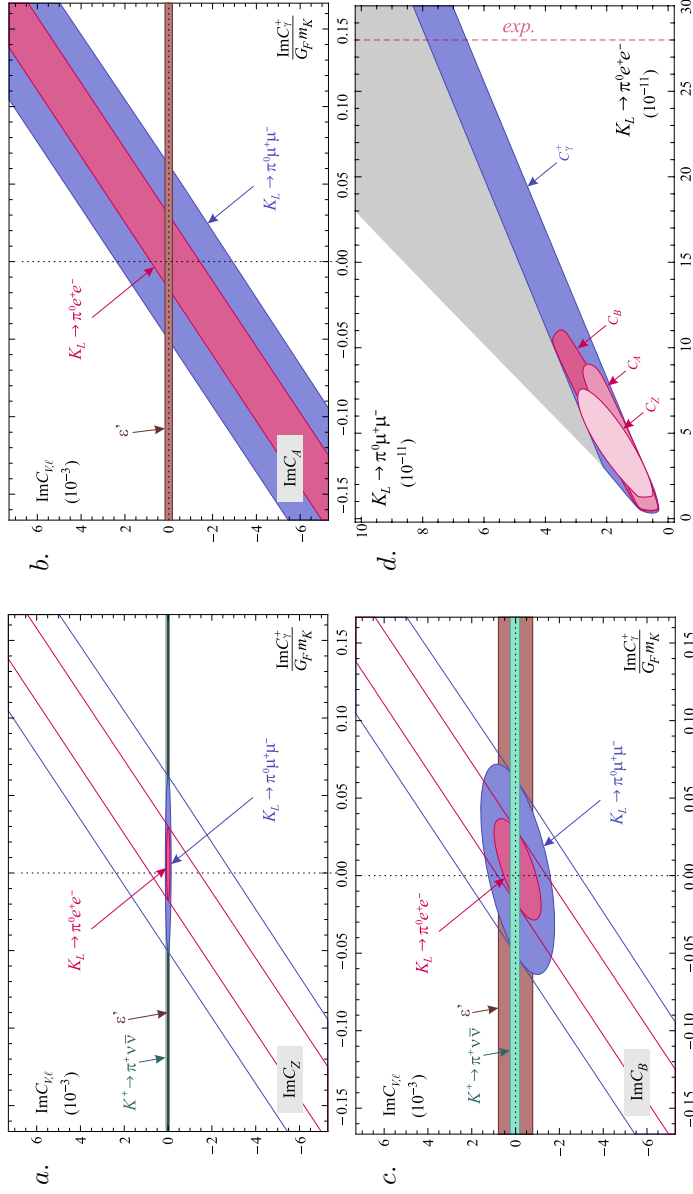


**Fig. 3.4:** Loop-level FCNC scenario, with each electroweak operator separately turned on together with  $Q_{\gamma}^{\pm}$ . (a – c) Contours in the  $\text{Im} C_{V\ell} - \text{Im} C_{\gamma}^{\pm}$  plane as allowed by the  $K^+ \rightarrow \pi^+ \nu \bar{\nu}$ ,  $K_L \rightarrow \pi^0 \ell^+ \ell^-$  and  $\epsilon'$  experimental bounds. (d) The correlation between  $K_L \rightarrow \pi^0 e^+ e^-$  and  $K_L \rightarrow \pi^0 \mu^+ \mu^-$ , when generated exclusively by  $Q_Z$ ,  $Q_A$ , or  $Q_B$  (red), or with one of these together with  $Q_{\gamma}^+$  (blue). The grey background is the area accessible with uncorrelated vector and axial-vector currents (assuming leptonic universality). See Ref. [89] for more information.

However, the current  $K^+ \rightarrow \pi^+ \nu \bar{\nu}$  experimental limit can be saturated when  $C_B \simeq C_Z$ , in which case  $K_L \rightarrow \pi^0 \nu \bar{\nu}$  could reach the model-independent upper limit of Eq.(3.8)

$$\begin{aligned} \text{Br}(K_L \rightarrow \pi^0 \nu \bar{\nu}) &\simeq 4.3(\text{Br}(K^+ \rightarrow \pi^+ \nu \bar{\nu}) - \text{Br}(K^+ \rightarrow \pi^+ \nu \bar{\nu})^{\text{SM}}) \\ &< 1.2 \times 10^{-9}. \end{aligned} \quad (3.31)$$

With  $\varepsilon'$  so constraining, even a slight cancellation among the electroweak penguins could have a significant outcome for  $\text{Im} C_\gamma^+$ . This could occur in most models since the  $\mathcal{H}_{\text{PB}}$  operators are usually not independent but arise simultaneously. Indeed, the intermediate loop particles are, in general, coupled to both the  $\gamma$  and  $Z$  bosons. Let us stress that, as previously mentioned, we do not expect a fine-tuning among these electroweak penguins. At most, we expect some cancellations because their  $SU(2)_L$ -breaking properties are significantly different. Still, it is worth investigating this possibility. Let us, therefore, relax the one-operator-at-a-time procedure.

Once Eq.(3.28) is added to  $K \rightarrow \pi \nu \bar{\nu}$  and  $K_L \rightarrow \pi^0 \ell^+ \ell^-$ , the system is sufficiently constrained and the bounds can be resolved even when all the semileptonic operators are turned on simultaneously

$\text{Re}(\varepsilon'/\varepsilon)$	$ \text{Im} C_A + 3.9 \text{Im} C_Z  < 19$	), (3.32)
$K^+ \rightarrow \pi^+ \nu \bar{\nu}$	$-15 < \text{Im} C_Z - 4 \text{Im} C_B < 21$	
$K_L \rightarrow \pi^0 e^+ e^-$	$-32 < \text{Im} C_Z < 35 \wedge -14 < \rho \text{Im} C_\gamma^+ < 18$	
$K_L \rightarrow \pi^0 \mu^+ \mu^-$	$-49 < \text{Im} C_Z < 53 \wedge -30 < \rho \text{Im} C_\gamma^+ < 35$	

where all the bounds are in units of  $10^{-4}$ . We indicate the main source driving each bound, but it should be clear that all the experimental constraints are entangled, and all are necessary to get a finite-size area in parameter space.

Interestingly, these bounds are not very different from those derived on the  $SU(2)_L \otimes U(1)_Y$  operators of Eq.(3.17). The reason is that  $\text{Re}(\varepsilon'/\varepsilon)$  in Eq.(3.28) imposes the tight correlation  $C_A \simeq -4C_Z$ , upon which  $C_Z$ ,  $C_A$ , and  $C_B$  are all ultimately bound by the rare decays through  $C_{\nu,\ell}$  and  $C_{A,\ell}$ , exactly like  $C_L$ ,  $C'_L$ , and  $C_R$  were (see Eq.(3.18)). Still, the origin of the observed correlations among  $C_{\nu,\ell}$ ,  $C_{A,\ell}$  and  $C_{V,\ell}$  in these two scenarios is obviously very different. It comes directly from the assumed NP dynamics when using the  $\mathcal{H}_{\text{Gauge}}$  basis, but is entirely driven by the sensitivity of  $\text{Re}(\varepsilon'/\varepsilon)$  to electroweak penguins when using the  $\mathcal{H}_{\text{PB}}$  basis.

If the electroweak operators are induced by SM-like  $Z$  and  $\gamma^*$  penguins, such a tight  $C_A \simeq -4C_Z$  correlation is rather unlikely given the intrinsic differences

between those FCNC (dim-4 versus dim-6). So, when

$$r_{ZA} \doteq \frac{C_A + 4C_Z}{C_A - 4C_Z} \ll 1, \quad (3.33)$$

one would rather conclude that a non-standard FCNC, not aligned with the SM penguins, is present. Since  $C_A + 4C_Z$  is the gauge-invariant combination driving the vector coupling (which is known to dominate in  $\varepsilon'$  [150], as is obvious in Eq.(3.28)), one would need a new enhanced penguin, not coupled to the vector current or not coupled to quarks.

The experimental signature for this scenario requires disentangling  $C_A$  and  $C_Z$ . Since the experimental  $K^+ \rightarrow \pi^+ \nu \bar{\nu}$  bound can be saturated with the help of  $C_B$  only, it has no discriminating power in  $r_{AZ}$ . The maximal attainable value for  $\text{Im} C_\gamma^+$  and, thus, for the CP-asymmetries, is not very sensitive to  $r_{ZA}$  either, see Fig.(3.5). On the contrary, the correlation between  $K_L \rightarrow \pi^0 e^+ e^-$  and  $K_L \rightarrow \pi^0 \mu^+ \mu^-$  shown in Fig.(3.5) could signal such a scenario. Indeed, on the one hand, without fine-tuning, one is back to the situation shown in Fig.(3.4) where both rates are saturated by a large  $Q_\gamma^+$  contribution in their vector current when they deviate from their SM predictions. While, on the other hand, as  $r_{AZ}$  decreases, more and more of the model-independent region in the  $K_L \rightarrow \pi^0 e^+ e^- - K_L \rightarrow \pi^0 \mu^+ \mu^-$  plane gets covered.



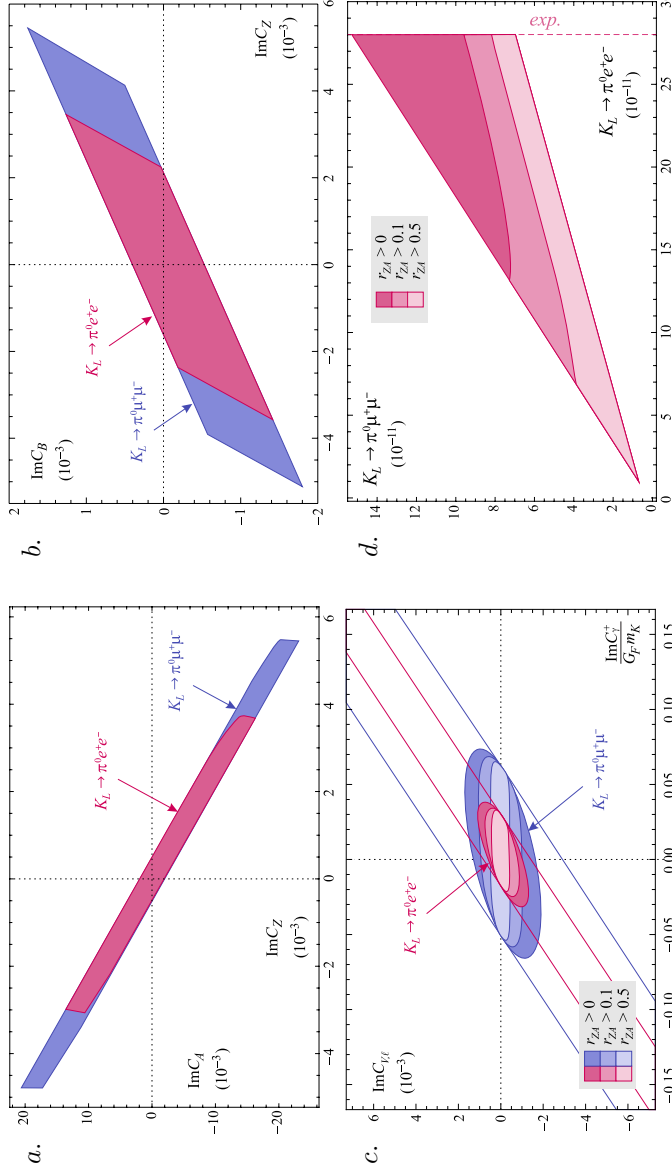


**Fig. 3.5:** Loop-level FCNC scenario, with all the electroweak operators as well as  $Q_{\gamma}^{\pm}$  simultaneously turned on. (a–b) Correlations between  $\text{Im} C_A$ ,  $\text{Im} C_B$ , and  $\text{Im} C_Z$ , as implied by the experimental bounds on  $K^+ \rightarrow \pi^+ \nu \bar{\nu}$ ,  $K_L \rightarrow \pi^0 \ell^+ \ell^-$ , and  $\epsilon'$ . (c) Contours in the  $\text{Im} C_{V,\ell} - \text{Im} C_{\gamma}^+$  plane, with the color lightness indicating the level of fine-tuning between  $C_A$  and  $C_Z$ , see Eq.(3.33). (d) The correlation between  $K_L \rightarrow \pi^0 e^+ e^-$  and  $K_L \rightarrow \pi^0 \mu^+ \mu^-$ , again as a function of the fine-tuning between  $C_A$  and  $C_Z$ . Note that here, the theoretical errors in  $K_L \rightarrow \pi^0 \ell^+ \ell^-$  are discarded for clarity.

## QCD penguins

If  $SU(3)_C \otimes U(1)_{em}$  remains unbroken at the low scale, the FCNC loops must involve intermediate charged and colored particle(s). The photonic penguin is, thus, necessarily accompanied by the gluonic one. Further, if NP enhances significantly the chromomagnetic operators  $Q_g^\pm$  (defined in Eq.(2.70)), the magnetic operators  $Q_\gamma^\pm$  are then directly affected through the RGE (2.71). So,  $C_g^\pm(\mu_{NP})$  act as lower bounds for  $C_\gamma^\pm(\mu_c)$ . The opposite cannot be asserted from Eq.(2.71), since the  $\mathcal{O}(\alpha_{em})$  mixings  $Q_\gamma^\pm \rightarrow Q_g^\pm$  are missing. However, those mixings are presumably long-distance dominated, hence have to be dealt with at the matrix-element level. For instance, in the case of  $\varepsilon'$ , the  $Q_\gamma^-$  contribution is subleading even when  $\text{Im } C_\gamma^-$  saturates the experimental limit on the  $K^+ \rightarrow \pi^+\pi^0\gamma$  CP-asymmetry, see Eq.(2.67). As such, the mixing effects do not forbid a large splitting  $C_\gamma^\pm(\mu_c) \gg C_g^\pm(\mu_c)$ .

Still, owing to their similar dynamics,  $C_\gamma^\pm(\mu_{NP})$  and  $C_g^\pm(\mu_{NP})$  may have similar sizes. If so, since  $Q_g^-$  contributes to  $\varepsilon'$ , both magnetic operators are tightly bounded

$$\frac{|\text{Im } C_\gamma^-|}{G_F m_K} \simeq \frac{|\text{Im } C_g^-|}{G_F m_K} \lesssim 5 \times 10^{-4}, \quad (3.34)$$

if we require  $|\text{Re}(\varepsilon'/\varepsilon)_g| < \text{Re}(\varepsilon'/\varepsilon)_{\text{exp}}$  and set  $B_G = 1$ . This is extremely constraining and would rule out any effect of the magnetic operators in rare decays or in CP-asymmetries.

The presence of the other FCNC could significantly alter this bound. So, let us again turn on all the penguin operators but freeze the relation among the magnetic ones to be given by  $|\text{Im } C_\gamma^+| = 1.5|\text{Im } C_g^-|$ . We also neglect the chromoelectric operators (the usual QCD penguins), as their impact is less important [33]. Then, using Eq.(3.28) with Eq.(3.5), the bounds can be resolved except when  $\varepsilon'$  and  $K_L \rightarrow \pi^0\ell^+\ell^-$  just happen to depend on the same combination of  $\text{Im } C_A$  and  $\text{Im } C_{\gamma,g}^+$ , which occurs for  $\text{Im } C_\gamma^+ \simeq -3\text{Im } C_g^-$  (with  $B_G = +1$ ).

In this scenario, the driving force is the cancellation between the two largest contributions to  $\varepsilon'$ , i.e. between  $\text{Im } C_g^-$  and  $\text{Im}(4C_Z + C_A)$ . The electroweak operators are not fine-tuned, except for the  $\text{Im } C_Z - \text{Im } C_B$  correlation imposed by the rare decays, which stays as in Fig.(3.5). So, in this scenario, large effects are possible in  $K \rightarrow \pi\nu\bar{\nu}$  thanks to  $Q_B$  and  $Q_Z$ , while  $K_L \rightarrow \pi^0\ell^+\ell^-$  receive sizeable contributions in both their vector and axial-vector currents. Contrary to the situation without  $Q_g^\pm$ , these latter decays can no longer be used to probe the cancellations in  $\varepsilon'$ , since they do not directly depend on the chromomagnetic operators.

Actual numbers for the bounds on the Wilson coefficients would not make much sense here, because the fine-tuning in  $\text{Re}(\varepsilon'/\varepsilon)$  reaches horrendous values before the rare decay constraints can kick in. As shown in Fig.(3.6), individual contributions to  $\text{Re}(\varepsilon'/\varepsilon)$  can be as large as 10%. Instead, let us freeze the situation and set the  $Q_g^-$  contribution to  $\text{Re}(\varepsilon'/\varepsilon)$  at  $2 \times 10^{-2}$ . As shown in Fig.(3.6), this requires a large but not impossible 90% cancellation between the electroweak and the gluonic penguins.

To uniquely identify this cancellation, the best strategy relies on the direct CP-asymmetries (see Fig.(3.6)). The first step is to exploit the RGE constraint  $C_\gamma^\pm(\mu_c) \gtrsim C_g^\pm(\mu_c)$ , which implies that the asymmetries in Eq.(3.1) are all at the percent level

$$\frac{\text{Im } C_\gamma^-}{G_F m_K} \gtrsim \frac{\text{Im } C_g^-}{G_F m_K} \simeq \frac{\text{Re}(\varepsilon'/\varepsilon)_g}{3B_G} \simeq 10^{-2} . \quad (3.35)$$

Since  $\varepsilon'_{+0\gamma}$ ,  $\varepsilon'_{+-\gamma}$ , and  $\varepsilon'_{||}$  are mostly insensitive to the hadronic penguin fraction in  $\varepsilon'$ , they would cleanly signal the presence of NP in  $Q_\gamma^-$ . The second step derives from the pure  $\Delta I = 1/2$  nature of the chromomagnetic operator. Since it enters only in  $K \rightarrow \pi\pi_0$ , its presence would be felt in  $\varepsilon'_\perp$  (see Eq.(3.3)), in addition to that of  $Q_\gamma^+$ . So, using Eq.(3.5) and enforcing  $|\text{Im } C_\gamma^+| = 1.5|\text{Im } C_g^-|$ , we can write

$$|\varepsilon'_\perp/\varepsilon|_g = \frac{\sqrt{2}}{\omega} \text{Re}(\varepsilon'/\varepsilon)_g \simeq 0.65 , \quad |\varepsilon'_\perp/\varepsilon|_\gamma = \frac{1}{4|\varepsilon|} \text{Re}(\varepsilon'/\varepsilon)_g \simeq 2.2 , \quad (3.36)$$

with  $B_G = +1$ . By contrast, electroweak penguins contribute mostly to the  $K \rightarrow \pi\pi_2$  amplitude and have, thus, a negligible impact on  $\varepsilon'_\perp$  compared to  $Q_g^-$ . So, in principle, by combining  $\varepsilon'_\perp$  with  $\varepsilon'_{+0\gamma}$ ,  $\varepsilon'_{+-\gamma}$ , or  $\varepsilon'_{||}$ , it is possible to put into evidence NP in both  $Q_\gamma^\pm$  and  $Q_g^-$ . Of course, this whole program is very challenging experimentally, but completing the first step may be feasible, since  $Q_\gamma^-$  could push  $\varepsilon'_{+0\gamma}$  and  $\varepsilon'_{+-\gamma}$  up to less than an order of magnitude away from their current limits.

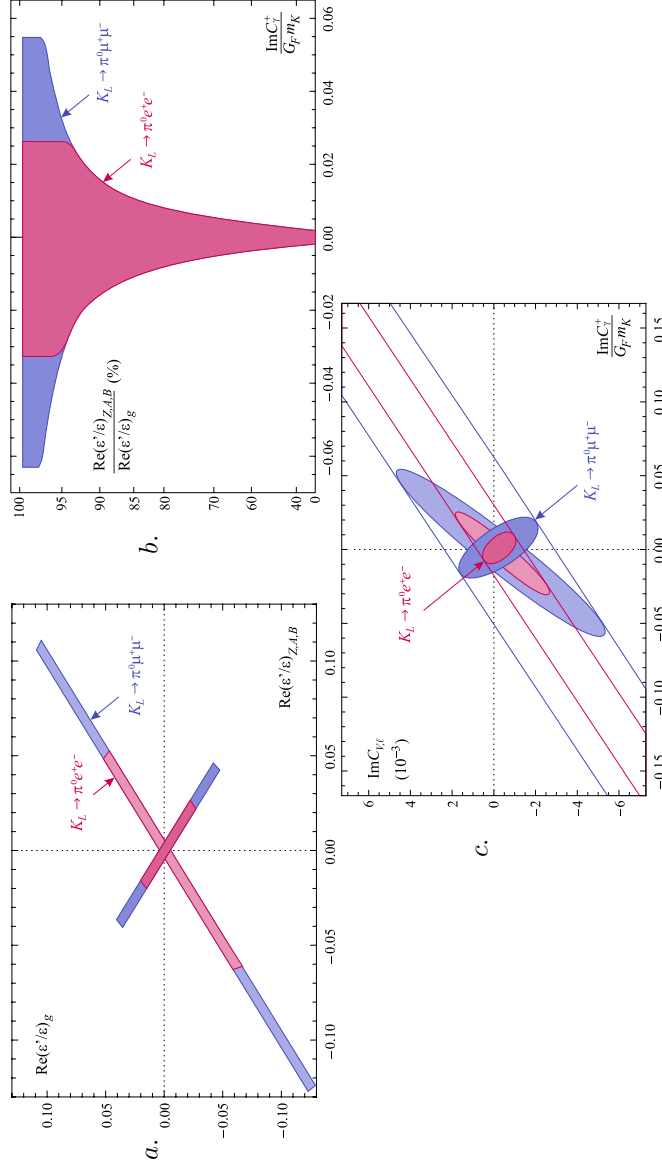


**Fig. 3.6:** Loop-level FCNC scenario, with all the electroweak operators as well as  $Q_{\gamma,g}^\pm$  simultaneously turned on, but imposing  $\text{Im}C_\gamma^+ = \pm 1.5 \text{Im}C_g^-$ . (a) Correlation between the electroweak and gluonic contributions to  $\varepsilon'$ , imposing  $|\text{Re}(\varepsilon'/\varepsilon)^{\text{NP}}| < 2 \text{Re}(\varepsilon'/\varepsilon)_{\text{exp}}$ . (b) The  $\text{Im}C_\gamma^+$  range as a function of the fine-tuning between  $\text{Re}(\varepsilon'/\varepsilon)_{EW}$  and  $\text{Re}(\varepsilon'/\varepsilon)_g$ . (c) The corresponding contours in the  $\text{Im}C_{V,\ell} - \text{Im}C_\gamma^+$  plane. In (a) and (c), the lighter (darker) colors denote destructive (constructive) interference between  $Q_A$  and  $Q_\gamma^+$  in  $K_L \rightarrow \pi^0 \ell^+ \ell^-$ .

### Minimal Supersymmetric Standard Model

The MSSM with R-parity is a particular implementation of the loop-level FCNC scenario discussed in the previous section. All the bounds derived there are, thus, not only valid, but could become tighter. Indeed, the various FCNC could be more directly correlated once the NP dynamics is specified. In addition, the MSSM introduces only a finite number of new sources of flavor-breaking through its soft-breaking squark mass terms and trilinear couplings.

The most important correlation is that between the gluonic and photonic penguins, as analyzed in detail in Refs. [81,125]. Both can be generated by gluino-down squark loops, so that [153]

$$C_\gamma^\pm(m_{\tilde{g}}) = \frac{\pi\alpha_s(m_{\tilde{g}})}{m_{\tilde{g}}} [(\delta_{LR}^D)_{21} \pm (\delta_{RL}^D)_{21}] F(x_{qg}), \quad (3.37a)$$

$$C_g^\pm(m_{\tilde{g}}) = \frac{\pi\alpha_s(m_{\tilde{g}})}{m_{\tilde{g}}} [(\delta_{LR}^D)_{21} \pm (\delta_{RL}^D)_{21}] G(x_{qg}), \quad (3.37b)$$

with

$$F(x_{qg}) \simeq F(1) = \frac{2}{9}, \quad G(x_{qg}) \simeq G(1) = -\frac{5}{18}, \quad (3.38)$$

where  $x_{qg} = m_q^2/m_{\tilde{g}}^2$ ,  $m_{\tilde{q}(\tilde{g})}$  is the squark (gluino) mass and where  $F(x_{qg})$  and  $G(x_{qg})$  are loop functions. The chirality flips are induced by the  $SU(2)_L$  breaking trilinear term  $\mathbf{A}^D$ , parametrized through the mass insertions  $(\delta_{RL}^D)_{21} = (\delta_{LR}^D)_{12}^*$ . At the low-scale, the Wilson coefficients obey

$$C_\gamma^\pm(\mu_c) = \left( \eta \frac{F(x_{qg})}{G(x_{qg})} + 8(\eta - 1) \right) C_g^\pm(\mu_c) \simeq -1.6 C_g^\pm(\mu_c). \quad (3.39)$$

In the absence of any other supersymmetric contributions to  $\varepsilon'$ , this leads to the tight constraint [154–156]

$$\text{Re}(\varepsilon'/\varepsilon) \Rightarrow \frac{|\text{Im} C_g^-(\mu_c)|}{G_F m_K} \lesssim 5 \times 10^{-4} \rightarrow |\text{Im}(\delta_{RL}^D)_{21,12}| \lesssim 2 \times 10^{-5}. \quad (3.40)$$

Before discussing how this bound could get relaxed by NP effects in the other FCNC, let us consider the MFV prediction for  $\delta_{RL}^D$ , to get a handle on the “minimal” size of  $C_{\gamma,g}^\pm$ . The flavor symmetry-breaking of  $\mathbf{A}^D$  imposes an expansion at least linear in the Yukawa couplings [128–132]

$$\mathbf{A}^D \sim A_0(a_0 \mathbf{1} + a_1 \mathbf{Y}_u \mathbf{Y}_u^\dagger + \dots) \mathbf{Y}_d, \quad (3.41)$$

with  $\mathbf{Y}_d = \sqrt{2} \mathbf{m}_d / v_d$ ,  $\mathbf{Y}_u = \sqrt{2} V^\dagger \mathbf{m}_u / v_u$ ,  $v_{u,d}$  the vacuum expectation values of the  $H_{u,d}^0$  Higgs boson,  $A_0$  setting the SUSY breaking scale, and  $a_i$  some free

$\mathcal{O}(1)$  parameters (which can be complex [157, 158]). In that case,  $(\delta_{LR}^D)_{IJ} \sim m_{d^j}/m_{\bar{d}} \sim 10^{-4}$ , and no visible deviations could arise in  $\varepsilon'$  or in the other CP-violation parameters in Eq.(3.1). Turned around, this means that these observables are particularly sensitive to deviation with respect to MFV. As a matter of fact, this framework is only one particular realization of the flavor sector of the MSSM. It is motivated in part by its rather natural occurrence starting from universal soft-breaking terms at the high scale and in part by the tight constraints in the  $b \rightarrow s, d$  or  $\ell \rightarrow \ell'$  sectors. It would, therefore, be interesting to confront it to experimental information about the  $s \rightarrow d$  sector as well.

Before exploiting the analysis of Sec.3.3, there is another important correlation arising in the MSSM. The  $\Delta S = 2$  observables can be induced by the same source of flavor-breaking as the magnetic operators. One derives for  $m_{\bar{g}} = 500$  GeV [154–156]:

$$\Delta M_K \Rightarrow \sqrt{\text{Re}(\delta_{RL}^D)_{21}^2} < 3 \times 10^{-3} \rightarrow \frac{|\text{Re } C_\gamma^\pm|}{G_F m_K} \lesssim 0.1, \quad (3.42a)$$

$$\varepsilon \Rightarrow \sqrt{\text{Im}(\delta_{RL}^D)_{21}^2} < 4 \times 10^{-4} \rightarrow \frac{|\text{Im } C_\gamma^\pm|}{G_F m_K} \lesssim 0.01. \quad (3.42b)$$

The absence of a large cancellation among the supersymmetric contributions, such as processes where the flavor-breaking originates from the  $SU(2)_L$  conserving squark masses (most notably  $\delta_{LL}^D$ ), is explicitly assumed. At this stage, we want to point out that the bounds on  $\text{Re } C_\gamma^\pm$  obtained from radiative decays are competitive with that from  $\Delta M_K$ :

$$K^+ \rightarrow \pi^+ \pi^0 \gamma \Rightarrow \frac{|\text{Re } C_\gamma^-|}{G_F m_K} \lesssim 0.1 \rightarrow |\text{Re}(\delta_{RL}^D)_{21}| < 3 \times 10^{-3}, \quad (3.43a)$$

$$K^0 \rightarrow \gamma \gamma \Rightarrow \frac{|\text{Re } C_\gamma^+|}{G_F m_K} \lesssim 0.3 \rightarrow |\text{Re}(\delta_{RL}^D)_{21}| < 10^{-2}, \quad (3.43b)$$

assuming  $C_\gamma^+ \simeq \pm C_\gamma^-$ . Compared to the bound from  $\Delta M_K$ , radiative decays directly constrain  $\text{Re}(\delta_{RL}^D)_{21}$ , and there can be no weakening through interferences among SUSY contributions, since only  $Q_\gamma^\pm$  enter.

Let us consider the bound from  $\varepsilon$  as the maximal allowed value for  $\text{Im } C_\gamma^\pm$ . We can now directly connect the present MSSM scenario to that discussed in Sec.3.3, since the bound (3.42b) matches that in Eq.(3.35). Given the constraint (3.39), which also matches that of Sec.3.3, such values for  $\text{Im } C_{\gamma,g}^\pm$  are only possible provided there is a large electroweak-gluonic penguin cancellation in  $\varepsilon'$ , of about 90% of their respective contributions, see Fig.(3.6).

This cannot be excluded, a priori, even though the electroweak penguins are not directly correlated with gluonic penguins in the MSSM. With the  $SU(2)_L$

conserving mass insertions  $\delta_{LL}^D$  limited by the  $\Delta S = 2$  observables, electroweak penguins arise essentially from the flavor-breaking in the up-squark sector. Indeed, when  $\mathbf{A}^U = A_0 \mathbf{Y}_u + \dots$ , the quadratic combination of mass-insertion  $(\delta_{LR}^U)_{13}(\delta_{LR}^U)_{23}^*$  gets significantly enhanced by the large top mass [159]. This scenario was analyzed in detail e.g. in Refs. [125, 160], where significant deviations with respect to the SM were found to be possible for  $K \rightarrow \pi \nu \bar{\nu}$ . In particular, the box diagram was found to be sizeable in Ref. [161]. Though these scenarios concentrated on the low to moderate  $\tan \beta \doteq v_u/v_d$  regime, the situation is similar at large  $\tan \beta$ . Indeed, on one hand,  $C_{\gamma,g}^\pm$  and, thus,  $\text{Re}(\varepsilon'/\varepsilon)_g$  could reach larger values even under MFV, since  $\mathbf{Y}_d = \mathbf{m}_d/v_d$  gets enhanced. On the other hand, however, the charged Higgs contribution to the electroweak penguins can kick in, making them sensitive to the flavor-breakings in the  $\delta_{RR}^D$  sector<sup>1</sup>.

Altogether, there can be two different situations in the MSSM:

- If there is a large cancellation between gluonic and electroweak penguins in  $\varepsilon'$ , large enhancements are possible in the rare decays. This is the scenario of Sec.3.3. The  $K^+ \rightarrow \pi^+ \nu \bar{\nu}$  mode can saturate its current limit, and  $K_L \rightarrow \pi^0 \nu \bar{\nu}$  can reach the model-independent bound (3.31). The  $K_L \rightarrow \pi^0 e^+ e^-$  can also saturate its experimental bound, while leptonic universality then limits  $K_L \rightarrow \pi^0 \mu^+ \mu^-$  to about 40% of its current (looser) bound. As in Sec.3.3, the direct CP-violating parameters in radiative  $K$  decays could reach the percent level, see Fig.(3.6), and would be the cleanest signatures for this scenario.
- On the contrary, if there is no large cancellation in  $\varepsilon'$ , say not beyond about 10%, then  $C_\gamma^\pm$  are indirectly limited by the tight correlation (3.39) and all the direct CP-violating parameters would be small, presumably beyond the experimental reach. Further, a fine-tuning between the  $Z$  and virtual  $\gamma$  penguins able to push  $r_{ZA}$  in Eq.(3.33) to small values is not possible. Both are driven by the same mass insertions, with the generic result  $C_Z > C_A$  (see e.g. Ref. [160]). So, this corresponds to the first scenario of Sec.3.3, characterized by the bounds (3.29). The  $K^+ \rightarrow \pi^+ \nu \bar{\nu}$  and  $K_L \rightarrow \pi^0 \nu \bar{\nu}$  could still be very large if the boxes are sizeable ( $C_Z \simeq C_B$ ), but  $K_L \rightarrow \pi^0 e^+ e^-$  and  $K_L \rightarrow \pi^0 \mu^+ \mu^-$  cannot because  $C_\gamma^+ \simeq -1.6 C_g^\pm$  is too small to enhance them (see the red areas in Fig.(3.4d)).

<sup>1</sup>At large  $\tan \beta$ , Higgs mediated penguins could also appear. Those are embedded in helicity-suppressed scalar and pseudoscalar semileptonic operators. We refer to Ref. [89] for an analysis of their possible impact.

In summary, to probe for a possible large electroweak and QCD penguin cancellations in  $\varepsilon'$ , the  $K \rightarrow \pi\nu\bar{\nu}$  are useful only if the scaling between box and penguins is known. However, telltale signatures would be large enhancements of  $K_L \rightarrow \pi^0 e^+ e^-$  and  $K_L \rightarrow \pi^0 \mu^+ \mu^-$ , as well as large CP-violating parameters in radiative  $K$  decays.

### 3.4 Conclusions

In this chapter, the possible NP impacts on the  $s \rightarrow d\gamma$  process were analyzed. The direct CP-violating parameters in radiative decays offer the cleanest accesses to  $s \rightarrow d\gamma$ , since they are free from any competing NP effect (except  $\varepsilon'_\perp$ ) once the  $Q_{3,\dots,10}$  contributions are fixed in terms of  $\text{Re}(\varepsilon'/\varepsilon)_{\text{exp}}$ . However, these parameters are not yet tightly bounded experimentally. By contrast, the  $K_L \rightarrow \pi^0 \ell^+ \ell^-$  decays are sensitive to both  $s \rightarrow d\gamma$  and  $s \rightarrow d\gamma^*$  processes, as well as to many other possible FCNC, but are already tightly bounded experimentally. So, to resolve the possible interferences among NP contributions and, thereby, assess how large the CP-violating parameters could be, several scenarios were considered. The main discriminator was chosen as the assumed NP dynamics, which translates as a choice of basis for the effective four-fermion semi-leptonic operators. To summarize each scenario:

1. **Model-independent** The basis (3.6) is constructed so as to minimize the interferences between the NP contributions in physical observables [126]. Its main characteristic is the entanglement of the magnetic operator  $Q_\gamma^+$  with the semileptonic operator  $Q_{V,\ell} = \bar{s}\gamma_\mu d \otimes \bar{\ell}\gamma^\mu \ell$ , since they both produce the  $\ell^+ \ell^-$  pair in the same  $1^{--}$  state. So, if these two interfere destructively, the CP-violating parameters in radiative decays could be large. For example, if there is an 80% cancellation between  $Q_\gamma^+$  and  $Q_{V,e}$  in  $K_L \rightarrow \pi^0 e^+ e^-$ ,  $\varepsilon'_{+0\gamma}$  could saturate its current experimental limit  $-22(36)\%$  [8], see Fig.(3.2). By comparison, a strict enforcement of the MFV hypothesis would suppress all these CP-violating parameters down to the  $10^{-4}$  range. This shows the power of these parameters in exhibiting deviations with respect to MFV.
2. **Tree-level FCNC** The basis (3.17) assumes that the NP is invariant under  $SU(2)_L \otimes U(1)_Y$  and generates the semileptonic operators through tree-level processes. The main characteristic is the strong correlation between  $K \rightarrow \pi\nu\bar{\nu}$ ,  $K_L \rightarrow \pi^0(\ell^+ \ell^-)_{1^{--}}$  and  $K_L \rightarrow \pi^0(\ell^+ \ell^-)_{1^{++},0^{-+}}$  for a given lepton flavor but the absence of leptonic universality. This is



sufficient to resolve the entanglement between  $Q_\gamma^+$  and  $Q_{V,\ell}$ . The CP-violating parameters are then bounded by  $K_L \rightarrow \pi^0 e^+ e^-$ , see Fig.(3.3), with e.g.  $|\varepsilon'_{+0\gamma}| \lesssim 11\%$ . Also, each rare decay can saturate its experimental bound, though all cannot simultaneously be large but for  $K_L \rightarrow \pi^0 \nu \bar{\nu}$ , which must satisfy its model-independent bound (3.8).

3. **Loop-level FCNC / electroweak penguins only** The basis (3.22) provided by the SM electroweak penguin and box operators is adequate when the FCNC originates entirely from loop processes. The main characteristic of this scenario is the entanglement of the  $s \rightarrow d\gamma$  and  $s \rightarrow d\gamma^*$  photon penguins in  $K_L \rightarrow \pi^0(\ell^+\ell^-)_{1--}$ . However, once in this basis, it is natural to allow the photon and  $Z$  to couple also to quarks, bringing  $\varepsilon'$  into the picture. Then, the only way to have sizeable effects in rare decays is to allow for a large box operator to fine-tune the electroweak penguins, so as to avoid the large vector current contribution in  $\varepsilon'$ , or to allow for  $Q_\gamma^\pm$  to be large. The main issue is, thus, to resolve the fine-tuning in  $\varepsilon'$ . Indeed, if it is extreme, one would conclude that the chosen basis is inadequate, and NP is not aligned with the  $Z$  or  $\gamma$  penguins. While the direct CP-violating parameters are rather insensitive, and could reach a few percents, at most, the correlation between the  $K_L \rightarrow \pi^0 e^+ e^-$  and  $K_L \rightarrow \pi^0 \mu^+ \mu^-$  modes can be used to signal such a fine-tuning in  $\varepsilon'$ , see Fig.(3.5).
4. **Loop-level FCNC / electroweak and chromomagnetic penguins** When generated at loop level, the magnetic operators are always accompanied by the chromomagnetic operators since the  $SU(3)_C \otimes U(1)_{em}$  quantum numbers must flow through the loop. Their relative strength, however, cannot be assessed model-independently. If one forces the two to be of similar strengths, the main characteristic of this scenario is the tight fine-tuning required by  $\varepsilon'$  between the gluonic and the electroweak penguins, see Fig.(3.6). To resolve this, rare decays are rather ineffective but the direct CP-violating parameters are perfectly suited, since they directly measure  $Q_\gamma^\pm$ . The parameter  $\varepsilon'_\perp$  is particularly interesting, considering that it is also directly sensitive to the  $\Delta I = 1/2$  chromomagnetic operator  $Q_g^-$  through its dependence on  $\xi_0$ .
5. **Loop-level FCNC / MSSM** The main characteristic of the MSSM is the strict correlation between the magnetic and chromomagnetic penguins, Eq.(3.39). Depending on the level of fine-tuning between gluonic and electroweak penguins in  $\varepsilon'$ , this scenario collapses either to scenario 3 or 4. In the former case, both magnetic penguins have to be small due to the fact that they are correlated, and the MSSM further forbids

the specific fine-tuning between the electroweak penguins required by  $\varepsilon'$ . As a result, the rare decays are tightly constrained, see Fig.(3.4), with the possible exception of  $K \rightarrow \pi\nu\bar{\nu}$  if the box amplitudes are exceptionally large. It should be stressed, though, that the cancellation between the gluonic and electroweak penguins required in  $\varepsilon'$  needs not be extreme to leave room for sizeable supersymmetric contributions to both  $K_L \rightarrow \pi^0\ell^+\ell^-$  and direct CP-violating parameters, see Fig.(3.6). Finally, radiative decays were found to provide a competitive bound on  $\text{Re}\delta_{12}^D$ , see Eq.(3.43).

# Chapter 4

## Weakly-induced strong CP-violation

In the SM, both the electroweak gauge interactions and the Higgs self interactions turn out to be CP-invariant. Yet, in absence of any flavor theory, the most general Yukawa interactions of the Higgs field with three generations of quarks are responsible for two independent CP-violating phases. The first one,  $e^{i\delta_{\text{CKM}}}$ , preserves parity (P) whilst the second one,  $e^{i\theta_{\text{QFD}}}$ , preserves charge conjugation (C). Indeed, these phases are rooted in the complex up (and down) quark mass matrices  $M^{u(d)}$ : induced by the Higgs field frozen at its vacuum expectation value, these matrices can always be polar decomposed into Hermitian ones multiplied by a global phase [162], but are neither symmetric nor Hermitian.

As a matter of fact, the  $\delta_{\text{CKM}}$  and  $\theta_{\text{QFD}}$  angles are not observables by themselves. On the one hand, the unitarity of the three-by-three Cabibbo-Kobayashi-Maskawa (CKM) mixing matrix allows nine independent parametrizations in terms of Euler rotations such that flavour physics only implies the lower bound [163]

$$\delta_{\text{CKM}} \gtrsim \frac{\pi}{200}. \quad (4.1)$$

In particular, in the usual CKM matrix parametrization, we saw in Eq.(1.15) that  $\delta_{\text{CKM}} \simeq 74(\pi/200)$ . On the other hand, the axial anomaly in strong gauge interactions is such that nuclear physics only requires the upper bound [164,165]

$$\theta \doteq \theta_{\text{QFD}} + \theta_{\text{QCD}} \lesssim 10^{-10} \quad (4.2)$$

with  $\theta_{\text{QFD}}$ , the argument of  $\det(M^u M^d)$  in Quantum Flavour Dynamics (QFD) and  $\theta_{\text{QCD}}$ , the coefficient in front of the  $G_{\mu\nu}\tilde{G}^{\mu\nu}$  term in Quantum Chromo Dynamics (QCD) [166].

The striking hierarchy between Eq.(4.1) and Eq.(4.2) suggests that  $\delta_{\text{CKM}} \neq 0$  and  $\theta = 0$  at the classical level. A natural way to implement such a scenario would be to impose the parity invariance on the full Lagrangian. However, in the SM, C and P discrete symmetries are explicitly broken by the gauge sector such that quantum corrections to the  $\theta$  parameter are expected to arise at the second-order in the electroweak interactions. In the past, two complementary short-distance attempts to estimate  $\Delta_w\theta$  within the SM have been suggested. The first one [167] was based on loop corrections for the light quark masses, leading to

$$\Delta_w\theta_{\text{QFD}} \simeq 10^{-16} \quad \text{at} \quad \mathcal{O}(G_F^2\alpha_s^3), \quad (4.3)$$

while the second one [168] has considered the induced gluon pseudo-strength field to get

$$\Delta_w\theta_{\text{QCD}} \simeq 10^{-19} \quad \text{at} \quad \mathcal{O}(G_F^2\alpha_s). \quad (4.4)$$

In this chapter, we estimate  $\Delta_w\theta$  through the physical  $\eta^{(\prime)} \rightarrow \pi\pi$  hadronic decays and find rather

$$\Delta_w\theta \simeq 10^{-17} \quad \text{at} \quad \mathcal{O}(G_F^2\varepsilon') \quad (4.5)$$

once again with  $\varepsilon'$ , the penguin-induced CP-violation parameter in  $K \rightarrow \pi\pi$  decays.

## 4.1 $\eta^{(\prime)} \rightarrow \pi\pi$ from strong interactions

At low energy, all the basic aspects of strong interactions are encapsulated in the truncated  $\mathcal{O}(p^2)$  effective Lagrangian [56–58]

$$\mathcal{L}_s = \frac{F^2}{4} \langle \partial_\mu U \partial^\mu U^\dagger \rangle + \mathcal{L}_s^M + \mathcal{L}_s^\theta, \quad (4.6)$$

which is the  $U(3)_L \times U(3)_R$  generalization of the strong effective Lagrangian of Eq.(1.46) that includes a  $\mathcal{O}(p^0, N_C^{-1})$  axial  $U_A(1)$  breaking term weighted by the mass parameter  $m_0$  in

$$\mathcal{L}_s^M = \frac{F^2}{4} \left[ \langle \mu^2 (U + U^\dagger) \rangle + \frac{m_0^2}{4N_C} \langle \ln U - \ln U^\dagger \rangle^2 \right] \quad (4.7)$$

and encodes effectively the presence of the  $\theta$ -term as

$$\mathcal{L}_s^\theta = iK_\theta \frac{F^2}{4} [-\langle U - U^\dagger \rangle + \langle \ln U - \ln U^\dagger \rangle] . \quad (4.8)$$

An important consequence of this extension is that an extra GB emerges from the spontaneous symmetry breaking  $U(3)_L \times U(3)_R \rightarrow U(3)_V$ . This is, of course, the reason why, in this  $1/N_C$  extension, we may identify the  $\eta'$  as a new GB with an anomalously large mass due to the  $m_0^2$  symmetry breaking term in Eq.(4.7) by including a new singlet scalar field  $\eta_0$  in  $\phi$ , defined in Sec.(1.3.2), as

$$\phi \rightarrow \phi + \sqrt{\frac{2}{3}} \eta_0 \mathbf{1}_{3 \times 3} . \quad (4.9)$$

It is worth recalling some of the main properties of this extended Lagrangian.

## Mass spectrum and mixing from $\mathcal{L}_S^M$

On the one hand, and as previously mentioned, the vacuum expectation value of the  $\mu^2$  matrix field is proportional to the real and diagonal light quark mass matrix and provides the pions and kaons with a mass:

$$\mu_u^2 = \mu_d^2 = m_\pi^2 \quad \text{and} \quad \mu_s^2 = 2m_K^2 - m_\pi^2 . \quad (4.10)$$

As such, it breaks the flavour  $SU(3)$  symmetry but preserves its isospin subgroup  $SU(2)_I$  in the limit  $\mu_u^2 = \mu_d^2$ . On the other hand, the colour-suppressed operator proportional to  $m_0^2$  in Eq.(4.7), responsible for the breaking of the anomalous axial  $U(1)_A$ , allows us to consider  $\eta_0$  as the ninth GB of the  $U(3)$  multiplet  $\phi$  in the large- $N_C$  limit [169]. However, since  $\eta_8$  and  $\eta_0$  mix, it is suitable to introduce the single mixing angle  $\varphi$  which relates the  $SU(3)$  eigenstates  $(\eta_8, \eta_0)$  and the mass eigenstates  $(\eta, \eta')$  in the isospin limit as

$$\begin{pmatrix} \eta \\ \eta' \end{pmatrix} = \begin{pmatrix} \cos \varphi & -\sin \varphi \\ \sin \varphi & \cos \varphi \end{pmatrix} \begin{pmatrix} \eta_8 \\ \eta_0 \end{pmatrix} \quad \text{with} \quad -\frac{\pi}{4} < \varphi < \frac{\pi}{4} . \quad (4.11)$$

We then obtain the following  $\mathcal{O}(p^2)$  mass spectrum for the iso-singlet states

$$m_{\eta'}^2 = \frac{1}{3} \left( 4m_K^2 - m_\pi^2 - 2\sqrt{2}(m_K^2 - m_\pi^2) \cot \varphi \right) \quad (4.12a)$$

$$m_\eta^2 = \frac{1}{3} \left( 4m_K^2 - m_\pi^2 + 2\sqrt{2}(m_K^2 - m_\pi^2) \tan \varphi \right) , \quad (4.12b)$$

with the mixing angle  $\varphi$  and the scale parameter  $m_0$  intimately related through

$$\tan 2\varphi = 2\sqrt{2} \left[ 1 - \frac{3}{2} \frac{3}{N_C} \frac{m_0^2}{m_K^2 - m_\pi^2} \right]^{-1} . \quad (4.13)$$

Interestingly, the Eqs.(4.12) allow for two mass degeneracies :

$$\begin{aligned} 1) \quad m_{\eta'} = m_\pi \quad \text{when} \quad m_0^2 = 0 \quad \quad \quad \text{or} \quad \varphi = +35.3^\circ, \\ 2) \quad m_\eta = m_K \quad \text{when} \quad m_0^2 = 3(m_K^2 - m_\pi^2) \quad \text{or} \quad \varphi = -19.5^\circ. \end{aligned} \quad (4.14)$$

The first one ( $m_{\eta'} = m_\pi$ ), at the source of the so-called  $U(1)_A$  problem [170], requires a non-vanishing  $m_0$  parameter. More precisely, in order to reproduce the  $\eta'(958)$  mass we should set  $m_0 = 817$  MeV or equivalently  $\varphi \simeq -20^\circ$  if the physical masses for  $K(498)$  and  $\pi(135)$  are imposed in Eq.(4.12a). This particular mixing angle turns out to be very close to the one at which the second degeneracy ( $m_\eta = m_K$ ) occurs. However,  $m_\eta^2$  almost fulfills the Gell-Mann-Okubo (GMO) mass relation of Eq.(1.50). So, to reproduce exactly the mass of  $\eta(548)$  one should rather impose a mixing angle close to zero in Eq.(4.12b). In other words, the physical mass spectrum for  $\eta(548)$ ,  $\eta'(958)$ ,  $K(498)$  and  $\pi(135)$  cannot be simultaneously reproduced within the truncated frame adopted here. This can be nicely quantified by the  $\varphi$ -independent upper bound [171,172]

$$\frac{m_\eta^2 - m_\pi^2}{m_{\eta'}^2 - m_\pi^2} < 2 - \sqrt{3} \simeq 0.27, \quad (4.15)$$

which calls for a 20% correction to be compatible with the measured ratio 0.33. To accommodate the full nonet mass spectrum, higher-order operators such as

$$\langle \mu^2(U - U^\dagger) \rangle \langle \ln U - \ln U^\dagger \rangle \ni \langle \phi \rangle \eta_0 \quad (4.16)$$

have to be considered [172]. Yet, this  $\mathcal{O}(p^2, N_C^{-1})$  operator along with  $\mathcal{O}(p^4, 1)$  ones will not be considered in this chapter since the effective Lagrangian in Eq.(4.6) is restricted to the leading  $\mathcal{O}(p^2, 1)$  and  $\mathcal{O}(p^0, N_C^{-1})$  terms, respectively.

## CP-violating interactions from $\mathcal{L}_S^\theta$

The full effect of the strong  $\theta$  angle is encoded into Eq.(4.8), which contains no linear term in  $\phi$  and whose derivation might be found in Refs. [173–175], for example. At this level, any strongly induced P- and T-violating observable quantity will, thus, depend on the constant factor  $K_\theta$  rather than on the  $\theta$  parameter itself. Consequently, in the SM, the first and simplest manifestation of a non-zero  $\theta$  is the occurrence of C-conserving two-body decays among which solely  $\eta^{(\prime)} \rightarrow \pi\pi$  on-shell decays are allowed by energy conservation. The corresponding strong amplitudes are purely  $\Delta I = 0$  and read

$$A(\eta^{(\prime)} \rightarrow \pi\pi)_s = \frac{K_\theta}{\sqrt{3}F} \left( s_\varphi + \sqrt{2} c_\varphi \right) \quad (4.17a)$$

$$A(\eta \rightarrow \pi\pi)_s = \frac{K_\theta}{\sqrt{3}F} \left( c_\varphi - \sqrt{2} s_\varphi \right) , \quad (4.17b)$$

having set  $s_\varphi = \sin \varphi$  and  $c_\varphi = \cos \varphi$  for short. By comparing the subsequent prediction  $\Gamma(\eta \rightarrow \pi^+\pi^-) \simeq 2.6 |K_\theta|^2 \text{ GeV}^{-3}$ , obtained for the phenomenological mixing angle  $\varphi \simeq -20^\circ$ , with the experimental limit  $\text{Br}(\eta \rightarrow \pi^+\pi^-) < 1.3 \times 10^{-5}$  [17], we infer the upper bound  $|K_\theta| \lesssim 2.6 \times 10^{-6} \text{ GeV}^2$ . As a consequence,  $K_\theta$  is small enough to be approximated by [162, 173]

$$K_\theta \doteq \frac{m_\pi^2}{2} \theta , \quad (4.18)$$

in the realistic limit where  $\mu_u^2 = \mu_d^2 \ll \mu_s^2, m_0^2$ .

The  $(\eta, \eta')$  mass eigenstates being complementary in the trigonometric sense, see Eq.(4.11), we conclude that the relation

$$A(\eta \rightarrow \pi\pi) = A(\eta' \rightarrow \pi\pi)|_{\varphi \rightarrow \varphi + \frac{\pi}{2}} , \quad (4.19)$$

fulfilled by Eqs.(4.17), constitutes a good cross-check for our forthcoming computations. Note also that the mixing angle dependences appearing in Eqs.(4.17) are specific to the single anomalous term ( $\mathcal{L}_S^\theta \ni \langle \phi^3 \rangle$ ) appearing at order  $\mathcal{O}(p^0, N_C^{-1})$ . In principle, other mixing angle dependences can be induced. For example, the P- and T-violating operator going along with the  $\mathcal{O}(p^2, N_C^{-1})$  one in Eq.(4.16), namely

$$\langle U + U^\dagger - 2 \rangle \langle \ln U - \ln U^\dagger \rangle \ni \langle \phi^2 \rangle \eta_0 , \quad (4.20)$$

generates pure  $\sin \varphi$  ( $\cos \varphi$ ) contribution to  $A(\eta^{(\prime)} \rightarrow \pi\pi)_s$ . This observation will be of some relevance in our confrontation with the weak interaction contributions to these decay processes.

## 4.2 $\eta^{(\prime)} \rightarrow \pi\pi$ from weak interactions

Such CP-violating, but flavour-conserving, weak processes require a two step change of flavor [176]. At low energy, the  $|\Delta S| = 1$  weak interactions involving the GB are also ruled by the chiral  $U(3)_L \otimes U(3)_R$  transformations acting on the  $U$  field. These interactions are encoded in the  $\mathcal{O}(p^2)$  effective weak Lagrangians of Eq.(1.55). Besides these contributions known to saturate the  $K \rightarrow \pi\pi$  decay amplitudes in the isospin limit, the current-current operator of Eq.(B.13) given by

$$\mathcal{L}_{8s}^{(2)} = F^4 G_s \langle \lambda_{32} L_\mu \rangle \langle L^\mu \rangle + \text{h.c.} , \quad (4.21)$$



**Fig. 4.1:** The  $\mathcal{O}(p^2)$  topologies generating (a) possible tadpole amplitudes and (b) two-body decay amplitudes. Blue disks stand for  $\mathcal{O}(p^2)$  weak vertices as in Fig.(1.5).

is proper to  $U(3)$  as it is proportional to the flavour singlet  $\eta_0$  field. For an analysis of this extra operator see Ref. [114].

In order to generate  $\Delta S = 0$  and CP-violating amplitudes from the  $|\Delta S| = 1$  weak Lagrangian, successive  $\Delta S = \pm 1$  and  $\Delta S = \mp 1$  transitions must interfere so that any such amplitude assumes the following structures

$$A(i \rightarrow f)_w = \sum_{I \neq J} A_{IJ}(i \rightarrow f) \text{Im}(G_I^* G_J). \quad (4.22)$$

Among the second-order weak amplitudes in Eq.(4.22), tadpole-like ones represented in Fig.(4.1a) vanish trivially. Indeed, any inclusion of a current-current  $\mathcal{L}_I$  Lagrangian ( $I \neq s, ew$ ) in the  $\eta^{(i)} \rightarrow K$  vertex generates an amplitude proportional to the square of the incoming four-momentum. Considering now the two-body decays generated by the non-local topologies of Fig.(4.1b), we obtain, in the isospin limit, the tree-level weak  $\eta'$  amplitudes

$$A(\eta' \rightarrow \pi^+ \pi^-)_w = \frac{4}{3\sqrt{3}} F^3 \alpha(m_{\eta'}^2) \left[ 5I_{8,27} s_\varphi - (4I_{8,27} - 9I_{8,s} - 6I_{27,s}) \sqrt{2} c_\varphi \right], \quad (4.23a)$$

$$A(\eta' \rightarrow \pi^0 \pi^0)_w = \frac{4}{3\sqrt{3}} F^3 \alpha(m_{\eta'}^2) [6I_{8,27} + 9(I_{8,s} - I_{27,s})] \sqrt{2} c_\varphi, \quad (4.23b)$$

where

$$\alpha(p^2) \doteq p^2 \left( \frac{p^2 - m_\pi^2}{p^2 - m_K^2} \right) \quad (4.24)$$

and

$$I_{I,J} \doteq \text{Im}(G_I^* G_J). \quad (4.25)$$

The complete computation is detailed in Appendix.(C.4). As explicitly checked, the weak  $\eta \rightarrow \pi\pi$  amplitudes fulfil the complementary relation mentioned in



Eq.(4.19), namely they are deduced from Eqs.(4.23) after replacing  $s_\varphi$  by  $c_\varphi$  and  $c_\varphi$  by  $-s_\varphi$ . In principle, we should also include the effect of the  $\mathcal{L}_{ew}^{(0)}$  Lagrangian, explicitly given in Eq.(C.95). However, these effects can be neglected as far as the  $\eta^{(\prime)} \rightarrow \pi\pi$  decays are concerned. Indeed, the neutral  $\eta^{(\prime)} \rightarrow \pi^0\pi^0$  decay amplitudes are not affected, while the charged ones are affected by less than ten percent, namely, using the results of Appendix C.4 we found that

$$\frac{A(\eta' \rightarrow \pi^+\pi^-)_w - A(\eta' \rightarrow \pi^+\pi^-)_{w|G_{ew}=0}}{A(\eta' \rightarrow \pi^+\pi^-)_w} = (-6.1 \text{ to } 9.1)\% . \quad (4.26)$$

The main reason is that, contrary to the CP-violating parameter  $\varepsilon'$  proportional to the ratio of  $G_I$  effective couplings, the CP-violating  $\eta^{(\prime)} \rightarrow \pi\pi$  decay amplitudes are proportional to their product. So, here there is no possible  $\varepsilon'$ -like  $\Delta I = 1/2$  enhancement to compensate for the naive  $\alpha_{em}/\alpha_s$  suppression factor.

### 4.3 From $\delta_{\text{CKM}}$ to $\theta_{\text{QCD}}$

As proved in the previous section, weak interactions do contribute to the P- and T- violating  $\eta^{(\prime)} \rightarrow \pi\pi$  decays at second-order. Therefore, within the SM, these weak corrections contribute to the  $K_\theta$  parameter or, equivalently, to the strong  $\theta$  term. In this section, we show how this can be achieved assuming again both the isospin and large- $N_C$  limits. To begin with, let us have a first look at the  $G_I$  effective coupling constants. Below the charm mass scale, the QCD-induced  $|\Delta S| = 1$  effective Hamiltonian approximatively reads

$$\begin{aligned} \mathcal{H}_W^{|\Delta S|=1}(\mu < m_c) \simeq & \frac{G_F}{\sqrt{2}} \lambda_u [z_1(\mu)Q_1(\mu) + z_2(\mu)Q_2(\mu)] + \\ & + [\lambda_u z_6(\mu) - \lambda_t y_6(\mu)] Q_6(\mu) \} + \text{h.c.} . \end{aligned} \quad (4.27)$$

In principle, it should be possible to assign the CKM phase to the  $G_I$  couplings. However, to do so, we first have to include the long-distance (LD) evolution down to the hadronization scale  $\mu_{\text{had}}$  lying well below one GeV where perturbative QCD breaks down. Fortunately, Chiral Perturbation Theory supplemented with the  $1/N_C$  expansion allows us to go from the quark-gluon picture to the meson one to get [76, 77]

$$\mathcal{H}^{|\Delta S|=1}(\mu_{\text{had}}) \simeq \frac{G_F}{\sqrt{2}} \{x_1\hat{Q}_1 + x_2\hat{Q}_2 + x_6\hat{Q}_6\} + \text{h.c.} , \quad (4.28)$$

with

$$\hat{Q}_1 = (L_\alpha)_{23}(L^\alpha)_{11}, \quad \hat{Q}_2 = (L_\alpha)_{13}(L^\alpha)_{21}, \quad \hat{Q}_6 = (L_\alpha L^\alpha)_{23} . \quad (4.29)$$

In other words, no additional chiral structures appear beyond the one already present in weak effective Lagrangian, since the product of quark currents factorizes into a product of meson ones at the hadronization scale. At this scale, we, thus, have a one-to-one formal correspondence between the  $G_I$  effective couplings and the  $x_i$  (SD plus LD) coefficients [114]:

$$G_8 \simeq \frac{G_F}{\sqrt{2}} \left[ -\frac{2}{5}x_1 + \frac{3}{5}x_2 + x_6 \right], \quad (4.30a)$$

$$G_{27} \simeq \frac{G_F}{\sqrt{2}} \left[ \frac{3}{5}(x_1 + x_2) \right], \quad (4.30b)$$

$$G_s \simeq \frac{G_F}{\sqrt{2}} \left[ \frac{3}{5}x_1 - \frac{2}{5}x_2 \right]. \quad (4.30c)$$

Within this matching approach, the CP-violating  $I_{I,J}$  elements defined in Eq.(4.25) arise then exclusively from quark  $Q_{1,2} - Q_6$  interference (i.e.,  $\lambda_u - \lambda_t$  interference) such that the subdominant  $27 - s$  contributions are real:

$$I_{27,s} = 0. \quad (4.31)$$

Let us now use the strong amplitudes given in Eq.(4.17) as a guideline to identify the weak contributions to the  $K_\theta$  parameter. The exhibited isospin symmetry between charge and neutral pion final states might be enforced on the  $\eta \rightarrow \pi\pi$  amplitudes:

$$A(\eta \rightarrow \pi^+\pi^-)_w = A(\eta \rightarrow \pi^0\pi^0)_w = \frac{4}{3}\sqrt{\frac{2}{3}}F^3\alpha(m_\eta^2) [2I_{8,27} + 3I_{8,s}], \quad (4.32)$$

if and only if we assess a specific mixing angle, i.e.,

$$\tan \varphi = -\frac{1}{2\sqrt{2}} \quad \text{or} \quad \varphi = -19.5^\circ, \quad (4.33)$$

as has been done in Ref. [176]. However, this phenomenological angle is rather problematic here, since the  $A(\eta \rightarrow \pi\pi)_w$  amplitude proportional to  $\text{Im}(x_6^*x_1)$  would then develop a pole (see Eqs.(4.14) and (C.94)). Moreover, it would also imply  $A(\eta' \rightarrow \pi^+\pi^-)_w \neq A(\eta' \rightarrow \pi^0\pi^0)_w$ . So, we find more appropriate to isolate the  $\Delta I = 0$  component of the  $\eta^{(\prime)} \rightarrow \pi\pi$  weak amplitudes:

$$A(\eta' \rightarrow \pi\pi)_w^0 = \frac{4}{3\sqrt{3}}F^3\alpha(m_{\eta'}^2) \left[ \frac{10}{3}I_{8,27}(s_\varphi + \sqrt{2}c_\varphi) - (4I_{8,27} - 9I_{8,s})\sqrt{2}c_\varphi \right], \quad (4.34a)$$

$$A(\eta \rightarrow \pi\pi)_w^0 = \frac{4}{3\sqrt{3}}F^3\alpha(m_\eta^2) \left[ \frac{10}{3}I_{8,27}(c_\varphi - \sqrt{2}s_\varphi) + (4I_{8,27} - 9I_{8,s})\sqrt{2}s_\varphi \right], \quad (4.34b)$$

leaving aside their  $\Delta I = 2$  components explicitly given by

$$\begin{aligned} A(\eta \rightarrow \pi^+ \pi^-)_w^2 &= -2 A(\eta \rightarrow \pi^0 \pi^0)_w^2 \\ &= \frac{20}{9\sqrt{3}} F^3 \alpha(m_\eta^2) I_{8,27} (c_\varphi + 2\sqrt{2} s_\varphi) \end{aligned} \quad (4.35)$$

in the case of  $\eta \rightarrow \pi\pi$ . A direct identification based now on the mixing angle dependence of Eqs.(4.17) provides then the  $\mathcal{O}(G_F^2)$  corrections to the strong P- and T- violating amplitudes :

$$\Delta_w A(\eta' \rightarrow \pi\pi) = \frac{40}{9\sqrt{3}} F^3 I_{8,27} \alpha(m_{\eta'}^2) (s_\varphi + \sqrt{2} c_\varphi) , \quad (4.36a)$$

$$\Delta_w A(\eta \rightarrow \pi\pi) = \frac{40}{9\sqrt{3}} F^3 I_{8,27} \alpha(m_\eta^2) (c_\varphi - \sqrt{2} s_\varphi) . \quad (4.36b)$$

Note that the pure  $\sin \varphi$  ( $\cos \varphi$ ) component of  $A(\eta^{(\prime)} \rightarrow \pi\pi)_w^0$  will affect contributions induced by a strong operator like the one given in Eq.(4.20).

Still, contrary to what is predicted by the strong amplitudes in Eqs.(4.17), the coefficients in front of the mixing angles in Eqs.(4.36) do not match exactly if the  $\eta$  and  $\eta'$  physical masses are enforced :

$$\alpha(m_\eta^2) = 1.62 \text{ GeV}^2 \quad \neq \quad 1.23 \text{ GeV}^2 = \alpha(m_{\eta'}^2) . \quad (4.37)$$

In other words, a 30% splitting in the effective  $\Delta_w K_\theta$  factor is obtained if the physical mass spectrum for the  $\eta(548)$ ,  $\eta'(958)$ ,  $K(498)$  and  $\pi(135)$  states is imposed. However, we have already noted that this assumption is not allowed in the truncated theory adopted here. Besides,  $\alpha(p^2)$  turns out to be rather unstable against  $p^2$  variations around the physical value of  $m_\eta^2$ . For illustration, allowing the  $\eta$  mass to be equal to the GMO prediction, i.e., 570 MeV, we obtain  $\alpha(m_{88}^2) = 1.30 \text{ GeV}^2$ , namely a value closer to  $\alpha(m_{\eta'}^2)$ . For these reasons, we use the less sensitive  $\Delta_w A(\eta' \rightarrow \pi\pi)$  amplitude to conclude that weak interactions shift  $\theta$  by the amount

$$\Delta_w \theta = \frac{2}{m_\pi^2} \Delta_w K_\theta = \frac{80}{9} \frac{\alpha(m_{\eta'}^2)}{m_\pi^2} F^4 I_{8,27} . \quad (4.38)$$

From the formal correspondence relations given in Eq.(4.30), we have in addition that

$$I_{8,27} \doteq \text{Im}(G_8^* G_{27}) = \frac{3}{10} G_F^2 \text{Im} [x_6^* (x_1 + x_2)] , \quad (4.39)$$

with the  $x_{1,2,6}$  coefficients defined at the hadronization scale, namely around  $m_{K,\pi}$ . So, at this stage, either we exploit information from the SD evolution to infer an upper bound on  $\Delta_w \theta$  or we extract these coefficients from the available data to get an estimate of it.

## An upper bound on $\Delta_w \theta$

Let us leave aside LD evolution effects by directly matching the Hamiltonians given in Eqs.(4.27) and (4.28). As far as the  $Q_6$  penguin operator is concerned, that won't do any harm since the  $\mu$  dependence of its Wilson coefficient (almost) cancels the one of the corresponding hadronic matrix element [177]. We then obtain

$$x_6 \simeq -4 \left( \frac{m_K}{1 \text{ GeV}} \right)^2 \frac{m_K^2}{[m_s + m_d]^2} [V_{ud}V_{us}^* z_6 - V_{td}V_{ts}^* y_6] , \quad (4.40)$$

with

$$z_6(1 \text{ GeV}) \simeq -0.02 , \quad y_6(1 \text{ GeV}) \simeq -0.10 \quad (4.41)$$

obtained by using the naive dimensional reduction scheme [38], and

$$(m_s + m_d)(1 \text{ GeV}) \simeq 131 \text{ MeV} , \quad (4.42)$$

by letting the lattice quark masses given in Ref. [178] evolve down to the GeV scale. Regarding the  $Q_1 + Q_2$  combination, what we know from perturbative QCD is that its Wilson coefficient smoothly decreases as  $\mu$  is decreasing (see the  $\Delta I = 1/2$  rule). Therefore, by imposing

$$x_1 + x_2 < (z_1 + z_2)(1 \text{ GeV}) \times V_{ud}V_{us}^* , \quad (4.43)$$

where

$$(z_1 + z_2)(1 \text{ GeV}) \simeq 0.76 , \quad (4.44)$$

we can infer the upper bound

$$I_{8,27} \lesssim 0.32 \times G_F^2 \times J(\delta_{\text{CKM}}) . \quad (4.45)$$

The necessity for the CKM phase to appear only through the Jarlskog invariant [179]

$$J(\delta_{\text{CKM}}) \doteq \text{Im}(V_{ts}^* V_{td} V_{ud}^* V_{us}) \quad (4.46)$$

explains, a posteriori, why one has to go to the second-order in the weak interactions to induce a correction to the physical strong  $\theta$  parameter. Such would not be the case if other sources of CP-violation beyond the SM were considered [167]. Taking  $J = (2.91_{-0.11}^{+0.19}) \times 10^{-5}$  from Ref. [17], we then infer the rather conservative bound

$$\Delta_w \theta < 6 \times 10^{-17} . \quad (4.47)$$

### An estimate of $\Delta_w\theta$

To this end, let us first extract the  $G_{8,27}$  effective couplings from the isospin decomposition of the  $K \rightarrow \pi\pi$  decay amplitudes. Following Ref. [180], the measured  $K \rightarrow \pi\pi$  decay widths are well reproduced if

$$|G_8|_{\text{exp}} = 0.77 G_F, \quad |G_{27}|_{\text{exp}} = 0.044 G_F \quad \text{and} \quad (\delta_2 - \delta_0)_{\text{exp}} = 47.5^\circ. \quad (4.48)$$

To go further and extract the imaginary part of  $G_{8,27}$  we need to consider the CP-violating observable  $\varepsilon'$ . It turns out [107] that  $\varepsilon'$  is theoretically well reproduced in the isospin limit, provided we compute the hadronic matrix elements in the large- $N_C$  limit, i.e., at the hadronization scale. It is, therefore, legitimate to expect a rather consistent and reliable estimate for  $I_{8,27}$ . As a matter of fact, we have at our disposal a CKM convention-independent direct CP-asymmetry, namely

$$\text{Re}(\varepsilon') = \frac{1}{\sqrt{2}} \text{Im} \left( \frac{A_2}{A_0} \right) \sin(\delta_2 - \delta_0), \quad (4.49)$$

from which using the usual isospin amplitudes, defined in Eqs.(C.71), we roughly get

$$I_{8,27} \simeq G_F^2 \times \text{Re}(\varepsilon'), \quad (4.50)$$

in the limit where  $\text{Im}G_8 \gg \text{Im}G_{27}$  and where  $G_{ew}$  is set to zero. To be more precise, we have to take into account the fact that the electroweak penguins interfere destructively with the strong one in  $\varepsilon'$  [180]. Including their leading effect, we can extract  $I_{8,27}$  either from  $\varepsilon'$ :

$$I_{8,27} = (1.7 \text{ to } 2.8) \times G_F^2 \times \text{Re}(\varepsilon'). \quad (4.51)$$

or from  $\text{Re}(\varepsilon'/\varepsilon)$  as done in Appendix C.4. The two extraction methods produce results that are in good agreement as the latter give the more conservative estimation  $I_{8,27} = (1.5 \text{ to } 3.9) \times G_F^2 \times \text{Re}(\varepsilon')$ . Taking  $\text{Re}(\varepsilon') = (2.5 \pm 0.4) \times 10^{-6}$  from Ref. [17], we obtain

$$\Delta_w\theta = (2.0 \text{ to } 4.6) \times 10^{-17}, \quad (4.52)$$

while using  $\text{Re}(\varepsilon'/\varepsilon)$  we rather find

$$\Delta_w\theta = (2.3 \text{ to } 5.2) \times 10^{-17}, \quad (4.53)$$

both values being compatible with the upper bound given in Eq.(4.47).

## 4.4 Conclusion

The strong CP problem, i.e., the smallness of  $\theta$ , is a long-standing one [181] and scenarios going beyond the SM have been suggested to bring it to an issue [182]. However, the status of this parameter within the SM itself is already a subject of some controversy. In this chapter, we have presented a coherent way to estimate weak interaction corrections to the strong  $\theta$  term. In the frame of a large- $N_C$  Chiral Perturbation Theory, we considered the physical  $\eta^{(\prime)} \rightarrow \pi\pi$  amplitudes. Compared to the previous quark-gluon estimates given in Refs. [167] and [168], our hadronic approach provides a direct access to the parameter  $\theta \doteq \theta_{\text{QFD}} + \theta_{\text{QCD}}$  rather than to its un-physical  $\theta_{\text{QFD}}$  and  $\theta_{\text{QCD}}$  components. We, thus, overcome phase convention issues as well as  $\alpha_s$  power counting problems. Concerning this latter point, our final result given in Eq.(4.5) is qualitatively compatible with the one of Ref. [168] given in Eq.(4.4) although, quantitatively, it rather agrees with the numerical result of Ref. [167] given in Eq.(4.3). An important point, not addressed in this work, is the possibility of infinite weak corrections to  $\theta$  as suggested in Ref. [167]. This would, however, require the study of the  $\eta^{(\prime)} \rightarrow \pi\pi$  decay amplitudes beyond the tree-level approximation considered here.

# Conclusions

The undefeated Standard Model is the best theory we have to describe the most elementary pieces of matter identified so far. This is even more true as its scalar sector, which has been hidden from us for sixty years, finally appears to be in agreement with the recent discovery of a scalar resonance at the LHC. And yet, physicists keep on trying to find something beyond. There are two main reasons for that. Firstly, we hope to open the doors of new uncharted territories waiting to be understood. Secondly, many problems are not yet successfully answered by the Standard Model.

In this thesis, we have addressed issues related to both concerns from a specific point of view, which is the typical CP violating dynamics of the Standard Model. In a nutshell, we have prepared the ground for future experimental studies of CP violating observables in radiative kaon decays, which, hopefully, will indirectly signal the presence of New Physics, and we have revisited the interplay between weak and strong interactions at play in the  $\theta_{\text{QCD}}$  parameter in an original way.

With regards to the hunt for New Physics, the news coming from the LHC are not encouraging these days. Even though this terrestrial machine probes the quantum dynamics of our world at the highest energy ever reached, it did not see any new particle yet. This lack of direct discovery is frustrating but, turned around, it might, in fact, re-enforce our interest into indirect searches. These complementary searches, which are mainly based on rare processes, are indeed very promising as they already provide severe constraints on possible New Physics models and will, for sure, benefit from future developments. However, a lot of work, both on the theoretical and on the experimental sides, is needed for these rare processes to constitute a perfect trap for New Physics. As new phenomena can manifest themselves through various portals, it is important to

get control over several rare processes, which put together, provide us with a complementary and fully constraining picture of what New Physics could be.

In this respect, we have established the cleanest Standard Model predictions of the best observables giving access to the elementary  $s \rightarrow d\gamma$  process. These results constitute the core of chapter 2. It is shown there, that we have sufficient theoretical control over the  $s \rightarrow d\gamma$  process to fully exploit the future results that will be released by several kaon decays experiments. Besides, providing new insights into our theoretical description of the low energy Standard Model dynamics, this process is complementary to  $b \rightarrow s\gamma$  and  $\mu \rightarrow e\gamma$  processes regarding the search for New Physics. We have, therefore, dedicated the third chapter of this work to a detailed analysis showing how these particular windows on  $s \rightarrow d\gamma$  should be combined with other rare processes in order to look for and/or to discriminate between New Physics effects. In other words, we have prepared the theoretical ground for a new indirect New Physics search direction.

This work does not only offer new opportunities in New Physics searches but it also suggests new ways to resolve some internal Standard Model issues. One of them being the long-standing and unfortunate lack of theoretical precision we encounter regarding  $\varepsilon'$ . As a matter of fact, in the process of improving the predictions of the  $s \rightarrow d\gamma$  probes, we were able to put forward a interesting relation between the pure QCD content of  $\varepsilon'$  and the CP violating parameter  $\varepsilon'_\perp$  occurring in  $K \rightarrow \gamma\gamma$ . Even though this parameter will be challenging to measure, its experimental determination would be extremely rewarding as it gives a direct access to the QCD-penguin induced parameter  $\xi_0$ . This quantity is the most problematic piece in the computation of  $\varepsilon'$  and, to a less dramatic extend, it also precludes a precise estimation of  $\varepsilon$ .

The second internal progress we made concerns the  $\theta$ -term. As mentioned in the introduction of the fourth chapter, the Standard Model contains in fact two sources of CP violation. The first is the complex phase of the CKM matrix whose phenomenological implications constitute the basic subject of the second chapter of this work. The second source is neither  $\theta_{\text{QCD}}$  nor  $\theta_{\text{QFD}}$  but the physical combination  $\theta = \theta_{\text{QCD}} + \theta_{\text{QFD}}$ . This distinction is primordial since  $\theta$  is the only angle that is independent of the basis chosen to describe the quark wave functions. The problem here is that, because possible solutions to the strong CP problem are based on the hypothesis that the smallness of  $\theta$  is due to the fact that it is loop induced, it is important to understand how radiative corrections and, in particular, weak radiative corrections affect  $\theta$ . This is indeed important as, in principle, even in the Standard Model, these radiative corrections might be infinite.



Previous attempts to compute these weak corrections overlooked the fact that only  $\theta$  is physical. The radiative corrections were either extracted from the quark mass matrix and, therefore, from  $\theta_{\text{QFD}}$  or they were extracted from loop induced effective  $G \cdot \tilde{G}$  operators and, therefore, from  $\theta_{\text{QCD}}$ . However, the issue of combining these results has not been addressed. This is why we have suggested a new estimation procedure that takes care of this physical requirement. The corresponding computation is detailed in chapter 4 and has several advantages compared to the previous attempts. Besides quantifying the physical corrections of the physical  $\theta$  angle, it is quite simple as it consists in the computation of simple (physical) tree-level decay amplitudes.

Let us end this conclusion by stressing the fact that, the experimental determination of the direct CP violating parameter  $\varepsilon'$  has played a crucial role in almost all the developments presented in this work. Even though, it cannot be precisely predicted from theory yet, its experimental determination already gives us some control over the basic CP violating phases present in the Standard Model and beyond. Since these CP violating quantities are involved in many other CP violating observables, numerous phenomenological links can be established with  $\varepsilon'$ . As demonstrated in this work, some of these connections are not only helpful, they are also gainful. This was, in essence, the guiding force of this work.



# Appendix **A**

## Useful formulae

### A.1 The $\Gamma(z)$ function

$\Gamma(z)$  is a special function particularly useful to compute probability amplitudes in Quantum Field Theories. Depending on the nature of its argument,  $z$ , its definition may vary. For example, if  $z$  is a non zero positive natural number  $n$  then

$$\Gamma(n) = (n - 1)! , \quad (\text{A.1})$$

while if  $z$  is a complex number, with strictly positive real part,  $\Gamma(z)$  may as well be defined by

$$\Gamma(z) = \int_0^\infty dt t^{z-1} e^{-t} .$$

Its domain can be analytically extended over the complex plan with the exception of  $z = 0$  and  $z = -n$  where  $\Gamma(z)$  has poles around which we may use the following expansions

$$\Gamma(z - n) = \frac{(-1)^n}{n!} \left[ \frac{1}{z} + \psi(n + 1) \right] + \mathcal{O}(z) ,$$

where the Digamma function  $\psi \doteq \Gamma'(z)/\Gamma(z)$  satisfies the following properties

$$\psi(1) = -\gamma , \quad \psi(z + 1) = \psi(z) + \frac{1}{z} ,$$

with  $\gamma = 0.577\dots$  the Euler-Mascheroni constant. Two of these poles,  $z = 0$  and  $z = -1$ , where

$$\Gamma(2 - d/2) = \Gamma(\epsilon/2) = + \left[ \frac{2}{\epsilon} + \psi(1) \right] + \mathcal{O}(\epsilon) , \quad (\text{A.2a})$$

$$\Gamma(1 - d/2) = \Gamma(\epsilon/2 - 1) = - \left[ \frac{2}{\epsilon} + \psi(1) + 1 \right] + \mathcal{O}(\epsilon) , \quad (\text{A.2b})$$

if

$$\epsilon \doteq 4 - d \rightarrow 0 \quad (\text{A.3})$$

will be relevant below.

## Basic integrals

As a first illustration of the  $\Gamma(z)$  utility, let us recall the integration formula of a  $d$ -dimensional solid angle  $d\Omega_d$  in spherical coordinates:

$$\int d\Omega_d = \int \prod_{k=1}^{d-1} \sin^{d-1-k} \theta_k d\theta_k = \frac{2\pi^{d/2}}{\Gamma(d/2)} \quad (\text{A.4})$$

and the integral definition of the Beta function  $B(p, q)$ ,

$$\begin{aligned} B(p, q) &\doteq \int_0^\infty dt \frac{t^{p-1}}{(1+t)^{p+q}} = \int_0^1 du u^{p-1} (1-u)^{q-1} \\ &= \frac{\Gamma(p)\Gamma(q)}{\Gamma(p+q)} , \end{aligned} \quad (\text{A.5})$$

particularly useful to integrate ratios of polynomials.

## Feynman parametrization

The gamma function also steps in the Feynman combination of denominator as:

$$\prod_{i=1}^N \frac{1}{a_i^{\alpha_i}} = \frac{\Gamma(\alpha)}{\prod_{i=1}^N \Gamma(\alpha_i)} \int_0^1 \left( \prod_{i=1}^N dx_i x_i^{\alpha_i-1} \right) \frac{\delta(1-x)}{[\sum_{i=1}^N x_i a_i]^\alpha} ,$$

with  $\alpha = \sum_{i=1}^N \alpha_i$  and  $x = \sum_{i=1}^N x_i$  where  $x_i$  are Feynman parameters. In the following, we use the following cases:

$$\frac{1}{a_1 a_2} = \int_0^1 dx \frac{1}{[x a_1 + (1-x) a_2]^2}, \quad (\text{A.6a})$$

$$\frac{1}{a_1 a_2 a_3} = 2 \int_0^1 dx \int_0^{1-x} dy \frac{1}{[x a_1 + y a_2 + (1-x-y) a_3]^3}. \quad (\text{A.6b})$$

## A.2 Dilogarithmic functions

Polylogarithms of arbitrary order  $s$  are defined by the series

$$\text{Li}_s(z) = \sum_{k=1}^{\infty} \frac{z^k}{k^s},$$

where  $z$  is a complex number such that  $|z| < 1$ . By analytic continuation it is, however, possible to define  $\text{Li}_s(z)$  for  $|z| \geq 1$ . The dilogarithm function is the  $s = 2$  polylogarithm defined by

$$\begin{aligned} \text{Li}_2(z) &= - \int_0^z \frac{dt}{t} \ln(1-t) = - \int_0^1 \frac{dt}{t} \ln(1-zt) \\ &= \sum_{n=1}^{\infty} \frac{z^n}{n} \int_0^1 dt t^{n-1} = \sum_{n=1}^{\infty} \frac{z^n}{n^2}, \end{aligned}$$

where we used the expansion  $-\ln(1-z) = \sum_{n=1}^{\infty} z^n/n$  valid for  $|z| \leq 1$ . The integral definition makes perfect sense as long as  $\text{Im}z \neq 0$ . However, on the real axis the logarithm has a branch cut on  $1 \leq x < +\infty$  where the logarithm has to be analytically continued in order for the integral definition to make sense. Yet, the dilogarithm itself is well defined all over the complex plane. To illustrate this, let us consider the following functional relation

$$\text{Li}_2(z) + \text{Li}_2\left(\frac{z}{z-1}\right) = -\frac{1}{2} \ln^2(1-z), \quad (\text{A.7})$$

valid for any complex number  $z$ . If  $z$  is real and bigger than 1, the right hand side of Eq.(A.7) involves a logarithm evaluated on its branch cut. In order to make sense, the logarithm should be analytically continued for  $\text{Li}_2(z)$  to acquire an imaginary part over the logarithm branch cut. It is, therefore, worth to recall some of the properties of logarithms of complex argument. If  $a$  and  $b$  are complex numbers, then

$$\begin{aligned} \ln(ab) &= \ln(a) + \ln(b) & \text{if } \text{Im}(a)\text{Im}(b) < 0, \\ \ln(a/b) &= \ln(a) - \ln(b) & \text{if } \text{Im}(a)\text{Im}(b) > 0, \end{aligned} \quad (\text{A.8})$$

whereas for real and positive  $z$  and  $\epsilon$  we have

$$\ln(-z \pm i\epsilon) = \ln|z| \pm i\pi, \quad (\text{A.9})$$

provided that  $\epsilon \rightarrow 0$ . Logarithms of complex argument may be related to reciprocal trigonometric functions. For example,

$$\begin{aligned} \arctan z &= \frac{i}{2} [\ln(1 - iz) - \ln(1 + iz)] \\ &= \arccos \frac{1}{\sqrt{1+z^2}} = \frac{\pi}{2} - \arcsin \frac{1}{\sqrt{1+z^2}}. \end{aligned} \quad (\text{A.10})$$

### A.3 Scalar one-loop functions

#### The $A_0$ function

The simplest Passarino-Veltman scalar function  $A_0$  is defined in four and  $d$ -dimension by

$$A_0(m^2) \doteq -\frac{i}{\pi^2} \int \frac{d^4\ell}{\ell^2 - m^2} \rightarrow \frac{(2\pi\mu)^\epsilon}{i\pi^2} \int \frac{d^d\ell}{\ell^2 - m^2},$$

where the arbitrary mass scale  $\mu$  is introduced to maintain the dimension of the integral. In four dimensions,  $A_0(m^2)$  has mass dimension two and the integration over the four momentum (pseudo-)norm is not defined such that  $A_0(m^2)$  diverges. Indeed, in the Euclidian space, reached using the Wick rotation defined by the variable change

$$\ell^0 \rightarrow iK^0 \quad \text{and} \quad \ell^i \rightarrow K^i,$$

$A_0$  assumes the following form

$$A_0(m^2) = -\frac{m^2}{2\pi^2} \left(\frac{2\pi\mu}{m}\right)^\epsilon \left[ \int d\Omega_d \right] \left[ \int_0^\infty dt \frac{t^{1-\epsilon/2}}{1+t} \right],$$

where  $m^2 t \doteq K^2 = K^0 K^0 + K^i K^i > 0$ . Using Eqs.(A.4) and (A.5) we obtain

$$A_0(m^2) = -m^2 \left(\frac{2\sqrt{\pi}\mu}{m}\right)^\epsilon \Gamma(\epsilon/2 - 1),$$

which diverges since  $\Gamma(\epsilon/2 - 1)$  diverges as  $\epsilon \rightarrow 0$ . Combining the expansion Eq.(A.2b) with

$$a^\epsilon = \sum_{i=0}^{\infty} \frac{\epsilon^i}{i!} \log^i a = 1 + \epsilon \log a + \mathcal{O}(\epsilon^2), \quad (\text{A.11})$$

this divergence is isolated as

$$A_0(m^2) = m^2 \left[ D_\epsilon + 1 - \log \left( \frac{m^2}{\mu^2} \right) \right] , \quad (\text{A.12})$$

where we defined

$$D_\epsilon \doteq \frac{2}{\epsilon} + \psi(1) + \log 4\pi = \frac{2}{\epsilon} + \log 4\pi e^{-\gamma} .$$

## The $B_0$ function

Another interesting scalar integral,  $B_0$ , is defined in  $d$ -dimensions by

$$B_0((p+q)^2, m_i^2, m_j^2) \doteq \frac{(2\pi\mu)^\epsilon}{i\pi^2} \int \frac{d^d\ell}{[(\ell+q)^2 - m_i^2][(\ell-p)^2 - m_j^2]} ,$$

where without loss of generality and for further convenience, we introduced the four momentum  $q$ , which satisfies  $q^2 = 0$ . Since it has mass dimension zero,  $B_0$  diverges. Using the parametrization of Eq.(A.6a) we may write

$$B_0((p+q)^2, m_i^2, m_j^2) = \frac{(2\pi\mu)^\epsilon}{i\pi^2} \int_0^1 dx \int \frac{d^d\ell}{[\ell^2 - \Delta]^2} ,$$

where

$$\Delta = x(x-1)p^2 + xm_j^2 + (1-x)m_i^2 - 2x(1-x)p \cdot q .$$

Applying the same manipulations used for  $A_0$  we find

$$B_0((p+q)^2, m_i^2, m_j^2) = \frac{\Gamma(\epsilon/2)}{\Gamma(2)} \int_0^1 dx \left( \frac{2\sqrt{\pi}\mu}{\sqrt{\Delta}} \right)^\epsilon ,$$

which, expanded around  $\epsilon = 0$  using Eqs.(A.2a) and (A.11), leads to

$$B_0((p+q)^2, m_i^2, m_j^2) = D_\epsilon - \int_0^1 dx \log \left[ \frac{x(x-1)(p^2 + 2p \cdot q) + (1-x)m_i^2 + xm_j^2}{\mu^2} \right] . \quad (\text{A.13})$$

The usual  $B_0(p^2, m_i^2, m_j^2)$  function is then obtained from Eq.(A.13) imposing  $q = 0$  and satisfies

$$B_0(p^2, m_i^2, m_j^2) = B_0(p^2, m_j^2, m_i^2) ,$$

$$B_0(0, m_i^2, m_j^2) = \frac{A_0(m_i^2) - A_0(m_j^2)}{m_i^2 - m_j^2} ,$$

as well as

$$B_0(m^2, 0, m^2) - 1 = B_0(0, 0, m^2) = \frac{A_0(m^2)}{m^2} = B_0(0, m^2, m^2) + 1.$$

The integration over the Feynman parameter  $x$  in Eq.(A.13) can be performed analytically, see e.g. Ref. [183].

## The $C_0$ function

The first non divergent one-loop scalar function in four dimensions is called  $C_0$  and has the dimension of an inverse mass squared. In the present work we are not interested in its most general form but in the simplified case where

$$C_0(p^2, (p+q)^2, m_j^2, m_i^2) \doteq \frac{1}{i\pi^2} \int \frac{d^4\ell}{[\ell^2 - m_i^2][(\ell+q)^2 - m_i^2][(\ell-p)^2 - m_j^2]},$$

with  $q^2 = 0$ . Here, it is important to recall that the  $i\epsilon$  prescription, defined by the pole mass shifts

$$m_i^2 \rightarrow m_i^2 - i\epsilon,$$

is implicitly understood. Using Eq.(A.6b) and applying the Wick rotation we obtain

$$C_0(p^2, (p+q)^2, m_j^2, m_i^2) = \frac{1}{2p \cdot q} \times \int_0^1 \frac{dx}{x} \ln \left( \frac{x(x-1)(p^2 + 2p \cdot q) + (1-x)m_i^2 + xm_j^2}{x(x-1)p^2 + (1-x)m_i^2 + xm_j^2} \right). \quad (\text{A.14})$$

To our knowledge, this integral has never been performed analytically unless further assumptions are made. Numerical evaluations are, however, easy to perform.

## A.4 Particular one-loop functions

This section is devoted to the calculation of two kinds of loop functions, which intervene in radiative decays. These functions are finite combinations of the  $A_0$ ,  $B_0$  and  $C_0$  functions presented above and will be expressed in terms of the reduced variables

$$z \doteq \frac{2p \cdot q}{m^2}, \quad r_i \doteq \frac{m_i}{m}, \quad a \doteq \frac{z}{r_i^2}, \quad (\text{A.15})$$



and

$$\beta_i \doteq \sqrt{1 - 4r_i^2}, \quad \beta_i(z) \doteq \sqrt{1 - \frac{4r_i^2}{1 + 2z}}.$$

## The $\mathcal{F}$ function

The function  $\mathcal{F}$  appears in decay amplitude whose final state contains at least two photons,  $K \rightarrow \gamma\gamma$  being an example of such decays. It is constructed from the  $C_0$  function

$$I_{\mathcal{F}} \doteq C_0(0, zm^2, m_i^2, m_i^2) = \frac{1}{zm^2} \int_0^1 \frac{dx}{x} \log[1 + x(x-1)a], \quad (\text{A.16})$$

obtained from Eq.(A.14) imposing  $p^2 = 0$ , where  $z$  is a kinematic variable:  $0 \leq z \leq z_{\max}$  with  $z_{\max}$  a finite real number. If we split the logarithm argument in Eq.(A.16) as

$$1 + x(x-1)a = (1 - x_+x)(1 - x_-x),$$

it is easy to realize that the numbers

$$x_{\pm} = \frac{2}{1 \pm \sqrt{1 - 4/a}},$$

related to each other as

$$x_{\pm} = \frac{x_{\mp}}{x_{\mp} - 1},$$

are complex since the  $i\epsilon$  prescription gives to  $a$  an imaginary part, which can be explicitly recovered using

$$a \rightarrow a + i\epsilon',$$

where  $\epsilon' > 0$ . It is as easy to notice that  $\text{sign}(\text{Im}x_{\mp}) = \pm \text{sign}(\epsilon) = \pm 1$  whatever the value of  $a$ . We may, therefore, use Eq.(A.8) with Eq.(A.7) to conclude that

$$I_{\mathcal{F}} = -\frac{1}{zm^2} [\text{Li}_2(x_+) + \text{Li}_2(x_-)] = \frac{1}{2zm^2} \ln^2(1 - x_+)$$

or, equivalently, that

$$I_{\mathcal{F}} = \frac{1}{2zm^2} \ln^2 \left( -\frac{1 - \sqrt{1 - 4/a}}{1 + \sqrt{1 - 4/a}} \right). \quad (\text{A.17})$$

The  $i\epsilon$  prescription now acquires its full interest. If  $\epsilon = 0$ , the last expression is undetermined for  $a \geq 4$ , since the argument of the logarithm is negative. However, for  $\epsilon \neq 0$  the same argument has a positive imaginary part, say  $i\eta$ , thanks to which Eq.(A.9) may be applied to find

$$\begin{aligned} I_{\mathcal{F}} &\stackrel{i\epsilon}{=} \frac{1}{2zm^2} \ln^2 \left( -\frac{1 - \sqrt{1 - 4/a}}{1 + \sqrt{1 - 4/a}} + i\eta \right) \\ &= \frac{1}{2zm^2} \left[ \ln \left( \frac{1 - \sqrt{1 - 4/a}}{1 + \sqrt{1 - 4/a}} \right) + i\pi \right]^2, \end{aligned} \quad (\text{A.18})$$

in the limit where  $\eta$  (or equivalently  $\epsilon$ ) is eventually sent to zero. In the complementary case where  $0 \leq a < 4$ , Eq.(A.17) is perfectly well defined even if we assume that  $\epsilon = 0$  from the beginning because  $\sqrt{1 - 4/a}$  is now imaginary. In that case, using Eqs.(A.8) we get

$$I_{\mathcal{F}} = \frac{1}{2zm^2} \left[ i(2k+1)\pi + \ln(1 - i\sqrt{4/a-1}) - \ln(1 + i\sqrt{4/a-1}) \right],$$

with  $k \geq 0$  an undetermined integer. Using Eq.(A.10), this expression further simplifies into

$$I_{\mathcal{F}} = -\frac{2}{zm^2} \left[ \arcsin \sqrt{a}/2 + k\pi \right]^2. \quad (\text{A.19})$$

Of course, both Eq.(A.18) and Eq.(A.19) originate from the same number, namely, that of Eq.(A.17). This is only when  $a$  ends up on one or an other interval of the real axis that  $I_{\mathcal{F}}$  may either be given by Eq.(A.18) or Eq.(A.19). But, if  $a$  is complex, this distinction is irrelevant so that both Eq.(A.18) and Eq.(A.19) give the same value: the one given by Eq.(A.17). Therefore, equating Eq.(A.19) with Eq.(A.17) anywhere in the complex plane, but on real axis, forces  $k$  to vanish so that  $I_{\mathcal{F}}$  is now defined everywhere on the real axis. We can now introduce the  $\mathcal{F}$  function defined by

$$\begin{aligned} \mathcal{F}(a) &\doteq 1 + 2m_i^2 I_{\mathcal{F}} \\ &= \begin{cases} 1 - \frac{4}{a} \arcsin^2 \sqrt{a}/2 & 0 \leq a < 4, \\ 1 + \frac{1}{a} \left[ \ln \left( \frac{1 - \sqrt{1 - 4/a}}{1 + \sqrt{1 - 4/a}} \right) + i\pi \right]^2 & 4 \leq a, \end{cases} \end{aligned} \quad (\text{A.20})$$

and displayed in Fig.(A.1).

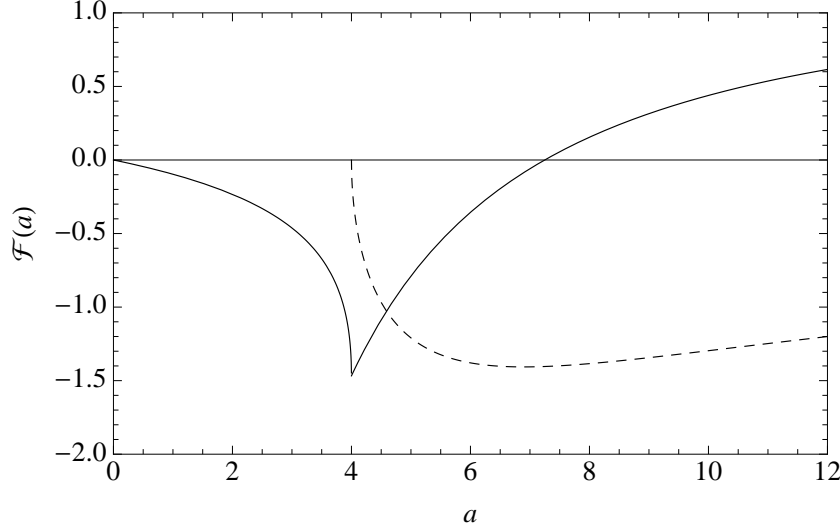


**Fig. A.1:** The plain line tending towards 1 at infinity represents  $\text{Re}\mathcal{F}(a)$  whilst the dashed line tending towards zero at infinity represents  $\text{Im}\mathcal{F}(a)$ .

## The $h_{ij}$ functions

The basic loop functions appearing in  $K \rightarrow \pi\pi\gamma$  decays are presented in this section. These functions are given by

$$h_{ij}(z) \doteq \frac{1}{4z} \left[ f_1^{ij}(z) + f_2^{ij}(z) + f_3^{ij}(z) \right] , \quad (\text{A.21})$$

where the separately finite  $f_k^{ij}$  functions are given by

$$f_1^{ij}(z) = -2m_i^2 C_0(p^2, zm_K^2 + p^2, m_j^2, m_i^2) , \quad (\text{A.22a})$$

$$f_2^{ij}(z) = \frac{p^2 + m_i^2 - m_j^2 + zm_K^2}{2zm_K^2} \times \\ \times \left[ B_0(p^2, m_i^2, m_j^2) - B_0(zm_K^2 + p^2, m_i^2, m_j^2) \right] , \quad (\text{A.22b})$$

$$f_3^{ij}(z) = -1 + \frac{1}{p^2} (A_0(m_i^2) - A_0(m_j^2)) - \\ - \frac{m_i^2 - m_j^2}{p^2} B_0(p^2, m_i^2, m_j^2) . \quad (\text{A.22c})$$

Even though they all have a pole at  $z = 0$ , once combined together to define  $h_{ij}(z)$ , no  $z$  pole remains:

$$\lim_{z \rightarrow 0} h_{ij}(z) = \text{constant} . \quad (\text{A.23})$$

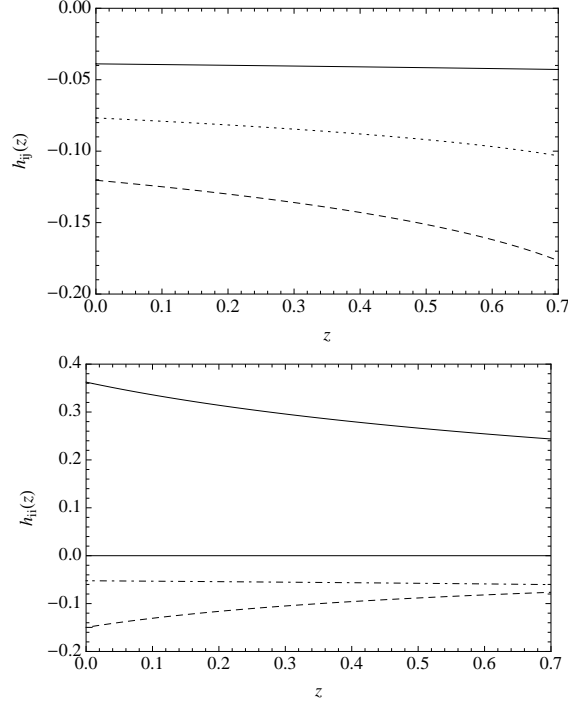


**Fig. A.2:** On the top, we plotted  $h_{\eta K}$  in plain,  $h_{\pi K}$  in dashed and  $h_{K\pi}$  in dotted line. On the bottom, are shown  $\text{Re}h_{\pi\pi} > 0$  in plain,  $\text{Im}h_{\pi\pi}$  in dashed and  $h_{KK}$  in dotted-dashed line.

When  $m_i = m_j$ , the integration over the Feynman parameters can be performed analytically and gives

$$h_{ii}(z) = \frac{r_i^2}{8z^2} \left[ \ln^2 \left( \frac{\beta_i + 1}{\beta_i - 1} \right) - \ln^2 \left( \frac{\beta_i(z) + 1}{\beta_i(z) - 1} \right) + \frac{1 + 2z}{r_i^2} \left[ \beta_i(z) \ln \left( \frac{\beta_i(z) + 1}{\beta_i(z) - 1} \right) - \beta_i \ln \left( \frac{\beta_i + 1}{\beta_i - 1} \right) \right] - \frac{2z}{r_i^2} \right] \quad (\text{A.24})$$

where  $p^2 = m_K^2$ . The  $h_{ij}(z)$  with  $i \neq j$ , defined for  $p^2 = m_\pi^2$ , are evaluated numerically and displayed in Fig.(A.2).

# Appendix B

## Effective Lagrangians

In this section, various effective Lagrangians used in this work are presented. In order to shorten the notations, we define the following objects

$$\begin{aligned} \chi_{\pm} &\doteq U^\dagger \chi \pm \chi^\dagger U, & f_{\pm}^{\mu\nu} &\doteq F_L^{\mu\nu} \pm U^\dagger F_R^{\mu\nu} U, \\ \tilde{F}_{L(R)}^{\mu\nu} &\doteq \epsilon^{\mu\nu\rho\sigma} F_{L(R)\rho\sigma}, & \tilde{f}_{\pm}^{\mu\nu} &\doteq \epsilon^{\mu\nu\rho\sigma} f_{\pm\rho\sigma}, \end{aligned}$$

and collect important constants in Tab.(B.1).

$i$	$\Gamma_i^L$	$\Gamma_i^N$	$\Gamma_i^D$	$\Gamma_i^Z$	$i$	$\Gamma_i^L$	$\Gamma_i^N$	$\Gamma_i^D$	$\Gamma_i^Z$
1	—	—	-1/6	-3/2	10	-1/4	2/3	—	—
2	—	—	0	-1	11	-1/8	-13/18	—	—
3	—	—	—	—	12	—	-5/12	—	—
4	1/8	—	3	—	13	—	0	8/3	-1
5	3/8	3/2	1	—	14	—	1/4	-4/3	—
6	11/144	-1/4	-3/2	-3/2	15	—	1/2	4/3	—
7	0	-9/8	1	—	16	—	-1/4	0	—
8	5/48	-1/2	—	—	17	—	0	—	—
9	1/4	3/4	—	-2	18	—	-1/8	—	—

**Tab. B.1:** Specification of the renormalization constant factor  $\Gamma_i^X$  ( $X = L, N, D, Z$ ).

## B.1 Effective QCD at $\mathcal{O}(p^4)$

The effective strong Lagrangian at  $\mathcal{O}(p^4)$  is expanded over twelve independent operators [184]

$$\begin{aligned} \mathcal{L}_s^{(4)} = & L_4 \langle D_\mu U^\dagger D^\mu U \rangle \langle \chi^\dagger U + \chi U^\dagger \rangle + L_5 \langle D_\mu U^\dagger D^\mu U (\chi^\dagger U + \chi U^\dagger) \rangle + \\ & + L_6 \langle \chi^\dagger U + \chi U^\dagger \rangle^2 + L_7 \langle \chi^\dagger U - \chi U^\dagger \rangle^2 + L_8 \langle \chi^\dagger U \chi^\dagger + \chi U^\dagger \chi U^\dagger \rangle + \\ & - i L_9 \langle F_R^{\mu\nu} D_\mu U D_\nu U^\dagger + F_L^{\mu\nu} D_\mu U^\dagger D_\nu U \rangle + L_{10} \langle U^\dagger F_R^{\mu\nu} U F_{L\mu\nu} \rangle + \\ & + L_{11} \langle F_{R\mu\nu} F_R^{\mu\nu} + F_{L\mu\nu} F_L^{\mu\nu} \rangle + L_{12} \langle \chi \chi^\dagger \rangle + \text{h.c.} \end{aligned} \quad (\text{B.1})$$

It is worth noting that all the divergences appearing at NLO can be re-absorbed in the bare  $L_i$ , appearing in  $\mathcal{L}_s^{(4)}$ . Using dimensional regularization, all the strong divergences appearing at one-loop are absorbed by the bare  $L_i$  as

$$L_i = L_i^r(\mu) + \Gamma_i^L \Lambda(\mu) ,$$

with

$$\begin{aligned} \Lambda(\mu) & \doteq \frac{\mu^{d-4}}{(4\pi)^2} \left\{ \frac{1}{d-4} - \frac{1}{2} (\ln 4\pi + 1 + \Gamma'(1)) \right\} \\ & = - \frac{\mu^\epsilon}{2(4\pi)^2} \{D_\epsilon + 1\} , \end{aligned} \quad (\text{B.2})$$

where the  $\Gamma_i^L$  are specified in Tab.(B.1).

## B.2 The Wess-Zumino-Witten Lagrangian

A nice presentation of the problem is due to Witten [67] and goes as follows. Let us call the *outer* parity transformation of space-time coordinates,  $(\vec{x}, t) \leftrightarrow (-\vec{x}, t), P_0$ . This external symmetry does not affect the scalar fields  $\phi^a$  contained in  $U$  such that under  $P_0$  we have  $\phi^a \leftrightarrow \phi^a$  or equivalently  $U \leftrightarrow U$ . The *inner* parity transformation, which leaves the space-time coordinates unchanged but acts on the pseudo-scalar field as  $\phi^a \leftrightarrow -\phi^a$  (or equivalently  $U \leftrightarrow U^\dagger$ ) is called  $(-1)^{N_B}$  because once applied to a state formed by  $N_B$  mesons its eigenvalue is  $(-1)^{N_B}$ . As a matter of fact, the parity transformation under which QCD remains invariant, is neither  $P_0$  nor  $(-1)^{N_B}$  but rather  $P = P_0(-1)^{N_B}$ . It is then expected from its effective representation to respect the exact same symmetry. However, in the CP conserving limit, it is easy to observe that  $\mathcal{L}_s^{(2)}$  given in Eq.(1.46) is invariant under both  $P_0$  and  $(-1)^{N_B}$  separately. In particular, its  $(-1)^{N_B}$  invariance implies that  $A(\pi^0 \rightarrow \gamma\gamma) = 0$  while

this particular process is the dominant decay channel of the neutral pion [17]:  $\text{Br}(\pi^0 \rightarrow \gamma\gamma)_{\text{exp}} = (98.823 \pm 0.034)\%$ .

The resolution of this paradox lies in the chiral anomaly of QCD [185]. In fact, a non-abelian Yang-Mills theory, which contains only vector gauge fields (as is the case of QCD) carries the non-abelian axial anomaly given by

$$D_\mu j_A^{a\mu} = \frac{1}{(4\pi)^2} \text{Tr}(T^a \tilde{F}_{\mu\nu} F_{\rho\sigma}) ,$$

where the axial vector current is given by  $j_5^{a\mu} = \bar{q} T^a \gamma^\mu \gamma_5 q$ . At the effective level, this anomaly is represented by an anomalous symmetry breaking term which, in the context of the present work, is truncated to the Lagrangian shifts [66, 67, 114]

$$\mathcal{L}_s^{(2)} \rightarrow \mathcal{L}_s^{(2)} + \mathcal{L}_{\text{WZW}}^{1\gamma} + \mathcal{L}_{\text{WZW}}^{2\gamma} ,$$

where

$$\mathcal{L}_{\text{WZW}}^{1\gamma} \doteq \frac{N_c}{48\pi^2} e \epsilon^{\mu\nu\rho\sigma} A_\mu \langle \partial_\nu U \partial_\rho^\dagger \partial_\sigma U \{U^\dagger, Q\} \rangle , \quad (\text{B.3a})$$

$$\begin{aligned} \mathcal{L}_{\text{WZW}}^{2\gamma} \doteq & \frac{iN_c}{48\pi^2} e^2 \epsilon^{\mu\nu\rho\sigma} F_{\mu\nu} A_\rho \left( \langle QQ \{ \partial_\sigma U, U^\dagger \} \rangle + \right. \\ & \left. + \frac{1}{2} \langle QU^\dagger Q \partial_\sigma U - QUQ \partial_\sigma U^\dagger \rangle \right) , \end{aligned} \quad (\text{B.3b})$$

where only the QED contribution is kept.

### B.3 Effective $|\Delta S| = 1$ sector

In order to construct the chiral realization of the four-quark operators, we need to determine their chiral symmetry properties first. So, if  $q = \{u, d, s\}$  is considered as a  $U(3)$  triplet, the quark bilinear  $u_j^i \doteq \bar{q}^i \Gamma q^j$ , where  $\Gamma$  stands for any Lorentz structures, transforms as a nonet,  $9 = 8 \oplus 1$ , of  $U(3)$ . Therefore, as any of the four-quark operator can be represented by a symmetric direct product  $u_j^i v_l^k \sim 9 \otimes 9$ , we can conclude that they transform either as irreducible symmetric octets or as an irreducible symmetric 27-plets of  $SU(3)$ :

$$(8 \otimes 8)_S = 27_S \oplus 8_S \oplus 1_S .$$

The singlet can be discarded as we are here interested in flavor violating operators only. The explicit construction of the 27-plet in terms of  $U(3)$  nonet is a bit tricky.

## The 27-plet

This traceless and symmetric tensor may be written in terms of two nonets  $u$  and  $v$  as

$$\begin{aligned}
27_{jl}^{ik} = & \frac{1}{4}(u_j^i v_l^k + u_j^k v_l^i + u_l^i v_j^k + u_l^k v_j^i) - \\
& - \frac{1}{20} \left[ \delta_j^i (\langle u \rangle v_l^k + u_l^k \langle v \rangle + u_l^x v_x^k + u_x^k v_l^x) + \right. \\
& + \delta_l^k (\langle u \rangle v_j^i + u_j^i \langle v \rangle + u_j^x v_x^i + u_x^i v_j^x) + \\
& + \delta_l^i (\langle u \rangle v_j^k + u_j^k \langle v \rangle + u_j^x v_x^k + u_x^k v_j^x) + \\
& \left. + \delta_j^k (\langle u \rangle v_l^i + u_l^i \langle v \rangle + u_l^x v_x^i + u_x^i v_l^x) \right] + \\
& + \frac{1}{40} (\delta_j^i \delta_l^k + \delta_l^i \delta_j^k) (\langle u \rangle \langle v \rangle + u_x^x v_x^x) .
\end{aligned} \tag{B.4}$$

The members of this multiplet are able to generate  $\Delta F = 0, \pm 1, \pm 2$  flavor violating interactions. Here, we are interested in the most general operator  $\mathcal{O}_{27}$  that generates  $\Delta S(D) = +1(-1)$  transitions where  $S = -1$  is the strangeness of the  $s$ -quark and  $D = +1$  is the flavor of the  $d$ -quark. We are, thus, looking for a 27-plet operators that turns a  $d$  quark into a  $\bar{s}$  quark. The most general  $\mathcal{O}_{27}$  operator is given by a linear combination of the elements

$$27_{21}^{31}, 27_{22}^{32}, 27_{23}^{33}$$

and their symmetric as all satisfy  $\Delta S(D) = +1(-1)$ . However, since they belong to the same multiplet, these elements are interchangeable, i.e.,  $\mathcal{O}_{27}$  should be invariant under the exchange of, say,  $27_{21}^{31}$  and  $27_{21}^{13}$ . In practice it means that all the  $\Delta S(D) = +1(-1)$  elements should appear weighted by the same coupling, say  $a$ , in the linear combination that constitutes  $\mathcal{O}_{27}$ . In other words,

$$\mathcal{O}_{27} = a [2 27_{22}^{32} + 2 27_{23}^{33} + 4 27_{21}^{31}] . \tag{B.5}$$

In the particular case where  $v = u$ , a re-scaling of the coupling  $a$  to  $G_{27}$ , together with Eq.(B.4), give

$$\mathcal{O}_{27} = G_{27} \left[ u_2^3 u_1^1 + \frac{2}{3} u_1^3 u_2^1 - \frac{1}{3} u_2^3 \langle u \rangle \right] .$$

Under this form,  $\mathcal{O}_{27}$  is general enough to describe both  $SU(3)$  and  $U(3)$  cases. Indeed in the former case we have automatically  $\langle u \rangle = 0$ . As a matter of fact, the operator  $\mathcal{O}_{27}$  can be further decomposed into more fundamental building



blocks. This second decomposition is based upon the fact that  $u$  and  $d$  quarks are members of an isospin doublet. To see this, let us write

$$\mathcal{O}_{27} = G_{27\bar{s}} \left[ \frac{1}{2}(d\bar{u}u - d\bar{d}d) + \frac{2}{3}u\bar{u}d + \frac{1}{6}d(\bar{u}u + \bar{d}d - 2\bar{s}s) \right], \quad (\text{B.6})$$

keeping in mind that  $q$  always connects with its immediate right-neighbor to form a  $u_j^i$  nonet. Recalling that  $s$  is an isospin 0 state, while  $\bar{u}u + \bar{d}d$  is an isospin 0 one, we observe that the isospin of the third term in Eq.(B.6) is fixed by that of the overall  $d$ -quark, namely,  $I = 1/2$ . On the other hand, the first two terms happen to be mixtures of  $I = 1/2$  and  $3/2$  states. Indeed, the direct isospin product  $1 \otimes \frac{1}{2}$  contains two states with definite isospin, namely,

$$\begin{aligned} |3/2, -1/2\rangle &= \frac{1}{\sqrt{3}}(d\bar{u}u - d\bar{d}d + u\bar{u}d) \doteq \frac{1}{\sqrt{2}}A, \\ |1/2, -1/2\rangle &= \sqrt{\frac{2}{3}}(d\bar{u}u - d\bar{d}d - 2u\bar{u}d) \doteq \sqrt{\frac{2}{3}}B, \end{aligned}$$

upon which the first two terms of Eq.(B.6) can be expanded as

$$\frac{1}{2}(d\bar{u}u - d\bar{d}d) + \frac{2}{3}u\bar{u}d = \frac{5}{9}A - \frac{1}{18}B.$$

Collecting the various  $I = 1/2$  and  $I = 3/2$  components together, we conclude that  $\mathcal{O}_{27}$  may as well be written as

$$\mathcal{O}_{27} = \left[ \frac{5}{9}G_{27}^{3/2}\mathcal{O}_{27}^{3/2} + \frac{1}{9}G_{27}^{1/2}\mathcal{O}_{27}^{1/2} \right], \quad (\text{B.7})$$

with

$$\begin{aligned} \mathcal{O}_{27}^{3/2} &\doteq u_1^3u_2^1 + u_2^3(u_1^1 - u_2^2), \\ \mathcal{O}_{27}^{1/2} &\doteq u_1^3u_2^1 + u_2^3(4u_1^1 + 5u_2^2) - 3u_2^3\langle u \rangle, \end{aligned}$$

where the possibility of an isospin breaking of  $G_{27}$  is assumed. It is sometimes useful to write these 27-plet operators in the form a tensor contraction

$$\mathcal{O}_{27}^I = \mathcal{T}_{ij;kl} u_j^i u_l^k, \quad (\text{B.8})$$

where

$$\mathcal{T}_{ij;kl} \doteq \left[ \frac{5}{9}G_{27}^{3/2}T_{ij;kl}^{3/2} + \frac{1}{9}G_{27}^{1/2}T_{ij;kl}^{1/2} \right], \quad (\text{B.9})$$

such that any 27-plet object with isospin  $I$  may be obtained from the contraction of the  $T^I$  tensors with two nonets. The non vanishing components of these tensors being

$$T_{31;12}^{3/2} = T_{32;11}^{3/2} = -T_{32;22}^{3/2} = +1$$

and

$$T_{31;12}^{1/2} = T_{32;11}^{1/2} = \frac{1}{2}T_{32;22}^{1/2} = -\frac{1}{3}T_{32;33}^{1/2} = +1 .$$

Another parametrization extensively used in the present work is based on the following projection technique. If we define

$$(\lambda_{ij})_{ab} \doteq \delta_{ib}\delta_{ja} ,$$

then for any  $3 \times 3$  matrix  $A$

$$\langle \lambda_{ij} A \rangle = A_{ij} .$$

These projecting matrices  $\lambda$  can be expressed in terms of the Gell-Mann matrices :

$$\begin{aligned} \lambda_{11} &= \frac{1}{\sqrt{6}} \left( \lambda_0 + \sqrt{\frac{3}{2}}\lambda_3 + \frac{1}{\sqrt{2}}\lambda_8 \right), & \lambda_{33} &= \frac{1}{\sqrt{6}}(\lambda_0 - \sqrt{2}\lambda_8), \\ \lambda_{22} &= \frac{1}{\sqrt{6}} \left( \lambda_0 - \sqrt{\frac{3}{2}}\lambda_3 + \frac{1}{\sqrt{2}}\lambda_8 \right), & & \\ \lambda_{12} &= \frac{1}{2}(\lambda_1 + i\lambda_2), & \lambda_{21} &= \frac{1}{2}(\lambda_1 - i\lambda_2), & \lambda_{13} &= \frac{1}{2}(\lambda_4 + i\lambda_5), \\ \lambda_{31} &= \frac{1}{2}(\lambda_4 - i\lambda_5), & \lambda_{23} &= \frac{1}{2}(\lambda_6 + i\lambda_7), & \lambda_{32} &= \frac{1}{2}(\lambda_6 - i\lambda_7), \end{aligned} \tag{B.10}$$

where  $\lambda_8$  may also be expressed in terms of the electric charge matrix  $Q = \text{diag}(2/3, -1/3, -1/3)$  as

$$\lambda_8 = 2\sqrt{3}\left(Q - \frac{1}{2}\lambda_3\right) .$$

These results are very useful to construct and understand the effective representation of  $(27_L, 1_R)$  weak interactions detailed in the next section. However, we stress the fact that many other operators with different flavor structures can be built from Eq.(B.4). As another well known example, we find the most general  $\Delta S(D) = +2(-2)$  operators which, using the same normalization as in Eq.(B.5), reads

$$\mathcal{O}_{27}^{\Delta S=2} = G_{27} \frac{5}{6} u_2^3 u_2^3 .$$

### B.3.1 The effective Lagrangian at $\mathcal{O}(p^2)$

In this section we give the hadronic realization of the effective  $H^{\Delta S=1}$  Hamiltonian given in Eq.(1.33). The four quarks operators are, there, products of left- or right-handed currents. At the hadronic level, the simplest objects that transform accordingly are the left- and right-handed currents

$$L_\mu = U^\dagger D_\mu U \quad \text{and} \quad R_\mu = U D_\mu U^\dagger .$$

The  $(8_L, 1_R)$  component of the  $|\Delta S| = 1$  effective Lagrangian is readily obtained by contracting two of such left-handed current and we normalized it as

$$\mathcal{L}_8^{(2)} = F^4 G_8 \langle \lambda_{32} L_\mu L^\mu \rangle + \text{h.c.} , \quad (\text{B.11})$$

where CP violation is allowed thanks to the complex coupling constant  $G_8$ .  $\mathcal{L}_8^{(2)}$  is not the only possible octet Lagrangian at  $\mathcal{O}(p^2)$  as

$$\mathcal{L}_m^{(2)} = F^4 G_m \langle \lambda_{32} \chi_+ \rangle + \text{h.c.} \quad (\text{B.12})$$

is also perfectly well suited to represent weak  $(8_L, 1_R)$  interactions. Even though it eventually turns out to be irrelevant in the context of the present work (see e.g. Ref. [186]), it can not be discarded from scratch. Another candidate is

$$\mathcal{L}_{8s}^{(2)} = F^4 G_s \langle \lambda_{32} L_\mu \rangle \langle L^\mu \rangle + \text{h.c.} , \quad (\text{B.13})$$

which is proper to  $U(3)$  as it involves  $\langle L^\mu \rangle \neq 0$  which vanishes in  $SU(3)$ .

With regards to the  $(27_L, 1_R)$  component, we use Eq.(B.7) and the Gell-Mann correspondence of Eq.(B.10) to find

$$\begin{aligned} \mathcal{L}_{27}^{(2)} = & \frac{F^4}{36} G_{27}^{(1/2)} \left[ \langle \lambda_1 L_\mu \rangle \langle \lambda_{4-i5} L^\mu \rangle + \langle \lambda_2 L_\mu \rangle \langle \lambda_{4+i5} L^\mu \rangle + \right. \\ & \left. + 2 \langle (9Q - 5\lambda_3) L^\mu \rangle \langle \lambda_{6-i7} L_\mu \rangle \right] \\ & + \frac{5}{36} F^4 G_{27}^{(3/2)} \left[ \langle \lambda_1 L_\mu \rangle \langle \lambda_{4-i5} L^\mu \rangle + \langle \lambda_2 L_\mu \rangle \langle \lambda_{5+i4} L^\mu \rangle + \right. \\ & \left. + 2 \langle \lambda_3 L_\mu \rangle \langle \lambda_{6-i7} L^\mu \rangle \right] + \text{h.c.} , \end{aligned} \quad (\text{B.14})$$

where we also allowed for CP violation and where the shorten notation  $\lambda_{a\pm ib} \doteq \lambda_a \pm i\lambda_b$  has been used. Note that the difference between  $U(3)$  or  $SU(3)$  embedding is taken into account by the term proportional to electric charge

matrix  $Q = \lambda_{11} - \frac{1}{3}1_{3 \times 3}$ , which involves the trace of the left-handed current,  $\langle L \rangle$ .

We may now turn our attention to the effective electroweak interactions generated by the  $Q_7$  and  $Q_8$  operators, which transform as  $(8_L, 8_R)$  multiplets. Something peculiar happens here: we may build them at  $\mathcal{O}(p^0)$  using  $U$  and  $U^\dagger$  because  $U^\dagger \otimes U \sim (\mathfrak{3}_L^* \otimes \mathfrak{3}_L, \mathfrak{3}_R \otimes \mathfrak{3}_R^*) \ni (8_L, 8_R)$ . However, the unitarity of  $U$  implies that  $U$  and  $U^\dagger$  must be contracted in a non trivial way. In fact, we may write

$$\mathcal{L}_{ew}^{(0)} = F^6 e^2 G_{ew} \langle \lambda_{32} U^\dagger Q U \rangle + \text{h.c.} \quad (\text{B.15})$$

This form could have been already guessed from the fact that  $Q_8$  may be written as a density-density product, density which, at the lowest order, is represented by the  $U$  matrix, see Eq.(1.47). The important point here is that the presence of the electric charge matrix  $Q$  allows us to get a  $\mathcal{O}(p^0)$  hadronic operator. In fact, QCD penguin operator  $Q_6$  is also a density-density operator. However, as we have no  $Q$  matrix substitute at our disposal, the hadronic realization of  $Q_6$  is of  $\mathcal{O}(p^4)$  at least. Thus, even though a  $\alpha_{em}/\alpha_s$  suppression of the electroweak penguin over the QCD one is expected, the former are chirally enhanced and deserve, therefore, a careful treatment.

### B.3.2 The effective Lagrangian at $\mathcal{O}(p^4)$

The weak  $SU(3)$  effective Lagrangian at  $\mathcal{O}(p^4)$  is expanded over 22 independent operators among which we keep [74, 187]

$$\begin{aligned} \mathcal{L}_8^{(4)} = & G_8 F^2 [N_5 \langle \lambda_{32} \{ \chi_+, D_\mu U^\dagger D^\mu U \} \rangle \\ & + N_6 \langle \lambda_{32} D_\mu U^\dagger U \rangle \langle U^\dagger D^\mu U \chi_+ \rangle + \\ & + N_7 \langle \lambda_{32} \chi_+ \rangle \langle D_\mu U^\dagger D^\mu U \rangle + N_8 \langle \lambda_{32} D_\mu U^\dagger D^\mu U \rangle \langle \chi_+ \rangle \\ & + N_9 \langle \lambda_{32} [\chi_-, D_\mu U^\dagger D^\mu U] \rangle + \langle \lambda_{32} (N_{10} \chi_+^2 + N_{12} \chi_-^2) \rangle \\ & + N_{11} \langle \lambda_{32} \chi_+ \rangle \langle \chi_+ \rangle + N_{13} \langle \lambda_{32} \chi_- \rangle \langle \chi_- \rangle + \\ & + i \langle \lambda_{32} \{ N_{14} f_+^{\mu\nu} + N_{16} f_-^{\mu\nu}, D_\mu U^\dagger D_\nu U \} \rangle + \\ & i \langle \lambda_{32} D_\mu U^\dagger U (N_{15} f_+^{\mu\nu} + N_{17} f_-^{\mu\nu}) U^\dagger D_\nu U \rangle + \text{h.c.} \end{aligned} \quad (\text{B.16})$$

It is worth noting that the presence of the  $G_8$  coupling constant is purely conventional here as it merely helps to keep track of the chiral behavior of the various operators. As for the strong sector, all one-loop divergences appearing at NLO can be absorbed through a renormalization of the bare  $N_i$  coefficients as

$$N_i = N_i^r(\mu) + \Gamma_i^N \Lambda(\mu) ,$$

with  $\Gamma_i^N$  given in Tab.(B.1).

The 27-plet Lagrangian used in the present work is taken from Ref. [183] and is complemented by four radiative operators taken from Ref. [188]. In this minimal basis we have

$$\begin{aligned}
\mathcal{L}_{27}^{(4)} = F^2 \mathcal{T}_{ij;kl} & \left[ D_1 \langle \lambda_{ij} \chi_+ \rangle \langle \lambda_{kl} \chi_+ \rangle + D_2 \langle \lambda_{ij} \chi_- \rangle \langle \lambda_{kl} \chi_- \rangle + \right. \\
& + D_4 \langle \lambda_{ij} U^\dagger D_\mu U \rangle \langle \lambda_{kl} \{ D^\mu U^\dagger U, \chi_+ \} \rangle + \\
& + D_5 \langle \lambda_{ij} U^\dagger D_\mu U \rangle \langle \lambda_{kl} [ D^\mu U^\dagger U, \chi_- ] \rangle + \\
& + D_6 \langle \lambda_{ij} U^\dagger \chi_+ \rangle \langle \lambda_{kl} D_\mu U^\dagger D^\mu U \rangle + \\
& + D_7 \langle \lambda_{ij} U^\dagger D_\mu U \rangle \langle \lambda_{kl} D^\mu U^\dagger U \rangle \langle \chi_- \rangle + \\
& + i D_{13} \langle \lambda_{ij} f_{\mu\nu}^+ \rangle \langle \lambda_{kl} D^\mu U^\dagger D^\nu U \rangle + \\
& + i D_{14} \langle \lambda_{ij} f_{\mu\nu}^- \rangle \langle \lambda_{kl} U^\dagger D^\mu U U^\dagger D^\nu U \rangle + \\
& + i D_{15} \langle \lambda_{ij} [ U^\dagger D^\mu U, f_{\mu\nu}^+ ] \rangle \langle \lambda_{kl} U^\dagger D^\nu U \rangle + \\
& \left. + i D_{16} \langle \lambda_{ij} [ f_{\mu\nu}^-, U^\dagger D^\mu U ] \rangle \langle \lambda_{kl} U^\dagger D^\nu U \rangle \right] + \text{h.c.} \tag{B.17}
\end{aligned}$$

with the projector tensors given in Eq.(B.9). As previously, these operators renormalize the LO via

$$D_i = D_i^r(\mu) + \Gamma_i^D \Lambda(\mu)$$

with  $\Gamma_i^D$  specified in Tab.(B.1).

Finally, we consider the NLO representation of the electroweak sector. Since this Lagrangian is of  $\mathcal{O}(p^0)$ , the corresponding NLO local terms are of  $\mathcal{O}(p^2)$ . As a consequence, none of the  $\mathcal{O}(p^2)$  local operators may contain  $F_{L,R}^{\mu\nu}$ . Indeed, Lorentz invariance would require two extra partial derivatives leading to  $\mathcal{O}(p^4)$  local interactions. The corresponding minimal Lagrangian is given by

$$\begin{aligned}
\mathcal{L}_{\text{ew}}^{(4)} = F^4 e^2 G_{\text{ew}} & \left[ Z_1 \langle \lambda_{32} U^\dagger \{ Q, \chi_+ \} U \rangle + Z_2 \langle \lambda_{32} U^\dagger Q U \rangle \langle \chi_+ \rangle + \right. \\
& + Z_6 \langle \lambda_{32} \{ U^\dagger Q U, D_\mu U^\dagger D^\mu U \} \rangle + \\
& + Z_9 \langle \lambda_{32} U^\dagger D_\mu U \rangle \langle Q U D^\mu U^\dagger \rangle + \\
& \left. + Z_{13} \langle \lambda_{32} U^\dagger Q U \rangle \langle D_\mu U^\dagger D^\mu U \rangle \right] \tag{B.18}
\end{aligned}$$

while the renormalization of the various coefficients read

$$Z_i = Z_i^r(\mu) + \Gamma_i^Z \Lambda(\mu)$$






where the  $\Gamma_i^Z$  constants are given in Tab.(B.1).



# Appendix C

## Amplitudes in ChPT

This section contains a detailed presentation of the various amplitude calculations used in the present thesis. These rather technical results are exposed here in order to lighten the main text where their implications and consequences are analyzed in more depth. Since these computations involve numerous loop diagrams, it is desirable to automatize these analytic computations using `Mathematica` [189] supplemented by `FeynRules` [190], `FeynArts` [191] and `FeynCalc` [192]. Before going into detail let us first introduce some conventions. While Feynman diagrams are displayed in a neat and colored form in the main text, here, they are drawn in black and white using the following vertex conventions:

-  indicates a  $\mathcal{O}(p^2)$  strong vertex obtained from Eq.(1.46).
-  indicates a  $\mathcal{O}(p^4)$  strong vertex obtained from Eq.(B.1).
-  indicates a  $\mathcal{O}(p^4)$  strong WZW vertex obtained from Eqs.(B.3).
-  indicates a  $\mathcal{O}(p^2)$  weak vertex obtained from Eqs.(1.55) and (B.12).
-  indicates a  $\mathcal{O}(p^4)$  weak vertex obtained from either Eq.(B.16), (B.17) or (B.18).

As several NLO calculations detailed below require to be renormalized, we dedicate the next section to the determination of all the corresponding renormalization constants.

## C.1 Renormalization

Renormalized masses, wave functions and decay constants, respectively denoted by  $M_\phi$ ,  $\Phi$  and  $F_{\phi_a}^r$ , are defined by

$$M_\phi^2 \doteq Z_\phi^m m_\phi^2, \quad (\text{C.1a})$$

$$\Phi \doteq Z_\phi^{-1/2} \phi, \quad (\text{C.1b})$$

$$F_{\phi_a}^r \doteq Z_{\phi_a}^F F_{\phi_a}, \quad (\text{C.1c})$$

where  $m_\phi$ ,  $\phi$  and  $F_{\phi_a}$  represent the *bare* masses, wave functions and decay constants, respectively. The  $Z_\phi^m$ ,  $Z_\phi^m$  and  $Z_{\phi_a}^F$  coefficients are called renormalization constants. While  $Z_\phi^m$  and  $Z^m$  are extracted from the same object, the  $\phi$  meson propagator,  $Z_{\phi_a}^F$  is obtained from the definition of  $F_{\phi_a}$ , i.e.,

$$\langle 0|A_\mu(0)|\phi_a(p)\rangle \doteq i\sqrt{2}F_{\phi_a}p_\mu, \quad (\text{C.2})$$

where the  $\sqrt{2}$  is a conventional normalization factor used in the present work.

### Mass and wave functions

Let us consider the generic case of a scalar field  $\phi$  of bare mass  $m$ . Its propagator given by the two-point Green function

$$i\Pi(p) \doteq \int d^4x e^{-ip \cdot x} \langle 0|T\{\phi(x)\phi(0)\}|0\rangle$$

may be represented by the Dyson sum

$$\begin{aligned} i\Pi(p) &= \text{---} + \text{---} \textcircled{\text{X}} \text{---} + \text{---} \textcircled{\text{X}} \textcircled{\text{X}} \text{---} + \dots \\ &= \frac{i}{p^2 - m^2 - \Sigma(p^2) + i\varepsilon}. \end{aligned} \quad (\text{C.3})$$

Since we did not yet specify the structure of the self-energy  $\Sigma$  or equivalently the structure of the underlying theory this result is quite general. All we



know is that  $\Sigma$  represents one-loop one particle irreducible corrections to the propagator of the scalar field  $\phi$ . This is, however, sufficient to make some important statements. First of all, it is clear from Eq.(C.3) that the pole of the propagator has been shifted from the bare mass  $m$ . The pole mass, or equivalently the physical mass, defined by  $p^2 = M^2$  reads now

$$M^2 = m^2 + \Sigma(m^2) + \text{higher order corrections} ,$$

where higher order corrections due to  $\Sigma(m^2) - \Sigma(M^2)$  are neglected at NLO. From this simple result we infer directly that the mass renormalization constant at NLO is given by

$$Z^m = 1 + \frac{\Sigma(m^2)}{m^2} . \quad (\text{C.4})$$

Furthermore, expanding  $\Sigma(p^2)$  around an arbitrary mass scale  $\mu^2$  we observe that

$$\Sigma(p^2) = \Sigma(\mu^2) + (p^2 - \mu^2)\Sigma'(\mu^2) + \tilde{\Sigma}(p^2) ,$$

where  $\tilde{\Sigma}(p^2) \doteq \frac{1}{2}(p^2 - \mu^2)^2\Sigma''(\mu^2) + \mathcal{O}((p^2 - \mu^2)^3)$  vanishes at  $p^2 = \mu^2$  by definition. Here, primes indicate partial derivatives with respect to  $p^2$ . A simple dimensional analysis teaches us that the divergence of  $\Sigma(\mu^2)$  is, at most, quadratic that of  $\Sigma'(\mu^2)$  is, at most, logarithmic whereas  $\tilde{\Sigma}(p^2)$  turns out to be finite. The mass scale  $\mu$ , being arbitrary, we may set  $\mu^2 = M^2$  to obtain

$$i\Pi(p^2) = \frac{i}{(p^2 - M^2) [1 - \Sigma'(M^2)] - \tilde{\Sigma}(p^2)} ,$$

with the nice result that the possible quadratic divergence of  $\Sigma$  has been absorbed by the mass renormalization. The pole mass has not changed ( $\tilde{\Sigma}(M^2) = 0$ ) but the propagator still carries a potential logarithmic divergence. This is where the wave function renormalization enters into play. Indeed, writing

$$i\Pi(p^2) = \frac{iZ}{(p^2 - M^2) - \tilde{\Sigma}(p^2)} + \text{higher order corrections} ,$$

where

$$Z = \frac{1}{1 - \Sigma'(M^2)} = 1 + \Sigma'(m^2) + \text{higher order corrections} ,$$

we conclude that the remaining logarithmic divergence of the propagator, hidden in  $Z$ , may be absorbed in the renormalization of the scalar field wave-function defined by

$$\phi \rightarrow \Phi = Z^{-1/2} \phi .$$

To review, the mass and wave-function renormalization constants are expressed in terms of the self-energy amplitude as

$$Z_\phi^m \doteq 1 + \frac{\Sigma_\phi(m^2)}{m^2}, \quad (\text{C.5})$$

$$Z_\phi \doteq 1 + \Sigma'_\phi(m^2). \quad (\text{C.6})$$

In ChPT, the self energies receive both loops and counter-term contribution :

$$\begin{aligned} -i\Sigma(p) &\doteq \text{---} \textcircled{\text{---}} \text{---} \\ &= \text{---} \textcircled{\text{---}} \text{---} + \text{---} \textcircled{\text{---}} \text{---} + \text{---} \blacksquare \text{---} . \end{aligned}$$

Evaluating these diagrams is straightforward and the result is expressed in terms of the  $A_0$  one-loop scalar function defined in Eq.(A.12). In the isospin limit ( $m_u = m_d$ ), we find

$$Z_\pi^m = 1 + \frac{1}{6(4\pi F)^2} [A_0(m_{\eta_8}^2) - 3A_0(m_\pi^2)] + \text{L}'(m_\pi^2), \quad (\text{C.7a})$$

$$Z_K^m = 1 - \frac{1}{3(4\pi F)^2} A_0(m_{\eta_8}^2) + \text{L}'(m_K^2), \quad (\text{C.7b})$$

$$\begin{aligned} Z_{\eta_8}^m &= 1 + \frac{1}{2(4\pi F)^2} [2A_0(m_{\eta_8}^2) - 3A_0(m_K^2)] + \\ &+ \text{L}'(m_{\eta_8}^2) + \frac{128}{9F^2} (3L_7 + L_8) \frac{(m_K^2 - m_\pi^2)^2}{m_{\eta_8}^2} + \\ &+ \frac{1}{6(4\pi F)^2} \frac{m_\pi^2}{m_{\eta_8}^2} [3A_0(m_\pi^2) - 2A_0(m_K^2) - A_0(m_{\eta_8}^2)], \end{aligned} \quad (\text{C.7c})$$

with the recurrent local contribution

$$\text{L}'(m^2) \doteq \frac{8}{F^2} [(2L_6 - L_4)(2m_K^2 + m_\pi^2) + (2L_8 - L_5)m^2]. \quad (\text{C.8})$$

With regards to the wave function renormalization constants, we rather find

$$Z_\pi = 1 - \frac{1}{3(4\pi F)^2} [2A_0(m_\pi^2) + A_0(m_K^2)] - \text{L}''(m_\pi^2), \quad (\text{C.9a})$$

$$\begin{aligned} Z_K &= 1 - \frac{1}{4(4\pi F)^2} [A_0(m_\pi^2) + 2A_0(m_K^2) + A_0(m_{\eta_8}^2)] - \\ &\quad - \text{L}''(m_K^2), \end{aligned} \quad (\text{C.9b})$$

Induced couplings							
$\pi^0$	$\pi^+$	$\pi^-$	$K^0$	$\bar{K}^0$	$K^+$	$K^-$	$\eta_8$
$a_\mu^1$	$a_\mu^3$	$a_\mu^4$	$a_\mu^7$	$a_\mu^8$	$a_\mu^5$	$a_\mu^6$	$a_\mu^2$

**Tab. C.1:** Pseudo-scalar meson coupling to  $A_\mu$  defined in Eq.(C.12).

$$Z_{\eta_8} = 1 - \frac{1}{(4\pi F)^2} A_0(m_K^2) - \mathbf{L}''(m_{\eta_8}^2) , \quad (\text{C.9c})$$

with the common local contribution

$$\mathbf{L}''(m^2) \doteq \frac{8}{F^2} [L_4(2m_K^2 + m_\pi^2) + L_5 m^2] . \quad (\text{C.10})$$

Note that since we assumed the isospin limit, the index  $\pi$  in  $Z_\pi^{(m)}$  stands for  $\pi^0$  or  $\pi^\pm$ , whilst the  $K$  index  $Z_K^{(m)}$  stands for  $K^0$ ,  $\bar{K}^0$  or  $K^\pm$ .

## Decay constants

Now we turn our attention to the renormalization of the decay constants. As stated above, the decay constant  $F_\phi$  of a pseudo-scalar field  $\phi$  is given by

$$F_\phi \doteq \frac{-i p^\mu}{\sqrt{2} p^2} \langle 0 | A_\mu(0) | \phi(p) \rangle . \quad (\text{C.11})$$

In  $SU(3)_L \otimes SU(3)_R$  Chiral Perturbation theory, the axial gauge field  $A_\mu$  may be decomposed in the pseudo-scalar basis as follow

$$A_\mu \doteq \begin{pmatrix} \frac{a_\mu^1}{\sqrt{2}} + \frac{a_\mu^2}{\sqrt{2}} & a_\mu^3 & a_\mu^5 \\ a_\mu^4 & -\frac{a_\mu^1}{\sqrt{2}} + \frac{a_\mu^2}{\sqrt{2}} & a_\mu^7 \\ a_\mu^6 & a_\mu^8 & \frac{-2a_\mu^2}{\sqrt{2}} \end{pmatrix} . \quad (\text{C.12})$$

This natural basis is useful because each pseudo-scalar couple to only one of these  $a_\mu^a$  fields according to Tab.(C.1). These couplings have two different origins: the covariant derivative of the  $U$

$$D_\mu U = \partial_\mu U - i \{U, A_\mu\} , \quad (\text{C.13})$$

and the direct couplings to the gauge field strength tensors

$$F_L^{\mu\nu} = \partial^\mu A^\nu - \partial^\nu A^\mu - i [A^\mu, A^\nu] , \quad (\text{C.14a})$$

$$F_R^{\mu\nu} = -\partial^\mu A^\nu + \partial^\nu A^\mu - i [A^\mu, A^\nu] . \quad (\text{C.14b})$$

At LO, we recover the following identical amplitudes

$$\langle 0|A_\mu(0)|\phi_a(p)\rangle_{\mathcal{O}(p^2)} = \text{---}\bullet\text{---} = i\sqrt{2}p_\mu$$

showing that at  $\mathcal{O}(p^2)$ , all the decay constants are degenerated. At  $\mathcal{O}(p^4)$ , things get more involved since amplitudes defined in Eq.(C.11) receive both loops and local contributions

$$\begin{aligned} F_{\phi_a}^{\mathcal{O}(p^4)} &= \frac{-i}{\sqrt{2}} \frac{p^\mu}{p^2} \langle 0|A_\mu(0)|\phi_a(p)\rangle_{\mathcal{O}(p^4)} \\ &= \frac{-i}{\sqrt{2}} \frac{p^\mu}{p^2} \left( \text{---}\bullet\text{---} + \text{---}\blacksquare\text{---} \right). \end{aligned} \quad (\text{C.15})$$

Once the wave-function renormalization is applied on these  $\mathcal{O}(p^4)$  amplitudes, the NLO decay constants get renormalized by

$$Z_\pi^F = 1 + \frac{1}{2(4\pi F)^2} [2A_0(m_\pi^2) + A_0(m_K^2)] + \frac{1}{2}L''(m_\pi^2), \quad (\text{C.16a})$$

$$\begin{aligned} Z_K^F &= 1 + \frac{3}{8(4\pi F)^2} [A_0(m_\pi^2) + 2A_0(m_K^2) + A_0(m_{\eta_8}^2)] + \\ &\quad + \frac{1}{2}L''(m_K^2), \end{aligned} \quad (\text{C.16b})$$

$$Z_{\eta_8}^F = 1 + \frac{3}{2(4\pi F)^2} A_0(m_K^2) + \frac{1}{2}L''(m_{\eta_8}^2). \quad (\text{C.16c})$$

## C.2 $K \rightarrow \gamma\gamma$

Parametrizing this process as  $K^0(P) \rightarrow \gamma(q_1, \mu)\gamma(q_2, \nu)$ , the kinematics imposes the following relations

$$P = q_1 + q_2, \quad q_1^2 = q_2^2 = 0 \quad \text{and} \quad P^2 = 2q_1 \cdot q_2 = M_K^2, \quad (\text{C.17})$$

while the most general expression of the corresponding amplitude allowed by Lorentz and gauge invariance is given by

$$\begin{aligned} A(K^0 \rightarrow \gamma\gamma) &= \frac{1}{\sqrt{2}} [A(P^2)(q_1^\nu q_2^\mu - q_1 \cdot q_2 g^{\mu\nu}) + \\ &\quad + B(P^2)\epsilon^{\mu\nu\rho\sigma} q_{1\rho} q_{2\sigma}] \epsilon_{1\mu}^* \epsilon_{2\nu}^*. \end{aligned} \quad (\text{C.18})$$

Since  $K$  is a pseudo-scalar particle, the photons have either positive or negative helicity :  $|++\rangle$  or  $|--\rangle$ <sup>1</sup>. Therefore, as a parity transformation acts only in the momentum space, the parity transformation  $|++\rangle \xrightarrow{P} |--\rangle$  suggests to consider the equivalent state decomposition:

$$|\gamma\gamma_{\parallel,\perp}\rangle = \frac{1}{\sqrt{2}}(|++\rangle \pm |--\rangle) \quad \text{with} \quad CP|\gamma\gamma_{\parallel,\perp}\rangle = \pm|\gamma\gamma_{\parallel,\perp}\rangle. \quad (\text{C.19})$$

From an operator point of view, a  $\gamma\gamma_{\parallel}$  state is produced by the  $CP$  even operator  $F_{\mu\nu}F^{\mu\nu}$  whereas a  $\gamma\gamma_{\perp}$  state is produced by the  $CP$  odd  $F_{\mu\nu}\tilde{F}^{\mu\nu}$  operator. In the momentum space it is, therefore, easy to realize that the  $A$  amplitude in Eq.(C.18) produces the two photons with parallel helicities ( $F \cdot F$ ), whereas the  $B$  term produces them with perpendicular helicities ( $F \cdot \tilde{F}$ ). Therefore, these two amplitudes do not interfere in the branching ratio.

Before computing all the possible  $K \rightarrow \gamma\gamma$  amplitudes, it is greatly rewarding to analyze first how the  $CP$  properties of the two photon states intermix with those of the  $K^0 - \bar{K}^0$  system. The  $CPT$  theorem is the key here because it implies the following relations

$$A(K^0 \rightarrow \gamma\gamma_{\parallel,\perp}) = \mp A(\bar{K}^0 \rightarrow \gamma\gamma_{\parallel,\perp})^*. \quad (\text{C.20})$$

In other words, these four amplitudes are not independent as two of them may be deduced from the other two. Explicitly, if we computed the amplitudes  $A_{\gamma\gamma}^{\parallel}$  and  $A_{\gamma\gamma}^{\perp}$  that specify completely the decay amplitude

$$A(K^0 \rightarrow \gamma\gamma) = \frac{1}{\sqrt{2}} \left[ A_{\gamma\gamma}^{\parallel} (q_1^\nu q_2^\mu - q_1 \cdot q_2 g^{\mu\nu}) + A_{\gamma\gamma}^{\perp} \epsilon^{\mu\nu\rho\sigma} q_{1\rho} q_{2\sigma} \right] \epsilon_{1\mu}^* \epsilon_{2\nu}^*, \quad (\text{C.21})$$

we conclude that

$$A(K_S \rightarrow \gamma\gamma_{\parallel}) = N \left[ \text{Re}A_{\gamma\gamma}^{\parallel} + i\epsilon_m \text{Im}A_{\gamma\gamma}^{\parallel} \right] (q_1^\nu q_2^\mu - q_1 \cdot q_2 g^{\mu\nu}) \epsilon_{1\mu}^* \epsilon_{2\nu}^*, \quad (\text{C.22a})$$

$$A(K_S \rightarrow \gamma\gamma_{\perp}) = N \left[ i\text{Im}A_{\gamma\gamma}^{\perp} + \epsilon_m \text{Re}A_{\gamma\gamma}^{\perp} \right] \epsilon^{\mu\nu\rho\sigma} q_{1\rho} q_{2\sigma} \epsilon_{1\mu}^* \epsilon_{2\nu}^*, \quad (\text{C.22b})$$

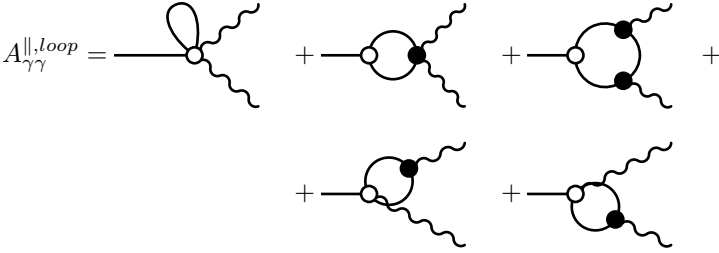
$$A(K_L \rightarrow \gamma\gamma_{\parallel}) = N \left[ i\text{Im}A_{\gamma\gamma}^{\parallel} + \epsilon_m \text{Re}A_{\gamma\gamma}^{\parallel} \right] (q_1^\nu q_2^\mu - q_1 \cdot q_2 g^{\mu\nu}) \epsilon_{1\mu}^* \epsilon_{2\nu}^*, \quad (\text{C.22c})$$

$$A(K_L \rightarrow \gamma\gamma_{\perp}) = N \left[ \text{Re}A_{\gamma\gamma}^{\perp} + i\epsilon_m \text{Im}A_{\gamma\gamma}^{\perp} \right] \epsilon^{\mu\nu\rho\sigma} q_{1\rho} q_{2\sigma} \epsilon_{1\mu}^* \epsilon_{2\nu}^*, \quad (\text{C.22d})$$

where  $N = (1 + |\bar{\epsilon}|^2)^{-1/2}$ . Let us now compute  $A_0^{\gamma\gamma} \doteq A(K^0 \rightarrow \gamma\gamma)$  in order to extract the independent partial amplitudes  $A_{\gamma\gamma}^{\parallel}$  and  $A_{\gamma\gamma}^{\perp}$ . Since the production of two on-shell photons is achieved by either  $F \cdot F$  or  $F \cdot \tilde{F}$  operators, both of dimension four, we conclude that  $A_0^{\gamma\gamma}$  starts at  $\mathcal{O}(p^4)$ . The absence of  $\mathcal{O}(p^2)$  contributions follows also from the fact that photon do not couple to neutral

<sup>1</sup>Indeed, a two photons state with opposite helicities has a non zero spin.

particle directly, i.e., there is no  $K^0\gamma\gamma$  coupling at tree-level. The only chance for this process to occur is through charged  $\pi\pi$  or  $KK$  loops. Consequently, potential  $\mathcal{O}(p^4)$  loop divergences cannot be absorbed in a  $\mathcal{O}(p^2)$  amplitude. In other words, the  $\mathcal{O}(p^4)$  amplitude is finite. Note however that this does not mean that the  $A_0^{\gamma\gamma}$  is automatically free of local contributions. It rather means that, a priori, local contributions, if any, appear in finite combinations. Following the standard power counting of ChPT,  $\mathcal{O}(p^4)$  topologies consist of either loop diagrams or tree diagrams involving one WZW vertex. In fact, WZW vertices are the only ones able to produce the  $\epsilon_{\mu\nu\rho\sigma}$  amplitudes that generate  $A_{\gamma\gamma}^\perp$ . Tackling the loop contributions first, we get



$$\begin{aligned}
A_{\gamma\gamma}^{\parallel,loop} = & \text{[Diagram 1]} + \text{[Diagram 2]} + \text{[Diagram 3]} + \\
& \text{[Diagram 4]} + \text{[Diagram 5]} \\
= & -\frac{2\alpha_{em}}{\pi} F(1-r_\pi^2) \mathcal{F}(r_\pi^{-2}) G_8 (1+\delta_{27}-\delta_m) + \\
& + 8\alpha_{em}^2 \frac{F^3}{m_K^2} [\mathcal{F}(1) - \mathcal{F}(r_\pi^{-2})] G_{ew} , \tag{C.23a}
\end{aligned}$$

where  $r_\pi = m_\pi/m_K$ ,  $\alpha_{em} = e^2/4\pi$  and the non-octet contributions collected in

$$\delta_{27} = \frac{1}{9G_8} (G_{27}^{(1/2)} + 5G_{27}^{(3/2)}) \quad \text{and} \quad \delta_m = \frac{2}{3} \frac{G_m}{G_8} (\mathcal{F}(1) + \mathcal{F}(r_\pi^{-2})) , \tag{C.24}$$

where  $\mathcal{F}(r_\pi^{-2}) \simeq (0.7 - 1.1i)$  indicates pion loops whilst  $\mathcal{F}(1) \simeq -1.1$  signals kaon loops,  $\mathcal{F}$  being the scalar loop function defined in Eq.(A.20). It seems that the weak mass term of Eq.(B.12) contributes here. In principle, this is allowed because the lowest order contribution to the present process is  $\mathcal{O}(p^4)$  (see Ref. [186]). However,  $A_{\gamma\gamma}^\parallel$  is still incomplete since it does not yet take into account the weak mass term ability to produce tadpoles. These effects are

given by

$$\begin{aligned}
 A_{\gamma\gamma}^{\parallel,tad} = & \text{[Diagram 1]} + \text{[Diagram 2]} + \text{[Diagram 3]} + \\
 & \text{[Diagram 4]} + \text{[Diagram 5]} \\
 = & -\frac{2\alpha_{em}}{\pi} F(1-r_\pi^2) \mathcal{F}(r_\pi^{-2}) G_8 (+\delta_m) , \tag{C.25a}
 \end{aligned}$$

and cancel exactly the  $G_m$  term of  $A_{\gamma\gamma}^{\parallel,loop}$  in Eq.(C.23a). The complete  $\mathcal{O}(p^4)$  amplitude  $A_{\gamma\gamma}^{\parallel} \doteq A_{\gamma\gamma}^{\parallel,loop} + A_{\gamma\gamma}^{\parallel,tad}$  is, therefore, given by

$$\begin{aligned}
 A_{\gamma\gamma}^{\parallel} = & -\frac{2\alpha_{em}}{\pi} F(1-r_\pi^2) \mathcal{F}(r_\pi^{-2}) G_8 (1 + \delta_{27}) + \\
 & + 8\alpha_{em}^2 \frac{F^3}{m_K^2} [\mathcal{F}(1) - \mathcal{F}(r_\pi^{-2})] G_{ew} . \tag{C.26}
 \end{aligned}$$

No local counter-term contributions are found here as no tree-level  $K^0\gamma\gamma$  vertex appear at  $\mathcal{O}(p^4)$ . It means that the predicted ChPT amplitude in Eq.(C.26) will not be affected by our poor knowledge of the weak local counter-terms.

Let us now turn our attention to the perpendicular helicity amplitude  $A_{\gamma\gamma}^\perp$ , which also starts at  $\mathcal{O}(p^4)$  and is driven by the WZW anomalous Lagrangian through the following pole exchange processes

$$\begin{aligned}
 A_{\gamma\gamma}^\perp = & \text{[Diagram]} = i \frac{2\alpha_{em}}{\pi} F m_K^2 \times \\
 & \times \left[ \frac{G_8 + G_m - G_{27}^{(3/2)} + \frac{1}{9}(G_{27}^{(1/2)} - G_{27}^{(3/2)})}{(m_K^2 - m_\pi^2)} - \frac{G_8 + G_m - G_{27}^{(1/2)}}{3(m_{\eta_8}^2 - m_K^2)} \right] \tag{C.27}
 \end{aligned}$$

where the  $\pi^0$  and  $\eta_8$  poles are clearly apparent, and where we assumed the overall factor  $N_C/3$  to equals unity. This amplitude vanishes in the isospin limit where  $G_{27}^{(1/2)} = G_{27}^{(3/2)}$  and  $m_K^2 - m_\pi^2 = 3(m_{\eta_8}^2 - m_K^2)$  holds. In order for this amplitude to differ from zero in the isospin limit we may either go at  $\mathcal{O}(p^6)$  or in  $U(3)$ , see Ref. [114].

Finally, we stress the fact that by  $\text{Re}A_{\parallel,\perp}$  and  $\text{Im}A_{\parallel,\perp}$  we refer to weak phases, i.e., the ones driven by the  $G_i$  coupling constants. The strong phases, broad

by the on-shell intermediate loop states are for their part included in  $\mathcal{F}$  and do not feel the  $CP$  transformation applied in Eq.(C.20) by definition.

### C.3 $K \rightarrow \pi\pi(\gamma)$

$K \rightarrow \pi\pi$

#### Kinematic

We choose to parametrize these decay amplitudes as  $A(K(P) \rightarrow \pi(q_1)\pi_2)$  with  $\pi\pi = \pi^+\pi^-, \pi^0\pi^0$  or  $\pi^+\pi^0$  so that in the rest frame of the decaying kaon and in the isospin limit, we have

$$P = q_1 + q_2, \quad P^2 = M_K^2, \quad q_1^2 = q_2^2 = M_\pi^2 \quad \text{and} \quad q_1 \cdot q_2 = \frac{1}{2} (M_K^2 - 2M_\pi^2),$$

where  $M_i$  indicate kinematic (or equivalently physical) masses which are degenerate with the bare masses  $m_i$  at tree-level only. This distinction is crucial in order for the renormalization process to work properly.

#### $\mathcal{O}(p^2)$ amplitudes

At the lowest order, the  $K \rightarrow \pi\pi$  amplitudes are obtained from the following tree-level topologies

$$A_{IJK} \doteq A(K^I \rightarrow \pi^J \pi^K) = \text{---} \bigcirc \begin{array}{l} / \\ \backslash \end{array} + \text{---} \bullet \begin{array}{l} / \\ \backslash \\ \bigcirc \end{array} \quad (\text{C.28})$$

and are explicitly given by

$$A_{0+-} = -\sqrt{2}F \left[ G_8 + \frac{1}{9}G_{27}^{(1/2)} + \frac{5}{9}G_{27}^{(3/2)} \right] (M_K^2 - M_\pi^2) - \sqrt{2}e^2 F^3 G_{ew}, \quad (\text{C.29a})$$

$$A_{000} = -\sqrt{2}F \left[ G_8 + \frac{1}{9}G_{27}^{(1/2)} - \frac{10}{9}G_{27}^{(3/2)} \right] (M_K^2 - M_\pi^2), \quad (\text{C.29b})$$

$$A_{++0} = -\frac{5}{3}FG_{27}^{(3/2)}(M_K^2 - M_\pi^2) + e^2 F^3 G_{ew}. \quad (\text{C.29c})$$



The second topology in Eq.(C.28) is in fact evanescent, it just cancels the  $G_m$  contribution generated by the first topology. Moreover, these amplitudes exhibit a dependence in the physical masses  $M_i$  only. Renormalizing masses at lowest order will, therefore, be useless. Still,  $\mathcal{O}(G_8 p^4)$  as well as  $\mathcal{O}(G_{27} p^4)$  amplitudes require the renormalization of both wave functions and decay constant while for the  $\mathcal{O}(G_{ew} e^2 p^2)$  contributions, the wave function renormalization is enough. Two different renormalization procedures are, therefore, needed:

$$A_{IJK} \rightarrow Z_K^{1/2} Z_\pi Z_K^F Z_\pi^{F^2} \left[ \frac{F_\pi^2}{F F_K} \right] A_{IJK} , \quad (\text{C.30a})$$

$$A_{IJK} \rightarrow Z_K^{1/2} Z_\pi Z_\pi^{F^3} \left[ \frac{F_\pi}{F} \right]^3 A_{IJK} , \quad (\text{C.30b})$$

for the  $G_8/G_{27}^{(I)}$  and  $G_{ew}$  components, respectively. In both cases, wave functions are renormalized using renormalization constants  $Z_{\pi,K}$  given in Eqs.(C.9) while renormalization constants for decay constant are given in Eqs.(C.16). Regarding the  $G_{ew}$  amplitudes, we simply substitute the bare  $F$  for  $F_\pi$ , though it is not required it allows us to express the decay amplitude in terms of a physical decay constant  $F_\pi$ . Concerning  $G_8$  and  $G_{27}$  amplitudes, the bare  $F$  is replaced by the particular combination  $F_\pi^2/F_K$ . This is not mandatory since we could have chosen to replace  $F$  by  $F_\pi$  as well. Yet, the advantage of pulling out the factor  $F_\pi^2/F_K$  lies in the fact that the associated factor  $Z_K^{1/2} Z_\pi Z_K^F Z_\pi^{F^2}$  does not depend on strong counter-terms in such a way that the renormalized amplitudes have no explicit dependence in the  $L_i$  constants, see e.g. Ref. [183]. Doing so, we obtain

$$A_{IJK} \rightarrow A_{IJK}^r + \delta A_{IJK} , \quad (\text{C.31})$$

where

$$A_{0+-}^r = -\sqrt{2} \frac{F_\pi^2}{F_K} \left[ G_8 + \frac{1}{9} G_{27}^{(1/2)} + \frac{5}{9} G_{27}^{(3/2)} \right] (M_K^2 - M_\pi^2) - \sqrt{2} e^2 F_\pi^3 G_{ew} , \quad (\text{C.32a})$$

$$A_{000}^r = -\sqrt{2} \frac{F_\pi^2}{F_K} \left[ G_8 + \frac{1}{9} G_{27}^{(1/2)} - \frac{10}{9} G_{27}^{(3/2)} \right] (M_K^2 - M_\pi^2) , \quad (\text{C.32b})$$

$$A_{++0}^r = -\frac{5}{3} \frac{F_\pi^2}{F_K} G_{27}^{(3/2)} (M_K^2 - M_\pi^2) - e^2 F_\pi^3 G_{ew} , \quad (\text{C.32c})$$

are the renormalized lowest order amplitudes whereas

$$\delta A_{0+-} = -\sqrt{2} \frac{m_K^2}{F_K} \left[ G_8 + \frac{1}{9} G_{27}^{(1/2)} + \frac{5}{9} G_{27}^{(3/2)} \right] (1 - r_\pi^2) \Delta - \sqrt{2} e^2 F_\pi G_{ew} \Delta' , \quad (\text{C.33a})$$

$$\delta A_{000} = -\sqrt{2} \frac{m_K^2}{F_K} \left[ G_8 + \frac{1}{9} G_{27}^{(1/2)} - \frac{10}{9} G_{27}^{(3/2)} \right] (1 - r_\pi^2) \Delta, \quad (\text{C.33b})$$

$$\delta A_{++0} = -\frac{5}{3} \frac{m_K^2}{F_K} G_{27}^{(3/2)} (1 - r_\pi^2) \Delta - e^2 F_\pi G_{ew} \Delta', \quad (\text{C.33c})$$

with

$$\Delta = \frac{1}{12(4\pi)^2} [19A_0(m_\pi^2) + 14A_0(m_K^2) + 3A_0(m_{\eta_8}^2)], \quad (\text{C.34a})$$

$$\Delta' = \frac{1}{24(4\pi)^2} [53A_0(m_\pi^2) + 22A_0(m_K^2) - 3A_0(m_{\eta_8}^2)] - 4L_5(m_K^2 - m_\pi^2), \quad (\text{C.34b})$$

are divergent higher order corrections regularizing the NLO loop and counter-term contributions computed in the next section. Notice that in these NLO contribution we use the bare masses  $m_i$  for pure convenience. Substituting the physical masses  $M_i$  for the bare masses at this order is allowed since it produced NNLO corrections which are beyond the order at which we are working. The same comment applies for the choice of the decay constant : in these NLO expression we can either use  $F_K$ ,  $F_\pi$  or  $F$ . However, once a choice is made, it has to be applied in all NLO contributions in order for the divergences to disappear properly.

### $\mathcal{O}(p^4)$ amplitudes

There are two types of NLO contributions to  $K \rightarrow \pi\pi$ : local counter-terms contributions and loop contributions. The former are driven by the following tree-level topologies

$$A_{JJK}^{ct} = \text{---} \square \text{---} + \text{---} \bullet \text{---} \square \text{---}, \quad (\text{C.35})$$

which are explicitly given by

$$A_{0+-}^{ct} = +\sqrt{2} \frac{m_K^4}{F_K} \left[ (1 - r_\pi^2) \left\{ G_8 \mathbf{N}_8 + \frac{1}{9} G_{27}^{(1/2)} \mathbf{D}_{1/2} + \frac{5}{9} G_{27}^{(3/2)} \mathbf{D}_{3/2} \right\} + e^2 \frac{F_\pi F_K}{m_K^2} G_{ew} \mathbf{Z}^{(1)} \right], \quad (\text{C.36a})$$

$$A_{000}^{ct} = +\sqrt{2} \frac{m_K^4}{F_K} \left[ (1 - r_\pi^2) \left\{ G_8 \mathbf{N}_8 + \frac{1}{9} G_{27}^{(1/2)} \mathbf{D}_{1/2} - \frac{10}{9} G_{27}^{(3/2)} \mathbf{D}_{3/2} \right\} + e^2 \frac{F_\pi F_K}{m_K^2} G_{ew} \mathbf{Z}^{(2)} \right], \quad (\text{C.36b})$$

$$A_{++0}^{ct} = -\frac{m_K^4}{F_K} \left[ \frac{5}{3}(1-r_\pi^2)G_{27}^{(3/2)}D_{3/2} + e^2 \frac{F_\pi F_K}{m_K^2} G_{ew} Z^{(3)} \right], \quad (\text{C.36c})$$

with the various counter-term combinations defined in Eqs.(C.40). It is worth noticing that here we kept only divergent counter-terms. More counter-terms should, in principle, appear in these expressions. However, as they appear in finite combinations, it is quite sufficient to hide them in the finite part of the various counter-terms combination in Eqs.(C.40), which eventually can be absorbed by a renormalization of the low energy coupling constants  $G_8, G_{27}$  and  $G_{ew}$ . Regarding the loop contributions, the situation is a bit more involved. The relevant topologies are given by

$$A_{IJK}^{\text{loop}} = \begin{array}{c} \text{---} \circ \text{---} \\ \text{---} \circ \text{---} \\ \text{---} \bullet \text{---} \\ \text{---} \bullet \text{---} \\ \text{---} \bullet \text{---} \\ \text{---} \bullet \text{---} \end{array} + \begin{array}{c} \text{---} \circ \text{---} \\ \text{---} \bullet \text{---} \\ \text{---} \bullet \text{---} \\ \text{---} \bullet \text{---} \end{array} + \begin{array}{c} \text{---} \circ \text{---} \\ \text{---} \bullet \text{---} \\ \text{---} \bullet \text{---} \\ \text{---} \bullet \text{---} \end{array} + \begin{array}{c} \text{---} \bullet \text{---} \\ \text{---} \bullet \text{---} \\ \text{---} \bullet \text{---} \\ \text{---} \bullet \text{---} \end{array} \quad (\text{C.37})$$

to which we should, in principle, add tadpole topologies. The overall effect of these contributions being the cancellation of all  $G_m$  contributions we do not show them explicitly even though this cancellation has been explicitly checked. After going through all the calculations we obtain the following loop amplitudes

$$A_{0+-}^{\text{loop}} = \frac{\sqrt{2}}{2(4\pi)^2} \frac{m_K^2}{F_K} \left[ G_8 F_A^{(8)} + \frac{1}{9} G_{27}^{(1/2)} F_A^{(1/2)} + \frac{5}{9} G_{27}^{(3/2)} F_A^{(3/2)} + \right. \\ \left. + e^2 \frac{F_\pi F_K}{m_K^2} G_{ew} E_A^{(1)} + m_K^2 \left\{ G_8 F_B^{(8)} + \frac{1}{9} G_{27}^{(1/2)} F_B^{(1/2)} + \right. \right. \\ \left. \left. + \frac{5}{9} G_{27}^{(3/2)} F_B^{(3/2)} + e^2 \frac{F_\pi F_K}{m_K^2} G_{ew} E_B^{(1)} \right\} \right], \quad (\text{C.38a})$$

$$A_{000}^{\text{loop}} = \frac{\sqrt{2}}{2(4\pi)^2} \frac{m_K^2}{F_K} \left[ G_8 F_A^{(8)} + \frac{1}{9} G_{27}^{(1/2)} F_A^{(1/2)} - \frac{10}{9} G_{27}^{(3/2)} F_A^{(3/2)} + \right. \\ \left. + e^2 \frac{F_\pi F_K}{m_K^2} G_{ew} E_A^{(2)} + m_K^2 \left\{ G_8 F_B^{(8)} + \frac{1}{9} G_{27}^{(1/2)} F_B^{(1/2)} - \right. \right. \\ \left. \left. - \frac{10}{9} G_{27}^{(3/2)} F_B^{(3/2)} + e^2 \frac{F_\pi F_K}{m_K^2} G_{ew} E_B^{(2)} \right\} \right], \quad (\text{C.38b})$$

$$A_{++0}^{\text{loop}} = \frac{1}{2(4\pi)^2} \frac{m_K^2}{F_K} \left[ \frac{5}{3} G_{27}^{(3/2)} F_A^{(3/2)} + e^2 \frac{F_\pi F_K}{m_K^2} G_{ew} E_A^{(3)} + \right. \\ \left. + m_K^2 \left\{ \frac{5}{3} G_{27}^{(3/2)} F_B^{(3/2)} + e^2 \frac{F_\pi F_K}{m_K^2} G_{ew} E_B^{(3)} \right\} \right], \quad (\text{C.38c})$$

where the various recurrent loop functions are collected in Eqs.(C.41). Using the results of Eq.(A.12) and Eq.(A.13), as well as the counter-term divergences of Tab.(B.1), it is now easy to check that the NLO amplitudes

$$A_{IJK} \doteq A_{IJK}^r + \delta A_{IJK} + A_{IJK}^{\text{ct}} + A_{IJK}^{\text{loop}} \quad (\text{C.39})$$

are finite. Our interest in these NLO amplitudes is in fact indirect. What really matters for us here is their implications to the radiative modes  $K \rightarrow \pi\pi\gamma$  analyzed in the following section.

## Counter-terms and loop functions

The various counter-term combinations relevant for the  $K \rightarrow \pi\pi$  renormalization are

$$\begin{aligned} N_8 = 2[(N_5 - 2N_7 + 2N_8 + N_9) + \\ + (2N_5 + 4N_7 + N_8 - 2N_{10} - 4N_{11} - 2N_{12})r_\pi^2] , \end{aligned} \quad (\text{C.40a})$$

$$\begin{aligned} D_{1/2} = (D_4 - D_5 - 9D_6 + 4D_7) - \\ - 2(6D_1 + 2D_2 - 2D_4 - 6D_6 - D_7)r_\pi^2 , \end{aligned} \quad (\text{C.40b})$$

$$D_{3/2} = (D_4 - D_5 + 4D_7) - 2(2D_2 - 2D_4 - D_7)r_\pi^2 , \quad (\text{C.40c})$$

$$Z^{(1)} = \frac{1}{3} [Z_6(1 + 2r_\pi^2) - 6Z_{\text{ew}}] , \quad (\text{C.40d})$$

$$Z^{(2)} = \frac{1}{3} (2Z_6 + 3Z_9)(r_\pi^2 - 1) , \quad (\text{C.40e})$$

$$Z^{(3)} = Z_6 + Z_9(1 - r_\pi^2) - 2Z_{\text{ew}} , \quad (\text{C.40f})$$

$$Z_{\text{ew}} = (Z_1 + 2Z_2) + (2Z_1 + Z_2)r_\pi^2 . \quad (\text{C.40g})$$

Here are collected the various one-loop functions occurring in  $K \rightarrow \pi\pi$  loop amplitudes:

$$F_A^{(8)} = \frac{2}{3} (-1 + 4r_\pi^2) \mathcal{A}_K - \frac{1}{2} (r_\pi^{-2} - 1 + 2r_\pi^2) \mathcal{A}_8 + \delta F_A , \quad (\text{C.41a})$$

$$\begin{aligned} F_A^{(1/2)} = \frac{1}{6} (-15r_\pi^{-2} - 19 + 46r_\pi^2) \mathcal{A}_K + (2r_\pi^{-2} - 7 + 4r_\pi^2) \mathcal{A}_8 + \\ + \delta F_A , \end{aligned} \quad (\text{C.41b})$$

$$\begin{aligned} F_A^{(3/2)} = \frac{1}{3} (-3r_\pi^{-2} - 5 + 5r_\pi^2) \mathcal{A}_K - \frac{1}{4} (r_\pi^{-2} + 1 + 2r_\pi^2) \mathcal{A}_8 + \\ + \frac{1}{12} (15r_\pi^{-2} - 97 + 106r_\pi^2) \mathcal{A}_\pi , \end{aligned} \quad (\text{C.41c})$$

$$\delta F_A = \frac{1}{6} (3r_\pi^{-2} + 1 - 10r_\pi^2) \mathcal{A}_\pi , \quad (\text{C.41d})$$

$$F_B^{(8)} = \frac{1}{9} r_\pi^2 (-1 + r_\pi^2) \mathcal{B}_{K88} + \frac{1}{6} (r_\pi^{-2} - 1) \mathcal{B}_{\pi K8} + \delta F_B , \quad (\text{C.41e})$$

$$F_B^{(1/2)} = r_\pi^2 (1 - r_\pi^2) \mathcal{B}_{K88} + \frac{2}{3} (-r_\pi^{-2} + 1) \mathcal{B}_{\pi K8} + \delta F_B , \quad (\text{C.41f})$$

$$F_B^{(3/2)} = (1 - 3r_\pi^2 + 2r_\pi^4) \mathcal{B}_{K\pi\pi} + \frac{1}{12} (r_\pi^{-2} - 1) \mathcal{B}_{\pi K8} + \frac{1}{4} (5r_\pi^{-2} - 13 + 8r_\pi^2) \mathcal{B}_{\pi K\pi} , \quad (\text{C.41g})$$

$$\delta F_B = - (2 - 3r_\pi^2 + r_\pi^4) \mathcal{B}_{K\pi\pi} + \frac{1}{2} (r_\pi^{-2} - 5 + 4r_\pi^2) \mathcal{B}_{\pi K\pi} , \quad (\text{C.41h})$$

$$E_A^{(1)} = -\frac{8}{3} \mathcal{A}_K + \frac{1}{4} (2 - 3r_\pi^{-2}) \mathcal{A}_8 + \frac{1}{12} (9r_\pi^{-2} - 46) \mathcal{A}_\pi , \quad (\text{C.41i})$$

$$E_B^{(1)} = \frac{1}{2} \mathcal{B}_{KKK} - \mathcal{B}_{K\pi\pi} + \frac{1}{4} r_\pi^{-2} \mathcal{B}_{\pi K8} + \frac{1}{4} (3r_\pi^{-2} - 8) \mathcal{B}_{\pi K\pi} , \quad (\text{C.41j})$$

$$E_A^{(2)} = \frac{1}{2} (r_\pi^{-2} - 2) (\mathcal{A}_K - \mathcal{A}_\pi) , \quad (\text{C.41k})$$

$$E_B^{(2)} = \frac{1}{2} \mathcal{B}_{KKK} + 2 (-1 + r_\pi^2) \mathcal{B}_{K\pi\pi} - \frac{1}{2} r_\pi^{-2} \mathcal{B}_{\pi K\pi} , \quad (\text{C.41l})$$

$$E_A^{(3)} = -\frac{1}{6} (3r_\pi^{-2} + 10) \mathcal{A}_K + \frac{1}{24} (30r_\pi^{-2} - 116) \mathcal{A}_\pi - \frac{1}{4} (3r_\pi^{-2} - 2) \mathcal{A}_8 , \quad (\text{C.41m})$$

$$E_B^{(3)} = (1 - 2r_\pi^2) \mathcal{B}_{K\pi\pi} + \frac{1}{4} r_\pi^{-2} \mathcal{B}_{\pi K8} + \frac{1}{4} (5r_\pi^{-2} - 8) \mathcal{B}_{\pi K\pi} , \quad (\text{C.41n})$$

where, for convenience, we defined

$$\mathcal{A}_I \doteq A_0(m_I^2) \quad \text{and} \quad \mathcal{B}_{IJK} \doteq B_0(m_I^2, m_J^2, m_K^2) . \quad (\text{C.42})$$

with  $A_0$  and  $B_0$  the one-loop scalar functions defined in Eq.(A.12) and Eq.(A.13), respectively.

$K \rightarrow \pi\pi\gamma$

## Kinematic

We parametrize the three body decay amplitudes  $K \rightarrow \pi\pi\gamma$  as follows

$$A(K(P) \rightarrow \pi(q_1)\pi(q_2)\gamma(q_3)) , \quad (\text{C.43})$$

with the pion pair  $\pi\pi = \pi^-\pi^+, \pi^0\pi^0$  or  $\pi^-\pi^0$ . Moreover, if the mass difference between charged and neutral pions is neglected, we have

$$P = q_1 + q_2 + q_3, \quad P^2 = M_K^2, \quad q_1^2 = q_2^2 = M_\pi^2 \quad \text{and} \quad q_3^2 = 0, \quad (\text{C.44})$$

where  $M_i$  indicates, as usual, the physical mass of the particle  $i$ . While a two body decay kinematic is completely fixed, a three body decay amplitude needs two kinematic variables to be completely specified. The amplitudes presented in this section are parametrized in terms of two of the following kinematic variables:

$$z_1 \doteq \frac{q_1 \cdot q_3}{M_K^2}, \quad z_2 \doteq \frac{q_2 \cdot q_3}{M_K^2} \quad \text{and} \quad z_3 \doteq \frac{P \cdot q_3}{M_K^2}, \quad (\text{C.45})$$

where, in the kaon rest frame, we have

$$z_3 = \frac{E_\gamma}{M_K}. \quad (\text{C.46})$$

These variables are not independent since the transversality of the on-shell photon implies that  $z_3 = z_1 + z_2$ . In particular, we will systematically use the relation

$$\begin{aligned} q_1 \cdot q_2 &= \frac{1}{2} [M_K^2 - 2M_\pi^2 - 2z_1 M_K^2 - 2z_2 M_K^2] \\ &= \frac{1}{2} [(1 - 2z_3)M_K^2 - 2M_\pi^2]. \end{aligned} \quad (\text{C.47})$$

This parametrization in terms of  $z_i$  is particularly well suited for analytic computations but, in order to compare them with experimental data, alternative parametrizations will be presented in Sec.C.3. From Lorentz and gauge invariance, the most general  $K \rightarrow \pi\pi\gamma$  amplitude reads [103, 104, 193]

$$\begin{aligned} A(K \rightarrow \pi(q_1)\pi_2(q_2)\gamma(q_3)) &= \left[ E(z_1, z_2) \frac{\lambda^\mu}{M_K} + \right. \\ &\quad \left. + iM(z_1, z_2) \frac{\epsilon^{\mu\nu\rho\sigma} q_{1\nu} q_{2\rho} q_{3\sigma}}{M_K^3} \right] \epsilon_\mu^*(q_3), \end{aligned} \quad (\text{C.48})$$

with  $\lambda^\mu \doteq z_2 q_1^\mu - z_1 q_2^\mu$  and where the two terms  $E(z_1, z_2)$  and  $M(z_1, z_2)$  are the dimensionless electric and magnetic amplitudes, respectively. Note that they do not interfere in the rate once the sum over the photon polarizations is done, since photons produced by  $E$  and  $M$  have opposite parity. The electric part can be further decomposed into a bremsstrahlung (QED emission) and a direct emission term as

$$E(z_1, z_2) \doteq E_{\text{IB}}(z_1, z_2) + E_{\text{DE}}(z_1, z_2), \quad (\text{C.49})$$



$$A_{2+-}^{(\gamma)} = -\frac{2eF \left( G_2 - \frac{25}{9} G_{27}^{(3/2)} \right)}{z_2 (2z_1 M_K^2 - \Delta_\pi)} \Delta_\pi \times \left[ \lambda \cdot \epsilon^*(q_3) - \frac{(4z_1 z_2 M_K^2 - z_3 \Delta_\pi)}{(2z_2 M_K^2 - \Delta_\pi)} q_2 \cdot \epsilon^*(q_3) \right], \quad (\text{C.52b})$$

$$A_{++0}^{(\gamma)} = -\frac{2eF}{z_2 (2z_1 M_K^2 - \Delta_\pi)} \left[ \Delta_\pi G_2 - \frac{e^2 F^2 G_{ew}}{(2z_3 M_K^2 + \Delta_K)} (2z_2 M_K^2 + \Delta_K + \Delta_\pi) + \frac{5G_{27}^{(3/2)}}{9(2z_3 M_K^2 + \Delta_K)} \left[ -3(M_K^2 - M_\pi^2)(2z_2 M_K^2 + \Delta_K + \Delta_\pi) + 2M_K^2(3z_1 \Delta_K + 4z_3 \Delta_\pi) + \Delta_K \Delta_\pi \right] \right] \times \lambda \cdot \epsilon^*(q_3) - \frac{2eF}{z_2 (2z_1 M_K^2 - \Delta_\pi)} \left[ -z_1 \Delta_\pi G_2 + \frac{e^2 F^2 G_{ew}}{(2z_3 M_K^2 + \Delta_K)} (z_1 \Delta_K + z_3 \Delta_\pi) + \frac{5G_{27}^{(3/2)}}{9(2z_3 M_K^2 + \Delta_K)} \left[ 3(M_K^2 - M_\pi^2)(z_1 \Delta_K + z_3 \Delta_\pi) - 2z_1 z_3 M_K^2 (3\Delta_K + 4\Delta_\pi) - \Delta_K \Delta_\pi (z_1 - 3z_2) \right] \right] \times q_2 \cdot \epsilon^*(q_3), \quad (\text{C.52c})$$

$$A_{100}^{(\gamma)} = A_{200}^{(\gamma)} = 0, \quad (\text{C.52d})$$

The bare mass and the physical mass differences vanish at lowest order and the gauge invariance is subsequently fulfilled since all the gauge symmetry violating pieces proportional to  $q_2 \cdot \epsilon^*(q_3)$  drop out. At NLO, on the other hand, masses are renormalized so that  $m_i^2 \neq M_i^2$  in such a way that the renormalized tree-level amplitudes are no more gauge invariant. Yet, as shown in the following section, these gauge violating contributions will cancel against loop and counter-terms induced gauge violating contributions.

We may, therefore, conclude that the  $K \rightarrow \pi\pi\gamma$  on-shell electric amplitudes are given at lowest order by

$$E^{1+-} = E_{\text{IB}}^{1+-} = -\frac{e}{z_1 z_2 M_K} A(K^1 \rightarrow \pi^+ \pi^-), \quad (\text{C.53a})$$

$$E^{++0} = E_{\text{IB}}^{++0} = -\frac{e}{z_2 z_3 M_K} A(K^+ \rightarrow \pi^+ \pi^0), \quad (\text{C.53b})$$





topology


(C.55)

which is the one responsible for the mass renormalization we already noted from the tree-level amplitude and which is also connected to the last two diagrams of Eq.(C.54), where only  $L_{4,\dots,8}$  strong counter-terms matter, see Eqs.(C.7) and Eq.(C.8). Yet, a simplification occurs regarding the loops: it is not possible to build a loop amplitude for which the weak vertex is a mixing term like  $K^+\pi^-$ . This can be easily checked by inspecting all the possible topologies.

Needless to say that the final NLO  $K \rightarrow \pi\pi\gamma$  are huge expressions. However, it is possible to get rather compact expressions if the non-radiative amplitudes are used. Here is how it goes:

1. the renormalization of the amplitudes in Eqs.(C.52) is performed. Regarding the wave functions and decay constants, we follow the same procedure as for the non-radiative amplitudes, see Eqs.(C.30). The mass renormalization is performed directly from the off-shell amplitudes using Eq.(C.4) and Eqs.(C.7). We then end up with non gauge invariant amplitudes

$$A_{IJK}^{(\gamma)} \rightarrow A_{IJK}^{(\gamma)\text{tree}} = A_{IJK}^{(\gamma)r} + \delta A_{IJK}^{(\gamma)} , \quad (\text{C.56})$$

where the non gauge invariant contributions come from the renormalization procedure, i.e., they are proportional to either scalar loop functions  $A_0$  or strong counter-terms.

2. the counter-terms contributions is then added to  $A_{IJK}^{(\gamma)\text{tree}}$  to give  $A_{IJK}^{(\gamma)\text{tree+ct}}$ , where all the gauge violating terms proportional to the strong counter-terms drop out.
3. the loop contributions are finally added to obtain the complete amplitudes

$$A_{IJK}^{(\gamma)\text{tot}} \doteq A_{IJK}^{(\gamma)\text{tree+ct+loop}} , \quad (\text{C.57})$$

which are now fully gauge invariant and finite.

4. the corresponding electrical amplitudes are extracted from the complete amplitudes and split into their bremsstrahlung , loop and counter-terms component as

$$E_{IJK}^{(\gamma)\text{tot}} \doteq E_{\text{IB}}^{IJK} + E_{\text{loop}}^{IJK} + E_{\text{CT}}^{IJK} . \quad (\text{C.58})$$

Doing so, we obtain

$$E_{\text{IB}}^{1+-} = -\frac{e}{z_1 z_2 M_K} A_{1+-} , \quad (\text{C.59a})$$

$$E_{\text{IB}}^{++0} = -\frac{e}{z_2 z_3 M_K} A_{++0} , \quad (\text{C.59b})$$

$$E_{\text{IB}}^{2+-} = E_{\text{IB}}^{100} = E_{\text{IB}}^{200} = 0 , \quad (\text{C.59c})$$

where the  $A_{IJK}$  are given in Eq.(C.39), namely, the full NLO on-shell  $K \rightarrow \pi\pi$  amplitudes that include both counter-terms and loops (which include, in particular, the strong phases arising from  $\pi\pi$  loops). Adopting this renormalization for the bremsstrahlung contributions, the loop contributions are given by

$$E_{\text{loop}}^{++0} = \mathcal{N} [h(z_1) + g(z_2) - 4A^+ h_{\pi\pi}(-z_3) + 2A^{ew} h_{KK}(-z_3)] , \quad (\text{C.60a})$$

$$E_{\text{loop}}^{1+-} = \mathcal{N} [h(z_1) + h(z_2) - 8A^0 h_{\pi\pi}(-z_3) - 4A^{ew} h_{KK}(-z_3)] , \quad (\text{C.60b})$$

$$E_{\text{loop}}^{2+-} = \mathcal{N} [\tilde{h}(z_1) - \tilde{h}(z_2)] , \quad (\text{C.60c})$$

$$E_{\text{loop}}^{200} = \mathcal{N} [\tilde{g}(z_1) - \tilde{g}(z_2)] , \quad (\text{C.60d})$$

$$E_{\text{loop}}^{100} = 0 , \quad (\text{C.60e})$$

where we introduced the normalization factor

$$\mathcal{N} \doteq -\frac{e(m_K^2 - m_\pi^2)}{8\pi^2 F_\pi} , \quad (\text{C.61})$$

while the composite loop functions  $h$  and  $g$  are given by

$$h(z) \doteq A^8 h_{K\eta}(z) + A^0 h_{\pi K}(z) - A^+ h_{K\pi}(z) , \quad (\text{C.62a})$$

$$g(z) \doteq 2A^+ (h_{\pi K}(z) + h_{K\pi}(z)) . \quad (\text{C.62b})$$

The loop functions  $h_{ij}(z)$  are given in Ref. [104] in terms of the subtracted three-point Passarino-Veltman function  $C_{20}$  and they are also explicitly given in Eq.(A.21). The  $A^i$  are, on the other hand, defined as follow

$$A^+ \doteq \frac{5}{6} G_{27}^{(3/2)} - \frac{1}{2} A^{ew} , \quad (\text{C.63a})$$

$$A^0 \doteq G_8 + \frac{1}{9} G_{27}^{(1/2)} + \frac{5}{9} G_{27}^{(3/2)} - A^{ew} , \quad (\text{C.63b})$$

$$A^8 \doteq G_8 - \frac{4}{9} G_{27}^{(1/2)} + \frac{5}{18} G_{27}^{(3/2)} - \frac{3}{2} A^{ew} , \quad (\text{C.63c})$$

with

$$A^{ew} \doteq \frac{e^2 F_\pi^2}{m_K^2 - m_\pi^2} G_{ew} . \quad (\text{C.64})$$

Note that in Eqs.(C.60),  $\tilde{h}$  and  $\tilde{g}$  are respectively given by  $h$  and  $g$  in the limit where  $G_{ew} = 0$ , while  $E_{\text{loop}}^{100}$  vanishes because of the combined effect of CP and Bose symmetries. It is also worth pointing out that all the loop contributions are finite (the  $f_k^{ij}(z)$  functions are, indeed, finite by construction, see Eq.(A.21) and Eqs.(A.22)) and constant in the  $z_i \rightarrow 0$  limit, see Eq.(A.23). As a consequence, the counter-term contributions must be finite too: we, indeed, find that

$$(E_{\text{CT}}^{++0}, E_{\text{CT}}^{1+-}, E_{\text{CT}}^{2+-}) = -\frac{2eG_8 M_K^3}{F_K}(-N_i, 2\text{Re}N_i, 2i\text{Im}N_i), \quad (\text{C.65a})$$

$$E_{\text{CT}}^{2+-} = E_{\text{CT}}^{100} = E_{\text{CT}}^{200} = 0, \quad (\text{C.65b})$$

where we relaxed the CP conservation limit in order to make the imaginary part of the counter-term explicit and where the counter-term combination is given by

$$\begin{aligned} N_i \doteq & N_{14} - N_{15} - N_{16} - N_{17+} \\ & + \frac{1}{18G_8} \left( G_{27}^{(1/2)} + 5G_{27}^{(3/2)} \right) (D_{13} + D_{14} + 3D_{15} - D_{16}), \end{aligned} \quad (\text{C.66})$$

where both octet and 27-plet combinations are separately finite, see Tab.(B.1). Since electroweak counter-term emerge from density-density operators, they always contain two derivatives power less than current-current four quark operators. Hence, Lorentz invariance forbid them to produce a real photon through  $F_{\mu\nu}$  at NLO as at that order they are of  $\mathcal{O}(p^2)$  and this explains why they do not appear in Eq.(C.66).

## Multipoles expansion

In the previous section, we gave the full  $K \rightarrow \pi\pi\gamma$  amplitudes at NLO in ChPT. In particular, we saw that the Low's theorem prediction holds at NLO since we were able to fully express the bremsstrahlung amplitude in terms of the NLO  $K \rightarrow \pi\pi$  amplitudes (see Eqs.(C.59)), which include the partial strong phases found at that order. At the same order, the direct emissions receive strong phases as well via their  $h_{\pi\pi}$  dependencies (see Eqs.(C.60a) and (C.60b)). We already mentioned in chapter 1 that a complete treatment of strong phases is tricky within a perturbative approach. In fact, the strong phases we found at NLO are only partial contributions expected to be corrected at higher order. Nonetheless, one of the basic ingredients when dealing with CP violating observable is weak and strong phases interferences. In the case of  $K \rightarrow \pi\pi$  decays it has become usual to put the strong phases by hand through

the so-called unitarization of the partial isospin amplitude. In a nutshell, it amounts to consider the strong phases as parameters fitted from experiment rather than robust theoretical numbers. In the case of  $K \rightarrow \pi\pi$  decays it is as easy to implement as it is easy to decompose the amplitudes in their isospin components, see Eq.(1.18). In the radiative case of  $K \rightarrow \pi\pi\gamma$ , the strong phase assignment procedure is more sophisticated but can still be achieved thanks to the so-called multipole expansion.

Let us recall that the parity of a photon of total angular momentum  $\mathbf{J}_\gamma = \mathbf{L} + \mathbf{S}$ ,  $\mathbf{S} = 1$  being its spin and  $\mathbf{L}$  its orbital momentum, is given by  $P_\gamma = (-1)(-1)^L = (-1)^{L+1}$  such that a photon may be in two different parity states : electrical  $2^J$ -poles with  $P_\gamma = (-1)^{J_\gamma+1}$  or magnetic  $2^J$ -poles with  $P_\gamma = (-1)^{J_\gamma}$ . In the context of  $K \rightarrow \pi\pi\gamma$  decays, they are respectively described by the electric amplitude  $E(z_1, z_2)$  and the magnetic amplitude  $M(z_1, z_2)$ . Let us now label the total angular momentum of the two pion states as  $\mathbf{J}_{2\pi}$  and notice that:

1. since kaons do not carry angular momentum, the angular momentum conservation tells us that, in order for the  $K \rightarrow \pi\pi\gamma$  decay to be allowed,  $\mathbf{J}_\gamma = \mathbf{J}_{2\pi}$  in such a way that  $\mathbf{J}_\gamma \otimes \mathbf{J}_{2\pi}$  contains 0,
2. Bose statistic imposes that, under the exchange of the two pions, the corresponding parity given by  $(-1)^{J_{2\pi}+I} = +1$ ,  $I$  being the isospin of the two pion state.

If  $F(z_1, z_2)$  represents now the electric (or the magnetic) direct emission amplitude for a given  $K \rightarrow \pi\pi\gamma$  channel, we may expand it in power of  $\delta_- \doteq z_1 - z_2$  using a simple Taylor expansion around  $z \doteq z_3/2$ ,

$$z_{1,2} = \frac{z_3}{2} \pm \frac{\delta_-}{2} = z \pm \frac{\delta_-}{2}, \quad (\text{C.67})$$

to split it in  $z_1 \leftrightarrow z_2$  symmetric  $F_+$  and anti-symmetric  $F_-$  components (by collecting even and odd power terms in  $\delta_-$ ). We, therefore, decompose the electric direct amplitude into two terms:

$$A_\pm = F_\mp \frac{\lambda^\mu}{m_K} \epsilon_\mu^*(q_3) \quad \text{where} \quad \lambda^\mu \doteq z_2 q_1^\mu - z_1 q_2^\mu, \quad (\text{C.68})$$

which are respectively symmetric and anti-symmetric under the exchange of the two pion as under such an exchange,  $z_1 \rightarrow z_2$  and  $\lambda^\mu \rightarrow -\lambda^\mu$ . These symmetry properties imply that the pions are in an  $I = 0, 2$  state in  $A_+$  while being in an  $I = 1$  states in  $A_-$ . Correspondingly, and due to Bose statistic,  $\mathbf{J}_\gamma$  is even ( $\mathbf{J}_\gamma = 2, 4, \dots$ ) for  $A_+$  and odd ( $\mathbf{J}_\gamma = 1, 3, \dots$ ) for  $A_-$ . In conclusion, the direct electric amplitudes can be expanded in multipoles, according to the

angular momentum of the two pions [98]:

$$E_{DE}(z_1, z_2)e^{i\delta_{DE}} = E_1(z_3)e^{i\delta_1} + E_2(z_3)e^{i\delta_2}(z_1 - z_2) + E_3(z_3)e^{i\delta_3}(z_1 - z_2)^2 + \dots, \quad (\text{C.69})$$

and similarly for  $M_{DE}$ . There are several interesting features in this expansion [69]:

1. for  $K^0$  decays, the odd and even multipoles produce the  $\pi\pi$  pair in opposite CP states. Indeed, the  $2\pi$  being a CP even eigenstate, the CP properties of the final state are dictated by the photon one, which is given by  $(-1)^L$ ,
2. when CP-conserving, the dipole emission  $E_1$  dominates over higher multipoles, which have to overcome the angular momentum barrier (in fact,  $|z_1 - z_2| < 0.2$ ),
3. the strong phases can be assigned consistently to each multipole, since it produces the  $\pi\pi$  state in a given angular momentum state,
4. if the  $E_{IB}$  and  $E_{DE}$  amplitudes interfere and have different weak and strong phases, a CP-asymmetry can be generated, see Eq.(2.11).

In the context of the present work, we will focus our attention on the dipole component  $E_1$  of  $K^0 \rightarrow \pi^+\pi^-\gamma$  and  $K^+ \rightarrow \pi^+\pi^0\gamma$  amplitudes extracted in the following section.

## Dipoles

For  $K \rightarrow \pi^+\pi^0\gamma$ , the function  $E^{loop}(W^2, T_c^*)$  occurring in Eq.(C.70) is

$$G_8 E^{loop}(z_1, z_2) = \text{Re} [h(z_1) + g(z_2) - 4A^+ h_{\pi\pi}(-z_3)] , \quad (\text{C.70})$$

as obtained from Eq.(C.60a) by neglecting  $\text{Re} A^{ew} \ll \text{Re} G_{8,27}$  (since  $G_{ew}$  is entirely generated by the electroweak penguins). The real part refers to the weak phases only. Performing the multipole expansion and expressing the  $K \rightarrow PP$  amplitudes parametrically in terms of the  $K \rightarrow \pi\pi$  isospin amplitudes

$$\begin{aligned} A_0 &= \sqrt{2}F_\pi(m_K^2 - m_\pi^2) \left[ G_8 + \frac{1}{9}G_{27}^{1/2} - \frac{2}{3}A^{ew} \right] , \\ A_2 &= 2F_\pi(m_K^2 - m_\pi^2) \left[ \frac{5}{9}G_{27}^{3/2} - \frac{1}{3}A^{ew} \right] , \end{aligned} \quad (\text{C.71})$$

we find

$$G_8 E_1^{loop}(z_3 = 2z) = \frac{-em_K}{(4\pi F_\pi)^2} [A_0 h_0(z) + A_2 h_2(z) + A_{\delta 2} \delta h_2(z)] , \quad (\text{C.72})$$

where

$$h_0(z) = \sqrt{2}(h_{K\eta}(z) + h_{\pi K}(z)) , \quad (\text{C.73a})$$

$$h_2(z) = 4h_{\pi K}(z) + \frac{3}{2}h_{K\pi}(z) - 6h_{\pi\pi}(-2z) - \frac{1}{2}h_{K\eta}(z) , \quad (\text{C.73b})$$

$$\delta h_2(z) = 3h_{K\eta}(z) - 6h_{KK}(-2z) , \quad (\text{C.73c})$$

with  $A_{\delta 2} = -(2/3)F_\pi(m_K^2 - m_\pi^2)A^{ew}$ . For the small  $\delta h_2(z)$  term, we can further set  $\text{Im } A_{\delta 2} \approx \text{Im } A_2$ , since CP-violation from  $Q_8$  dominates in the  $\Delta I = 3/2$  channel. Eq.(2.16) is then found by defining  $(\delta)h_{20}(z_3) = (\delta)h_2(z)/h_0(z)$ . Let us stress that  $A_0$  and  $A_2$  are just convenient parameters to keep track of the weak phases of  $G_8$ ,  $G_{27}$ , and  $G_{ew}$ . As such, they do not include any strong phase. Further, the strong phase originating from  $h_{\pi\pi}$  is discarded, as it has already been taken care of through the multipole expansion.

Similarly, the  $K^0 \rightarrow \pi^+\pi^-\gamma$  direct emission amplitude occurring in Eq.(2.31) is the dipole part of the amplitude in Eq.(C.60b),

$$E_{+-}(z_3 = 2z) = -\frac{2em_K}{(4\pi F_\pi)^2} [A_0 h'_0(z) + A_2 h'_2(z) + A_{\delta 2} \delta h'_2(z)] - \frac{4eG_8 m_K^3}{F_\pi} N_i ,$$

where

$$h'_0(z) = \sqrt{2}(h_{K\eta}(z) + h_{\pi K}(z) - 4h_{\pi\pi}(-2z)) , \quad (\text{C.74a})$$

$$h'_2(z) = -\frac{1}{2}h_{K\eta}(z) + h_{\pi K}(z) - \frac{3}{2}h_{K\pi}(z) - 4h_{\pi\pi}(-2z) , \quad (\text{C.74b})$$

$$\delta h'_2(z) = 3h_{K\eta}(z) + 6h_{KK}(-2z) . \quad (\text{C.74c})$$

Again, defining  $(\delta)h'_{20}(z_3) = (\delta)h'_2(z)/h'_0(z)$  immediately leads to Eq.(2.35).

It is worth noting that, contrary to what is generally stated, the amplitude for  $K_L \rightarrow \pi^0\pi^0\gamma$  does not vanish at  $\mathcal{O}(p^4)$ , but is suppressed by the  $\Delta I = 1/2$  rule. Being in addition a pure quadrupole emission, the rate is tiny

$$\mathcal{B}(K_L \rightarrow \pi^0\pi^0\gamma)_{G_{27}} = 7.3 \times 10^{-13} . \quad (\text{C.75})$$

For comparison, Ref. [103] found that, using dimensional arguments, the  $G_8$  contribution at  $\mathcal{O}(p^6)$  is of the order of  $10^{-10}$ , much larger but still far below the experimental bound  $2.43 \times 10^{-7}$ .

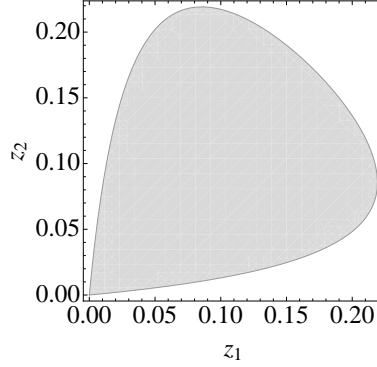


**Fig. C.1:** Representation of the phase-space in the  $(z_1, z_2)$  plane.

## Phase space parametrisations

We saw that  $z_{1,2(,3)}$  are well suited variables to investigate  $K \rightarrow \pi\pi\gamma$  theoretically. Yet, as we will see, alternative sets of variables are more suited for experimental investigations. From an experimental point of view, it is appreciable to describe a given process in terms of measurable quantities and in order to compare theory and experiment we must be able to go from one parametrization to another. This is the purpose of this section.

### $(z_1, z_2)$ parametrization

The parametrization of  $A(K \rightarrow \pi\pi\gamma)$  in terms of Lorentz invariant variables  $z_{1,2}$  was presented in Eq.(C.45). Let us now find the range over which they evolve. In the kaon rest frame, using the momentum conservation law, it is easy to see that

$$z_{1,2} = a_{2,1} - \frac{E_{2,1}}{M_K}, \quad (\text{C.76})$$

where  $E_i$  is the energy of  $\pi(q_i) \doteq \pi_i$  while

$$a_{1,2} \doteq \frac{1}{2} (1 + r_{1,2}^2 - r_{2,1}^2) \quad (\text{C.77})$$

is a constant where  $r_i \doteq M_{\pi_i}/M_K$ . Up to now,  $z_{1,2}$  are equivalent so, without loss of generality, we start by looking for the extrema of  $z_2$ . It is clear that  $z_2$  reaches its maximum when  $E_1$  is at its minimum, i.e.,  $E_1^{\min} = M_{\pi_1}$ , such that  $z_2^{\max} = a_1 - r_1$ . Conversely,  $z_2$  will reach its minimum when  $E_1$  hits its



maximum. Looking at the Mandelstam variable

$$s \doteq (q_2 + q_3)^2 = (P - q_1)^2 = M_{\pi_2}^2 + 2q_2 \cdot q_3 = M_K^2 + M_{\pi_1}^2 - 2M_K E_1, \quad (\text{C.78})$$

we see that it happens when  $q_3 = 0$  so that  $E_1^{\max} = M_K a_1$ , which subsequently leads to  $z_2^{\min} = 0$ . In order to find the bounds for  $z_1$  when a value of  $z_2$  is fixed, we ask for the angle between the two pions to exist, namely, we force

$$\cos \theta = \frac{E_1 E_2 - q_1 \cdot q_2}{|\vec{q}_1| |\vec{q}_2|} \quad (\text{C.79})$$

to satisfy

$$-1 \leq \cos \theta \leq +1. \quad (\text{C.80})$$

This is performed by rewriting  $\cos \theta$  in terms of  $z_{1,2}$  using Eq.(C.76) and if the  $\cos \theta$  indeed exists then

$$0 \leq z_2 \leq a_1 - r_1, \quad (\text{C.81a})$$

$$\frac{B - \sqrt{B^2 - Ar_1^2}}{A} z_2 \leq z_1 \leq \frac{B + \sqrt{B^2 - Ar_1^2}}{A} z_2, \quad (\text{C.81b})$$

where  $A = r_2^2 + 2z_2$  and  $B = a_1 - r_1^2 - z_2$ . The derivation of the  $z_2$  range is not detailed because it is just simple (but boring) algebra manipulations. Note that we could, of course, have started with  $z_1$  in which case we would have found the same range but with  $1 \leftrightarrow 2$  indexes exchanged. The corresponding phase-space displayed in Fig.(C.1) reflects, indeed, this symmetry.

### $(T_c^*, E_\gamma)$ parametrization

This parametrization is interesting because it consists of the kinetic energy  $T_c^*$  of one of the pion, say  $\pi_1$ , and the energy of the photon  $E_\gamma$ . Both variables have a simple physical interpretation and are particularly well suited for phenomenological investigations. The range for  $T_c^*$  is easily obtained from that of  $z_2$  since they are linearly related as

$$z_2 = a_1 - r_1 - \frac{T_c^*}{M_K}, \quad (\text{C.82})$$

it follows directly from Eq.(C.81a) that

$$0 \leq T_c^* \leq M_K(a_1 - r_1). \quad (\text{C.83})$$

Once again, the existence of  $\cos \theta$  gives us the allowed range for  $E_\gamma$ . In the present case, we write  $\cos \theta$  in terms of  $E_1$  and  $E_2 = M_K - E_1 - E_\gamma$  using the

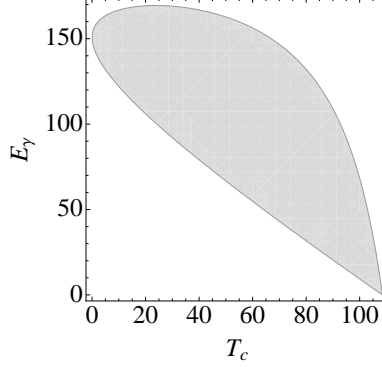


**Fig. C.2:** Representation of the phase-space in the  $(T_c^*, E_\gamma)$  plane.

energy conservation condition. Since  $E_1$  is fixed once  $T_c^*$  is fixed, the condition on  $\cos \theta$  can be solved following the same lines as before and it is found that

$$\frac{(M_K - E_1)^2 - M_{\pi_2}^2 - P^2}{2(M_K - E_1 + P)} \leq E_\gamma \leq \frac{(M_K - E_1)^2 - M_{\pi_2}^2 - P^2}{2(M_K - E_1 - P)}, \quad (\text{C.84})$$

where  $E_1 = T_c^* + M_{\pi_1}$  and  $P = \sqrt{T_c^*(T_c^* + 2M_{\pi_1})}$ . The corresponding graphical representation may be found in Fig.(C.2). Finally, note that the variable substitution  $(z_1, z_2) \rightarrow (T_c^*, E_\gamma)$  goes along with the simple Jacobian

$$\frac{\partial^2}{\partial z_1 \partial z_2} = M_K^2 \frac{\partial^2}{\partial T_c^* \partial E_\gamma}. \quad (\text{C.85})$$

### $(T_c^*, W^2)$ parametrization

The third and last parametrization presented here is derived from  $(T_c^*, E_\gamma)$  and is obtained by trading the photon energy for the variable

$$W^2 = \frac{M_{\pi_1}^2}{M_K^2} z_1 z_3 = \frac{E_\gamma}{M_{\pi_1}^2} \left( E_\gamma + T_c^* + M_{\pi_1} - \frac{M_K}{2} a_1 \right). \quad (\text{C.86})$$

The relevance of this particular variable is not obvious at first but it pops up when looking at Eq.(2.2). This variable differently weighs differently the various contributions entering the differential branching ratio of  $K^+ \rightarrow \pi^+ \pi^0 \gamma$ , namely the bremsstrahlung, interference and direct emissions. This is particularly interesting experimentally, since it allows to probe these various emissions by setting well suited  $W^2$  cuts. Its range is in fact easy to get because  $W^2$  is

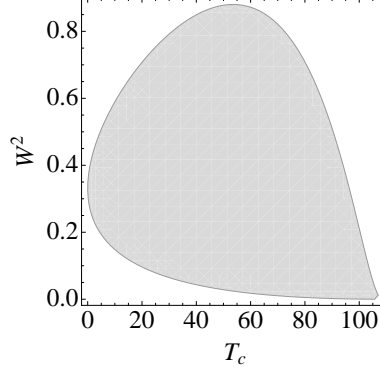


**Fig. C.3:** Representation of the phase-space in the  $(T_c^*, W^2)$  plane.

a monotonic increasing function of  $E_\gamma$ . So using the bounds for  $E_\gamma$  the corresponding bound on  $W^2$  are directly inferred to be

$$\frac{M_K(E_1 - P)(M_K - 2E_1)^2}{4M_{\pi_1}^2(P - E_1 + M_K)^2} \leq W^2 \leq \frac{M_K(E_1 + P)(M_K - 2E_1)^2}{4M_{\pi_1}^2(P + E_1 - M_K)^2} \quad (\text{C.87})$$

with the same conventions as in the last parametrization. For numerical analysis, the present parametrization is the most suited since it allows simple comparison with experimental results, in particular regarding the experimental cuts. We, thus, find it useful to mention the relation between  $z_i$  and  $(T_c^*, W^2)$  variables:

$$z_3 = \frac{1}{2} \left[ \left\{ (k_c + r_1 - a_1)^2 + 4r_1^2 W^2 \right\}^{\frac{1}{2}} - (k_c + r_1 - a_1) \right], \quad (\text{C.88a})$$

$$z_1 = \frac{1}{2} \left[ \left\{ (k_c + r_1 - a_1)^2 + 4r_1^2 W^2 \right\}^{\frac{1}{2}} + (k_c + r_1 - a_1) \right], \quad (\text{C.88b})$$

$$z_2 = a_1 - r_1 - k_c, \quad (\text{C.88c})$$

having introduced the dimensionless variable  $k_c \doteq T_c^*/M_K$ . The corresponding graphical representation is shown in Fig.(C.3). Note that because the relation between  $z_3$  (or  $E_\gamma$ ) and  $W^2$  is non-linear, the Jacobian associated to the variable substitution  $(z_1, z_2) \rightarrow (T_c^*, W^2)$  is not one but rather

$$\frac{\partial^2}{\partial z_1 \partial z_2} = \frac{M_K}{r_1^2} \left[ 4r_1^2 W^2 + (k_c + r_1 - a_1)^2 \right]^{\frac{1}{2}} \frac{\partial^2}{\partial T_c^* \partial W^2}. \quad (\text{C.89})$$



which sum up to give

$$A(\eta' \rightarrow \pi^0\pi^0) = \frac{4}{3\sqrt{3}}F^3\alpha(m_{\eta'}^2)[6I_{8,27} + 9(I_{8,s} - I_{27,s})]\sqrt{2}c_\varphi, \quad (\text{C.93a})$$

$$A(\eta' \rightarrow \pi^+\pi^-) = \frac{4}{3\sqrt{3}}F^3\alpha(m_{\eta'}^2)\left\{ [9I_{8,s} - 4I_{8,27} + 6I_{27,s}]\sqrt{2}c_\varphi + 5I_{8,27}s_\varphi \right\} + \delta'_{ew}, \quad (\text{C.93b})$$

where

$$\alpha(p^2) \doteq p^2 \left( \frac{p^2 - m_\pi^2}{p^2 - m_K^2} \right). \quad (\text{C.94})$$

The corresponding amplitudes for  $\eta$  are obtained applying the complementary relations of Eq.(4.19). The electroweak correction affecting the charged channel reads, for its part,

$$\delta'_{ew} = -\frac{16\pi F^5}{\sqrt{3}}\alpha_{em}\beta(m_{\eta'}^2)\left[ (2I_{8,ew} + 3I_{s,ew})\sqrt{2}c_\varphi + \left( \frac{3 - 4r'_K + r'_\pi}{r'_K - r'_\pi}I_{8,ew} + \frac{2 - (r'_K + r'_\pi)}{r'_K - r'_\pi}I_{27,ew} \right) s_\varphi \right], \quad (\text{C.95})$$

where we introduced the notations

$$r_i^{(\prime)} = \frac{m_i^2}{m_{\eta^{(\prime)}}^2} \quad \text{and} \quad \beta(p^2) = p^2 \frac{1}{p^2 - m_K^2}. \quad (\text{C.96})$$

In Eqs.(C.94) and (C.96), the simple pole at the  $K$ -mass indicates that the only relevant topology for  $\eta^{(\prime)} \rightarrow \pi\pi$  decays is eventually the first one depicted in Eq.C.92. Indeed, the remaining topologies cancel out once summed up, making the  $\mathcal{O}(G_F^2)$  amplitudes given in Eqs.(C.93)  $b$ -independent, as it should be, but also  $G_m$ -independent. Yet, in order to get some numerical insight, we estimate the  $I_{I,J}$  couplings in the following section.

## Phenomenological $I_{I,J}$ extraction

Following the analysis of Ref. [114], we observe that the low energy coupling constants  $G_8$ ,  $G_{27}$ ,  $G_s$  and  $G_{ew}$  find their origin in the following dominant four-quarks operators combinations:

$$Q_1 \oplus Q_2 \oplus Q_6 \rightarrow G_8, \quad (\text{C.97})$$

$$Q_1 \oplus Q_2 \rightarrow G_{27}, \quad (\text{C.98})$$

$$Q_1 \oplus Q_2 \rightarrow G_s, \quad (\text{C.99})$$

$$\alpha_{em}Q_8 \rightarrow G_{ew}. \quad (\text{C.100})$$

In principle, we should extract eight numbers to completely determine all these four couplings. Some simplifications are, however, possible. First of all, since the current-current operator  $Q_{1,2}$  are CP conserving in our conventions, we set

$$\text{Im}G_{27} = \text{Im}G_s = 0 . \quad (\text{C.101})$$

In addition, since the EW penguin is suppressed with respect to the QCD penguin<sup>2</sup> it is fair to strengthen the  $\text{Re}G_{ew} \ll \text{Re}G_8$  hierarchy assuming

$$\text{Re}G_{ew} = 0 . \quad (\text{C.102})$$

Under these assumptions, it remains to determine five quantities, namely,

$$\text{Re}G_8, \text{Re}G_{27}, \text{Re}G_s, \text{Im}G_8 \quad \text{and} \quad \text{Im}A_{ew} . \quad (\text{C.103})$$

The first two are usually obtained from  $K \rightarrow \pi\pi$  decay branching ratios with the corresponding strong re-scattering phase, see e.g. Ref. [180], with the result

$$\text{Re}G_8 = 9.1 \times 10^{-12} \text{ MeV}^{-2}, \quad \text{Re}G_{27} = 5.3 \times 10^{-13} \text{ MeV}^{-2} . \quad (\text{C.104})$$

Following then [114] it turns out that using the  $K_L \rightarrow \gamma\gamma$  decay we can extract

$$\frac{\text{Re}G_s}{\text{Re}G_8} = -0.30 \pm 0.05 , \quad (\text{C.105})$$

such that the imaginary parts of Eq.(C.103) remain to be determined. This can be achieved using the experimental information we have about  $\varepsilon'$ . First, in our present approximation, the  $K \rightarrow \pi\pi$  isospin amplitudes

$$\text{Re}A_0 = \sqrt{2}F(m_K^2 - m_\pi^2) \left( \text{Re}G_8 + \frac{1}{9}\text{Re}G_{27} \right) , \quad (\text{C.106})$$

$$\text{Re}A_2 = F(m_K^2 - m_\pi^2) \frac{10}{9}\text{Re}G_{27} , \quad (\text{C.107})$$

$$\text{Im}A_0 = \sqrt{2}F(m_K^2 - m_\pi^2) \left( \text{Im}G_8 - \frac{2}{3}\text{Im}A_{ew} \right) , \quad (\text{C.108})$$

$$\text{Im}A_2 = -\frac{2}{3}F(m_K^2 - m_\pi^2)\text{Im}A_{ew} , \quad (\text{C.109})$$

used in combination with the general expression of  $\varepsilon'$  given in Eq.(1.23) imply that

$$\frac{\text{Im}G_8}{\text{Re}G_8} = \frac{\sqrt{2}|\varepsilon|}{\omega} \frac{\text{Re}(\varepsilon'/\varepsilon)}{\Omega - 1} \left( \frac{1 + \frac{x}{2}}{1 - \frac{2y}{3}} \right) , \quad (\text{C.110})$$

<sup>2</sup>Their respective contribution to a given observable, as  $\varepsilon'$ , might however be of the same order.

where we defined

$$x \doteq \frac{\text{Re}G_{27}}{\text{Re}G_8} \quad \text{and} \quad y \doteq \frac{\text{Im}A_{ew}}{\text{Im}G_8} . \quad (\text{C.111})$$

While  $x$  is known from Eq.(C.104),  $y$  remains unknown as long as we don't resolve the content of  $\varepsilon'$ . Indeed, knowing the EW penguin versus QCD penguin fraction  $\Omega$  in  $\varepsilon'$  is equivalent to knowing  $y$  since

$$y \doteq \frac{3\omega\Omega}{-\sqrt{2} + 2\omega\Omega} . \quad (\text{C.112})$$

In order to remove this last uncertainty we just assume that the isospin breaking parameter  $\Omega$  lies in the SM favored range, see Fig.(2.2)

$$\Omega \in [0.2, 0.5] . \quad (\text{C.113})$$

Doing so, we conclude that:

$$I_{8,s} = -(4.44 \pm 2.44) \times 10^{-27} \text{ MeV}^{-4} , \quad (\text{C.114a})$$

$$I_{8,27} = +(8.62 \pm 3.30) \times 10^{-28} \text{ MeV}^{-4} , \quad (\text{C.114b})$$

$$I_{8,ew} = +(1.47 \pm 1.21) \times 10^{-25} \text{ MeV}^{-4} , \quad (\text{C.114c})$$

$$I_{s,ew} = -(4.40 \pm 4.36) \times 10^{-26} \text{ MeV}^{-4} , \quad (\text{C.114d})$$

$$I_{27,ew} = +(8.55 \pm 7.53) \times 10^{-27} \text{ MeV}^{-4} . \quad (\text{C.114e})$$

For some reassurance in these numbers, we can compare them with the ones obtained using the lattice determination of  $A_2$  given in Ref. [49]:

$$\text{Re}A_2 = +(1.436 \pm 0.265) \cdot 10^{-8} \text{ GeV} , \quad (\text{C.115})$$

$$\text{Im}A_2 = -(6.83 \pm 1.40) \cdot 10^{-13} \text{ GeV} , \quad (\text{C.116})$$

and their  $\varepsilon'$ -based extraction of

$$\frac{\text{Im}A_0}{\text{Re}A_0} = -(1.69 \pm 0.28) \cdot 10^{-4} . \quad (\text{C.117})$$

From these quantities, we can extract the imaginary part of  $A_{ew}$  through

$$\frac{\text{Im}A_{ew}}{\text{Re}G_{27}} = -\frac{5}{3} \frac{\text{Im}A_2}{\text{Re}A_2} \quad (\text{C.118})$$

and that of  $G_8$  using

$$\frac{\text{Im}G_8}{\text{Re}G_8} = \left(1 + \frac{x}{2}\right) \frac{\text{Im}A_0}{\text{Re}A_0} + \frac{2x}{3} \frac{\text{Im}A_{ew}}{\text{Re}G_{27}} . \quad (\text{C.119})$$

to find

$$I_{8,s}^{\text{Lat}} = -(4.24 \pm 0.74) \times 10^{-27} \text{ MeV}^{-4} , \quad (\text{C.120a})$$

$$I_{8,27}^{\text{Lat}} = +(8.24 \pm 0.06) \times 10^{-28} \text{ MeV}^{-4} , \quad (\text{C.120b})$$

$$I_{8,ew}^{\text{Lat}} = +(1.11 \pm 0.43) \times 10^{-25} \text{ MeV}^{-4} , \quad (\text{C.120c})$$

$$I_{s,ew}^{\text{Lat}} = -(3.33 \pm 1.85) \times 10^{-26} \text{ MeV}^{-4} , \quad (\text{C.120d})$$

$$I_{27,ew}^{\text{Lat}} = +(6.46 \pm 2.52) \times 10^{-27} \text{ MeV}^{-4} . \quad (\text{C.120e})$$

Our predictions based on the assumption made on  $\Omega$  are compatible with those Lattice predictions; they are less precise but somehow more conservative. In fact, using the Lattice results, we would get  $\Omega \in [0.19, 0.40]$ , which is a smaller allowed range for  $\Omega$ . Note finally that our estimation of Eq.(C.114b) is in full agreement with our estimation based on  $\text{Re}(\varepsilon')$  shown in Eq.(4.51).



# Bibliography

- [1] G. 'T HOOFT, *Nucl.Phys.* **B33**, 173 (1971).
- [2] R. PECCEI and H. R. QUINN, *Phys.Rev.Lett.* **38**, 1440 (1977).
- [3] M. MISIAK, H. ASATRIAN, K. BIERI, M. CZAKON, A. CZARNECKI, et al., *Phys.Rev.Lett.* **98**, 022002 (2007).
- [4] D. ASNER et al., *Heavy Flavor Averaging Group - hep-ex/1010.1589* (2010).
- [5] J. HISANO, M. NAGAI, P. PARADISI, and Y. SHIMIZU, *JHEP* **0912**, 030 (2009).
- [6] J. ADAM et al., *Nucl.Phys.* **B834**, 1 (2010).
- [7] A. ARTAMONOV et al., *Phys.Rev.Lett.* **101**, 191802 (2008).
- [8] J. BATLEY et al., *Eur.Phys.J.* **C68**, 75 (2010).
- [9] P. MERTENS and C. SMITH, *JHEP* **1108**, 069 (2011).
- [10] J.-M. GÉRARD and P. MERTENS, *Phys.Lett.* **B716**, 316 (2012).
- [11] P. MERTENS, *47th Rencontres de Moriond (EW) - arXiv:1205.1208* (2012).
- [12] H. WEYL, *Z.Phys.* **56**, 330 (1929).
- [13] C.-N. YANG and R. L. MILLS, *Phys.Rev.* **96**, 191 (1954).
- [14] S. GLASHOW, *Nucl.Phys.* **22**, 579 (1961).
- [15] A. SALAM and J. C. WARD, *Phys.Lett.* **13**, 168 (1964).

- [16] S. WEINBERG, *Phys.Rev.Lett.* **19**, 1264 (1967).
- [17] J. BERINGER et al., *Phys.Rev.* **D86**, 010001 (2012).
- [18] F. ENGLERT and R. BROUT, *Phys.Rev.Lett.* **13**, 321 (1964).
- [19] G. GURALNIK, C. HAGEN, and T. KIBBLE, *Phys.Rev.Lett.* **13**, 585 (1964).
- [20] P. W. HIGGS, *Phys.Lett.* **12**, 132 (1964).
- [21] P. W. HIGGS, *Phys.Rev.Lett.* **13**, 508 (1964).
- [22] G. 'T HOOFT, *Nucl.Phys.* **B35**, 167 (1971).
- [23] J. GOLDSTONE, *Nuovo Cim.* **19**, 154 (1961).
- [24] G. AAD et al., *Phys.Lett.* **B716**, 1 (2012).
- [25] S. CHATRCHYAN et al., *Phys.Lett.* **B716**, 30 (2012).
- [26] S. GLASHOW, J. ILIOPOULOS, and L. MAIANI, *Phys.Rev.* **D2**, 1285 (1970).
- [27] N. CABIBBO, *Phys.Rev.Lett.* **10**, 531 (1963).
- [28] J. CHARLES et al., *Eur.Phys.J.* **C41**, 1 (2005).
- [29] M. KOBAYASHI and T. MASKAWA, *Prog.Theor.Phys.* **49**, 652 (1973).
- [30] J. CHRISTENSON, J. CRONIN, V. FITCH, and R. TURLAY, *Phys.Rev.Lett.* **13**, 138 (1964).
- [31] G. COLANGELO, J. GASSER, and H. LEUTWYLER, *Nucl.Phys.* **B603**, 125 (2001).
- [32] J. BROD and M. GORBAHN, *Phys.Rev.Lett.* **108**, 121801 (2012).
- [33] A. J. BURAS and M. JAMIN, *JHEP* **0401**, 048 (2004).
- [34] A. PICH, *2004 ICHEP Proceedings - hep-ph/0410215* (2004).
- [35] D. GROSS and F. WILCZEK, *Phys.Rev.Lett.* **30**, 1343 (1973).
- [36] H. D. POLITZER, *Phys.Rev.Lett.* **30**, 1346 (1973).
- [37] T. INAMI and C. LIM, *Prog.Theor.Phys.* **65**, 297 (1981).
- [38] G. BUCHALLA, A. J. BURAS, and M. E. LAUTENBACHER, *Rev.Mod.Phys.* **68**, 1125 (1996).

- [39] J. BROD and M. GORBAHN, *Phys.Rev.* **D82**, 094026 (2010).
- [40] A. J. BURAS and D. GUADAGNOLI, *Phys.Rev.* **D78**, 033005 (2008).
- [41] A. J. BURAS and D. GUADAGNOLI, *Phys.Rev.* **D79**, 053010 (2009).
- [42] J.-M. GÉRARD, *JHEP* **1102**, 075 (2011).
- [43] A. J. BURAS, J.-M. GÉRARD, and W. A. BARDEEN, *arXiv:1401.1385* (2014).
- [44] A. LENZ, U. NIERSTE, J. CHARLES, S. DESCOTES-GENON, A. JANTSCH, et al., *Phys.Rev.* **D83**, 036004 (2011).
- [45] M. GAILLARD and B. W. LEE, *Phys.Rev.Lett.* **33**, 108 (1974).
- [46] G. ALTARELLI and L. MAIANI, *Phys.Lett.* **B52**, 351 (1974).
- [47] M. A. SHIFMAN, A. VAINSHTEIN, and V. I. ZAKHAROV, *Sov.Phys.JETP* **45**, 670 (1977).
- [48] A. PICH, *Nucl.Phys.Proc.Suppl.* **93**, 253 (2001).
- [49] T. BLUM, P. BOYLE, N. CHRIST, N. GARRON, E. GOODE, et al., *Phys.Rev.Lett.* **108**, 141601 (2012).
- [50] V. CIRIGLIANO, G. ECKER, H. NEUFELD, and A. PICH, *Eur.Phys.J.* **C33**, 369 (2004).
- [51] M. A. SHIFMAN, A. VAINSHTEIN, and V. I. ZAKHAROV, *Phys.Rev.* **D18**, 2583 (1978).
- [52] S. BERTOLINI, F. BORZUMATI, and A. MASIERO, *Phys.Rev.Lett.* **59**, 180 (1987).
- [53] N. DESHPANDE, P. LO, J. TRAMPETIC, G. EILAM, and P. SINGER, *Phys.Rev.Lett.* **59**, 183 (1987).
- [54] G. D'AMBROSIO, G. ECKER, G. ISIDORI, and J. PORTOLES, *JHEP* **9808**, 004 (1998).
- [55] S. BERTOLINI, M. FABBRICHESI, and E. GABRIELLI, *Phys.Lett.* **B327**, 136 (1994).
- [56] C. ROSENZWEIG, J. SCHECHTER, and C. TRAHERN, *Phys.Rev.* **D21**, 3388 (1980).
- [57] P. DI VECCHIA and G. VENEZIANO, *Nucl.Phys.* **B171**, 253 (1980).

- 
- [58] E. WITTEN, *Annals Phys.* **128**, 363 (1980).
- [59] S. R. COLEMAN, J. WESS, and B. ZUMINO, *Phys.Rev.* **177**, 2239 (1969).
- [60] J. CALLAN, C. G., S. R. COLEMAN, J. WESS, and B. ZUMINO, *Phys.Rev.* **177**, 2247 (1969).
- [61] J. A. CRONIN, *Phys.Rev.* **161**, 1483 (1967).
- [62] B. GRINSTEIN, S.-J. REY, and M. B. WISE, *Phys.Rev.* **D33**, 1495 (1986).
- [63] S. WEINBERG, *Physica* **A96**, 327 (1979).
- [64] H. LEUTWYLER, *Annals Phys.* **235**, 165 (1994).
- [65] J. GASSER and H. LEUTWYLER, *Annals Phys.* **158**, 142 (1984).
- [66] J. WESS and B. ZUMINO, *Phys.Lett.* **B37**, 95 (1971).
- [67] E. WITTEN, *Nucl.Phys.* **B223**, 422 (1983).
- [68] C. W. BERNARD, T. DRAPER, A. SONI, H. D. POLITZER, and M. B. WISE, *Phys.Rev.* **D32**, 2343 (1985).
- [69] G. D'AMBROSIO and G. ISIDORI, *Int.J.Mod.Phys.* **A13**, 1 (1998).
- [70] G. D'AMBROSIO, G. ECKER, G. ISIDORI, and H. NEUFELD, *Z.Phys.* **C76**, 301 (1997).
- [71] G. ECKER, A. PICH, and E. DE RAFAEL, *Nucl.Phys.* **B303**, 665 (1988).
- [72] G. D'AMBROSIO, G. ECKER, G. ISIDORI, and H. NEUFELD, *Phys.Lett.* **B380**, 165 (1996).
- [73] F. LOW, *Phys.Rev.* **110**, 974 (1958).
- [74] G. ECKER, J. KAMBOR, and D. WYLER, *Nucl.Phys.* **B394**, 101 (1993).
- [75] G. ECKER, J. GASSER, A. PICH, and E. DE RAFAEL, *Nucl.Phys.* **B321**, 311 (1989).
- [76] W. A. BARDEEN, A. BURAS, and J.-M. GÉRARD, *Phys.Lett.* **B192**, 138 (1987).
- [77] J.-M. GÉRARD, *Acta Phys.Polon.* **B21**, 257 (1990).
- [78] G. ISIDORI, F. MESCIA, and C. SMITH, *Nucl.Phys.* **B718**, 319 (2005).

- 
- [79] C. BRUNO and J. PRADES, *Z.Phys.* **C57**, 585 (1993).
- [80] D.-N. GAO, *Phys.Rev.* **D67**, 074028 (2003).
- [81] G. COLANGELO, G. ISIDORI, and J. PORTOLES, *Phys.Lett.* **B470**, 134 (1999).
- [82] D. BECIREVIC, V. LUBICZ, G. MARTINELLI, and F. MESCIA, *Phys.Lett.* **B501**, 98 (2001).
- [83] V. MATEU and J. PORTOLES, *Eur.Phys.J.* **C52**, 325 (2007).
- [84] P. BUIVIDOVICH, M. CHERNODUB, E. LUSCHEVSKAYA, and M. POLIKARPOV, (2009).
- [85] L. SEHGAL and M. WANNINGER, *Phys.Rev.* **D46**, 1035 (1992).
- [86] P. HEILIGER and L. SEHGAL, *Phys.Rev.* **D48**, 4146 (1993).
- [87] J. K. ELWOOD, M. B. WISE, and M. J. SAVAGE, *Phys.Rev.* **D52**, 5095 (1995).
- [88] G. ECKER and H. PICHL, *Phys.Lett.* **B507**, 193 (2001).
- [89] F. MESCIA, C. SMITH, and S. TRINE, *JHEP* **0608**, 088 (2006).
- [90] G. BUCHALLA, G. D'AMBROSIO, and G. ISIDORI, *Nucl.Phys.* **B672**, 387 (2003).
- [91] G. ISIDORI, C. SMITH, and R. UNTERDORFER, *Eur.Phys.J.* **C36**, 57 (2004).
- [92] D.-N. GAO, *Phys.Rev.* **D69**, 094030 (2004).
- [93] P. SINGER, *1996 Orsay K-Physics Workshop - hep-ph/9607429* (1996).
- [94] J. TANDEAN, *Phys.Rev.* **D61**, 114022 (2000).
- [95] G. EILAM, A. IOANNISIAN, R. MENDEL, and P. SINGER, *Phys.Rev.* **D53**, 3629 (1996).
- [96] S. FAJFER, S. PRELOVSEK, and P. SINGER, *Phys.Rev.* **D59**, 114003 (1999).
- [97] J. GOOD, *Phys.Rev.* **113**, 352 (1959).
- [98] N. CHRIST, *Phys.Rev.* **159**, 1292 (1967).
- [99] J. BIJNENS, G. ECKER, and A. PICH, *Phys.Lett.* **B286**, 341 (1992).

- 
- [100] G. D'AMBROSIO and J. PORTOLES, *Nucl.Phys.* **B533**, 523 (1998).
- [101] G. D'AMBROSIO and D.-N. GAO, *JHEP* **0010**, 043 (2000).
- [102] L. CAPPIELLO and G. D'AMBROSIO, *Phys.Rev.* **D75**, 094014 (2007).
- [103] G. ECKER, H. NEUFELD, and A. PICH, *Nucl.Phys.* **B413**, 321 (1994).
- [104] G. D'AMBROSIO and G. ISIDORI, *Z.Phys.* **C65**, 649 (1995).
- [105] B. ANANTHANARAYAN, G. COLANGELO, J. GASSER, and H. LEUTWYLER, *Phys.Rept.* **353**, 207 (2001).
- [106] C. DIB and R. PECCEI, *Phys.Lett.* **B249**, 325 (1990).
- [107] A. J. BURAS and J.-M. GÉRARD, *Phys.Lett.* **B517**, 129 (2001).
- [108] J. TANDEAN and G. VALENCIA, *Phys.Rev.* **D62**, 116007 (2000).
- [109] J. N. MATTHEWS, P. GU, P. HAAS, W. HOGAN, S. KIM, et al., *Phys.Rev.Lett.* **75**, 2803 (1995).
- [110] L. SEHGAL and L. WOLFENSTEIN, *Phys.Rev.* **162**, 1362 (1967).
- [111] B. MARTIN and E. DE RAFAEL, *Nucl.Phys.* **B8**, 131 (1968).
- [112] R. DECKER, P. PAVLOPOULOS, and G. ZOUPANOS, *Z.Phys.* **C28**, 117 (1985).
- [113] F. BUCCELLA, G. D'AMBROSIO, and M. MIRAGLIUOLO, *Nuovo Cim.* **A104**, 777 (1991).
- [114] J.-M. GÉRARD, C. SMITH, and S. TRINE, *Nucl.Phys.* **B730**, 1 (2005).
- [115] T. WU and C.-N. YANG, *Phys.Rev.Lett.* **13**, 380 (1964).
- [116] A. J. BURAS, D. GUADAGNOLI, and G. ISIDORI, *Phys.Lett.* **B688**, 309 (2010).
- [117] J. BROD, M. GORBAHN, and E. STAMOU, *Phys.Rev.* **D83**, 034030 (2011).
- [118] A. BURAS, M. GORBAHN, U. HAISCH, and U. NIERSTE, *Phys.Rev.Lett.* **95**, 261805 (2005).
- [119] A. J. BURAS, M. GORBAHN, U. HAISCH, and U. NIERSTE, *JHEP* **0611**, 002 (2006).
- [120] J. BROD and M. GORBAHN, *Phys.Rev.* **D78**, 034006 (2008).

- 
- [121] J. AHN et al., *Phys.Rev.* **D81**, 072004 (2010).
- [122] A. ALAVI-HARATI et al., *Phys.Rev.Lett.* **93**, 021805 (2004).
- [123] A. ALAVI-HARATI et al., *Phys.Rev.Lett.* **84**, 5279 (2000).
- [124] K. ADCOX et al., *Phys.Rev.Lett.* **88**, 192303 (2002).
- [125] A. BURAS, G. COLANGELO, G. ISIDORI, A. ROMANINO, and L. SILVESTRINI, *Nucl.Phys.* **B566**, 3 (2000).
- [126] M. CARPENTIER and S. DAVIDSON, *Eur.Phys.J.* **C70**, 1071 (2010).
- [127] Y. GROSSMAN and Y. NIR, *Phys.Lett.* **B398**, 163 (1997).
- [128] G. D'AMBROSIO, G. GIUDICE, G. ISIDORI, and A. STRUMIA, *Nucl.Phys.* **B645**, 155 (2002).
- [129] M. CIUCHINI, G. DEGRASSI, P. GAMBINO, and G. GIUDICE, *Nucl.Phys.* **B534**, 3 (1998).
- [130] A. ALI and D. LONDON, *Eur.Phys.J.* **C9**, 687 (1999).
- [131] A. BURAS, P. GAMBINO, M. GORBAHN, S. JAGER, and L. SILVESTRINI, *Phys.Lett.* **B500**, 161 (2001).
- [132] C. SMITH, *Acta Phys.Polon.Supp.* **3**, 53 (2010).
- [133] T. HURTH, G. ISIDORI, J. F. KAMENIK, and F. MESCIA, *Nucl.Phys.* **B808**, 326 (2009).
- [134] W. BUCHMULLER and D. WYLER, *Nucl.Phys.* **B268**, 621 (1986).
- [135] R. BARBIER, C. BERAT, M. BESANCON, P. BINETRUY, G. BORDES, et al., (1998).
- [136] Y. GROSSMAN, G. ISIDORI, and H. MURAYAMA, *Phys.Lett.* **B588**, 74 (2004).
- [137] N. DESHPANDE, D. K. GHOSH, and X.-G. HE, *Phys.Rev.* **D70**, 093003 (2004).
- [138] A. DEANDREA, J. WELZEL, and M. OERTEL, *JHEP* **0410**, 038 (2004).
- [139] S. DAVIDSON, D. C. BAILEY, and B. A. CAMPBELL, *Z.Phys.* **C61**, 613 (1994).
- [140] E. NIKOLIDAKIS and C. SMITH, *Phys.Rev.* **D77**, 015021 (2008).

- 
- [141] S. DAVIDSON and S. DESCOTES-GENON, *JHEP* **1011**, 073 (2010).
- [142] C. SMITH, *6th International Workshop on the CKM Unitarity Triangle - arXiv:1012.4398* (2010).
- [143] S. R. CHOUDHURY, N. GAUR, G. C. JOSHI, and B. MCKELLAR, (2004).
- [144] M. BLANKE, A. J. BURAS, B. DULING, S. RECKSIEGEL, and C. TARANTINO, *Acta Phys.Polon.* **B41**, 657 (2010).
- [145] T. GOTO, Y. OKADA, and Y. YAMAMOTO, *Phys.Lett.* **B670**, 378 (2009).
- [146] P. L. CHO and M. MISIAK, *Phys.Rev.* **D49**, 5894 (1994).
- [147] W.-S. HOU, M. NAGASHIMA, and A. SODDU, *Phys.Rev.* **D72**, 115007 (2005).
- [148] A. J. BURAS, B. DULING, T. FELDMANN, T. HEIDSIECK, C. PROMBERGER, et al., *JHEP* **1009**, 106 (2010).
- [149] A. J. BURAS, M. SPRANGER, and A. WEILER, *Nucl.Phys.* **B660**, 225 (2003).
- [150] G. BUCHALLA, A. J. BURAS, and M. K. HARLANDER, *Nucl.Phys.* **B349**, 1 (1991).
- [151] A. J. BURAS and L. SILVESTRINI, *Nucl.Phys.* **B546**, 299 (1999).
- [152] Y. NIR and M. P. WORAH, *Phys.Lett.* **B423**, 319 (1998).
- [153] F. GABBIANI, E. GABRIELLI, A. MASIERO, and L. SILVESTRINI, *Nucl.Phys.* **B477**, 321 (1996).
- [154] S. KHALIL, T. KOBAYASHI, and O. VIVES, *Nucl.Phys.* **B580**, 275 (2000).
- [155] A. MASIERO, S. VEMPATI, and O. VIVES, *Les Houches 2005, Particle physics beyond the standard model*, 1 (2005).
- [156] G. ISIDORI, Y. NIR, and G. PEREZ, *Ann.Rev.Nucl.Part.Sci.* **60**, 355 (2010).
- [157] G. COLANGELO, E. NIKOLIDAKIS, and C. SMITH, *Eur.Phys.J.* **C59**, 75 (2009).
- [158] L. MERCOLLI and C. SMITH, *Nucl.Phys.* **B817**, 1 (2009).
- [159] G. COLANGELO and G. ISIDORI, *JHEP* **9809**, 009 (1998).



- 
- [160] G. ISIDORI, F. MESCIA, P. PARADISI, C. SMITH, and S. TRINE, *JHEP* **0608**, 064 (2006).
- [161] A. J. BURAS, T. EWERTH, S. JAGER, and J. ROSIEK, *Nucl.Phys.* **B714**, 103 (2005).
- [162] J.-M. GÉRARD, *2008 European School of HEP - arXiv:0811.0540* (2008).
- [163] J.-M. GÉRARD and Z.-z. XING, *Phys.Lett.* **B713**, 29 (2012).
- [164] C. BAKER, D. DOYLE, P. GELTENBORT, K. GREEN, M. VAN DER GRINTEN, et al., *Phys.Rev.Lett.* **97**, 131801 (2006).
- [165] M. POSPELOV and A. RITZ, *Annals Phys.* **318**, 119 (2005).
- [166] G. 'T HOOFT, *Phys.Rev.Lett.* **37**, 8 (1976).
- [167] J. R. ELLIS and M. K. GAILLARD, *Nucl.Phys.* **B150**, 141 (1979).
- [168] I. KHRIPLOVICH, *Phys.Lett.* **B173**, 193 (1986).
- [169] E. WITTEN, *Nucl.Phys.* **B156**, 269 (1979).
- [170] S. WEINBERG, *Phys.Rev.* **D11**, 3583 (1975).
- [171] H. GEORGI, *Phys.Rev.* **D49**, 1666 (1994).
- [172] J.-M. GÉRARD and E. KOU, *Phys.Lett.* **B616**, 85 (2005).
- [173] A. PICH and E. DE RAFAEL, *Nucl.Phys.* **B367**, 313 (1991).
- [174] P. RAMOND, *Front.Phys.* **51**, 1 (1981).
- [175] P. DI VECCHIA and F. SANNINO, *Preprint - arXiv:1310.0954* (2013).
- [176] C. JARLSKOG and E. SHABALIN, *Phys.Rev.* **D52**, 248 (1995).
- [177] A. BURAS and J. GÉRARD, *Phys.Lett.* **B192**, 156 (1987).
- [178] A. JUTTNER, *XIV International Conference on Hadron Spectroscopy - arXiv:1109.1388* (2011).
- [179] C. JARLSKOG, *Phys.Rev.Lett.* **55**, 1039 (1985).
- [180] V. CIRIGLIANO, G. ECKER, H. NEUFELD, A. PICH, and J. PORTOLES, *Rev.Mod.Phys.* **84**, 399 (2012).
- [181] R. CREWETHER, P. DI VECCHIA, G. VENEZIANO, and E. WITTEN, *Phys.Lett.* **B88**, 123 (1979).

- 
- [182] R. PECCEI, *Lect.Notes Phys.* **741**, 3 (2008).
- [183] J. BIJNENS, E. PALLANTE, and J. PRADES, *Nucl.Phys.* **B521**, 305 (1998).
- [184] J. GASSER and H. LEUTWYLER, *Nucl.Phys.* **B250**, 465 (1985).
- [185] W. A. BARDEEN, *Phys.Rev.* **184**, 1848 (1969).
- [186] R. CREWETHER, *Nucl.Phys.* **B264**, 277 (1986).
- [187] J. KAMBOR, J. H. MISSIMER, and D. WYLER, *Nucl.Phys.* **B346**, 17 (1990).
- [188] G. ESPOSITO-FARESE, *Z.Phys.* **C50**, 255 (1991).
- [189] WOLFRAM RESEARCH INC., *Version 8.0, Champaign, IL (2010)* .
- [190] N. D. CHRISTENSEN and C. DUHR, *Comput.Phys.Commun.* **180**, 1614 (2009).
- [191] T. HAHN, *Comput.Phys.Commun.* **140**, 418 (2001).
- [192] R. MERTIG, M. BOHM, and A. DENNER, *Comput.Phys.Commun.* **64**, 345 (1991).
- [193] G. D'AMBROSIO, M. MIRAGLIUOLO, and F. SANNINO, *Z.Phys.* **C59**, 451 (1993).